

Central nervous system plasticity associated with pain in a mouse model of multiple sclerosis, and the antinociceptive effects of the antidepressant phenelzine.

by  
Liam E. Potter

A thesis submitted in partial fulfillment of the requirements for the degree of

Doctor of Philosophy

Neuroscience  
University of Alberta

© Liam E. Potter, 2017

## Abstract

Multiple sclerosis (MS) is a chronic, progressive disease that involves neuroinflammation, demyelination, and neurodegeneration within the central nervous system (CNS). While loss of motor function and paralysis are considered the primary clinical consequences of MS, the disease is also associated with a variety of secondary symptoms. One of the most common and debilitating secondary symptoms of MS is pain. The underlying neurobiological mechanisms of pain in MS are poorly understood, and the currently available treatments are generally inadequate. Pain in MS can be studied using the inducible animal disease model experimental autoimmune encephalomyelitis (EAE). This thesis focuses on elucidating the cellular and circuit/systems-level mechanisms underlying pain in the MOG<sub>35-55</sub>/C57/BL6 murine EAE model. Altered neuronal function and structural/synaptic plasticity are characterized within the dorsal horn (DH) and the primary somatosensory cortex (S1) in early EAE, using a variety of optical imaging and immunohistochemical methods. We also assess the effects of treatment with the antidepressant phenelzine (PLZ) on neuronal plasticity and behavioral measures of pain in EAE, and in the formalin model of subacute chemogenic pain. PLZ, which acts to raise CNS levels of the monoamines (5-HT, NA, DA) and GABA, reduced nociceptive responses in the second phase of the formalin model, and reversed allodynia in EAE. PLZ also reversed or attenuated many of the plastic changes that we identified in the CNS in EAE, and acts to restore or augment inhibition in the DH/S1. These experiments identify novel forms of CNS plasticity associated with pain in EAE, and also identify a novel use for PLZ in mitigating this plasticity and treating pain. This work helps validate and advance the use of MOG<sub>35-55</sub>/C57/BL6 EAE as a model for pain in MS, and may also inform the development of novel pain treatments.

## Preface

This thesis is an original work of Liam Potter. The research project that this thesis is part of received research ethics approval from the University of Alberta Health Sciences Animal Care and Use Committee, Protocol Title: “Assessing sensory function in EAE” – #: AUP00000274.

Some of the research in this thesis was conducted in collaboration with other laboratories/individuals at the University of Alberta, and at the University of Kentucky. The flavoprotein imaging experiments, and confocal microscopy in Chapter 4 were carried out by myself in the laboratory of Dr. Ian Winship. Jee Su Suh assisted with Golgi Cox/IHC/microscopy in Chapter 3/4. John Paylor assisted with IHC microscopy/analysis in Chapter 4. Dr. Fred Colbourne at the University of Alberta, and Jayalakshmi Caliaperumal instructed/assisted on Golgi Cox in Chapter 4. Dr. Glen Baker and Dr. Bradley Kerr formulated the idea to use phenelzine in EAE/for pain. The calcium imaging experiments in Chapter 2/3 were conducted at the University of Kentucky in Lexington, KY, USA, in the laboratory of Dr. Bradley Taylor. Dr. Suzanne Doolen helped design those experiments and developed the method, and also did the surgeries and assisted with analysis. Experiments at the University of Kentucky were conducted with ethics approval from the Institutional Animal Care and Use Committee of the University of Kentucky.

A version of Chapter 4 of this thesis was previously published in the Journal of Neuroinflammation as: “*Altered excitatory-inhibitory balance within somatosensory cortex is associated with enhanced plasticity and pain sensitivity in a mouse model of multiple sclerosis.*” Potter LE, Paylor JW, Suh J, Tenorio G, Caliaperumal J, Colbourne F, Baker G, Winship I, Kerr BJ. Journal of Neuroinflammation, 2016. 13(1): p. 142.”

## Acknowledgments

I would above all like to acknowledge my mentor / supervisor Dr. Bradley Kerr for providing me with the opportunity and resources to undertake my PhD, and for providing guidance and assistance throughout the process. Next I would like to my fiancée (and former Kerr lab member) Dr. Camille Olechowski - her guidance and support were critical to my success, and much of this thesis is built upon her foundational work. Other current and former members of the Kerr lab – Dr. Curtis Benson, Katherine Mifflin, Saad Yousuf, Kevin Thorburn – all contributed to the work in this thesis in various ways. Gustavo Tenorio helped with behavioral experiments, tissue processing, and with some of the figures. Jee Su Suh, Wes Paylor, and Kasia Zubkow helped with much of the tissue staining and quantifications. Dr. Ian Winship provided critical guidance and resources, especially for the *in vivo* imaging and confocal microscopy experiments. Bin Dong assisted and instructed me in the *in vivo* imaging experiments as well. Dr. Bradley Taylor and Dr. Suzanne Doolen at University of Kentucky provided me with resources and instruction for the *ex vivo* imaging experiments – and Suzanne did all of the necessary surgeries and assisted with analysis. Dr. Fred Colbourne and Dr. Jayalakshmi Caliaperumal provided instruction and resources for the Golgi Cox experiments. I would also like to thank Campus Alberta Neuroscience and Dr. Majid Mohajerani at University of Lethbridge for guidance and MATLAB code that was used for the peri-somatic parvalbumin analysis. The University of Alberta Neuroscience and Mental Health Institute and The MS Society of Canada / Alberta endMS provided key funding, support, opportunities and resources. Lastly I would like to thank my family, who also supported me in various ways throughout this process.

## Table of Contents

### Chapter 1

<i>Introduction</i>	1
1.1 – Pain	2
1.1.1 – Chronic / Pathological Pain	3
1.1.2 – Functional Neuroanatomy / Neurobiology of Pain	4
1.1.2.1 – Primary Afferent Neurons	4
1.1.2.2 – Dorsal Horn of the Spinal Cord	7
1.1.2.2.1 – Mechanisms of Central Sensitization: Activity-Dependent Changes	9
1.1.2.2.2 – Mechanisms of Central Sensitization: Loss of Inhibition	11
1.1.2.2.3 – Descending Inhibition / Monoamines	13
1.1.2.2.4 – Glial and Immune / Inflammatory Mechanisms	15
1.1.2.3 – Supraspinal Sites	16
1.1.2.3.1 – Midbrain / Brainstem	17
1.1.2.3.2 – Thalamus	17
1.1.2.3.3 – Primary and Secondary Somatosensory Cortices (S1/S2)	19
1.1.2.3.4 – Anterior Cingulate Cortex (ACC)	23
1.1.2.3.5 – Insular Cortex (IC)	24
1.1.2.3.6 – Other Brain Regions	25
1.1.2.3.7 – Caveat to the “Pain Matrix”	26
1.2 – Multiple Sclerosis	27
1.2.1 – MS Phenotypes	28
1.2.2 – Genetic Risk Factors for MS	29
1.2.3 – Environmental Risk Factors for MS	30
1.2.4 – Pathophysiology of MS	31
1.2.4.1 – The Blood Brain Barrier (BBB)	32
1.2.4.2 – Outside-In Model of MS	32
1.2.4.3 – Inside-Out Model of MS	33
1.2.4.4 – Immunopathogenesis of MS	33
1.2.4.5 – Cytokines	35
1.2.4.5.1 – IL-23	36
1.2.4.5.2 – IL-6	36
1.2.4.5.3 – IL-1( $\beta/\alpha$ )	36
1.2.4.5.4 – The Inflammasome	37
1.2.4.5.5 – TNF $\alpha$	37
1.2.4.5.6 – IFN $\gamma$	38
1.2.4.6 – Axonal Injury and Neurodegeneration	38
1.2.5 – Treatment of MS	40
1.3 – Experimental Autoimmune Encephalomyelitis (EAE)	42
1.3.1 – Pathology / Pathogenesis of EAE	43
1.3.2 – Secondary Symptoms of EAE/MS	47
1.4 – Pain in MS	47
1.5 – Pain (Altered Nociception) in EAE	49
1.6 – Phenelzine	53

1.7 – Aims and Scope	54
1.8 – Hypotheses	54
1.9 – Figures	56
1.10 – References	60
<b>Chapter 2</b>	<b>76</b>
<i>Acute antinociceptive effects of the antidepressant phenelzine are mediated by context-dependent inhibition of neuronal responses in the dorsal horn.</i>	
2.1 – Abstract	77
2.2 – Introduction	77
2.3 – Methods	79
2.3.1 – Animals and Ethics	79
2.3.2 – Drug Treatments	79
2.3.3 – Behavioral Pain Assays	80
2.3.3.1 – Von Frey Hairs	80
2.3.3.2 – Hot Plate	80
2.3.3.3 – Formalin	81
2.3.4 – Immunohistochemistry / Immunocytochemistry	81
2.3.4.1 – Tissue Collection / Preparation	82
2.3.4.2 – Immunohistochemistry Staining	82
2.3.4.3 – c-Fos/DAB	82
2.3.4.4 – Immunofluorescence	82
2.3.4.5 – IHC Image Acquisition and Quantification	82
2.3.5 – Calcium Imaging	83
2.3.5.1 – Preparation of Adult Mouse Spinal Cord Slices	83
2.3.5.2 – Ratiometric Ca <sup>2+</sup> Imaging	84
2.3.6 – Statistics	85
2.4 – Results	85
2.4.1 – Acute PLZ pretreatment ( <i>in vivo</i> ) does not affect basal mechanical or thermal nociceptive sensitivity.	85
2.4.2 – Acute PLZ pretreatment ( <i>in vivo</i> ) inhibits the second phase of the response to intraplantar formalin.	86
2.4.3 – Acute PLZ pretreatment ( <i>in vivo</i> ) reduces c-Fos+ immunoreactivity in the ipsilateral superficial dorsal horn following intraplantar formalin.	87
2.4.4 – Acute PLZ treatment ( <i>in vivo</i> ) increases 5-HT+ immunoreactivity in the superficial dorsal horn.	88
2.4.5 – PLZ produces a dose-dependent inhibition of glutamate-evoked calcium responses in <i>ex vivo</i> lumbar slices.	88
2.4.6 – Pretreatment with the 5HT <sub>1A</sub> R antagonist WAY-100,635, but not the adrenergic antagonist idazoxan, blocks the inhibition of glutamate-evoked calcium responses in the DH by PLZ.	89
2.5 – Discussion	91
2.6 – Figures	96
2.7 – References	102
<b>Chapter 3</b>	<b>104</b>

*Functional and structural plasticity in the dorsal horn associated with allodynia in EAE, and the effects of the antidepressant phenelzine.*

3.1 – Abstract	105
3.2 – Introduction	106
3.3 – Methods	108
3.3.1 – Animals and Ethics	108
3.3.2 – EAE Induction	108
3.3.3 – Disease Scoring	109
3.3.4 – Drug Treatments	110
3.3.5 – Pain Testing	110
3.3.5.1 – Von Frey Hairs	110
3.3.5.2 – Acetone	111
3.3.5.3 – Rotorod	111
3.3.6 – Additional Assays	112
3.3.7 – c-Fos Induction	112
3.3.8 – Tissue Collection / Preparation	112
3.3.9 – Immunohistochemistry / Immunocytochemistry	113
3.3.9.1 – c-Fos/DAB	113
3.3.9.2 – Immunofluorescence / Double-Labeling	113
3.3.9.3 – IHC Image Acquisition and Quantification	113
3.3.10 – Calcium Imaging	114
3.3.10.1 – Preparation of Adult Mouse Spinal Cord Slices	114
3.3.10.2 – Ratiometric Ca <sup>2+</sup> Imaging	115
3.3.11 – Statistics	116
3.4 – Results	116
3.4.1 – Pretreatment with PLZ normalizes nociceptive sensitivity in EAE animals at clinical onset.	116
3.4.2 – Vibromechanical stimulation evokes additional c-Fos <sup>+</sup> neurons in the superficial dorsal horn of VEH-treated EAE, but not PLZ-treated EAE animals or CFA controls.	117
3.4.3 – PLZ's actions in EAE are not mediated by a reduction of inflammatory cells in the dorsal horn.	119
3.4.4 – Intracellular calcium responses to glutamate are enhanced within the dorsal horn in EAE, and are normalized by bath-applied PLZ.	120
3.4.5 – Plasticity of excitatory synaptic terminals within the deeper laminae (III to VI) of the dorsal horn in EAE.	121
3.4.6 – 5-HT immunoreactivity is reduced in the dorsal horn in EAE, and is normalized by pretreatment with PLZ.	122
3.5 – Discussion	123
3.5.1 – Conclusions	128
3.6 – Figures	129
3.7 – References	136
<b>Chapter 4</b>	<b>140</b>
<i>Altered excitatory-inhibitory balance within somatosensory cortex is associated with enhanced plasticity and pain sensitivity in a mouse model of multiple sclerosis</i>	
4.1 – Abstract	141

4.2 – Introduction	142
4.3 – Methods	144
4.3.1 – Animals and Ethics	144
4.3.2 – EAE Induction	144
4.3.3 – Disease Scoring	144
4.3.4 – Drug Treatments	145
4.3.5 – Pain Testing	145
4.3.6 – <i>In Vivo</i> Flavoprotein Autofluorescence Imaging in S1	145
4.3.6.1 – Thin Window Preparation	146
4.3.6.2 – FA Imaging	147
4.3.6.3 – FA Image Processing and Data Analysis	148
4.3.7 – Histology	149
4.3.7.1 – Tissue Extraction and Fixation	150
4.3.7.2 – Free Floating Sections	150
4.3.7.3 – Golgi-Cox Staining	150
4.3.7.4 – Immunohistochemistry	152
4.3.7.4.1 – Antibodies / Reagents	152
4.3.7.4.2 – IHC: Image Acquisition	152
4.3.7.4.3 – IHC: Analysis	154
4.3.7.4.4 – IHC: Analysis (“Perisomatic” PV)	154
4.3.8 – Statistics	155
4.4 – Results	156
4.4.1 – Mice with EAE exhibit enhanced neuronal responses to tactile stimulation within S1 pre-symptomatically.	156
4.4.2 – Early EAE is associated with changes in the density of inhibitory and excitatory synaptic markers within S1.	157
4.4.3 – Chronic treatment with the antidepressant PLZ normalizes vibrotactile-evoked FAI responses in S1 of mice with EAE at clinical-onset.	158
4.4.4 – EAE is associated with morphological changes to excitatory neurons of cortical layers 2/3 and 4 of S1, which are prevented or reversed by PLZ treatment.	159
4.4.5 – Chronic PLZ treatment partially normalizes pre-synaptic excitatory synaptic densities in S1 of mice with established EAE.	160
4.4.6 – EAE is associated with a progressive loss of peri-neuronal nets and microgliosis in S1.	161
4.5 – Discussion	162
4.5.1 – Conclusions	167
4.6 – Figures	168
4.7 – References	177
<b>Chapter 5</b>	<b>182</b>
<i>Additional Commentary and Conclusions</i>	
5.0 – Chapter 2 Commentary	183
5.1 – Chapter 3 Commentary	196
5.3 – Chapter 4 Commentary	201
5.4 – Conclusions	206
5.5 – References	207
Works Cited	211
Appendix (Published Papers)	240

## List of Figures

1.1 – <i>Functional anatomy of the dorsal horn.</i>	56
1.2 – <i>Microcircuits in somatosensory cortex.</i>	57
1.3 – <i>CNS immune infiltration in EAE/MS.</i>	58
1.4 – <i>Neurodegeneration in EAE/MS.</i>	59
2.1 – <i>Acute effects of PLZ treatment on basal mechanical and thermal nociceptive sensitivity.</i>	96
2.2 – <i>Acute effects of PLZ treatment on formalin-evoked nociceptive behavior.</i>	97
2.3 – <i>Effect of PLZ treatment on formalin-evoked c-Fos in the dorsal horn.</i>	98
2.4 – <i>Effect of PLZ treatment on 5-HT+ immunoreactivity in the dorsal horn.</i>	99
2.5 – <i>Dose-dependent inhibition of glutamate-evoked calcium responses in the dorsal horn by bath-applied PLZ.</i>	100
2.6 – <i>Pretreatment with the 5HT1AR antagonist WAY-100,635, but not the adrenergic antagonist idazoxan, blocks the inhibition of intracellular calcium responses in the DH by PLZ.</i>	101
3.1 – <i>Effects of chronic pretreatment with PLZ on clinical score and nociceptive behaviors in EAE animals at onset.</i>	129
3.2 – <i>Vibromechanically evoked c-Fos in the dorsal horn in EAE is normalized by pretreatment with PLZ.</i>	130
3.3 – <i>c-Fos co-localizes with neurons, and not with inflammatory cell types, in the dorsal horn in VEH- and PLZ-treated EAE.</i>	131
3.4 – <i>PLZ's actions in EAE are not mediated by a reduction of inflammatory cells in the dorsal horn.</i>	132
3.5 – <i>Intracellular calcium responses are enhanced within the dorsal horn in EAE, and are normalized by bath-applied PLZ.</i>	133
3.6 – <i>Increased density of vGlut1+ presynaptic terminals in the deeper laminae (III-VI) of the dorsal horn in EAE.</i>	134
3.7 – <i>5-HT+ immunoreactivity is reduced in the dorsal horn in EAE, and is normalized by pretreatment with PLZ.</i>	135
4.1 – <i>In vivo FA imaging of vibrotactile-evoked responses in S1 at the pre-symptomatic stage of EAE.</i>	168
4.2 – <i>Perisomatic PV+ and VGLUT1+ reactivity in S1 at the pre-symptomatic stage of EAE.</i>	169
4.3 – <i>Chronic PLZ normalizes FAI responses in S1, and mechanical nociceptive thresholds, in EAE at clinical-onset.</i>	170
4.4 – <i>In vivo FAI of forelimb vibrotactile-evoked responses in S1 of EAE, and PLZ-treated EAE animals at clinical onset.</i>	171
4.5 – <i>Morphological changes in spiny excitatory neurons of S1 in EAE, and PLZ-treated EAE, at clinical onset.</i>	172
4.6 – <i>Perisomatic PV+ and VGLUT1+ reactivity and the effects of PLZ treatment in established EAE.</i>	173
4.7 – <i>S1 IHC in pre-symptomatic and clinical onset EAE: PV+ cell counts, PNN counts, and Iba-1+ microglia counts.</i>	174
4.8 – <i>Microglial activation and peri-neuronal net integrity in S1, and the effects of PLZ, in established EAE.</i>	175
4.9 – <i>S1 IHC in pre-symptomatic and clinical onset EAE: Absence of cortical-infiltrating CD3+ and/or CD45+ T-cells.</i>	176

## List of Tables

Table 1 – Ch. 4 Immunohistochemistry Sample Sizes

153

## List of Abbreviations

<b>(1H-)MRS</b>	(proton) magnetic resonance spectroscopy
<b>(p)CREB</b>	(phospho) cyclic adenosine monophosphate (cAMP)-response element binding protein
<b>4-AP</b>	4-aminopyridine
<b>5-HT</b>	5-hydroxytryptamine (serotonin)
<b>5-HT(#R)</b>	5-HT(#) receptor
<b>A1</b>	primary auditory cortex
<b>AC</b>	adenylyl cyclase
<b>ACC</b>	anterior cingulate cortex
<b>ACh</b>	acetylcholine
<b>aCSF</b>	artificial cerebrospinal fluid
<b>ADEM</b>	acute disseminated encephalomyelitis
<b>ADP</b>	adenosine diphosphate
<b>AIDS</b>	acquired immune deficiency syndrome
<b>ALS</b>	amyotrophic lateral sclerosis
<b>AMPA(R)</b>	$\alpha$ -amino-3-hydroxy-5-methyl-4-isoxazolepropionic acid (receptor)
<b>ANOVA</b>	analysis of variance
<b>AP</b>	action potential
<b>APC</b>	antigen presenting cell
<b>APP</b>	amyloid precursor protein
<b>ASL</b>	arterial spin labeling
<b>ATP</b>	adenosine triphosphate
<b>BBB</b>	blood-brain barrier
<b>BDNF</b>	brain-derived neurotrophic factor
<b>BG</b>	basal ganglia
<b>CaMK(2)</b>	calcium calmodulin-dependent protein kinase 2
<b>cAMP</b>	cyclic adenosine monophosphate
<b>CBV</b>	cerebral blood volume
<b>CCL</b>	chemokine ligand
<b>CCR</b>	chemokine receptor
<b>CD</b>	cluster of differentiation
<b>CFA</b>	complete Freund's adjuvant
<b>c-Fos</b>	(c) FOS proto-oncogene / FBJ murine osteosarcoma viral oncogene homolog
<b>CGRP</b>	calcitonin gene-related peptide
<b>CIS</b>	clinically isolated syndrome

<b>Cl</b>	chloride
<b>CNP</b>	chronic neuropathic pain
<b>CNS</b>	central nervous system
<b>COMT</b>	catechol-O-methyl-transferase
<b>COX(2)</b>	cyclooxygenase (2)
<b>CRPS</b>	complex regional pain syndrome
<b>CSF</b>	cerebrospinal fluid
<b>CSPG</b>	chondroitin sulfate proteoglycan
<b>CX3CL1</b>	fractalkine
<b>CX3CR1</b>	fractalkine receptor
<b>CXCL(10)</b>	C-X-C motif chemokine (10)
<b>CXCL8</b>	interleukin-8
<b>D2R</b>	dopamine 2 receptor
<b>DA</b>	dopamine
<b>DAB</b>	3,3'-diaminobenzidine
<b>DH</b>	dorsal horn
<b>DMAM</b>	disease modifying agent for MS
<b>DMT</b>	disease modifying therapy
<b>DNA</b>	deoxyribonucleic acid
<b>DNIC</b>	diffuse noxious inhibitory controls
<b>Dpi.</b>	days post-innoculation
<b>DRG</b>	dorsal root ganglion
<b>EAAT(-1/2)</b>	excitatory aminoacid transporter (1/2)
<b>EAE</b>	experimental autoimmune encephalomyelitis
<b>EBV</b>	epstein-barr virus
<b>ECM</b>	extracellular matrix
<b>ECMC</b>	extracellular matrix components
<b>E-I</b>	excitatory-inhibitory
<b>EPSP</b>	excitatory post-synaptic potential
<b>ERK</b>	extracellular signal related kinase
<b>FA/FAI</b>	flavoprotein autofluorescence (imaging)
<b>FL</b>	forelimb
<b>fMRI</b>	functional magnetic resonance imaging
<b>FosB</b>	(B) FOS proto-oncogene / FBJ murine osteosarcoma viral oncogene homolog
<b>FoxP3</b>	forkhead box P3
<b>FTY720</b>	fingolimod
<b>GA</b>	glatiramer acetate
<b>GA</b>	glutaraldehyde
<b>GABA</b>	gamma-amino butyric acid

<b>GABA-A/B(R)</b>	gamma-amino butyric acid A / B receptor
<b>GABA-T</b>	GABA-transaminase
<b>GDNF</b>	glial cell-line derived neurotrophic factor
<b>GFAP</b>	glial-fibrillary acidic protein
<b>GluR1</b>	glutamate receptor subunit 1
<b>GM</b>	grey matter
<b>GM-CSF</b>	granulocyte monocyte colony stimulating factor
<b>GPCR</b>	G-protein coupled receptor
<b>GWAS</b>	genome-wide association study
<b>HIV</b>	human immunodeficiency virus
<b>HL</b>	hindlimb
<b>HLA</b>	human leukocyte antigen
<b>I.P.</b>	intraperitoneal
<b>IASP</b>	International Association for the Study of Pain
<b>IB4</b>	isolectin B4
<b>Iba-1</b>	ionized calcium adapter binding-protein 1
<b>IBS</b>	irritable bowel syndrome
<b>IC</b>	insular cortex
<b>IDA</b>	idazoxan
<b>IFN</b>	interferon
<b>IL(-#) R</b>	interleukin(-#) receptor
<b>IL</b>	interleukin
<b>INF<math>\gamma</math></b>	interferon gamma
<b>iNOS</b>	inducible nitric oxide synthase
<b>IPSP</b>	inhibitory post-synaptic potential
<b>ISF</b>	interstitial fluid
<b>JunB/D</b>	JunB/D proto-oncogene
<b>KCC2</b>	potassium chloride cotransporter 2
<b>KROX24</b>	EGR1-early growth response protein 1 / Zif268 - zinc finger protein 1
<b>LC</b>	locus coeruleus
<b>LTD</b>	long-term depression
<b>LTP</b>	long-term potentiation
<b>M1</b>	primary motor cortex
<b>MAO</b>	monoamine oxidase
<b>MAOI</b>	monoamine oxidase inhibitor
<b>MAPK</b>	mitogen activated protein kinase
<b>MBP</b>	myelin basic protein
<b>MCP-1</b>	monocyte chemoattractant protein 1

<b>MEK</b>	mitogen activated protein kinase kinase
<b>memTNF<math>\alpha</math></b>	membrane-bound tumor necrosis factor alpha
<b>Mg</b>	magnesium
<b>mGluR</b>	metabotropic glutamate receptor
<b>MHC</b>	major histocompatibility complex
<b>MMP</b>	matrix metalloproteinase
<b>MOG</b>	myelin oligodendrocyte glycoprotein
<b>MRI</b>	magnetic resonance imaging
<b>MS</b>	multiple sclerosis
<b>N2-Ac-PLZ</b>	N2-acetyl-phenelzine
<b>NA</b>	noradrenaline
<b>Na</b>	sodium
<b>NA(WM/GM)</b>	normal-appearing (white matter/grey matter)
<b>NAA</b>	N-acetyl aspartate
<b>Nav(1.3)</b>	type 3 voltage gated sodium channel
<b>NGF</b>	nerve growth factor
<b>NK1(R)</b>	neurokinin 1 (receptor)
<b>NMDA(R)</b>	N-methyl-D-aspartate (receptor)
<b>NO</b>	nitric oxide
<b>NRLP3</b>	NACHT, LRR and PYD domains-containing protein 3
<b>NSAID</b>	non-steroidal anti-inflammatory drug
<b>NT</b>	neurotransmitters
<b>P2X(4)</b>	(ionotropic) purinoreceptor 4
<b>p38-MAPK</b>	p38 mitogen activated protein kinase
<b>PAG</b>	peri-aqueductal grey
<b>PAN</b>	peripheral afferent neuron
<b>PB</b>	phosphate buffer
<b>PBS</b>	phosphate buffered saline
<b>PEH</b>	phenylethylidenehydrazine
<b>PET</b>	positron emission tomography
<b>PFA</b>	paraformaldehyde
<b>PFC</b>	prefrontal cortex
<b>PKA</b>	protein kinase A
<b>PKC</b>	protein kinase C
<b>PLP</b>	phospholipoprotein
<b>PLZ</b>	phenelzine
<b>PML</b>	progressive multifocal leukoencephalopathy
<b>PNI</b>	peripheral nerve injury
<b>PNN</b>	peri-neuronal net

<b>PNS</b>	peripheral nervous system
<b>POm</b>	medial posterior
<b>PPMS</b>	primary progressive multiple sclerosis
<b>PSL</b>	partial sciatic nerve ligation
<b>PTX</b>	pertussis toxin
<b>PV</b>	parvalbumin
<b>RmANOVA</b>	repeated measures analysis of variance
<b>RNS</b>	reactive nitrogen species
<b>ROI</b>	region of interest
<b>ROS</b>	reactive oxygen species
<b>RRMS</b>	relapsing remitting multiple sclerosis
<b>RT</b>	room temperature
<b>RVM</b>	rostroventral medulla
<b>S.C.</b>	subcutaneous
<b>S1</b>	primary somatosensory cortex
<b>S2</b>	secondary somatosensory cortex
<b>SAS</b>	subarachnoid space
<b>SC</b>	spinal cord
<b>SCDH</b>	dorsal horn of the spinal cord
<b>SCI</b>	spinal cord injury
<b>SCN9a</b>	sodium voltage gated channel alpha subunit 9
<b>SNK</b>	Student-Newmann-Keuls
<b>SNRI</b>	serotonin norepinephrine reuptake inhibitor
<b>SPMS</b>	secondary progressive multiple sclerosis
<b>SSRI</b>	selective serotonin reuptake inhibitor
<b>sTNF<math>\alpha</math></b>	soluble tumor necrosis factor alpha
<b>TAAR</b>	trace amino acid receptor
<b>TC</b>	thalamocortical
<b>TCA</b>	tricyclic antidepressant
<b>TCR</b>	T-cell receptor
<b>TGF<math>\beta</math></b>	transforming growth factor beta
<b>Th</b>	T-helper cell
<b>TLR</b>	toll-like receptor
<b>TMEV</b>	Theiler's murine encephalomyelitis virus
<b>TNF<math>\alpha</math></b>	tumor necrosis factor alpha
<b>TNFR1/2</b>	tumor necrosis factor alpha receptor (1/2)
<b>Treg</b>	regulatory T cell
<b>Trk(B)</b>	tropomyosin receptor kinase (B)
<b>TRP</b>	transient receptor potential cation channel (vanilloid 1/ankyrin 1/M member 8)

**(V1/A1/M8)**

<b>TSP-1</b>	thrombospondin 1
<b>V1</b>	primary visual cortex
<b>VEH</b>	vehicle
<b>VF/VFH</b>	Von Frey (hairs)
<b>VGCC</b>	voltage-gated calcium channel
<b>VGLUT</b>	vesicular glutamate transporter
<b>VMPo</b>	ventromedial posterior
<b>VPI</b>	ventroposterior inferior
<b>VPL</b>	ventral posterolateral
<b>VPM</b>	ventral posteromedial
<b>WAY</b>	WAY-100,635
<b>WDR</b>	wide dynamic range
<b>WFA</b>	<i>Wisteria floribunda</i> agglutinin
<b>WM</b>	white matter

# Chapter 1

General Introduction

## 1.1 – Pain

The International Association for the Study of Pain (IASP) defines pain as “an unpleasant sensory or emotional experience associated with actual or potential tissue damage, or described in terms of such damage” [1]. This definition captures the phenomenological/experiential component of pain, as well as its multidimensional qualities and its relationship with processes of nociception. Nociception is the sensory process of detecting “noxious” or potentially damaging stimuli, and of distinguishing noxious from innocuous stimuli [1]. Nociception is a critical adaptive function, necessary for the long-term survival of any organism that interacts dynamically with a changing external environment, inasmuch as it enables the organism to respond to noxious and potentially damaging stimuli – generally through reflexes and avoidance [1-4]. Pain is thus only one possible outcome of nociception – that is, the conscious experience which results from underlying nociceptive processes [1]. Pain is multidimensional in that involves both a sensory-discriminative aspect, which allows the (conscious) organism to distinguish the source/origin of the pain; and an emotional/affective/aversive component, which promotes future avoidance behavior in relation to the noxious stimulus [1, 5]. Both acute and persistent pain may serve this adaptive function – in instances of actual tissue damage, pain which persists through the healing process is protective in that it prevents re-injury [4, 6]. Central to this function is the capacity for an organism to adjust the “threshold” at which sensory stimuli are perceived as being painful, as distinguished from innocuous stimuli. “Allodynia” and “hyperalgesia” both refer to conditions of altered sensitivity to painful/nociceptive stimuli. Allodynia is defined by IASP as “pain in response to a non-nociceptive stimulus” – that is, pain in response to a stimulus which is *known* not to elicit activity in primary nociceptors [1]. This definition is somewhat restrictive, in that the only stimulus which categorically fits this definition at present is light brushing of the skin (ie. by a feather) [1]. A broader, less formal/anatomical, definition of allodynia is that it refers to a decreased threshold of detection for pain, such that previously non-painful stimuli are perceived as painful [1]. This more general alternate meaning of allodynia is encompassed in the current IASP definition for hyperalgesia, which is simply

“increased pain sensitivity” – and may refer to either a reduction in pain threshold, or to an increased response to suprathreshold (ie. nociceptive) stimuli [1]. Under this definition, hyperalgesia is a “catch-all” term, which applies when it is not known whether or not a stimulus activates nociceptors [1]. A previous definition of hyperalgesia was that it applied only to the case of increased responsiveness to noxious/nociceptive stimuli. Hyperalgesia may be classed as either primary hyperalgesia – affecting the site of injury, or secondary hyperalgesia – affecting a site remote from the injury [1].

Allodynia/hyperalgesia are also modality specific, with thermal and mechanical allodynia/hyperalgesia being separately assessed and biologically distinct processes [1, 5, 7]. Specific cellular populations, with unique molecular compositions, underlie distinct sensory and nociceptive modalities (*described in greater detail in section-1.3.2*) [3, 5, 6, 8]. Generally, since pain itself is inaccessible to researchers (particularly in studies with animals), allodynia/hyperalgesia are measured in terms of indirect indices of nociception, such as nocifensive/withdrawal behaviors [1]. For human studies, both “objective” behavioral/physiological indices, and subjective self-report may be employed.

### **1.1.1 – Chronic / Pathological Pain**

Both allodynia and hyperalgesia may be part of adaptive pain, and are not necessarily pathological in and of themselves. However, pain may become pathological in cases where it outlives its protective function, and persists in the absence of any noxious stimuli or ongoing tissue damage (ie. becomes *chronic*) [9]. The IASP definition of chronic pain is pain which persists for longer than 3-6 months, OR pain that outlasts the time of healing [10]. The estimated global health burden of chronic pain is immense, with some analyses suggesting that as much as 25-30% of the general adult population is affected in certain regions (ie. the United States) [11]. Chronic pain may be thought of as being a “disease of pain” in and of itself, which can arise from diverse etiologies [1, 12]. Chronic pain may also exist as a consequence of, or in the context of, other diseases, such as MS, diabetes, or HIV/AIDS [9, 13-15]. Hyperalgesia and allodynia are common components of chronic pain, and particularly of chronic neuropathic pain (CNP) – which results from damage to and/or dysfunction of the sensory nervous

system [9, 13]. CNP may also involve spontaneous or ongoing pain, as well as painful dysaesthesia (ie. burning/tingling sensations) [13]. Some other major etiological or clinical categories of chronic pain include musculoskeletal pain, joint pain, lower-back pain, chronic headache / migraine, chronic facial pain, fibromyalgia / widespread pain, and complex regional pain syndrome (CRPS) [16, 17].

### **1.1.2 – Functional Neuroanatomy / Neurobiology of Pain**

Given its experiential or phenomenological nature, pain is intrinsically a function of the brain. The various ‘dimensions’ of the experience of pain – its sensory-discriminative aspect, its emotional features, its affective and attention-orienting qualities – are processed in the functionally discrete brain regions to which they correspond [5, 18]. Nociception, however, involves both the peripheral and central nervous systems. Noxious stimuli must first be detected by sensory elements in the peripheral nervous system (PNS). These peripheral sensory elements transduce noxious and non-noxious external stimuli to biologically (chemically/electrically) encoded information, and then transmit that information to the CNS – initially to the spinal cord and the spinal dorsal horn, and then to the brain [3, 5, 8]. “Plastic” or pathological changes may occur at each level of this ascending somatosensory/nociceptive system, resulting in altered nociceptive sensitivity and pain responses – and in some cases generating chronic pathological pain states [6, 7].

#### **1.1.2.1 – Primary Afferent Neurons**

The processes of nociception, and non-nociceptive somatosensation, are initially mediated by specialized neurons of the peripheral somatosensory system – known as primary afferent neurons (PANs) [3, 5]. These neurons innervate peripheral tissues and organs, and are specialized to detect and transduce various mechanical, thermal, chemical, and proprioceptive stimuli [3]. The cell-bodies of PANs are located in the dorsal root ganglia (DRGs), or in the trigeminal ganglia [3, 5]. Detection of peripheral stimuli is accomplished through specialized sensory organs located at the distal terminals of PANs, such as muscle spindles and hair follicles; and by specialized receptor molecules within the

terminal cell-membrane known as transient-receptor potential (TRP) channels [3]. PANs can be categorized based on their functional, anatomical, and molecular characteristics. PANs which are specifically responsive to nociceptive stimuli are known as nociceptors, and may be either 'C fibres' or 'A $\delta$  fibres'. C fibres are primarily high-threshold nociceptive afferents; and are thin, unmyelinated, and therefore slow-conducting [3, 5]. The peripheral terminals of C fibres are unspecialized, and are known as 'free' nerve endings. Endings of cutaneous C fibres are generally found deeper in the dermal tissue compared to non-nociceptive mechanosensory fibres [3, 5]. C fibres also innervate visceral organs and deep muscle tissues, where they detect visceral and muscle pain [3, 5]. C fibres are further subdivided into peptidergic and non-peptidergic classes, based on whether or not they express the peptide neurotransmitters substance P, galanin, and calcitonin gene-related peptide (CGRP) [3]. Non-peptidergic C fibres may be labelled by the lectin IB4, or by staining for the glial-derived neurotrophic factor (GDNF) receptor [3]. Centrally, C fibres project into the superficial dorsal horn (lamina I-III, but primarily lamina II), although some branches may extend into the deeper laminae as well [3, 8]. A $\delta$  fibres are medium-diameter, lightly myelinated fibres, with intermediate conduction velocity. A $\delta$  fibres may be either nociceptive or non-nociceptive, detecting low-threshold touch/mechanosensation [3, 8]. Some non-nociceptive A $\delta$  fibres innervate hair follicles (D-hair afferents) [8]. A $\delta$  fibres project centrally to dorsal horn lamina I and the outside of lamina II, and also to lamina V [8, 19] (**FIG. 1.1**). C fibres and A $\delta$  fibres may also be distinguished functionally in terms of their responsive modality – with some afferents being primarily thermoceptive, and others specifically mechanosensitive [3, 8]. The majority of nociceptive PANs are, however, polymodal [5]. Thermoceptive afferents may express specific TRP channels, such as TRPV1 and 2, which open and conduct ions in response to specific (high) temperatures – or TRPM8/TRPA1, which detect “cold” [3]. Mechanosensation is thought to be underlied by stretch receptors or stretch-sensitive ion channels, which open and conduct upon deformation of the cell membrane [3]. Nociceptive PANs are thought to encode the intensity of peripheral stimuli through the frequency of their action potentials, and through cellular specificity [3, 5].

The third major class of PANs are the large-diameter, thickly myelinated (fast conducting) A $\alpha$ / $\beta$  fibres. Large diameter PANs are primarily non-nociceptive, although a subpopulation (<~20%) of high-threshold nociceptive A $\beta$  fibres also exists [3, 5]. A $\beta$  fibres may innervate specialized sensory organs in the distal tissues such as proprioceptive Golgi-tendon organs and muscle spindles, or cutaneous structures such as Pacinian corpuscles, Ruffini's corpuscles, Meissner corpuscles and Merkel's disks [3]. These structures determine the A $\beta$  fibre's rate of adaptation to stimuli, as well as its sensitivity and receptive-field size [3, 8]. Centrally, A $\beta$  fibres directly ascend in the ipsilateral dorsal-column(/medial-lemniscus) pathway, but also send projections into the deeper laminae (II – IV) of the dorsal horn [8, 19]. **(FIG. 1.1)**

At their central terminals, all PANs release the excitatory neurotransmitter glutamate. Peptidergic C fibres may also release the peptide neurotransmitters (substance P, CGRP, galanin), at both their central and peripheral endings [20]. In the distal/peripheral tissues, these peptide transmitters act as inflammatory and excitatory/depolarizing signals, which tend to sensitize neighboring afferents [3]. These neuropeptides also promote neurogenic inflammation - affecting vascular leakage and plasma extravasation, vasodilation, and promoting cellular infiltration (eg. macrophages, neutrophils etc.) into the affected tissues [3]. Other pro-inflammatory/pro-excitatory signals which may sensitize PANs at their peripheral terminals include 5-HT (serotonin/5-hydroxytryptamine), bradykinin, NGF, protons, ATP, histamine, and prostaglandins [3, 21]. Many of these pro-inflammatory/excitatory signals may also be released from non-neuronal cells, such as mast cells, neutrophils, platelets, and fibroblasts - as components of the so-called "inflammatory soup" [3, 7].

In general, the process of sensitizing or altering the responsiveness of PANs is known as "peripheral sensitization" [22]. The intrinsic excitability and receptivity or sensitivity of PANs are dependent on the various ion-channels and receptors expressed in their cell-membranes [2, 3]. Inflammation, injury, and disease processes may trigger altered surface expression of these channels and receptors. These changes can in turn lead to peripheral sensitization, ectopic discharges, and even to "phenotypic

switching” - wherein previously non-nociceptive PANs start to behave functionally as nociceptors [1, 5, 19]. Previously “silent” (latent) nociceptive PANs may also become active after injury [5]. Peripheral sensitization, phenotypic switching, and silent nociceptor activation, may all contribute to hyperalgesia and allodynia in certain conditions (ie. after nerve injury) [1]. However, allodynia is more commonly thought of as being dependent on changes within the central nervous system (CNS) - which in some conditions may be initiated and/or maintained by activity and plasticity in the periphery, as is the case in nerve injury [1, 2, 6, 23].

#### **1.1.2.2 – Dorsal Horn of the Spinal Cord**

Upon entering the spinal cord, the central projections of PANs either branch and ascend rostrally within the dorsal column pathway (in the case of myelinated A $\beta$  fibres), or terminate in the dorsal horn, where they synapse onto second-order neurons [19]. Nociceptive fibre types (C and A $\delta$ ) project abundantly into the superficial laminae of the dorsal horn (lamina I and II), while non-nociceptive fibres (A $\beta$  fibres) project primarily into the deeper laminae (III to VI) [8, 19]. Second-order neurons may be either interneurons, of which there are both excitatory and inhibitory types within the dorsal horn, or projection neurons, with axons that ascend in spinal white matter tracts to innervate various targets in the brain and brainstem [8]. Excitatory interneurons within the dorsal horn also form polysynaptic connections and pathways between PANs and projection neurons [8, 19]. The specificity of neuronal connectivity within the dorsal horn - including its somatotopic anatomical organization - ensures the fidelity of information transfer regarding the body-centric location, type, intensity, and duration of peripheral sensory stimuli [8, 19]. Specific projection neurons may act as “labelled lines” for the transmission of nociceptive signals via the spinothalamic/spinoparabrachial tracts [5, 8, 19, 24]. In particular, projection neurons within lamina I of the dorsal horn which express the neurokinin-1 receptor (NK1R+), are thought to relay nociceptive signals – although they are not solely responsible for this function [8]. **(FIG. 1.1)**

The dorsal horn of the spinal cord is critical to the process of nociception - not only as a node which relays inputs from peripheral nociceptors and somatosensory fibres to the brain, but also as the first locus of synaptic integration and processing for nociceptive sensory information [6, 8]. Melzack and Wall first formulated the gate-control theory of pain in 1965 [25], which postulates that mechanisms in the dorsal horn control the dynamic threshold which distinguishes painful from non-painful inputs by “gating” the connection between the periphery and higher-order pain-perception centers (in the brain) [8]. Beyond the binary/digital logic of this model and the painful/non-painful distinction, this gating process may also be thought of as setting the analog “gain” on the intensity of sensory signals – and may involve either pro-algesic or analgesic modulations [6]. Neuronal plasticity within the dorsal horn, which may be strictly functional in nature, or may involve the structural modification of synapses and connections [26], is necessary for the mutability of the threshold for pain perception, and of pain-intensity – particularly across modalities and peripheral receptive fields (ie. for allodynia and secondary hyperalgesia). This cannot be accomplished through altered PAN activity/peripheral sensitization alone [6, 27]. Sensory integration within the dorsal horn is also necessary for the influence of top-down facilitation and inhibition of nociceptive transmission by descending inputs from brain regions which control higher-order functions such as attention, intention, and sympathetic arousal [6, 28]. Another role of the dorsal horn is to provide the anatomical substrate for the integration of sensory inputs with fast motor responses (ie. reflexes) [6].

The role of dorsal horn plasticity in hyperalgesia, allodynia, and chronic pain states is well established, both clinically and in experimental models [1, 9, 29]. The general term for plasticity which enhances the responsiveness, excitability, and/or output of the somatosensory/nociceptive CNS (esp. in the dorsal horn) is central sensitization [29]. A multitude of conditions, mechanisms, and stimuli may lead to the sensitization of dorsal horn neurons and networks [1, 29, 30]. Central sensitization may initially be the result of excitatory input from the periphery. Intense, ongoing, sustained, and/or repetitive drive from the PNS, as occurs in most types of acute injury or insult which result in pain hypersensitivity (ie.

peripheral nerve injury, cuts, burns, and chemical insults such as formalin, capsaicin and caragheen) can produce central sensitization [1, 9, 31]. Many of these forms of insult or injury also involve an inflammatory component that contributes to the resulting sensitization [1, 32]. Chemical inflammatory mediators/signals may access CNS tissues and influence the excitability of dorsal horn neurons, either through their local / central release (ie. from PAN terminals or microglia), or through the systemic circulatory system [8, 33]. Many disease states also involve the systemic circulation, or local release (ie. from immune cells and glia) of inflammatory mediators and cytokines – as is the case in pain related to infection and illness, and in diseases such as MS [16, 33, 34]. Another important general ‘central’ mechanism underlying enhanced nociceptive sensitivity, allodynia, and hyperalgesia - particularly in disease states – is disinhibition or loss of inhibitory tone [1, 6, 21]. Disinhibition can lead to the ‘unmasking’ of previously latent (suppressed/subthreshold) excitatory inputs or synaptic pathways in the dorsal horn [1, 6, 31]. There are many specific ways in which all of these general mechanisms can occur, and pathological pain states frequently involve multiple interacting factors which contribute to the overall sensitization of the CNS. Certain mechanisms are specifically relevant to the initiation of chronic/neuropathic pain, while other mechanisms may primarily contribute to the maintenance/chronicity of pain states [1, 2, 6].

#### **1.1.2.2.1 – Mechanisms of Central Sensitization: Activity-Dependent Changes**

One essential cellular mechanism for both the induction and maintenance of central sensitization and chronic/neuropathic pain, is activity-dependent plasticity at excitatory glutamatergic synapses [1, 2, 22, 29]. Excitatory post-synaptic potentials (EPSPs) can summate, both temporally and spatially, allowing for an amplification of responses to repetitive or combined/simultaneous inputs [1, 6]. On a longer time-scale, there can be changes in the efficacy of synaptic inputs, making them more or less likely to elicit an action-potential in the post synaptic neuron [1, 6]. These changes may involve both the pre-synaptic and post-synaptic cell, and can be either homosynaptic or heterosynaptic (“classical” central sensitization) [6]. At the pre-synaptic terminal, increased transmitter release-probability and quantal

release-content enhance the resulting EPSP [1, 6]. Additionally, the co-release of peptide neurotransmitters from pre-synaptic terminals (esp. of PANs, ie. substance P, CGRP, BDNF etc.) can act to depolarize and enhance the excitability of the post-synaptic cell through GPCR/Trk receptor-mediated effects [1, 6, 8]. Apart from ionotropic AMPA receptors (AMPA), glutamate can also act through group I metabotropic receptors (mGluRs) to evoke long-lasting “plateau potentials” in post-synaptic DH neurons [1]. Induction of pre-synaptic LTP at C fibre synapses has been demonstrated, and requires the co-activation of post-synaptic neurokinin 1 and 2 receptors, activation of group 1, but not group 2/3 mGluRs (which are inhibitory in the DH), and NMDA-channel opening / calcium entry into the post-synaptic cell [1, 6]. A number of retrograde signals may be involved in signaling from the post-synaptic cell to the pre-synaptic cell (or may act at pre-synaptic autoreceptors) to alter synaptic efficacy, including NO, ATP, glutamate (at autoreceptors) and endocannabinoids [3, 8]. Within the post-synaptic cell, NMDA receptor (NMDAR)-dependent, long-term potentiation (LTP)-like, mechanisms are necessary for the initiation of neuropathic pain states [2, 7]. Generally, this involves the entry of calcium into the post-synaptic cell, following removal of the  $Mg^{2+}$ -blockade of the NMDAR’s ion-channel due to partial depolarization [6]. At some synapses in the DH, calcium may also enter through voltage-gated calcium channels (VGCCs) or calcium-permeable AMPA receptors [6, 35]. Calcium then acts as an intracellular signal to initiate activity in downstream enzymes and kinases (such as AC, PKC, and CaMK2), most of which may generate additional second-messenger molecules (such as cAMP) and set off further signaling cascades (ie. PKA, CREB) [2, 6]. These kinases subsequently phosphorylate many targets in the cytoplasm and cell-membrane, including additional downstream kinases (MEK/MAPK/ERK), and AMPA receptor subunits – switching them to a high-conductance state, and enhancing the responsiveness of the post-synaptic cell [2, 6]. The trafficking, sequestering and diffusional-trapping of cell-surface receptors (ie. GluR1+ AMPARs), altered ion-channel expression (eg. Nav1.3), and altered receptor-subunit compositions, can also contribute to synaptic efficacy and intrinsic neuronal excitability [1, 6, 29]. Late-phase changes, which involve altered gene-expression (ie. transcriptional changes) and protein synthesis (ie. translation, either at the synapse or in the cell-body),

produce longer lasting alterations of excitability – and are implicated in the transition to chronicity and the maintenance of chronic pain states [6, 21, 26]. Effector genes upregulated following activity in dorsal horn neurons include the immediate-early genes c-Fos and cyclooxygenase-2 (COX-2), as well as Fos-B, Jun-B/D, KROX-24 - and later prodynorphin, NK1, and TrkB [1, 2, 6, 36].

Another mechanism underlying the persistent potentiation of neuronal connections in the dorsal horn is the formation of new synaptic contacts, which can be one result of activity-dependent changes in gene expression [1, 6, 26]. Peripheral-nerve injury has been demonstrated to elicit sprouting of the axons of A $\beta$  fibres into lamina II of the dorsal horn [1] – although these experiments have been challenged. Once late-phase changes are initiated in the dorsal horn, they may persist in the absence of ongoing drive from the PNS, leading to chronicity, although some changes may revert or resolve after a period of days-weeks-months [6, 21]. Additionally, endogenous analgesic, compensatory, and inhibitory mechanisms may naturally upregulate in order to “mask” or counteract persistent pro-excitatory changes [37]. Experimentally, blocking specific intracellular kinases (ie. MEK, ERK) or protein synthesis can interrupt late-phase changes and components of pain responses (ie. formalin / experimental inflammatory pain) [6]. If previously potentiated dorsal horn pathways are re-activated while simultaneously blocking protein synthesis, those pathways may be rendered labile, and potentiation can be reversed and extinguished [38]. Some synapses in the dorsal horn, including at central PAN terminals, may also undergo LTD-like processes - wherein the firing of the pre-synaptic cell repeatedly fails to elicit sufficient depolarization and AP-firing in the post-synaptic cell, and synapses are rendered less efficacious. The mechanism of this LTD primarily involves the activity of calcium-dependent phosphatases in the post-synaptic neuron [1, 6].

#### **1.1.2.2.2 – Mechanisms of Central Sensitization: Loss of Inhibition**

Another important mechanism of central sensitization, allodynia and hyperalgesia – which is particularly relevant in disease states and pathological pain – is the loss of inhibition [1, 6]. Both tonic and phasic

inhibition are necessary to the normal functioning of the nociceptive/somatosensory circuitry in the dorsal horn [1, 6, 8, 19]. Inhibition in the dorsal horn acts to control the spread of excitation between neighboring somatotopic regions and across modality specific “labelled lines”. It also ensures an appropriate level of responsiveness to peripheral inputs [1, 6, 8]. Locally projecting inhibitory interneurons, which release GABA or glycine, are found throughout the dorsal horn [8, 19]. Within the superficial dorsal horn (lamina I and II), 25-30% of intrinsic neurons are GABAergic, while glycinergic (as well as GABAergic neurons) are enriched in the deeper laminae (lamina III –VI) [8, 19]. These inhibitory interneurons can be innervated by PANs and/or excitatory interneurons, and form axodendritic/axosomatic contacts with other interneurons and projection neurons in the dorsal horn [8, 19]. They also form axoaxonic contacts with the central terminals of PANs, which mediate feed-forward inhibition from neighboring peripheral inputs [8, 19]. Dorsal horn neurons, as well as central PAN terminals, express both GABA-A and GABA-B receptors, mediating fast and slow GABAergic inhibition respectively [8, 19]. The observation that intrathecal administration of the GABA-A channel blockers/antagonists bicuculline or strychnine produces A $\beta$ -mediated allodynia demonstrates the importance of dorsal horn inhibition for nociceptive processing [1, 8]. Nociceptive projection neurons in the dorsal horn receive an abundance of inputs from peripheral low-threshold mechanosensitive fibres (ie. A $\beta$  fibres), which are ordinarily suppressed (or are ‘subthreshold’) under feed-forward inhibition – as postulated in the classic gate control theory of pain [1, 8, 24]. Synaptic plasticity which results in decreased excitatory input or efficacy onto inhibitory interneurons, or a loss of inhibitory connections, interneurons, or inhibitory synaptic strength can all similarly contribute to central sensitization [1]. NMDA-dependent LTD has been observed experimentally at excitatory synapses between PAN terminals and inhibitory interneurons [1]. Neuropathic pain models, such as peripheral nerve injury, can involve a substantial reduction in the inhibitory post-synaptic currents (IPSCs) elicited by GABAergic interneurons in the dorsal horn; and have also been demonstrated to unmask latent subthreshold connections between A $\beta$  fibres and lamina II dorsal horn neurons [1]. Additionally, GABA+ immunoreactivity and GABA content in the dorsal horn decline in neuropathic pain models [1, 39]. Part

of this decline is thought to involve reduced transmitter synthesis, but it is also thought to potentially involve the selective death of GABAergic interneurons (likely due to excitotoxicity) – suggesting a neurodegenerative component to neuropathic pain [1, 6]. Another mechanism of disinhibition which has been observed experimentally in the dorsal horn - and which may be specific to males - involves the conversion of GABA-AR mediated IPSCs into EPSCs, due to altered  $\text{Cl}^-$  reversal potential [1, 6, 40].

#### 1.1.2.2.3 – Descending Inhibition / Monoamines

Axons projecting caudally from the brain/brainstem to the dorsal horn mediate descending or “top-down” inhibition of nociception [28]. Some of these axons may contain and/or release GABA and glycine [6, 28]. Many more of them release the monoamine neurotransmitters 5-HT, NA, and dopamine (DA) [28]. Descending serotonergic neurons originate in the medial Raphe nucleus and their axons project throughout the dorsal horn - most abundantly to the superficial laminae (particularly lamina I and II) [1, 28]. Descending noradrenergic neurons originate in the *locus coeruleus* and the neighboring pons, and also project throughout the dorsal horn, with abundant terminations in the *substantia gelatinosa* (lamina II) [28, 41]. Evidence suggests that 5-HT and NA act both synaptically, and extrasynaptically through volume transmission [8, 28, 41]. Receptors for monoamines are present on dorsal horn projection neurons, local interneurons (both excitatory and inhibitory), and PAN central terminals [28, 42-45]. Wide-dynamic range (WDR) neurons, which are found in the deeper dorsal horn laminae (III-VI) and are innervated by both nociceptive and non-nociceptive PANs [5], are another important target of descending input [28]. Specific transmitter/receptor actions in the dorsal horn may either facilitate or inhibit nociceptive signal outflow, or in some cases do both. 5-HT may exert either facilitatory or inhibitory effects depending on the receptor which is bound, and the post-synaptic neuron acted upon: ionotropic 5-HT<sub>3</sub> receptors are excitatory and are primarily implicated in descending facilitation of nociception, while the metabotropic/GPCRs 5-HT<sub>1</sub>(A/B/D/F) (as well as 5-HT<sub>2,4,5,6</sub> and 7) receptors are frequently (but not exclusively) inhibitory [28]. Spinal 5HT<sub>1A</sub> - which generally produces cellular inhibition, and 5HT<sub>2A-C</sub> - which generally produce cellular excitation - have been

implicated in both facilitation and inhibition of nociception [28, 43, 44, 46-48]. This duality is likely reflective of the expression of these receptors on excitatory projection, interneuron, and PAN populations - *and* on inhibitory interneurons in the dorsal horn [28, 49]. NA is primarily inhibitory in the dorsal horn, acting mainly via alpha-2 receptors [28, 41], and generally promotes analgesia. Alpha-2a receptors are found on PAN central terminals, while alpha-2c receptors are found on excitatory interneurons which synapse onto NK1R+ projection neurons [28, 41, 42]. Spinal administration of alpha-2 agonists (eg. clonidine) effectively suppresses mechanical allodynia in experimental models of neuropathic pain [28, 41]. NA may also exert facilitatory effects, mediated by activation of alpha-1 receptors in the dorsal horn – although contradictory evidence suggesting an inhibitory effect of alpha-1 receptors exists as well [28, 41].

Descending modulatory systems have a role in stimulation-induced analgesia, forming direct and indirect “loops” between the dorsal horn and brainstem/higher-order CNS regions [28]. Glutamatergic and serotonergic neurons within the periaqueductal gray (PAG) - which is innervated by the ascending spinomesencephalic tract - form excitatory connections with serotonergic neurons in the Raphe [28]. Many of the excitatory links between the PAG and rostroventral medulla (RVM) are tonically suppressed by local inhibitory interneurons, and may be “unmasked” by drugs which inhibit those interneurons (ie. opioids, cannabinoids) [28]. Some GABAergic and enkephalinergic inhibitory projections extend from the PAG to the RVM and LC/subcoeruleus – and principally act to disinhibit descending inhibitory fibres in the target regions [28], facilitating analgesia. Apart from its direct afferent spinal inputs, the PAG is also innervated by a multitude of other connected brain regions (ie. the cortex, thalamus, hypothalamus, and amygdala), which form longer feedback “loops” [28]. These connections are involved in analgesia and facilitation related to complex environmental stimuli, cognition, and emotions such as fear, anxiety, and stress [28]. Some descending neurons are opioidergic, releasing dynorphin/enkephalin or  $\beta$ -endorphin into the dorsal horn [28]. Opioid receptors ( $\mu$ ,  $\delta$ , and  $\kappa$ ) are located on PAN central terminals and intrinsic dorsal horn neurons, and their activation generally

produces analgesia [28]. Descending cholinergic neurons are also implicated in facilitation and inhibition of nociception, and autonomic fibres may act both directly and indirectly to influence the activity of PANs [28]. Additionally, descending inputs expressing glutamate and/or peptide neurotransmitters such as substance P, galanin, and CGRP, are implicated in descending facilitation [28].

In pathological conditions, descending modulatory systems may be altered, engaged, or disrupted, leading to a loss of descending inhibitory control and/or converting inhibition to facilitation [1, 9, 21, 28]. Systemic illness and inflammation are thought to engage descending facilitation as part of 'sickness syndrome' [1]. Within the dorsal horn, receptors may up- or downregulate in pathological conditions, altering the post-synaptic response to modulatory monoamines and neuropeptides [28]. Depletion of monoamines in the dorsal horn - due to reduced synthesis, exhaustion of transmitter pools, and/or axonal degeneration and loss – may also contribute to pathological pain states [21, 28]. The clinical use of tricyclic anti-depressants (TCAs) and serotonin-norepinephrine reuptake inhibitors (SNRIs) for treating chronic pain conditions likely reflects the fact that they recapitulate or mimic the influence of descending inhibition by elevating extracellular monoamine concentrations in the dorsal horn (and possibly in supraspinal regions) [28]. Alternatively, ongoing noxious stimuli and injury may act to engage descending or local inhibition as a compensatory mechanism [28].

#### **1.1.2.2.4 – Glial and Immune/Inflammatory Mechanisms**

In addition to strictly neuronal mechanisms, a prominent role for glial cell populations in the induction and maintenance of chronic neuropathic and inflammatory pain states has now been firmly established [1, 6]. Within the dorsal horn, a role has been identified for both astrocytes and microglia in various models of persistent/chronic pain [1]. Both astrocytes and microglia may become "activated" following injury, inflammation, and in disease conditions. Activated glia respond by altering their morphology and the expression and release of various signaling molecules, enzymes, cell-surface markers, and

receptors [1]. Activated astrocytes are thought to contribute to the maintenance of chronic/neuropathic pain [1]. One important mechanism involving astrocytes involves their role in the reuptake, clearance, and metabolism of glutamate at excitatory synapses [1, 50]. Reduced glutamate reuptake by astrocytes leads to elevated synaptic and extracellular/extrasynaptic glutamate concentrations, and enhances excitatory neurotransmission and excitotoxicity [1]. The role of microglia is more multifaceted, reflecting their diverse functionality [51]. Microglia respond to a variety of chemical stimuli, including glutamate, ATP, cytokines, chemokines, substance P, NO, prostaglandins, and endocannabinoids [1, 6]. Microglia may, in turn, release a wide variety of signaling molecules and enzymes, including: ROS, BDNF/NGF, IL-1 $\beta$  and TNF $\alpha$ , and proteolytic MMPs [1, 6]. Microglial activation tends to precede astrocyte activation in the dorsal horn in experimental models, and it is thought that microglia are relevant to both the induction and maintenance of neuropathic and inflammatory pain [1, 6]. Experimentally, blocking the fractalkine receptor (CX3CR1), the microglial P2X4 (ATP) receptor, Toll-like receptors (TLR-4), p38-MAPK, and the complement receptor type I - or inhibiting microglial activation and proliferation using minocycline - are all manipulations which have been found to reduce or reverse the expression of allodynia and/or hyperalgesia following peripheral nerve injury and/or injection of formalin or capsaicin [1, 6]. Microglia have also been implicated in the acquisition of tolerance to the analgesic effects of morphine, and in morphine-induced hyperalgesia [52]. Some of these microglial mechanisms may be sex-specific and primarily relevant in males [53, 54]. In females, T-cells have instead been implicated [53, 55]. In both sexes, immunocompetent cells other than microglia may contribute to central sensitization and pain in inflammatory conditions, through the systemic circulation of cytokines, or through CNS infiltration and/or actions in peripheral tissues [51, 56].

### **1.1.2.3 – Supraspinal Sites**

Pain perception involves neuronal activity within multiple interconnected supraspinal/brain regions, each processing a specific “dimension” of the overall experience of pain [18, 21]. This concept of the brain as being comprised of regionally segregated and functional discrete “modules” may be something

of an over-simplification; however, it is not entirely without merit. Human neuroimaging studies have identified a group of brain regions which are consistently activated or engaged during acute/evoked pain, and/or are functionally and/or anatomically altered in chronic pain patients [18, 57]. This group of brain regions, along with the spinal nociceptive circuitry, is sometimes referred to as the “pain (neuro)matrix” [57, 58]. In chronic pain, this pain matrix is abnormally (usually excessively) active or interconnected – and the composite regions undergo both functional plasticity and structural changes (ie. reflective of neuroanatomical plasticity, and/or neurodegenerative/excitotoxic processes) [18, 57, 59]. The extent to which supraspinal plasticity contributes in a causal manner to chronic pain is still being elucidated – some forms of plasticity and activity in certain brain regions may be purely epiphenomenal, or related to secondary (ie. cognitive/depressive) sequelae of chronic pain, contributing little to the actual manifestation and experience of chronic pain [18, 60]. However, activity and plasticity in some regions irrefutably appears to be causally related to both normal and altered pain perception [18, 23]. **(FIG. 1.1)**

#### **1.1.2.3.1 – Midbrain/Brainstem**

As discussed above, an abundance of midbrain / brainstem nuclei participate in descending “loops” with the dorsal horn / spinal nociceptive circuitry. These regions directly and/or indirectly receive inputs from the ascending (spinal) nociceptive circuitry, and send descending axonal projections back to the dorsal horn which modulate or gate its output (ie. descending inhibition and facilitation) [28]. These nuclei also receive inputs from other supraspinal regions of the pain “matrix”. Besides the brainstem monoaminergic nuclei (eg. RVM/Raphe, LC etc.) and the PAG, the nucleus tractus solitarius, parabrachial nucleus, and dorsal reticular nucleus also participate in descending modulation of nociception [28].

#### **1.1.2.3.2 – Thalamus**

The thalamus receives ascending inputs from the spinothalamic and dorsal column pathways (and other minor ascending pathways), and projects to most of the other supraspinal and cortical elements of the pain “matrix” and the (non-nociceptive) somatosensory CNS [5, 7, 18]. The thalamus thus forms the main central functional and anatomical sensory “relay hub”, connecting the various brain regions that comprise the pain neuromatrix, and the lower nociceptive circuitry [18]. Although projection areas vary by species, the spinothalamic pathway projects primarily to the medial posterior (POm), ventral posterolateral (VPL), ventral posteromedial (VPM), ventral posteroinferior (VPI), and posterolateral (VMPO) nuclei of the thalamus; while the dorsal column pathway projects to the POm, VPM and VPL [5, 7, 61]. The thalamus generally preserves the somatotopic arrangement of inputs, and activation within the thalamus is also correlated with the intensity of noxious stimulation [18, 61]. Thalamic projections to the primary and secondary somatosensory cortices (S1/S2) are a critical component of the sensory-discriminative dimension of pain and non-nociceptive somatosensation [5, 18, 61]. The thalamus also innervates the anterior cingulate cortex (ACC) and insular cortex (IC) - regions which are crucial to the affective, motivational, and emotional dimensions of pain perception [18]. Like the dorsal horn, the thalamus is not merely a passive “relay node”, but is actively involved in the gating and modulation of sensory and nociceptive signals [7, 62]. Pain perception may therefore be modulated by purely supraspinal (ie. thalamic/cortical) circuits, in addition to descending modulation of dorsal horn function [7, 18, 28]. Attention and arousal (ie. noradrenergic, glutamatergic/GABAergic, cholinergic, and histaminergic innervation) modulate activity in the thalamus, and thereby modulate sensory gating [18]. Endogenous opioid (analgesic) systems also influence activity within the thalamus [28, 62].

Thalamocortical neurons generally project to excitatory neurons within layer 4 of the neocortex – but also innervate cortical inhibitory interneuron populations which mediate ‘fast-spiking’ feed-forward (phasic) inhibition (ie. parvalbumin+, and other, GABAergic interneurons) [63-66]. A variety of studies of clinical (ie. complex regional pain syndrome/CRPS, central/neuropathic) pain patients have identified reduced ongoing thalamic blood flow and activity as a feature [18]. A consequence of this reduced ongoing thalamic output could be disinhibition of downstream targets, which may contribute to the

disconnection between ongoing pain and the (potentially resolved) underlying injury [18]. Proton magnetic resonance spectroscopy (1H-MRS) studies have also identified chemical abnormalities, such as increased NAA (initially, followed by a reduction) and glutamate, within the thalamus in chronic pain related to spinal cord injury [18, 67].

#### **1.1.2.3.3 – Primary and Secondary Somatosensory Cortices (S1/S2)**

As previously mentioned, the primary and secondary somatosensory cortices (S1/S2) are the key CNS regions underlying the sensory-discriminative dimension of pain and non-nociceptive somatosensation [18]. The somatotopic arrangement of S1 (ie. the “homunculus”) reflects this functional role. Individual neurons within S1/S2 have been identified which encode the body-centric spatial origin, duration, and intensity of noxious and non-noxious somatosensory stimuli [18, 68]. Some neurons within S1/S2 are activated only by either noxious or non-noxious stimuli, or are modality specific (ie. respond only to thermal or mechanical stimuli) – although in general, S1 is preferentially activated by mechanical stimuli [18]. The intensity of (sub)regional activation within S1/S2 (eg. S1 hindlimb cortex – S1HL) following a peripheral stimulus generally correlates with both the objective stimulus intensity, and with the “perceived” or “subjective” stimulus intensity – with noxious stimuli generally eliciting greater activation than non-noxious stimuli [18]. Non-nociceptive stimuli also generally elicit less S2 activity, preferentially activating S1 [18]. S1 activity has been suggested to underlie “first pain” (ie. fast / A $\delta$ -mediated pain) – whereas “second” pain (ie. slow / C fibre-mediated pain) has been associated with activity in S2 (and ACC/IC) [18]. It has also been suggested that painful stimuli activate S2 directly, whereas non-painful stimuli activate S2 indirectly via S1 [18], although this has been disputed [69].

S1 and S2 receive direct thalamic inputs (mainly to cortical layer 4, but also to layer 1 apical dendrites, and layers 5 and 6), as well as forming reciprocal intracortical connections with each other (ie. S1 to S2/S2 to S1) [18, 63, 70]. S1/S2 also form longer-range connections with the contralateral somatosensory cortex, and with other cortical areas such as the ACC, IC and the primary motor cortex

(M1) [18{Feldmeyer, 2012 #2667, 63, 70-73}. As such, activity within S1/S2 can modulate (or evoke/suppress) activity within these other cortical areas. Within S1 (or S2), there are abundant intracortical connections between neighboring cortical columns (ie. transcolumar connections) and somatotopic regions – primarily located within cortical layers 2/3 [63, 74, 75]. Layer 5 is the primary output layer of the somatosensory cortex, forming long distance projections [63]. Neurons in layer 6 also form corticothalamic “feedback” projections [63, 74]. In the “canonical” feed-forward excitatory circuit/loop through S1: the thalamus projects to stellate/star-pyramid neurons in layer 4, which subsequently project to pyramidal cells in layers 2/3, layer 2/3 pyramidal neurons project horizontally (to neurons within layer 2/3 in adjacent cortical columns) and to layer 5 pyramidal neurons, layer 5 pyramidal neurons project to long-range/subcortical targets and into layer 6, layer 6 neurons then feedback to the thalamus [74] (**FIG. 1.2**). A multitude of other circuits/loops within S1 are also known to exist (but are beyond the scope of this discussion, see: [63, 70, 74, 76]. Inhibitory (GABAergic) interneurons within S1 are functionally, neurochemically, and anatomically diverse, and are found throughout the various layers [64, 65, 77-81]. These interneurons exert considerable tonic and phasic control over the activity and behavior of the cortical network, and ultimately over cortical plasticity (esp. through spike-timing dependent mechanisms) [77, 79, 82, 83]. Specifically, parvalbumin+ (PV+) “basket” interneurons within the neocortex exert strong phasic (fast-spiking) inhibitory control over excitatory (pyramidal, principle, and stellate) neurons, and are thought to be crucial to regulating plasticity [84-88].

Plasticity within S1 has been extensively studied both in humans and in animals – indeed, S1 (esp. rodent barrel cortex - along with V1, and, to a lesser extent, A1) is perhaps the quintessential region in which to study adult and developmental neocortical plasticity [82, 87, 89-91]. To attempt to summarize the literature in this area would be well beyond the scope of the current discussion. However, it is relevant to observe that S1 is known to exhibit considerable experience-dependent plasticity - both purely functional in nature, and also neuroanatomical/synaptic [82, 92-94]. Enduring changes in the

pattern of functional activation evoked by peripheral (eg. mechanical or electrical) stimulation - and in the synaptic architecture within S1 - have been documented following manipulations such as: stroke, whisker-trimming, tail-cut, limb-restraint, repetitive stimulation, behavioral training, nerve injury/transfer, spinal cord injury, intraplantar capsaicin, peripheral ischemia, and inflammation. The diverse mechanisms of S1 plasticity have also been studied in extensive detail, and cannot easily be summarized here (see: [81, 82, 95]). A wide variety of neurotransmitters (eg. glutamate, GABA, 5-HT, NA, ACh, opioids/neuropeptides), receptors (eg. AMPARs, NMDARs, mGluRs, GABA-A/BRs, etc.), trophic factors (eg. BDNF/NGF), cell-types (ie. neuronal and glial), cellular signals (eg. NO, ATP, endocannabinoids, cytokines) etc. may participate in functional/synaptic changes within S1 (see: [81, 82, 95-97]). Many types of synapses in S1 including thalamocortical / corticocortical glutamatergic synapses, and intracortical GABAergic inhibitory synapses, exhibit: potentiation and/or depression, early LTP/LTD-like plasticity, and/or late LTP/LTD-like plasticity, morphological remodeling, sprouting, and pruning (ie. of axonal terminals / dendritic spines) [81, 82, 95]. There are, in general, extensive “subthreshold” latent connections within S1, which may be “unmasked” either through synaptic potentiation or through disinhibition [98-102]. This mechanism is likely implicated in cortical “remapping” following injury or stroke [98, 103].

Specifically with respect to pain, lesions to S1/S2 result in deficits in the ability to localize and describe painful stimuli, although noxious stimuli still evoke a “vague unpleasant feeling” – indicating that the affective/emotional component of pain is preserved [18]. Manipulations which reduce the perceived intensity of pain (eg. attentional modulation, hypnosis) generally reduce activity within S1/S2 – and the inverse is true as well (eg. attentional enhancement of pain intensity) [18, 104, 105]. Pathological pain states have been found to enhance activity (both evoked and ongoing) and plasticity (functional, and structural/anatomical) within S1 in clinical studies and animal models (eg. PNI, capsaicin) [93, 94, 104-112]. In clinical pain states and animal models of pain, functional somatotopic representations (or cortical ‘maps’ – obtained by imaging or electro-/magneto- physiology/encephalography) within S1 may

not only be potentiated/hyperexcitable, but also expanded in terms of activated cortical area [94, 113]. Biochemically, <sup>1</sup>H-MRS studies have also identified characteristic and related changes, such as decreased NAA and increased glutamate/glutamine in S1 in chronic pain patients (ie. chronic low-back pain) [114]. Animal models of neuropathic pain are often associated with increased synapse formation, dendritic spine turnover and motility, and altered spine maturation in excitatory neurons within S1 [93, 105, 107, 111, 112]. An interaction between astrocyte-secreted thrombospondin-1 - which promotes synaptogenesis through interactions with the extracellular matrix [115] - has also been recently implicated in plasticity within S1 following partial sciatic nerve ligation (PSL) [116]. Alteration of the extracellular space can affect the diffusion of neurotransmitters at, and adjacent to, the synapse, and provide (or deprive) space for synaptic remodeling [117, 118]. Additionally, PV+ GABAergic interneurons in S1 are associated with peri-neuronal nets (PNNs) - extracellular matrix components which subserve a variety of functions, and are closely linked to the developmental closure of critical period plasticity within S1. This critical period can be re-opened in adults following the digestion of PNNs by enzymes such as MMPs, or experimentally by chondroitinase - although this mechanism has not been previously implicated in pain models [84, 85, 88, 89, 119]. Nevertheless, loss of cortical inhibition - PV+ interneuron-mediated or otherwise – and disruption of cortical E-I (excitatory-inhibitory) balance, may play a critical role in promoting and maintaining chronic pain states [120, 121]. This general mechanism has been demonstrated within the ACC in experimental nerve injury models [122, 123]. In an experiment by Eto et al. (2012) [121], another pain model – intraplantar CFA – produced mechanical allodynia and increased excitability in cortical layer 4 and layer 2/3 (excitatory) pyramidal neurons within S1. Intraplantar CFA was also associated with reduced KCC2 (potassium-chloride cotransporter 2) expression and disrupted chloride homeostasis in S1, which diminished the magnitude of intracortical GABA-AR-mediated IPSCs. Interestingly, intracortical inhibitory output within layer 2/3 was actually enhanced, driven by excess (feed-forward) input onto local inhibitory interneurons from layer 4 pyramidal neurons – which partially compensated for the additional excitatory drive. In spite of the fact that this enhanced activity within inhibitory interneurons resulted in greater net inhibition

(compared to controls) – even in the presence of impaired chloride homeostasis - it was never-the-less insufficient to fully normalize excitability in S1, or reverse the associated mechanical allodynia [121]. However, experimentally restoring the disrupted E-I balance within S1 by locally administering diazepam (a GABA-A receptor positive-allosteric modulator) or muscimol (a GABA-A receptor agonist) was sufficient to overcome the pro-excitatory shift, and fully normalized mechanical withdrawal thresholds in that model [121].

Another, more widescale/structural form of neural plasticity – altered cortical volume (ie. increased cortical thickness in S1) – has been observed in chronic pain patients, and is positively correlated with pain intensity [108]. In amputees, ongoing phantom limb pain is positively correlated with the extent of cortical reorganization/functional remapping of the lost limb – however, this is typically measured by functional neuroimaging/fMRI following innocuous (non-painful) stimulation [18, 124-126]. Therefore, the causal nature of this link in phantom-limb pain is questionable. Indeed, it has been speculated that plasticity in S1 may be epiphenomenal to certain pain conditions – and in some painful conditions or in certain individuals with pain, plasticity in S1 may not be present at all [104, 127]. However, a direct causal link between functional and neuroanatomical plasticity in S1, enhanced activity in other “pain-matrix” regions (eg. ACC), and neuropathic pain, has been established in animal models [72, 105]. In general, the evidence in humans/clinical pain patients also supports an active role for cortical plasticity within S1/S2 in pathological pain – and interventions which directly target cortical somatosensory representations have been proposed [128, 129].

#### **1.1.2.3.4 – Anterior Cingulate Cortex (ACC)**

The anterior cingulate cortex (ACC) is thought to contribute to the affective-emotional components of pain perception [18, 21, 130]. Painful stimuli reliably evoke activity within the ACC, whereas non-noxious somatosensory stimuli typically do not (compare to S1) [5, 18, 73, 131]. Activity within the ACC is directly correlated with the intensity and subjective “unpleasantness” of painful stimuli [18]. Lesions to

the ACC or cingulotomy produce an attenuation of the emotional response to painful stimuli [5, 18]. However, in certain clinical pain syndromes, such as in patients with irritable bowel syndrome (IBS) – the positive correlation between ACC activity and subjective pain rating following noxious stimulation (eg. rectal distention) may be abolished [18]. This loss of correlation may be associated with the “chronicization”/centralization of pain and/or basal hyperexcitability within ACC [18]. Clinical pain syndromes, and animal models of neuropathic pain (PNI/SCI) generally involve functional/synaptic plasticity (hyperexcitability) within the ACC [18, 21, 57, 131-136]. Plasticity in the ACC is thought to play a direct causal role in encoding the affective dimension of pain, and is also implicated in pathological pain states and altered pain behaviors following injury [18, 130, 132, 136-139]. Allodynia generally involves activation of the ACC [18], as does “illusory” thermal pain [140]. Optogenetic studies targeting the ACC have demonstrated bi-directional control over the expression of pain behaviors and thalamic neuronal activity in response to formalin, pinch, and Von Frey hairs [123, 141]. Approaches which directly target or reverse plasticity within the ACC have been attempted experimentally as a method of reversing pathological pain [142]. The ACC is a critical locus of cortical pain modulation, such as analgesia produced by endogenous and exogenous opioids [18, 73, 143, 144]. Positron-emission tomography (PET) and fMRI studies indicate that activation of  $\mu$ -opioid receptor sites in the ACC is associated with suppression of the affective component of pain [18, 139, 144]. Placebo-induced analgesia is also thought to involve modulation of the ACC by endogenous opioids [145]. The ACC is generally believed to be an important region for mediating interactions between emotional state and pain, for the modulation of pain by emotion (and vice-versa), and for motivational aspects of pain processing [18, 28, 73, 130, 146-149]. Activation of the ACC may enhance descending facilitation via the RVM nuclei, and thereby also modulate subthalamic nociceptive processing [28, 150].

#### **1.1.2.3.5 – Insular Cortex**

Like the ACC, the insular cortex (IC) also contributes to the affective-emotional components of pain perception [18, 151]. The IC is also important to pain-related memory function, and to visceral

interoception, sensorimotor integration, and autonomic control [18, 151, 152]. For certain painful (thermal) stimuli, the IC may also perform some of the sensory-discriminatory functions normally subserved by S1 [153]. The IC, like the ACC, is activated by painful stimuli (but not innocuous touch) - and activity within the IC is correlated with stimulus intensity and subjective pain rating [18, 73, 131]. Thermal stimuli (noxious heat, graded heat, noxious cold) are particularly associated with IC activation [5, 140]. Recent neuroimaging (fMRI, arterial spin-labelling, ASL) studies have speculated that one or two subregions of the insula (the dorsal posterior insula, and the anterior insula) may be key regions which, by their activity, differentiate painful from non-painful stimuli – comprising part of a unique/specific neuroimaging “pain signature”, and/or encoding subjective pain intensity/rating [154-156]. The IC, like S1/S2, is likely activated directly via the thalamus during pain perception [18]. The IC is basally activated in chronic pain patients, and also in neuropathic pain patients during allodynia [18, 154, 157]. Artificial (electrical) stimulation of the IC has been noted to produce “extremely unpleasant” and painful sensations [18, 158]. Lesions of the IC may produce the condition known as “pain asymbolia”, in which the emotional valence and “meaning” of noxious sensory stimuli are disrupted, and behavioral and physiological responses to pain are inappropriate despite normal sensation and nociceptive “awareness” [18, 159]. An antinociceptive role for the insula is also documented – patients with lesioned IC exhibited enhanced S1 activation and subjective pain intensity in response to an acute noxious stimulus [159]. Like the ACC, modulation of the IC has been identified as playing a role in placebo-induced analgesia [5, 157]. IC, like S1/S2 and ACC, is heavily and reciprocally connected with other “pain matrix” regions and modulatory centers – and is itself modulated by manipulations or processes which alter pain perception, such as exogenous and endogenous opioids, attention/distraction, etc. [7, 18, 28, 57, 73, 157, 160]. Altered insular function may also have a role in pain related to depression [161].

#### **1.1.2.3.6 – Other Brain Regions**

While the above mentioned brain regions are the most consistently and directly implicated areas underlying the experience of pain, many other regions have been reported to be activated or modulated by painful stimuli and conditions - and contribute to the overall response to pain [7, 18, 21, 28]. Like S1 and ACC/IC, these regions may serve specific functional roles or underlie specific dimensions of the response to acute or chronic pain. They may also modulate activity within the other components of the pain “matrix”. The prefrontal cortex (PFC) is one such region, and is frequently (but not always) reported as being activated during pain in imaging studies [18, 131, 157]. However, activity in the PFC does not correlate linearly with stimulus intensity or subjective pain rating [18, 162]. It is believed that activity within the PFC likely reflects cognitive processes related to the experience of pain, rather than the sensation of pain itself [18]. The PFC also likely participates in “top-down” (ie. executive/cognitive) control of pain, by engaging descending and/or supraspinal modulatory circuits [18, 28]. The basal ganglia (BG) – esp. the striatum/nucleus accumbens - is another region with an important role in pain modulation (eg. by dopaminergic circuits), and in motivational aspects of pain [18, 157]. Decreased dopamine content and D2-receptor (D2R) density within the BG has been observed in clinical pain conditions, and D2R concentration within the BG correlates with tolerance to tonic pain in healthy subjects [18]. The subcortical / anterior cortical monoaminergic systems and circuits represent an important point of interface between processes such as stress, salience, and reward, and pain modulation - including through interactions between opioidergic and monoaminergic systems [7, 18, 21, 28]. Other limbic or “motivation-associated” regions involved in pain – and the modulation of, or the response to, pain - include the amygdala, habenula, hypothalamus, and hippocampus [7, 18, 21, 57, 73]. The cerebellum is also activated by noxious stimuli, and there are reciprocal connections between the cerebellum and spinal cord [18]. However, cerebellar activity is present following noxious stimulation even in anesthetized patients who are completely unconscious of pain, suggesting it subserves secondary functions related to pain, as opposed to processing pain itself [18].

#### **1.1.2.3.7 – Caveat to the “Pain Matrix”**

Despite the usefulness of the “pain matrix” concept, and its correspondence with multiple lines of experimental data, activity within the pain matrix should not be considered the neural correlate of pain per se. All of these brain regions perform multiple functions, and are involved in processing (internal/external) stimuli/states other than (merely) those which evoke or involve pain [60, 163]. Current concepts of how pain is represented in the brain predict that specific subregional circuits or neuronal ensembles within areas of the “pain matrix” encode the actual experience of pain / pain-related information [23]. Imaging and recording methods/models which only resolve neuronal function/activity at the regional level can therefore not distinguish between painful and similar (or related), but non-painful, responses [23]. This is exemplified by recent functional imaging studies contrasting responses to noxious stimulation in *SCN9a*-deficient patients - who are congenitally insensitive to pain - and healthy controls [23]. The reported intensity of the sensation experienced was similar in both groups, and both groups exhibited similar patterns of resultant brain activation (ie. within the pain neuromatrix); however, in the *SCN9a*-deficient group, the experience was not painful [23]. Therefore, the precise detailed mechanism of how the experience of pain is represented or encoded in the brain will remain elusive until sufficiently high-resolution (spatial/temporal), and high-throughput, imaging/recording and analysis methods – which might be powerful enough to pinpoint the critical neurobiological distinctions in the aforementioned experiment - become available.

## **1.2 – Multiple Sclerosis**

Multiple sclerosis (MS) is a progressive degenerative disease affecting the human central nervous system (CNS) [164, 165]. First characterized by Jean-Martin Charcot in 1868 [166], the hallmark pathological features of MS are central neuroinflammation and demyelination leading to the formation of white matter (WM) lesions or ‘scars’ – hence ‘sclerosis’. More recently, it has been acknowledged that grey matter (GM) is also disrupted in the disease [167]. The location of these lesions in the brain and spinal cord (SC) influences the clinical manifestation of MS; however, the primary symptoms include paralysis and motor dysfunction, as well as a range of cognitive, sensory, and affective

disturbances [165, 168]. MS affects roughly 100,000 Canadians (according to the World Health Organization/MS Society of Canada [169]), or 2.5 million people worldwide by World Health Organization estimates (2008) [169]. The typical age of onset is between 20 and 50 years of age – and by 25 years past onset, roughly 50% of those affected will require the use of a wheelchair [170]. Women are affected at a rate of roughly two or three to one over males [167]. MS is currently a disease of idiopathic origin; however, studies have confirmed an association with multiple genetic and environmental risk factors [171-173].

### **1.2.1 – MS Phenotypes**

MS is a heterogeneous condition with multiple disease phenotypes or clinical presentations. The most common form of MS is referred to as relapsing-remitting MS (RRMS), due to characteristic recurring episodes of acute disability and neurological decline (relapse), followed by a partial or complete recovery of function (remission) [165, 167, 174]. RRMS accounts for roughly 85% of total MS cases, and is frequently diagnosed following an initial diagnosis of clinically isolated syndrome (CIS) [167, 168]. CIS is a nascent form of inflammatory demyelinating disorder involving only a single discrete episode of neurological deficit and – typically – a single discrete lesioned area [175]. CIS commonly affects the optic nerve, leading to optic neuritis, but it may also affect the brainstem, cerebellum, spinal cord, or cerebrum [175]. Roughly 45% of cases of CIS progress to MS within the first 2 years following diagnosis, and most cases of CIS which progress to MS do so within the first 5 years [175, 176]. The presence or absence of active demyelinating lesions (diagnosed by magnetic resonance imaging, MRI) strongly influences the prognosis for CIS, with ~80% of patients with MRI abnormalities progressing to clinically-defined MS within 20 years – compared to only ~20% of patients whose MRIs had normal appearance [176-178]. For those patients who go on to develop RRMS, continued relapses are generally correlated with periods of increasing lesion formation/load [168]. Typically, the frequency and severity of the relapses increase with time. Eventually, in most cases – 65-80% by 10-20 years after diagnosis – RRMS will become secondary progressive MS (SPMS) [165, 170]. In SPMS, disability is no

longer correlated with lesion load, and does not undergo spontaneous remission [179], although widespread neuroinflammation persists/remains. Whereas inflammatory demyelination is characteristic of RRMS, SPMS is characterized by gradual progressive neurological decline and CNS atrophy – including diminished brain volume and widespread neuroaxonal degeneration [170, 174]. However, no specific clinical, imaging, or pathological criteria which define the conversion between RRMS and SPMS have yet been established or identified [167, 174, 179]. A much smaller proportion of MS cases (~15%) involve no initial period of relapsing-remitting disease prior to this progressive phase, and are thus termed primary progressive MS (PPMS) [180]. PPMS generally onsets ~10 years later in life than RRMS, and is equally prevalent in either gender [180]. The underlying causes of the intrinsic clinical heterogeneity of MS, in its various phenotypic forms, are the subject of current investigation and debate [181, 182]. It has, however, been postulated that the progressive forms of the disease emerge when the pathological processes that drive MS (ie. inflammation, demyelination, and neurodegeneration) – which *may* be similar or identical across disease phenotypes – overwhelm innate compensatory and repair mechanisms (ie. remyelination, neurogenesis, neuroplasticity) [167, 170, 183, 184]. Alternatively, it has also been hypothesized that the progressive disease results from ongoing, simultaneous, yet independently occurring pathological processes – distinct from those which dominate the relapsing-remitting phase [167, 170, 171, 185].

### **1.2.2 – Genetic Risk Factors for MS**

Based in large part on the pathological processes observed in RRMS, and in the animal model experimental autoimmune encephalomyelitis (EAE) – which both involve peripheral adaptive immune system activation against self-antigens, and subsequent infiltration of the CNS by autoreactive T lymphocytes - MS is generally considered to be an autoimmune disease [170]. In support of this view is the fact that the vast majority of the 100+ genetic variants identified as risk-factors for MS by genome-wide association studies (GWAS) have immunological function [170, 171]. Based on epidemiological studies, it is estimated that approximately 30% of the overall risk for developing MS is attributable to

genetic factors [170, 171]. The remaining ~70% of the overall risk is therefore ascribed to as-yet unidentified environmental factors and “stochastic” (endogenous or external) events [170, 171]. Most of the genetic alleles identified as being associated with MS are non-coding, and rather function as repressors or enhancers for specific immune cells/functions [170]. Many of the genes associated with a predisposition towards MS overlap with genetic determinants identified for other autoimmune diseases (eg. ankylosing spondylitis) [170].

The most prominent genetic associations conferring risk for MS yet identified are for allelic variants of the *HLA* (human leukocyte antigen) gene complex [170, 171]. The *HLA* gene complex encodes the major histocompatibility complex (MHC) proteins – cell surface proteins which define the specificity of T/B-cell mediated immune responses [171]. The allele *HLA-DRB1* – part of the gene cluster encoding the MHC class II protein – has consistently been identified as conferring risk for MS [170, 171]. The allele *HLA-A\*02:01*, which encodes part of the interleukin-2 (IL-2) receptor (IL-2Ra) has also been implicated [170]. It is estimated that genes within the *HLA* superlocus account for some 20-60% of the overall genetic risk for MS [171]. Apart from the *HLA* variants, many of the genes that are associated with MS generally influence the threshold of activation for cellular immune-responses [170, 171]. Notably, few genes which would be implicated in classical neurodegenerative disorders have been implicated in the initiation of MS [170]. These “neurological” genes may, however, play a role in determining disease phenotype and severity [170]. Despite these limited insights, much about the role of genetics in MS remains to be discovered and elucidated. Ultimately, it is understood that complex interactions between a multitude of genes (ie. an ‘interactome’) and the internal/external environment are necessary to generate and maintain the disease [170, 171].

### **1.2.3 – Environmental Risk Factors for MS**

Compared with our knowledge of the genetics of MS, current understanding of the environmental factors which confer susceptibility to MS is very limited. Regional variations in susceptibility, including

an association with latitude, have been noted [165, 168]. This association prompted hypotheses relating to the role of vitamin D (which requires sunlight for its biosynthesis) [167, 172, 173]. Other studies have implicated smoking and circadian rhythm disruption as risk factors for MS [167, 170, 172, 173]. Viral and microbial infections have also been repeatedly implicated, most notably Epstein-Barr virus (EBV) [167, 170, 172, 173]. It is hypothesized that microbial or viral infections may trigger autoimmune T-cell responses through the process of molecular mimicry – ie. similarity between external and self-antigens [167, 186, 187]. Another possibility - observed in the Theiler's murine encephalomyelitis virus (TMEV) model - is that CNS-targeting infections may cause sequestered CNS self-antigens to be released into the peripheral systemic circulation [170]. Furthermore, peripheral infections and inflammation may influence the CNS through circulating cytokines and cytokine-nerve interactions [170, 188]. Along these lines of reasoning, the role of the gut microbiota is currently being investigated [170, 189]. At this point, however, most of these associations remain largely hypothetical.

#### **1.2.4 – Pathophysiology of MS**

As mentioned, the primary pathological characteristics of MS include widespread neuroinflammation, demyelinated plaques/lesions of the WM/GM, and gradual axonal loss/neurodegeneration [165, 167, 185]. These pathological features/lesions can be distributed throughout the CNS (including in the spinal WM), although MS is often thought of as primarily affecting the brain. Ventricular enlargement is frequently observed in MS brains, an indication of brain atrophy [170]. Within demyelinated WM lesions, a loss of oligodendrocytes (which form the neuronal myelin sheath) is consistently observed [167, 170]. Glial scarring – regions comprised of reactive astrocytes – is also regularly observed [170]. Demyelination also affects the GM of the cerebral cortex, deep brain/brain stem nuclei, and the spinal cord [167, 185, 190, 191]. While relapses in RRMS are associated with the formation and increasing load of inflammatory/demyelinated lesions, disability in the progressive phase is mainly correlated with neuronal/axonal loss [185].

#### 1.2.4.1 – The Blood Brain Barrier (BBB)

Conceptions of MS as an autoimmune disease have clear merit, based on pathological observations in MS tissues (as well as genetic studies, treatment mechanisms, animal models etc.). Inflammation, immune activation, and infiltration are present in the CNS at all stages of MS, though are most pronounced/active in the early/acute disease [170, 192]. How and why (and to what effect) the CNS comes to be targeted and infiltrated by the immune system is debated. The CNS is often considered an ‘immune-privileged’ site - largely segregated from the peripheral immune system by the blood-brain barrier (BBB) [170, 192]. The BBB is comprised of tight endothelial junctions and astrocytic end-feet (the *glia limitans*) surrounding CNS-penetrant blood vessels, which serve to exclude peripheral immunocompetent cells, microorganisms, molecules and antigens from the CNS parenchyma [170, 192]. Adaptive-immune cells (T/B-lymphocytes) are not normally endogenously present in the CNS (parenchyma), and must therefore be recruited from the periphery and cross the BBB to gain access to the CNS [170, 192]. **(FIG. 1.3)**

#### 1.2.4.2 – Outside-In Model of MS

Two broad and competing theories of MS pathogenesis are currently debated. The first concept is known as the ‘CNS extrinsic’ or ‘outside-in’ model. This theory postulates that the disease is triggered from outside of the CNS, in the periphery [170, 186, 193]. The primary drivers of the disease in this model are autoreactive T-cells, as well as B-cells and monocytes, which are activated in the periphery and subsequently trafficked across the BBB into the CNS [170, 192]. This model fits well with what is observed in the relapsing-remitting/acute phase of MS, and is also consistent with the pathogenesis of EAE – the most popular animal model for studying MS (*see below-section 1.2.1*) [187, 192, 194]. The outside-in model accords less well with what is observed in progressive or chronic MS (especially PPMS), in which neurodegeneration and disability are less correlated with inflammation and immune infiltration [170, 195]. **(FIG. 1.3)**

#### 1.2.4.3 – Inside-Out Model of MS

The other broad theory of MS pathogenesis is the ‘CNS intrinsic’ or ‘inside-out’ model. This model postulates that peripheral immune infiltration is a secondary phenomenon, triggered by events endogenous to the CNS [170, 193]. Several versions of this concept exist, with varying notions of the contribution from the periphery to the disease. One hypothesis is that a CNS-viral trigger initiates the secondary recruitment of the peripheral immune system [170]. Another hypothesis is that MS is a primary neurodegenerative disease, similar to Parkinson’s or Alzheimer’s [193]. In this version, the immune infiltration and inflammation observed in the CNS is largely secondary, epiphenomenal, or perhaps compensatory. The central driver of disease progression and disability in this model would be some (unknown) intrinsic neuronal pathology, such as mitochondrial dysfunction, that leads to neuronal atrophy and death [170, 196]. The inside-out model fits well with the apparent uncoupling of neurodegeneration and disease progression from inflammation and immune infiltration in the progressive and chronic forms of the disease [193]. **(FIG. 1.3)**

#### 1.2.4.4 – Immunopathogenesis of MS

The initiating etiological events in both “models” are currently obscure [185, 193]. However, the immunopathological sequence of events in early/RRMS has been fairly well characterized [170, 187, 192, 194, 197]. Altered central and peripheral immune tolerance is thought to be a precondition for autoimmune activation [170, 192]. This refers to the process by which spontaneously generated autoreactive T-cells are deleted or suppressed in the thymus and bone-marrow (“central tolerance”), or after being released into the periphery (“peripheral tolerance”) [170]. Regulatory T-cells, known as Tregs, are involved in activating and differentiating T/B lymphocytes into effector or helper classes. Tregs are also involved in the suppression of autoreactive T/B cells [170]. In MS, altered Treg functionality, or resistant (to suppressive mechanisms) T/B cells, are thought to permit the proliferation of CNS-directed autoreactive T/B effector cells [170, 192, 197]. These autoreactive T/B-cells are

thought to arise and become activated in the periphery by molecular mimicry, or by recognition of (ordinarily) sequestered CNS autoantigens which have been released into the periphery [167, 170, 187]. Initial activation may also occur by recognition of a novel autoantigen, or by bystander activation (ie. cytokine mediated heterologous T-cell activation) [167, 170, 187]. Candidates for the initiating autoantigen(s) are generally myelin-associated proteins such as myelin basic protein (MBP), myelin oligodendrocyte glycoprotein (MOG), and proteolipid protein (PLP) [167, 170, 187]. Once activated in the periphery, autoreactive T/B-cells travel through the systemic circulation to the cerebral vasculature [170, 192]. Either through cell-surface receptor-mediated interactions, or through 'leaky' regions of the BBB, autoreactive lymphocytes and monocytes/macrophages gain access to the CNS (directly or via the CSF) [170, 192]. Infiltrating T/B-cells accumulate in the CSF in the perivascular / subarachnoid space (SAS), and in the choroid plexus [170, 192]. Antigen presenting cells (APCs), such as dendritic cells and macrophages, can then reactivate infiltrating lymphocytes in the CSF, allowing them to secondarily pass into the CNS parenchyma [170, 192]. **(FIG. 1.3)**

Early MS lesions are generally perivascular, and are rich in infiltrating peripheral immune cells [167, 192]. The cellular infiltrate in these early lesions is mainly composed of macrophages and CD8+ T-cells [167, 170]. Cytotoxic CD8+ T-cells, reactive against self myelin epitopes, are thought to mediate - and are quantitatively correlated with - the destruction of oligodendrocytes, leading to demyelination and axon damage [167]. Monocytes/macrophages are also implicated in demyelination and neuronal injury [167, 170, 187, 192]. Relatively fewer CD4+ T-cells, primarily of the T-helper T<sub>H</sub>1 / T<sub>H</sub>17 classes, are also present, alongside B-cells and plasma cells [170, 192]. B-cells producing autoantibodies and complement proteins are also likely involved in tissue damage [170, 192]. CNS tissue damage and demyelination in the early stages is generally confined to lesioned areas [167]. Later in the disease, diffuse T/B-cell infiltrates are present in the CNS, along with diffuse demyelination and axonal injury [167]. Resident/innate immune cells of the CNS, namely microglia/macrophages, are also activated, as are astrocytes [170, 187, 192]. Innate immune and glial cells likely contribute to the ongoing

neuroinflammation and damage, help to disrupt the BBB, and recruit additional peripheral immune cells through the secretion of cytokines, chemokines, and proteolytic enzymes – such as the matrix-metalloproteinases (MMPs) [187, 195]. Innate immune cells may also contribute to epitope-spreading, whereby additional self-antigens become targeted by infiltrating leukocytes [167, 170, 192]. **(FIG. 1.3)**

#### 1.2.4.5 – Cytokines

Cytokines are signaling molecules with a diverse array of functions [188]. They are released from immune cells such as lymphocytes and myeloid cells, or from various other cell-types including endothelial cells and fibroblasts [167, 188]. They can act in an autocrine, paracrine, or endocrine fashion, and exert receptor-mediated effects on a wide variety of cell-types, including immune cells, glial cells, neurons, and endothelial cells [188, 198]. The role of cytokines in MS is complex and only partially understood. However, apart from MHC genes, genes which encode (or regulate) cytokines and their receptors are the most prominent genetic risk factors associated with MS [170, 171]. Much of what is understood about the role of cytokines in MS is derived from experiments in EAE (*see below-section 1.2.1*). In general, a cascade of cytokine signaling is necessary for the initiation, coordination, and perpetuation of the self-directed immune/inflammatory response which characterizes MS [167, 170, 188, 192]. One of the major functions of cytokines is to direct immune-cell behaviors, including: proliferation/apoptosis, activation, chemotaxis, and polarization/differentiation [188]. Most of the cytokines associated with MS are considered to be pro-inflammatory; however, some may have alternate or even opposite functions depending on context (ie. cytokine/inflammasome networks, tissue-specific effects, temporally-specific effects, etc.) [170, 188]. CD4+ T-helper (T<sub>H</sub>) cells, which are strongly implicated in the pathogenesis of EAE, likely contribute to the cytokine response which drives MS [192]. T<sub>H</sub>1-polarized CD4+ T-cells release IFN $\gamma$  (interferon-gamma), TNF $\alpha$  (tumor necrosis factor-alpha), and IL-12 (interleukin-12) [192]. These cytokines act to promote cell-mediated immune responses and phagocyte-dependent inflammation [170, 188, 192]. T<sub>H</sub>17-polarized CD4+ T-cells, which secrete IL-7F, IL-17(A-F), and IL-22, are also strongly associated with MS/EAE pathogenesis [170, 188,

192]. T<sub>H</sub>2-polarized CD4<sup>+</sup> T-cells - which secrete IL-4, IL-5, IL-6, IL-9, IL-10 and IL-13, and promote humoral (ie. antibody-mediated) immune responses – play a smaller role in MS pathogenesis [167, 170]. Beside lymphocytes, peripheral monocytes and CNS-resident microglia also produce cytokines which contribute to MS [167, 170, 188]. IL-1 $\beta$ , IL-6, IL-12, IL-17, IL-23, TNF $\alpha$ , and INF $\gamma$  are all thought to be important in the immunopathogenesis of MS [167, 170, 188, 192]. A brief description of some of their roles follows (*see section-1.2.1: EAE Pathogenesis*):

#### 1.2.4.5.1 – IL-23

IL-23 is released from both invading and CNS resident myeloid cells [188], and is thought to play a critical role in promoting the polarization of T-cells towards pro-inflammatory/pathogenic effector cell-types [188] – and in inducing cytokine (IL-17, GM-CSF) expression [167, 188].

#### 1.2.4.5.2 – IL-6

IL-6 is also thought to play a critical role in T-cell polarization, promoting T<sub>H</sub>17 polarization in differentiating T-cells, and suppressing FoxP3 expression and polarization towards regulatory T-cell types (Tregs) [188]. It also promotes expression of the IL-1 receptor (IL-1R) on T-cells [188]. IL-6 is present in both acute and chronic MS plaques, and is associated with active/ongoing demyelination [199].

#### 1.2.4.5.3 – IL-1( $\beta/\alpha$ )

IL-1 exerts multiple pro-inflammatory effects [188], and is expressed by peripheral and resident myeloid cells (monocytes/macrophages and microglia) in acute WM/GM lesions [200]. IL-1 is thought to stabilize the polarization of pathogenic T<sub>H</sub> cells [188]. Active IL-1 $\beta$  can be generated from its inactive precursor pro-IL-1 $\beta$  by the proteolytic actions of the enzyme caspase-1, which is the major end-product of inflammasome activation. [201]

#### 1.2.4.5.4 – The Inflammasome

The “inflammasome” refers to an intracellular macromolecular system/oligomeric assembly that coordinates and promotes the inflammatory response in innate immune cells, following the receptor-mediated detection of extracellular pathogen/danger-associated molecular patterns (PAMPs/DAMPs), and/or intracellular stress signals such ROS/mitochondrial DNA. EAE, MS, and the cuprizone model of demyelination/MS, are all specifically associated with activation of the NLRP3 inflammasome. The NLRP3 inflammasome is thought to contribute to  $T_H1$  and  $T_H17$  cellular responses and migration in EAE, and *Nrlp3*-deficient mice exhibit reduced disease severity and delayed onset of EAE. [201]

#### 1.2.4.5.5 – TNF $\alpha$

TNF $\alpha$  is pleiotropic cytokine, with multiple functions including both pro- and anti-inflammatory effects, effects on cellular proliferation, differentiation, and apoptosis [188]. TNF $\alpha$  is elevated in the CSF of MS patients, and CSF levels are correlated with disease severity [202]. Serum levels of TNF $\alpha$  are, however, normal in MS patients, suggesting that production by CNS resident cells is critical [203]. TNF $\alpha$  is produced by multiple cell-types, and can exist in multiple forms (soluble/insoluble) and bind to multiple receptor subtypes (TNFR1/2) [188]. TNF $\alpha$  contributes to the pathogenesis of EAE in multiple ways. It can induce apoptosis of oligodendrocytes, and can impede the reuptake of extracellular glutamate by astrocytes, contributing to neurotoxicity, (*see below-section 1.1.4.6*) [188]. It can also promote the expression of MHC molecules on astrocytes and oligodendrocytes, making them susceptible to CD8+ T-cell-mediated cytotoxicity [188]. TNF $\alpha$  also promotes the expression of adhesion molecules on endothelial cells and astrocytes, which enable peripheral immune cells to cross the BBB [188].

Apart from its pathogenic effects, TNF $\alpha$  can also, somewhat paradoxically, have protective effects in MS, as evidenced by the fact that neutralization of TNF $\alpha$  in MS patients increases the frequency and severity of relapses [188, 204]. This is likely due to functionally opposite and contrasting effects between the soluble (sTNF $\alpha$ ) and insoluble/membrane-bound (memTNF $\alpha$ ) forms of TNF $\alpha$ , as

mediated through the proinflammatory TNFR1 receptor, or the prohomeostatic / immunomodulatory TNFR2 receptor, respectively. [188]

#### 1.2.4.5.6 – IFN $\gamma$

IFN $\gamma$  is produced exclusively by lymphocytes [188]. Like TNF $\alpha$ , IFN $\gamma$  exerts multiple and sometimes opposing effects. It can be either pro- or anti-inflammatory depending on context (*see EAE Pathology-section 1.2.1*) [188]. IFN $\gamma$  can promote T-cell apoptosis, and may reduce T<sub>H</sub>17 cell counts and IL-17 production, while also promoting the expression of regulatory T-cell types [188]. IFN $\gamma$  can apparently also have bidirectional effects on the BBB, alternatively promoting or disrupting it [188]. It can also promote phagocytosis - which may help 'clean up' myelin debris and contribute to repair, but may also contribute to pathogenicity [188].

Apart from these actions, many of these cytokines (ie. IL-1 $\beta$ , TNF $\alpha$ ) also affect neuronal function, and can influence neuronal plasticity and structure [205-207]. These effects are likely relevant in the secondary symptoms of MS such as pain, depression, cognitive dysfunction, and fatigue [208-212].

#### 1.2.4.6 – Axonal Injury and Neurodegeneration

Neurodegeneration begins early in MS, with decreased cerebral N-acetyl-aspartate (NAA, a marker of axonal integrity) being detected by magnetic resonance spectroscopy (MRS), and brain atrophy observable by MRI, very early in the disease course [196]. Neurodegenerative processes and axonal injury gradually accumulate as the disease progresses, with the transition to progressive MS potentially representing the point at which a critical mass of axonal/neuronal loss is reached, or at which innate compensatory and repair mechanisms are overwhelmed [167, 184, 185, 196]. Several mechanisms may contribute to axonopathy and neurodegeneration in MS. These mechanisms may be secondary to inflammation and demyelination, or may be a primary underlying pathological characteristic of MS, as

postulated in the inside-out/primary neurodegenerative model [184, 185, 193, 196, 213]. Notably, the currently available immunotherapies which are used to reduce relapse rates in MS do not impede long-term disease progression [185]. This may be accounted for by the induction of self-sustaining neurodegenerative processes following autoimmune injury [170, 196].

One mechanism which has been implicated in MS involves a cascade of events triggered by demyelination: Demyelinated axons are known to redistribute  $\text{Na}^+$  channels and mitochondria between nodes of Ranvier in order to compensate for the loss of saltatory conduction [184, 214, 215]. While this may resolve conduction block, actively maintaining ionic gradients along greater lengths of axon creates additional energetic demands on the neuron [214]. Energy deficiencies can lead to ion imbalances as active transport mechanisms, such as the  $\text{Na}^+/\text{K}^+$ -ATPase, fail [214]. The  $\text{Na}^+/\text{Ca}^{2+}$  exchanger can start operating in reverse under these conditions [215, 216]. This and other mechanisms can cause an accumulation of intracellular/cytosolic calcium, leading to excessive glutamate release from axon terminals [167, 217]. Increased extracellular glutamate can, in turn, create additional energy demands on neighboring neurons, and at high levels becomes excitotoxic, leading to apoptosis/necrosis [214, 217]. In this way, the excitotoxic cascade spreads and becomes self-sustaining, particularly when neuroprotective and regenerative mechanisms fail [217]. **(FIG. 1.4)**

Altered glial functionality, fueled by chronic inflammation, can further contribute to neurodegeneration [170, 214, 218]. Normally, astrocytes remove excess glutamate from the synapse, and can help to limit the diffusion of toxic chemical mediators and byproducts, and assist in remyelination. However, in the disease state, astrocytic glutamate reuptake can be reversed, contributing to excitotoxicity. Microglia, which can clear cellular/myelin debris, among other actions, may also become pathogenic in their functioning – releasing various proinflammatory chemical mediators [170, 214, 218]. Apoptotic and necrotic cells release additional toxic factors which can disrupt neighboring neurons and further activate innate immune cells [218]. Myelin debris from damaged/apoptotic oligodendrocytes can lead to the formation of toxic lipid peroxidation byproducts [167, 218]. Reactive oxygen and nitrogen species

(RONS) can damage cells/mitochondria, and are produced by activated immune cells, as well as by neuronal mitochondria during oxidative phosphorylation [167, 196, 218]. Several mitochondrial respiratory complex proteins are known to be disrupted in MS/EAE, particularly in demyelinated axons – and mitochondrial DNA can become damaged [196, 215]. Mitochondrial disruption and respiratory deficiency can cause neurons in MS brains to become energetically dependent on glycolysis - and ultimately to become “virtually” (functionally) hypoxic [215, 218, 219]. Cytoskeletal proteins and axonal/mitochondrial transport are also altered, which can lead to the accumulation of toxic proteins such as amyloid precursor protein (APP) and tau [196]. All of these processes ultimately lead to the diffuse, non-focal neurodegeneration and axonopathy observed in ‘normal appearing’ (NA)WM/GM in chronic MS [185, 196]. **(FIG. 1.4)**

Altered functional connectivity between neurons, and synaptopathy, have also been described in MS/EAE [196, 220, 221]. Inhibitory GABAergic interneurons are specifically disrupted in EAE brains [222-224] – and may also be disrupted in MS [215, 225]. The resulting disinhibition may promote additional excitotoxicity. Pro-inflammatory cytokines can also directly promote hyperexcitability and abnormal plasticity [206, 211], and activated microglia can directly ablate specific synapses [226, 227]. Functional MRI (fMRI) changes within the neocortex have been observed in early MS and EAE [228-231]. Some of the altered functional connectivity observed in the MS/EAE cortex may be due to the need to compensate for lost network nodes/connections, due to focal neurodegeneration/demyelination [184, 190, 232]. Ultimately, it is these neuronal alterations and neuronal loss which primarily mediate the diverse symptoms of MS, and which are most correlated with disability throughout the disease course [167, 184, 213].

### **1.2.5 – Treatment of MS**

As previously mentioned, virtually all currently available treatments for MS target the immune component of the disease [167, 170, 233]. As such, they are - almost without exception - only effective

at reducing attacks (relapses) in the early disease/RRMS. At the moment, there are no approved treatments which directly target the neurodegenerative component of the disease, or are effective for primary progressive MS [170, 233]. Mitoxantrone is the only treatment recognized as delaying (but not arresting) disease progression in SPMS – though methotrexate and interferon-beta 1b (IFNB1b) may also have some modest effect [234].

The immunomodulatory/immunosuppressive agents used to treat RRMS - apart from the corticosteroids - are also known as ‘disease modifying therapies’/‘disease modifying agents for MS’ (DMTs/DMAMs). These agents generally act to suppress or modify specific immune cell populations or responses [167, 233]. Some commonly prescribed DMTs are the beta interferons (IFNB1b/interferon-beta 1a) and glatiramer acetate (GA). IFNB(1b/1a) are endogenous cytokines which are thought to slow progression of MS by reducing the rate of cellular differentiation for specific lymphocyte subsets (ie. T<sub>H</sub>17 T-cells), among other immunomodulatory effects [167, 233]. GA is synthetic peptide which is thought to mimic MBP, and may promote the differentiation of a subset of regulatory T-cells [167]. Some DMTs specifically prevent peripheral immune infiltration into the CNS - such as fingolimod (FTY720), which sequesters activated T-cells in the lymph nodes [167, 233]; and natalizumab, which blocks the alpha-4 integrin cell-adhesion molecule that mediates the crossing of the BBB for a subset of lymphocytes [167, 233]. Other agents act to ablate or prevent the proliferation of specific lymphocyte populations – such as alemtuzumab, an anti-CD52 monoclonal antibody which promotes antibody dependent cell lysis; and teriflunomide, which blocks synthesis of pyrimidines (ie. nucleic acids) necessary for mitosis/cell-turnover [167, 233]. Many of these agents, which decrease white blood cell counts or block the renewal of somatic cellular populations, possess potentially serious side-effects, such as reduced immunocompetence or hepatotoxicity [167, 233]. Some of these agents create risks for secondary disorders/infections, such as progressive multifocal leukoencephalopathy (PML) – “an opportunistic infection of the brain that can lead to death or severe disability”, and a potential side effect of natalizumab [167, 233]. Apart from fingolimod, which is orally administered, these DMTs are

injectable, and may create tissue injury or irritation at the site of injection [167, 233]. Other side effects of specific DMTs include cardiovascular problems (fingolimod, mitoxantrone), autoimmune side effects (alemtuzemab), teratogenicity (teriflunomide), and flu-like symptoms (beta interferon) [167, 233]. The effect size of these DMTs in reducing relapse rates generally ranges between an approximate 30 to 60% reduction over the course of ~1 or 2 years treatment [167, 233]. As mentioned, no approved treatment can prevent the eventual transformation to progressive MS – DMTs merely reduce relapse rates and delay/postpone disease progression [167] [233]. Certain highly aggressive and experimental immunoablative protocols have been described in the literature which seem to ‘cure’ MS – however, these treatments are potentially lethal and have only been attempted in extremely severe/rapidly progressing cases of fulminant MS (Marburg’s variant) [167, 235].

Apart from DMTs, symptomatic treatments may be prescribed for the ‘secondary symptoms’ of MS. This includes antidepressants (ie. SSRIs) for depression/fatigue (also amantadine, psychostimulants) [236], treatments for spasticity (baclofen, benzodiazepines) [237], bladder problems, sexual dysfunction, diarrhea/constipation, and treatments for pain (*see below-section 1.4/5*). Donepezil, an acetylcholinesterase inhibitor used in the treatment of Alzheimer’s disease, was explored in MS-associated cognitive dysfunction, but was ineffective [238]. At present, there are no pharmacotherapeutic agents that are known to effectively treat cognitive dysfunction or tremor in MS. Dalfampridine (4-aminopyridine/4-AP) is a pro-convulsant potassium channel blocker that has been approved for the treatment of ‘impaired ambulation’ in MS. [233, 239]

### **1.3 – Experimental Autoimmune Encephalomyelitis (EAE)**

There are several inducible animal models which are used to study MS, each recapitulating specific features of the human disease. The most commonly used model, experimental autoimmune encephalomyelitis (EAE), possesses many similarities to MS in terms of its underlying pathology and behavioral symptoms. EAE was first discovered in 1933 following the observation that antirabies

vaccination - involving the injection of heterologous brain material - and recovery from certain viral infections, occasionally produce acute demyelination of the CNS and paralysis (known as acute disseminated encephalomyelitis – ADEM) [240-242]. It had also been observed the repeated injections of normal (rabbit) brain tissue in rabbits sometimes produced paralysis [240, 243]. Rivers, Sprunt and Berry [243] (followed by Rivers and Schwentker in 1935 [244]) determined that intramuscular injection of rabies vaccine alongside rabbit brain extract produced an acute disseminated encephalomyelitis with paralysis in monkeys. Subsequently it was realized that better results could be obtained by using purified myelin proteins alongside adjuvants (ie. complete Freund's adjuvant – CFA – heat-killed bacteria particles, designed to provoke an immune response). This method of inducing EAE is known as 'active' EAE/induction. The choice of myelin antigen used, and the amount of adjuvant - as well as the addition of pertussis toxin injections, and the choice of animal/strain - strongly influence the disease that results [241, 245]. The most commonly used antigens are the same myelin proteins which are currently suspected to be the initiating autoantigen(s) in MS – namely MBP, MOG, and PLP. Generally EAE is monophasic or progressive, although 'relapsing-remitting' models have sometimes been described in the literature [246]. The characteristic 'clinical' course of (murine/esp. MOG<sub>35-55</sub>) EAE involves an ascending paralysis progressing caudal to rostral, beginning with flaccid paralysis of the tail (around 5-15 days post induction), followed by weakness/paralysis of the hindlimbs [240, 247, 248]. EAE can also be induced by 'passive-' or 'adoptive-transfer', which involves transferring autoreactive T-cells from an animal in which active EAE has previously been induced, into a naïve animal [245]. More recently, 'spontaneous' EAE has been generated in transgenic mice engineered to over-express autoantigen-specific T-cell receptor molecules (TCRs) [192, 249, 250].

### **1.3.1 – Pathology/Pathogenesis of EAE**

The pathology of EAE has been extensively studied and is now well understood [240, 241, 245, 247, 249, 251]. As in MS, disruption of the BBB, widespread neuroinflammation (peripheral immune cell recruitment to the CNS, innate immune activation, and cytokine secretion), demyelination,

neurodegeneration, and axonopathy, are all primary pathological features of the disease [192, 245, 247, 251]. Despite obvious differences in the induction/etiology of the diseases, the pathology/pathogenic sequence of EAE is substantially similar to what is believed to occur in early (RR)MS, according to 'outside-in' (peripheral activation/infiltration) models [245, 246, 251]. Multiple lines of evidence indicate that EAE is primarily a CD4<sup>+</sup> T-cell driven disease [192, 249]. CD4<sup>+</sup> T-cells of the T<sub>H</sub>1 and T<sub>H</sub>17 classes are especially implicated in the pathogenesis of EAE [192, 247]. Autoreactive (T<sub>H</sub>1/T<sub>H</sub>17) CD4<sup>+</sup> T-cells - generated in the periphery following immunization - gain access to the CNS via the CSF (SAS, cisterna magna, choroid plexus), or by directly crossing the BBB [192]. Pertussis toxin is administered in most active EAE induction protocols, which is thought to promote the disease by helping disrupt the BBB and facilitate peripheral infiltration [252, 253]. There may, however, be immunomodulatory effects of pertussis toxin as well [254]. Once CD4<sup>+</sup> T-cells have infiltrated the CNS, they are reactivated by MHC class II APCs such as CD11c<sup>+</sup> dendritic cells [170, 192, 255]. The resulting neuroinflammatory response recruits peripheral monocytes into the CNS, a requirement for EAE initiation [192, 252]. It has been speculated that peripheral myeloid cells (ie. phagocytic macrophages, neutrophils) may be the major effector cells which mediate tissue damage in EAE - through phagocytosis, receptor-mediated cytotoxicity, and ROS production [188]. Additional nonpolarized CD4<sup>+</sup> T-cells are also recruited, and epitope spreading perpetuates and broadens the autoimmune/inflammatory response [192]. The production and circulation of pro-inflammatory cytokines is critical to EAE initiation and progression [188]. Cytokines may be derived from invading lymphocytes and myeloid cells, or from CNS-resident microglia [188]. T<sub>H</sub>1 lymphocyte-produced IFN $\gamma$ , and T<sub>H</sub>17-produced IL-17A and IL-7F, have been implicated in directing CNS infiltration and disrupting the BBB [188, 192]. As mentioned, the effects of IFN $\gamma$  are variable depending on context – for instance: blocking IFN $\gamma$  expression in astrocytes reduces the severity of EAE, while knocking out or blocking IFN $\gamma$  systemically exacerbates it [188]. Administering IFN $\gamma$  during the pre-onset 'priming' phase of EAE, exacerbates severity, while administering IFN $\gamma$  in the 'effector' stage (after onset) ameliorates it [188]. IL-17 is not critical to the development of EAE, but genetic deletion delays the onset and progression of

EAE [188]. IL-17R is expressed on endothelial cells, and activation of this receptor likely disrupts BBB integrity, promoting CNS infiltration (*see below*) [188]. Other pro-inflammatory cytokines driving EAE include: IL-1, IL-6, IL-12, IL-23, TGF $\beta$ , TNF $\alpha$ , and GM-CSF (granulocyte/macrophage colony stimulating factor) [167, 170, 188, 192]. IL-23 is thought to be critical to the initiation of EAE, as is IL-6 [188]. Blocking TNF $\alpha$  with anti-TNF antibodies delays the onset of EAE, though the severity of the disease is unchanged once initiated [188]. This contrasts with MS, wherein blocking TNF $\alpha$  actually increased the rate and severity of relapses – a counterintuitive effect that is likely related to the fact that TNF $\alpha$  can exist in different forms and bind to multiple receptors [188, 256]. Deficiency or blocking of IL-1/IL-1 receptors reduces the severity of EAE [188, 257]. Chemokines such as MCP-1/CCL2 (also CCL20/CCR6, CXCL8, CXCL10), and various cell-adhesion molecules (eg. integrins) - which may be secreted/expressed by astrocytes - are all elevated in the CNS in EAE [258, 259]. Additionally, expression of the fractalkine receptor CX3CR1 increases in microglia, and appears *de novo* in astrocytes during EAE [260]. Microglia also secrete elevated levels of proteolytic enzymes such as the MMPs (MMP-2, MMP-9, MMP-12) in the CNS during EAE [261]. All of these molecules generally facilitate recruitment of peripheral leukocytes across the BBB [167, 170, 188, 192]. CCL/CCR2 specifically are required for chemoattraction of monocytes in EAE; and CCR2+ monocyte-derived cells are thought to play an active role in demyelination during inflammation [188]. Mice lacking CCR2 are resistant to EAE (and are monocytopenic) [188].

Regulatory T-cells such as FoxP3+ CD4+ cells, and anti-inflammatory cytokines such as IL-10, can suppress T-cell recruitment/CNS infiltration: overexpression or heterologous transfer of FoxP3+/CD4+ cells can suppress spontaneous EAE [192]. However, these innate regulatory effects become overwhelmed in the disease [170]. Autoreactive CD8+ T-cells, which are thought to play a large role in the pathogenesis of MS, are less critically implicated in EAE [170, 192]. Nevertheless, autoreactive CD8+ T-cells are found in the CNS in EAE, and CD8+ cell depletion reduces the severity and mortality of EAE [192]. The role of B-cells in EAE is unclear, although MOG-specific antibodies (exogenous or

transgenically expressed) have been found to exacerbate EAE [187, 192]. Apart from adaptive immune cells, activated CNS-resident microglia are also critically implicated in EAE, as in MS [167, 170].

Reactive microglia promote and maintain inflammation and CNS lymphocyte infiltration, as well as contributing directly to myelin disruption and neuropathology/plasticity [170]. Astrocytes are also activated in the CNS in EAE, although they are not believed to directly contribute to disease initiation [170]. Astrocytes can, however, contribute to pathology and progression in the disease; for instance, through defective astrocytic glutamate reuptake, chemokine secretion, and BBB-disruption [167, 170].

The mechanisms by which EAE preferentially affects the spinal cord - leading initially to tail paralysis - whereas MS tends to favour the brain, are not fully understood [192, 246]. In both diseases, the location of inflammatory/ demyelinating lesions in the CNS is a major determinant of clinical outcomes [170]. One important factor in the anatomical specificity of EAE/MS may be differences in the ratio of  $T_H1$  to  $T_H17$  cells, and in the levels of their respective cytokines (IFN $\gamma$  and IL-17) [192]. The phenotypic consequences of these differing T-cell/cytokine ratios have been studied experimentally in animals with EAE induced by novel autoantigens [192]. These studies showed that adoptive transfer of T-cells specific for differing MOG epitopes produces different EAE phenotypes; with certain epitopes (eg. MOG<sub>35-55</sub>) tending to produce a 'spinal cord specific' disease, and others (specifically MOG<sub>97-114</sub>) producing a disease which *also* involves significant immune infiltration of the brain [192]. In adoptive transfer MOG<sub>35-55</sub> EAE, a preponderance of  $T_H1$  CD4+ T-cells, and of IFN $\gamma$ , tended to promote spinal cord inflammation [192]. Systemic depletion of IFN $\gamma$  has also been found to promote brain infiltration over spinal cord inflammation [192]. In MOG<sub>97-114</sub> adoptive transfer EAE, a preponderance of  $T_H17$  cells over  $T_H1$  cells, and of IL-17, favoured immune infiltration and inflammation of the brain [192]. The precise details of this mechanism, and its applicability to MS, are currently the subject(s) of investigation.

As in MS, diffuse GM pathology has also been observed in EAE brain and SC [167, 190, 262].

Structural and functional alterations, synaptopathy, and altered neuronal metabolism have all been

observed in various regions of the CNS - including the cerebral cortex, the striatum, and the amygdala [206, 220-222, 263-266]. Various studies have pointed to neuronal hyperexcitability and excessive glutamatergic neurotransmission leading to excitotoxicity, and subsequent synaptic loss and axonal degeneration, in the CNS in EAE [264, 266-270]. Loss of inhibition / GABAergic neuronal dysfunction and degeneration has also been observed [223, 225]. This topic is the subject of more detailed discussion in subsequent chapters.

### **1.3.2 – Secondary Symptoms of EAE/MS**

Apart from pain (*discussed in detail in section-1.4/1.5*), EAE can also be used to model several other 'secondary symptoms' of MS [241, 270-272]. These are symptoms and behaviors other than the primary clinical outcomes and measures (ie. paralysis / motor dysfunction). These include depressive/sickness behaviors, and cognitive/memory dysfunction, both of which have been previously investigated in the C57/BL6 MOG<sub>35-55</sub> EAE model in our lab [273, 274]. Musgrave et al. (2011) [275] noted that mice in this model express sickness behaviors, such as consistently gazing below the horizon, reduced exploratory ambulation, and increased production of fecal boli, compared to controls. Olechowski et al. (2013) [274] examined cognitive function in the model with the novel-object recognition assay, and found the EAE mice to be significantly impaired.

## **1.4 – Pain in MS**

Pain, along with cognitive dysfunction, is one of the most common and debilitating secondary symptoms of MS [15, 276, 277]. Roughly 50% (29-86%) of MS patients experience pain as a symptom of their disease at some point in their progression [276, 278-280], making pain significantly more common in MS patients than in the non-MS population; and for 1/5 patients, pain is present at disease onset [281]. Pain in MS significantly impacts quality of life and impedes rehabilitation, with roughly a third of patients considering pain as one of the worst symptoms of their disease [15, 278]. A variety of pain phenotypes have been identified in MS, including: continuous or intermittent central neuropathic

pain, musculoskeletal pain, mixed neuropathic/non-neuropathic pain, and MS-related facial pain/trigeminal neuralgia [276, 281, 282]. Other sensory abnormalities and pain syndromes associated with MS include painful dysaesthesias (tingling) affecting the extremities, Lhermitte's sign, painful spasms, headache/migraine and low back pain [276, 282, 283]. Women tend to experience more severe pain, but susceptibility is comparable between the genders [284]. Although pain has no specific relationship to disease severity, as MS progresses clinically, the severity of MS-related pain may also progress/increase [276].

Some reports indicate that more than half of MS patients with pain (or 30% of overall MS patients) are affected by central neuropathic pain [284]. Central neuropathic pain generally results from a CNS lesion (or lesions) located in the somatosensory/nociceptive circuitry [283]. Typically this involves a lesion within the posterior column and/or ascending spinothalamic tract [283]. Lesions within the thalamus or PAG are also sometimes associated with pain in MS [285, 286]. Central neuropathic pain may manifest in multiple areas simultaneously, with lesion placement influencing pain location [283]. MS associated trigeminal neuralgia invariably involves a lesion in the trigeminal nucleus or nerves [286]. Pain in MS may be either evoked and/or spontaneous, paroxysmal, or ongoing [276, 281, 283, 284]. Pain (or tingling/numbness) in the extremities is extremely common in MS-related central neuropathic pain [287]. Enhanced pain sensitivity and reduced pain-perceptual thresholds are another common feature [278, 281, 283, 284]. Many MS patients with central neuropathic pain also experience thermal and mechanical allodynia [284],[278]. The precise mechanistic details of central neuropathic pain in MS have not been elucidated. However, deafferentation effects due to demyelinating/inflammatory lesions, possibly leading to conduction block and disinhibition, or hyperexcitability/ectopic discharges (upsetting the central E-I balance), appear to be involved [283]. The systemic inflammatory environment, and dorsal horn, thalamic, and cortical (grey matter) perturbations (again: consisting of hyperexcitability/excessive glutamate levels/excitotoxicity, gliosis and immune infiltration, circulating cytokines/chemokines/complement proteins/antibodies/proteolytic

enzymes/inflammatory mediators, metabolic dysfunction and virtual hypoxia, ROS, toxic cellular/myelin debris and lipid peroxidation byproducts, neurodegeneration and axonal loss, loss of inhibition, BBB disruption, altered trophic support, and synaptic/structural plasticity etc.) are also likely involved [34, 288-290].

No specific treatments exist for pain (or central neuropathic pain) in MS. As in other forms of chronic pathological pain, the first-line treatments for pain in MS include SNRIs/TCAs, and anticonvulsants such as gabapentin, carbamazepine, lamotrigine, and topiramate [34, 290-292]. Opioids, cannabinoids (eg. dronabinol, sativex), and intrathecal baclofen (a GABA-B agonist) are second/third line treatment options [291]. None of these treatments is particularly effective in a majority of cases [34, 278, 292, 293].

### **1.5 – Pain (Altered Nociception) in EAE**

In recent years, EAE has been established as a useful model for studying pain in MS (esp. central neuropathic pain / trigeminal neuralgia), and many mechanistic insights into the underlying neurobiology/pathology have been gleaned from it [34, 290, 294, 295]. As noted in previous sections, there may be limits to the applicability and translatability of mechanistic insights garnered from EAE to MS, due to differences in the underlying pathological mechanisms and clinical/symptomatic profile of each disease [240, 242, 246, 249, 251, 296]. Nevertheless, EAE still represents the only viable model for many types of studies, and the relative dearth of studies on pain in MS makes studies in EAE even more necessary. Several models have been employed, with differing pain phenotypes (and likely somewhat divergent underlying pathobiologies) [273, 290, 294, 297]. C57/BL6 mice (esp. females) with MOG<sub>35-55</sub>-induced EAE are the focus of this thesis. Olechowski et al. [273] performed the foundational work and initial characterization of nociceptive behaviors in this model in 2009. These mice develop robust mechanical and (less frequently) thermal (cold) allodynia affecting their hindlimbs in the early stages the disease, before paralysis sets in. More recently, Thorburne et al. (2016) [298] established

that these mice also exhibit exaggerated facial pain behaviors – assessed by the facial grimace scale, in later stages or more clinically advanced disease - when hindlimb motor dysfunction confounds conventional pain testing. Several other groups have also looked at pain behaviors in the MOG<sub>35-55</sub> C57/BL6 EAE model, and have used the model to evaluate potential treatment strategies [290, 299-307]. Mechanical sensitivity is the most commonly observed behavioral measure of pain in MOG EAE mice, although a few studies have also found increased heat sensitivity (hotplate/Hargreave's test) in this model [273, 274, 294, 301, 308]. This discrepancy may be related to differences in induction protocols (eg. use of PTX, volumes of MOG/CFA, age/source of mice etc.).

Other studies have examined nociceptive behaviors or neurophysiological correlates (ie. electrophysiological measures) of nociception in the Lewis rat EAE model (various antigens/induction methods) or in the SJL/J mouse / PLP<sub>139-151</sub> EAE model [294, 297]. Generally, the disease produced in the Lewis rat is monophasic/transient, whereas SJL/J + PLP<sub>139-151</sub> mice exhibit a “relapsing remitting” or “progressive” disease course (similar to MOG EAE) [240, 241, 245, 247, 248, 251, 290, 296]. In both models (Lewis rat / SJL/J), thermal (heat) hyperalgesia has been observed, and SJL/J + PLP mice also develop mechanical allodynia/hypersensitivity at later disease time points (compared to the early mechanical allodynia in MOG EAE) [34, 290, 295, 306]. Thibault et al. (2011) [295] directly compared the efficacy of many of the most widely used pain treatments in the Lewis rat EAE model (ie. duloxetine, gabapentin, morphine, NSAIDs etc.). Kuner/Lu et al. (2012) [306] directly compared pain behaviors in SJL/J PLP mice to C57/BL6 MOG EAE, and noted differences in the time course of pain symptoms in these models. Electrophysiological studies in the Lewis rat and SJL/J PLP mice have pointed to altered function (hyperexcitability, or reduced conduction velocity/conduction block indicative of demyelination) of DRG primary afferent neurons – especially low-threshold myelinated afferents - which may drive central sensitization in these models [306, 309-312]. However, Khan et al. (2014) [290] noted that the antigens used in these models (PLP, MBP etc.) are ubiquitous in both the PNS and CNS, whereas MOG is found only in the CNS (although this assertion has been challenged). Because pain in

humans with MS generally follows from a CNS lesion, it has been argued that MOG may be a more valid model (if the preceding assertion is true) [290]. Other groups have pointed out that, given the heterogeneity of MS - and pain conditions in MS - multiple models are needed to study pain in MS [306]. Several recent studies have also suggested that MOG EAE may too involve sensitization (or disruption/blockade) of primary afferents in the DRG/PNS (ie. demyelinated A fibres) [313, 314]. Whether these PNS changes precede and drive CNS changes, or are merely contemporaneous, is not currently known. Likewise, while demyelinating lesions within the CNS seem to be a prerequisite for the development of neuropathic pain in MS, the role and contribution of central demyelination in altered nociceptive sensitivity in EAE is not clear [34, 290, 306, 313]. MOG EAE mice do develop widespread central demyelination and axonal loss, but this may occur at later stages of the disease - whereas pain presents in the early stages [290]. However, Gritsch/Kuner et al. (2014) were able to recapitulate a similar pain phenotype to MOG EAE by selectively ablating oligodendrocytes in the CNS (using a genetically targeted diphtheria toxin system) in otherwise naïve mice [315]. This finding demonstrates that, at least in principle, oligodendrocyte loss and accompanying demyelination, in the absence of a central autoimmune/neuroinflammatory response is sufficient to produce EAE-like pain behaviors.

Within the dorsal horn, EAE (MOG/PLP) mice exhibit elevated grey-matter penetrating (infiltrating) CD3/CD45+ T-cells, elevated glial-fibrillary acid protein (GFAP)+ immunoreactivity (reactive astrocytes), and elevated ionizing calcium-binding adaptor-1 (Iba-1)+ reactive microglia [273, 306, 313]. Infiltrating T-cells peak in the dorsal horn early in the disease and then decline, whereas GFAP/Iba-1+ staining persist [273, 306]. Peripheral and central (dorsal horn) CGRP+ and galanin+ staining is unaltered in EAE, suggesting peptidergic C fibres are (grossly) unperturbed in the disease [273]. c-Fos+ cell bodies - an indicator of neuronal activity and of central-sensitization - are basally elevated in the dorsal horn of EAE mice [273]. These findings suggested that gliosis within the dorsal horn might be involved in producing central sensitization, and the observed pain phenotype (ie. allodynia) in EAE [33, 316, 317]. A role for astrocytes was confirmed by Olechowski et al. (2010) [318], who identified

disruption and reversal of the astrocytic glutamate reuptake transporters (EAAT-1/2) in the dorsal horn, leading to elevations in extracellular glutamate (confirmed in Musgrave et al. (2011) [319]) and hyperexcitability/allodynia [50, 269, 320-322]. Treatment with the glutamate transporter activator MS-153 reduced dorsal horn c-Fos+ puncta [318], and the EAAT-2 upregulating drug ceftriaxone normalized mechanical withdrawal thresholds in MOG EAE mice [274]. In addition to elevated glutamate levels, Musgrave et al. (2011) also found that the concentrations of monoamine neurotransmitters (5-HT, NA, and DA) were reduced in spinal cord, brain stem, and brain homogenate from EAE mice early in the disease, and progressively declined [319]. In later disease, GABA concentrations in the CNS were also reduced.

Several studies have also highlighted the role of proinflammatory cytokines acting in the dorsal horn (or DRG) to produce central sensitization in EAE [290, 304, 323-326]. Similarly, anti-inflammatory cytokines may counteract these effects; intrathecal administration of a plasmid driving the (over)-expression of IL-10 reduced mechanical hypersensitivity in murine EAE [327]. Melanson et al. (2009) [324] found evidence of elevated TNF $\alpha$  levels in DRGs in (Lewis rat) EAE, and surmised that TNF $\alpha$  underwent anterograde transport to the dorsal horn. Begum et al. (2013) [325] found that TNF $\alpha$  levels in the dorsal horn correlated with tail sensitivity (ie. to noxious heat) in EAE. Olechowski et al. (2013) [274] measured circulating pro-inflammatory cytokines (IL-1 $\beta$ , IL-6) in MOG EAE, and found them to be elevated early in the disease (at clinical onset) when pain behaviors were present. Other studies have suggested that chemokines such as CCL2/MCP-1, CCR5, and CX3CL1/CX3CR1, and MMPs (-2/9), or even prostaglandins - which are elevated in EAE/MS tissues [34, 188, 261] - may be implicated in the development of central sensitization in EAE/MS [308, 326, 328-331]. Soluble TNF $\alpha$  was found to drive synaptic plasticity (dendritic spine turnover) in primary somatosensory cortex in both early and late MOG EAE [207]. Many of these cytokines and enzymes may be produced and secreted by reactive microglia within the DH [33, 188, 316, 330, 332-334], supporting the proposed role of resident glia in promoting neuropathic pain-like behaviors and symptoms in EAE. Also supporting this role is the fact

that treatment with the microglial inhibitor minocycline normalized pain behaviors in EAE, although it also alleviated/interrupted the ‘clinical’ progression of the disease [335]. A non-pharmacological, behavioral intervention (voluntary exercise-wheel running) was found to reduce the severity of mechanical allodynia, and alleviate oxidative stress (increase the ratio of reduced glutathione to oxidized glutathione, and reduce inducible nitric oxide synthase (iNOS) expression) in the dorsal horn [336].

## **1.6 – Phenzelzine**

Much of this thesis concerns the effects of the drug phenzelzine (PLZ) on pain in naïve/formalin-treated mice, and in EAE. Although this drug will be described again in later sections, PLZ is an antidepressant from the monoamine-oxidase inhibitor (MAOI) class. This drug irreversibly inhibits both isoforms of monoamine oxidase (MAO-A/B) – one of the primary degradative enzymes for the monoamine neurotransmitters (5-HT, NA, and DA) – the other main degradative enzyme being catechol-O-methyltransferase (COMT) [337, 338]. Inhibition of MAO by PLZ produces sustained increases in CNS tissue concentrations of the monoamines [338]. The reaction between PLZ and MAO also produces an active metabolite, phenethylidenehydrazine (PEH), which has been established as having anxiolytic effects related to its ability to inhibit the enzyme GABA-transaminase (GABA-T) [339-341]. Inhibition of GABA-T by PEH leads to enhanced concentrations of GABA within inhibitory presynaptic terminals, enhanced extracellular GABA (CNS), and augmented inhibitory neurotransmission [337, 341, 342]. A range of other mechanisms have been attributed to PLZ, including reducing glutamatergic outflow (by interfering with GABA/glutamine interconversion) [343, 344], neuroprotection by “scrubbing” of reactive aldehyde species [337, 345], and possibly direct interactions with trace-amine receptors (TAARs) or monoamine receptors [337]. This thesis focuses on the monoaminergic component of PLZ’s effects, though other mechanisms will be discussed throughout.

Previously, Mifflin et al. (2016) [346] explored the effects of PLZ on formalin-evoked pain behaviors in male and female mice. PLZ and PEH were found to inhibit pain behaviors in both sexes. A PLZ analogue lacking the PEH-mediated component of PLZ's effect (ie. retaining only the monoaminergic component), known as N<sub>2</sub>-acetyl-PLZ (N<sub>2</sub>-Ac-PLZ) inhibited formalin evoked pain behaviors in males but not females. The inhibition in males could be blocked by intrathecal administration of the 5-HT<sub>1A</sub>R antagonist WAY-100,635, but not the adrenergic (alpha-2) antagonist idazoxan. In EAE, Benson and Musgrave [347, 348] found that acute and chronic PLZ treatment restored CNS concentrations of the monoamine neurotransmitters and GABA. Chronic PLZ treatment was found to delay the onset of clinical (paralytic) symptoms of EAE by several days, and to improve functional (motor) outcomes for a modest period of time. Providing the PLZ once every second day, as opposed to daily, sustained the functional/clinical effects of the drug. This dosing schedule likely extends the formation/action of the PLZ-metabolite PEH, which declines when PLZ is given daily, due to complete irreversible inhibition of the MAO necessary for the generation of PEH. These earlier experiments form the basis of the experiments with PLZ which are the focus of this thesis, and they will be discussed again in later chapters.

## **1.7 – Aims and Scope**

The purpose of this thesis was to characterize functional and structural (neuronal morphological/synaptic) plasticity within the CNS (specifically, in the dorsal horn and the primary somatosensory cortex) related to altered nociception in female C57/BL6 + MOG<sub>35-55</sub> EAE. A second aim was to evaluate the MAOI PLZ as a treatment for pain behaviors and pain-related CNS plasticity in EAE, and to examine PLZ's mechanism(s) of action in the disease. A third aim was to evaluate the effects of acute PLZ treatment on nociceptive behaviors and dorsal horn activity in naïve and/or (acute) formalin-treated (female C57/BL6) mice, and to explore the relevant mechanism(s) of action.

## **1.8 – Approaches / Hypotheses**

In **Chapter 2**, we tested the **hypothesis** that PLZ would reduce the expression of basal nociceptive behaviors and/or response durations in the formalin assay. We also tested the **hypothesis** that pretreatment with PLZ would reduce evoked neuronal activation in the dorsal horn, by measuring c-Fos expression following formalin injection, and by ratiometric calcium imaging in *ex vivo* spinal cord slices.

In **Chapter 3**, we tested the **hypothesis** that early time points in EAE disease progression would be associated with increased neuronal activity within the dorsal horn in response to a vibromechanical stimulus and/or bath-applied glutamate (in slice). We again made use of c-Fos immunohistochemistry (IHC) and ratiometric calcium imaging in *ex vivo* lumbar slices. We also tested the **hypothesis** that chronic treatment with PLZ, initiated at 7 days-post inoculation, would normalize nociceptive behaviors in early EAE. Furthermore, we examined the effects of chronic PLZ treatment on functional responses within the dorsal horn. Lastly, we used IHC to identify structural/synaptic plasticity in the dorsal horn in EAE, and to test the hypothesis that PLZ would reduce cellular markers of inflammation in the dorsal horn.

In **Chapter 4**, we tested the **hypothesis** that early time points in EAE would be associated with functional plasticity in the primary somatosensory cortex. We made use of *in vivo* flavoprotein autofluorescence optical imaging (FAI) to look at S1 neuronal-ensemble responses to vibromechanical stimulation of the paws. In addition we looked for structural/synaptic changes in S1 in EAE using Golgi-Cox staining and IHC. We found evidence of both proexcitatory synaptic changes in S1, and a loss of inhibitory function/synaptic structures. Lastly, we tested the effects of chronic PLZ treatment on all of these measures, and also looked at cellular inflammation in S1 with IHC.

Figure 1.1

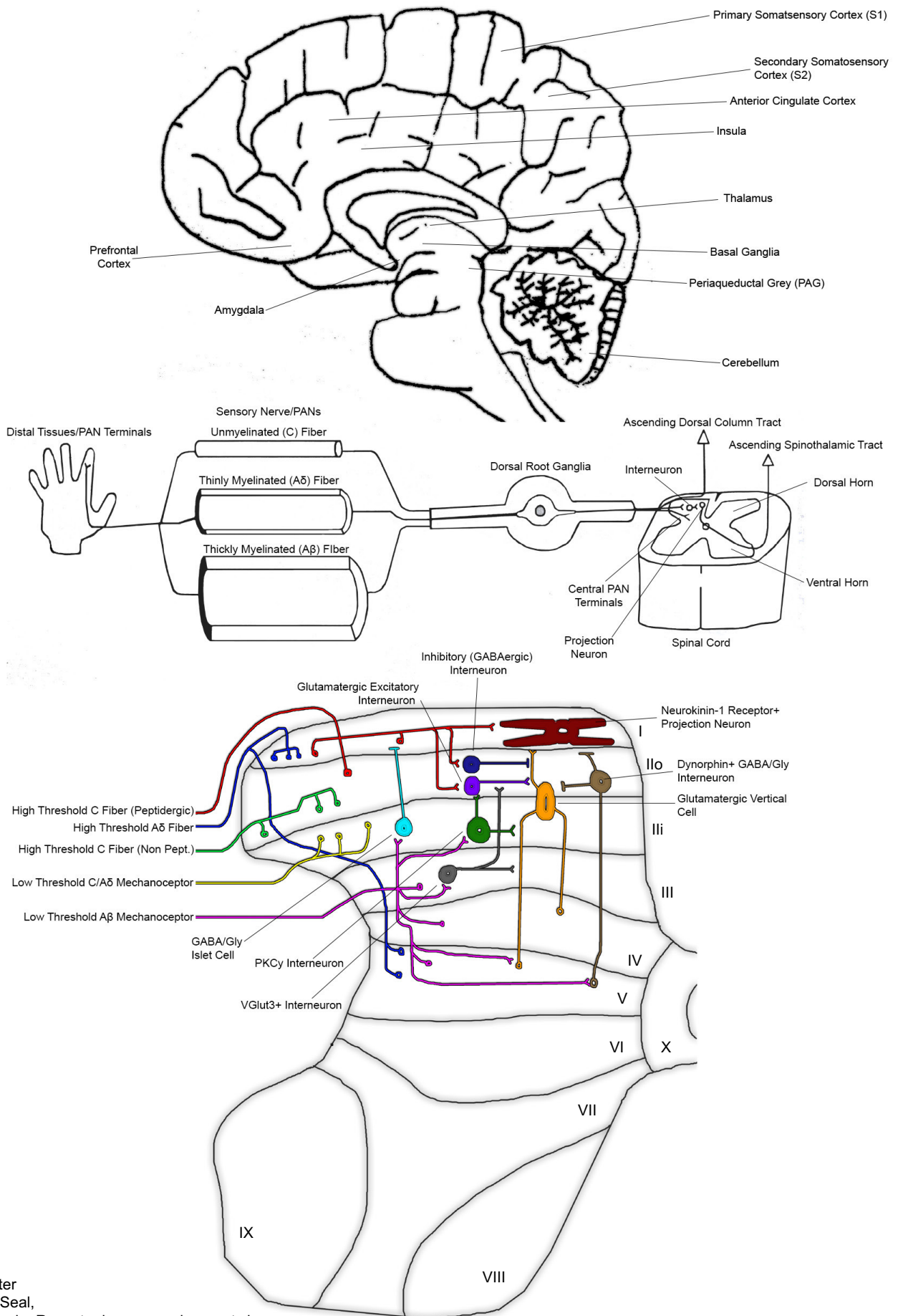


Figure modeled after Piers, C. and R.P. Seal, Neural circuits for pain: Recent advances and current views. Science, 2016. 354(6312): p. 578.

Figure 1.2

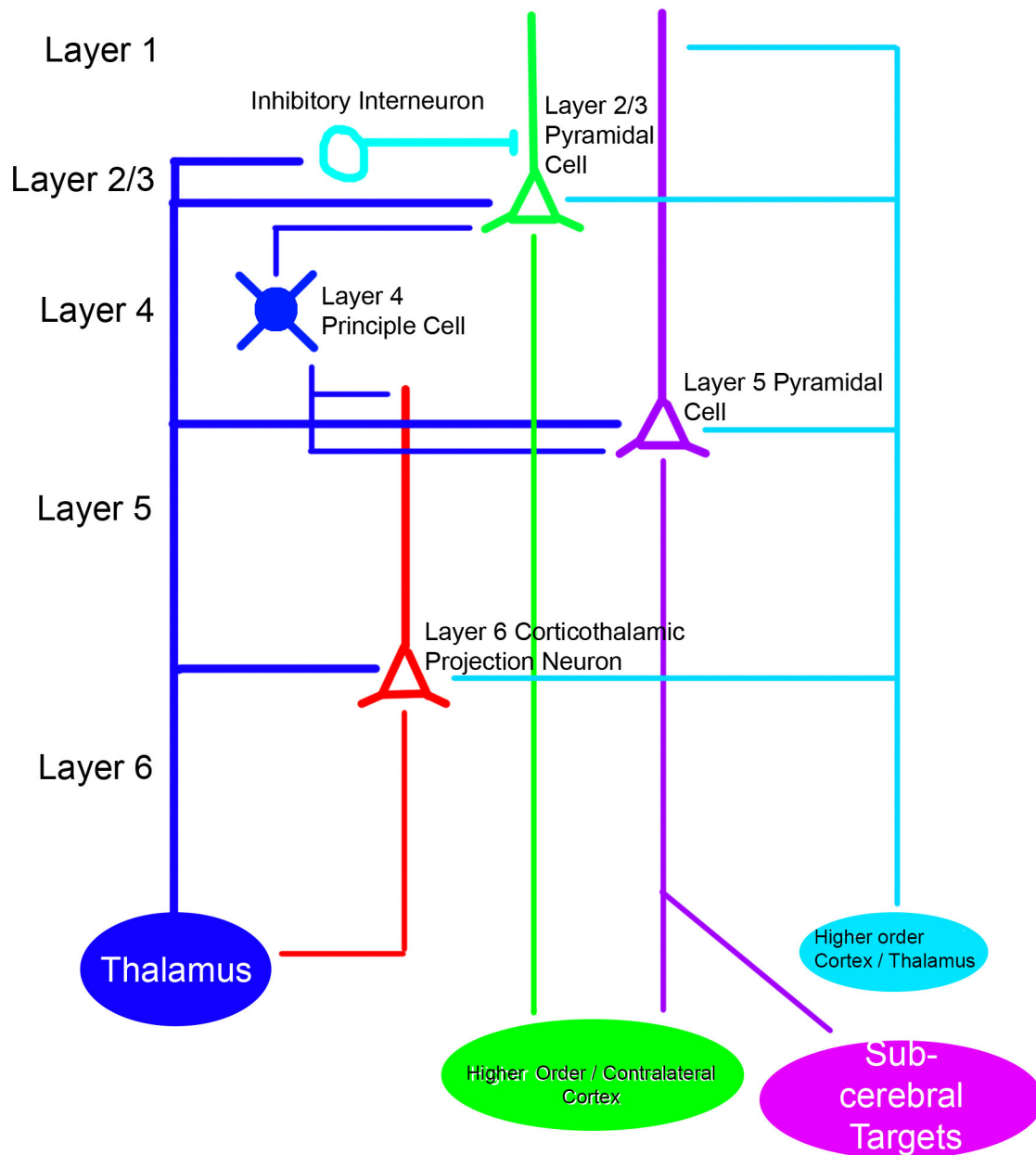


Figure modeled after

Box 1: Canonical connectivity of cortical principal cells From Cortical connectivity and sensory coding

Kenneth D. Harris & Thomas D. Mrsic-Flogel Nature 503, 51–58 (07 November 2013) doi:10.1038/nature12654

Figure 1.3

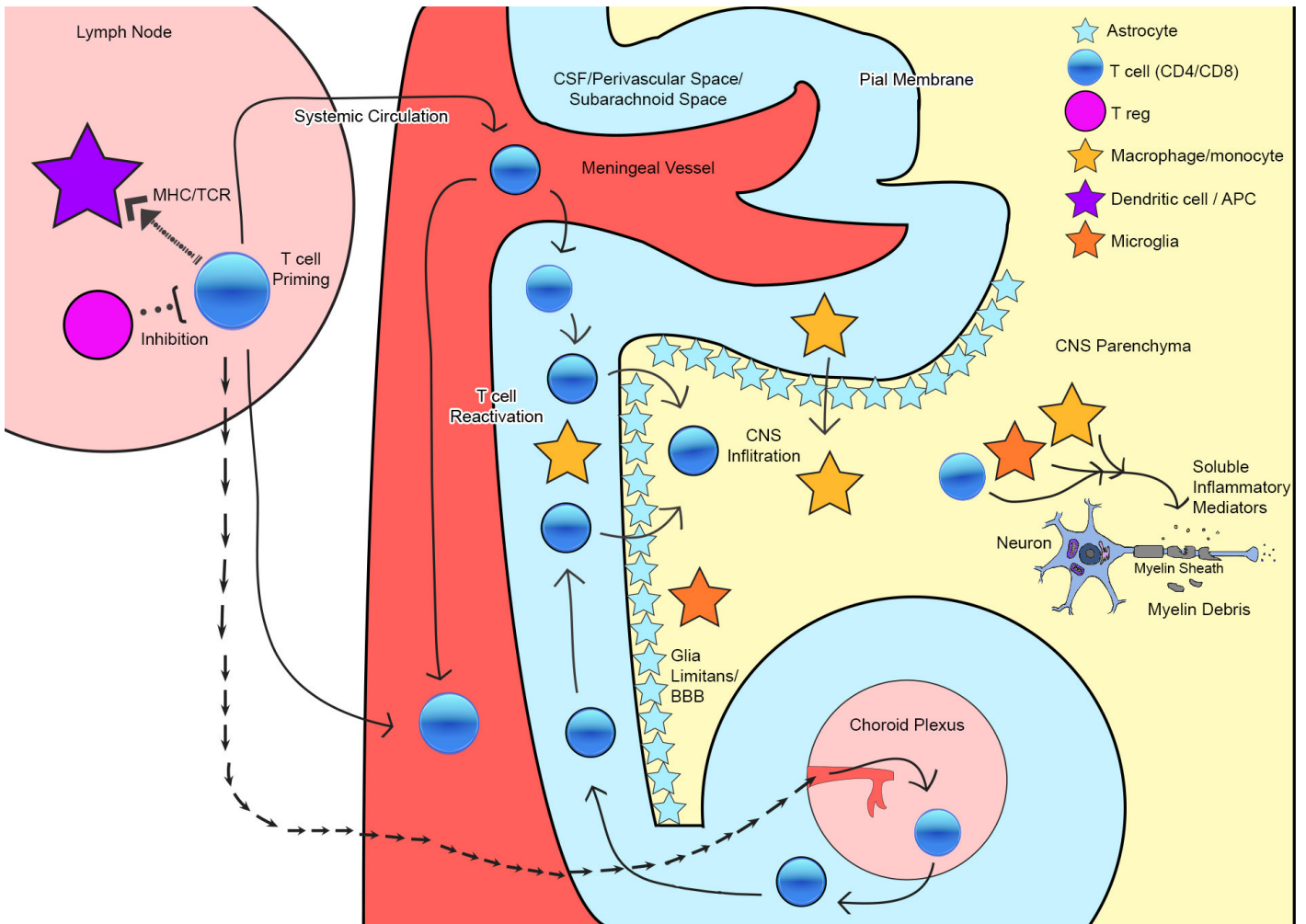
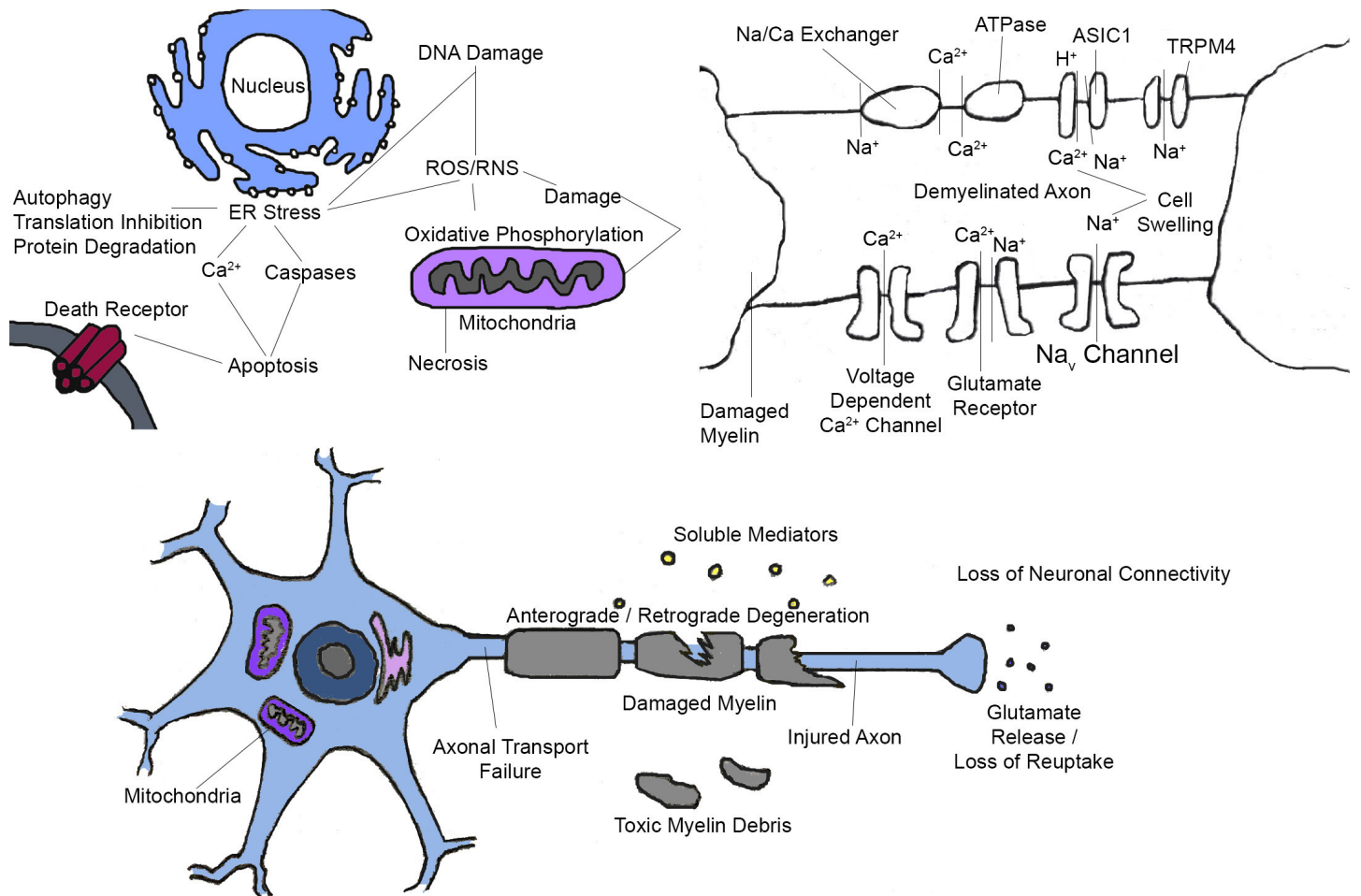


Figure modeled after  
Goverman, J., Autoimmune T cell responses in the central nervous system. Nature reviews. Immunology, 2009. 9(6): p. 393.

Figure 1.4



## 1.9 – REFERENCES

1. Sandkühler, J., *Models and Mechanisms of Hyperalgesia and Allodynia*. Physiological Reviews, 2009. **89**(2): p. 707.
2. Ji, R.-R., et al., *Central sensitization and LTP: do pain and memory share similar mechanisms?* Trends in Neurosciences, 2003. **26**(12): p. 696-705.
3. Julius, D.M., E.W., *Cellular and molecular properties of primary afferent neurons*, in in *Melzack & Wall's Textbook of Pain 5th Ed.*2005, Elsevier.
4. Woolf, C.J., *What is this thing called pain?* The Journal of clinical investigation, 2010. **120**(11): p. 3742-3744.
5. Craig, A.D., *Pain mechanisms: labeled lines versus convergence in central processing*. Annu Rev Neurosci, 2003. **26**: p. 1-30.
6. Woolf, C.J.S., M. W., *Plasticity and pain: role of the dorsal horn*, in in *Wall & Melzack's Textbook of Pain, 5th ed.*2005, Elsevier.
7. Millan, M.J., *The induction of pain: an integrative review*. Progress in neurobiology, 1999. **57**(1): p. 1-164.
8. Todd, A.K., H.R., *Neuroanatomical substrates of spinal nociception*, in in *Wall & Melzack's Textbook of Pain, 5th ed.*2005, Elsevier.
9. Costigan, M., J. Scholz, and C.J. Woolf, *Neuropathic Pain: A Maladaptive Response of the Nervous System to Damage*. Annual review of neuroscience, 2009. **32**: p. 1-32.
10. Doleys, D.M., *Chronic Pain as a Hypothetical Construct: A Practical and Philosophical Consideration*. Frontiers in Psychology, 2017. **8**: p. 664.
11. Goldberg, D.S. and S.J. McGee, *Pain as a global public health priority*. BMC Public Health, 2011. **11**: p. 770.
12. von Hehn, Christian A., R. Baron, and Clifford J. Woolf, *Deconstructing the Neuropathic Pain Phenotype to Reveal Neural Mechanisms*. Neuron, 2012. **73**(4): p. 638-652.
13. Campbell, J.N. and R.A. Meyer, *Mechanisms of Neuropathic Pain*. Neuron, 2006. **52**(1): p. 77-92.
14. Verma, S., L. Estanislao, and D. Simpson, *HIV-Associated Neuropathic Pain*. CNS drugs, 2005. **19**(4): p. 325-334.
15. Khan, F. and J. Pallant, *Chronic Pain in Multiple Sclerosis: Prevalence, Characteristics, and Impact on Quality of Life in an Australian Community Cohort*. The Journal of Pain, 2007. **8**(8): p. 614-623.
16. Woolf, C.J., *Central sensitization: Implications for the diagnosis and treatment of pain*. Pain, 2011. **152**(3 Suppl): p. S2-15.
17. Treede, R.-D., et al., *A classification of chronic pain for ICD-11*. Pain, 2015. **156**(6): p. 1003-1007.
18. Bushnell, C.M.A., A. V., *Representation of pain in the brain*, in in *Wall & Melzack's Textbook of Pain, 5th ed.*2005, Elsevier.
19. Todd, A.J., *Neuronal circuitry for pain processing in the dorsal horn*. Nature reviews. Neuroscience, 2010. **11**(12): p. 823-836.
20. Dubin, A.E. and A. Patapoutian, *Nociceptors: the sensors of the pain pathway*. The Journal of clinical investigation, 2010. **120**(11): p. 3760-3772.
21. Kuner, R., *Central mechanisms of pathological pain*. Nat Med, 2010. **16**(11): p. 1258-66.
22. Woolf, C.J., *Neuronal Plasticity: Increasing the Gain in Pain*. Science, 2000. **288**(5472): p. 1765-1768.
23. Peirs, C. and R.P. Seal, *Neural circuits for pain: Recent advances and current views*. Science, 2016. **354**(6312): p. 578.
24. Braz, J., et al., *Transmitting pain and itch messages: A contemporary view of the spinal cord circuits that generate Gate Control*. Neuron, 2014. **82**(3): p. 522-536.
25. Melzack, R. and P.D. Wall, *Pain mechanisms: a new theory*. Science, 1965. **150**(3699): p. 971-9.
26. Kuner, R. and H. Flor, *Structural plasticity and reorganisation in chronic pain*. Nat Rev Neurosci, 2017. **18**(1): p. 20-30.

27. Woolf, C.J., *Evidence for a central component of post-injury pain hypersensitivity*. Nature, 1983. **306**(5944): p. 686-8.
28. Millan, M.J., *Descending control of pain*. Progress in neurobiology, 2002. **66**(6): p. 355-474.
29. Latremoliere, A. and C.J. Woolf, *Central Sensitization: A Generator of Pain Hypersensitivity by Central Neural Plasticity*. The journal of pain : official journal of the American Pain Society, 2009. **10**(9): p. 895-926.
30. Peirs, C., et al., *Dorsal Horn Circuits for Persistent Mechanical Pain*. Neuron, 2015. **87**(4): p. 797-812.
31. Nickel, F.T., et al., *Mechanisms of neuropathic pain*. European Neuropsychopharmacology, 2012. **22**(2): p. 81-91.
32. Hunskaar, S. and K. Hole, *The formalin test in mice: dissociation between inflammatory and non-inflammatory pain*. Pain, 1987. **30**(1): p. 103-14.
33. Scholz, J. and C.J. Woolf, *The neuropathic pain triad: neurons, immune cells and glia*. Nat Neurosci, 2007. **10**(11): p. 1361-8.
34. Iannitti, T., B.J. Kerr, and B.K. Taylor, *Mechanisms and Pharmacology of Neuropathic Pain in Multiple Sclerosis*. Current topics in behavioral neurosciences, 2014. **20**: p. 75-97.
35. Luo, C., et al., *Activity-dependent potentiation of calcium signals in spinal sensory networks in inflammatory pain states*. Pain, 2008. **140**(2): p. 358-367.
36. Sandkühler, J., et al., *Synaptic mechanisms of hyperalgesia*. Prog Brain Res, 2000. **129**: p. 81-100.
37. Taylor, B.K. and G. Corder, *Endogenous analgesia, dependence, and latent pain sensitization*. Curr Top Behav Neurosci, 2014. **20**: p. 283-325.
38. Sandkühler, J. and J. Lee, *How to erase memory traces of pain and fear*. Trends in Neurosciences, 2013. **36**(6): p. 343-352.
39. Gwak, Y.S. and C.E. Hulsebosch, *GABA and central neuropathic pain following spinal cord injury*. Neuropharmacology, 2011. **60**(5): p. 799-808.
40. Coull, J.A., et al., *Trans-synaptic shift in anion gradient in spinal lamina I neurons as a mechanism of neuropathic pain*. Nature, 2003. **424**(6951): p. 938-42.
41. Pertovaara, A., *Noradrenergic pain modulation*. Progress in neurobiology, 2006. **80**(2): p. 53-83.
42. Sonohata, M., et al., *Actions of noradrenaline on substantia gelatinosa neurones in the rat spinal cord revealed by in vivo patch recording*. The Journal of physiology, 2004. **555**(2): p. 515-526.
43. Jeong, C.Y., J.I. Choi, and M.H. Yoon, *Roles of serotonin receptor subtypes for the antinociception of 5-HT in the spinal cord of rats*. European Journal of Pharmacology, 2004. **502**(3): p. 205-211.
44. Bardin, L., J. Lavarenne, and A. Eschalier, *Serotonin receptor subtypes involved in the spinal antinociceptive effect of 5-HT in rats*. Pain, 2000. **86**(1-2): p. 11-18.
45. Abe, K., et al., *Responses to 5-HT in morphologically identified neurons in the rat substantia gelatinosa in vitro*. Neuroscience, 2009. **159**(1): p. 316-324.
46. Xie, D.J., et al., *Identification of 5-HT receptor subtypes enhancing inhibitory transmission in the rat spinal dorsal horn in vitro*. Molecular pain, 2012. **8**: p. 58.
47. Buritova, J., et al., *Effects of the high-efficacy 5-HT1A receptor agonist, F 13640 in the formalin pain model: A c-Fos study*. European Journal of Pharmacology, 2005. **514**(2): p. 121-130.
48. Millan, M.J., *Serotonin and pain: evidence that activation of 5-HT1A receptors does not elicit antinociception against noxious thermal, mechanical and chemical stimuli in mice*. Pain, 1994. **58**(1): p. 45-61.
49. Bardin, L., *The complex role of serotonin and 5-HT receptors in chronic pain*. Behav Pharmacol, 2011. **22**(5-6): p. 390-404.
50. Chiang, C.-Y., et al., *Astroglial Glutamate-Glutamine Shuttle Is Involved in Central Sensitization of Nociceptive Neurons in Rat Medullary Dorsal Horn*. The Journal of Neuroscience, 2007. **27**(34): p. 9068.
51. Scholz, J. and C.J. Woolf, *The neuropathic pain triad: neurons, immune cells and glia*. Nature Neuroscience, 2007. **10**(11): p. 1361-1368.

52. Ferrini, F., et al., *Morphine hyperalgesia gated through microglia-mediated disruption of neuronal Cl<sup>-</sup> homeostasis*. Nat Neurosci, 2013. **16**(2): p. 183-192.
53. Sorge, R.E., et al., *Different immune cells mediate mechanical pain hypersensitivity in male and female mice*. Nature Neuroscience, 2015. **18**(8): p. 1081-1083.
54. Mapplebeck, J.C., S. Beggs, and M.W. Salter, *Sex differences in pain: a tale of two immune cells*. Pain, 2016. **157** Suppl 1: p. S2-6.
55. Brings, V.E. and M.J. Zylka, *Sex, drugs and pain control*. Nat Neurosci, 2015. **18**(8): p. 1059-60.
56. Ji, R.R., Z.Z. Xu, and Y.J. Gao, *Emerging targets in neuroinflammation-driven chronic pain*. Nat Rev Drug Discov, 2014. **13**(7): p. 533-48.
57. Tracey, I. and P.W. Mantyh, *The Cerebral Signature for Pain Perception and Its Modulation*. Neuron, 2007. **55**(3): p. 377-391.
58. Melzack, R., *From the gate to the neuromatrix*. Pain, 1999. **82**: p. S121-S126.
59. May, A., *Chronic pain may change the structure of the brain*. Pain, 2008. **137**(1): p. 7-15.
60. Legrain, V., et al., *The pain matrix reloaded: A salience detection system for the body*. Progress in neurobiology, 2011. **93**(1): p. 111-124.
61. Willis, W.D. and K.N. Westlund, *Neuroanatomy of the pain system and of the pathways that modulate pain*. J Clin Neurophysiol, 1997. **14**(1): p. 2-31.
62. Ab Aziz, C.B. and A.H. Ahmad, *The Role of the Thalamus in Modulating Pain*. The Malaysian Journal of Medical Sciences : MJMS, 2006. **13**(2): p. 11-18.
63. Feldmeyer, D., *Excitatory neuronal connectivity in the barrel cortex*. Frontiers in Neuroanatomy, 2012. **6**: p. 24.
64. Cruikshank, S.J., T.J. Lewis, and B.W. Connors, *Synaptic basis for intense thalamocortical activation of feedforward inhibitory cells in neocortex*. Nat Neurosci, 2007. **10**(4): p. 462-8.
65. Porter, J.T., C.K. Johnson, and A. Agmon, *Diverse Types of Interneurons Generate Thalamus-Evoked Feedforward Inhibition in the Mouse Barrel Cortex*. The Journal of Neuroscience, 2001. **21**(8): p. 2699.
66. Castro-Alamancos, M.A. and B.W. Connors, *THALAMOCORTICAL SYNAPSES*. Progress in neurobiology, 1997. **51**(6): p. 581-606.
67. Likavčanová, K., et al., *Metabolic changes in the thalamus after spinal cord injury followed by proton MR spectroscopy*. Magnetic Resonance in Medicine, 2008. **59**(3): p. 499-506.
68. Nakamura, A., et al., *Somatosensory Homunculus as Drawn by MEG*. NeuroImage, 1998. **7**(4): p. 377-386.
69. Liang, M., A. Mouraux, and G.D. Iannetti, *Parallel Processing of Nociceptive and Non-nociceptive Somatosensory Information in the Human Primary and Secondary Somatosensory Cortices: Evidence from Dynamic Causal Modeling of Functional Magnetic Resonance Imaging Data*. The Journal of Neuroscience, 2011. **31**(24): p. 8976.
70. Aronoff, R., et al., *Long-range connectivity of mouse primary somatosensory barrel cortex*. European Journal of Neuroscience, 2010. **31**(12): p. 2221-2233.
71. Mao, T., et al., *Long-Range Neuronal Circuits Underlying the Interaction between Sensory and Motor Cortex*. Neuron, 2011. **72**(1): p. 111-123.
72. Eto, K., et al., *Inter-regional contribution of enhanced activity of the primary somatosensory cortex to the anterior cingulate cortex accelerates chronic pain behavior*. J Neurosci, 2011. **31**(21): p. 7631-6.
73. Price, D.D., *Central neural mechanisms that interrelate sensory and affective dimensions of pain*. Mol Interv, 2002. **2**(6): p. 392-403, 339.
74. Lübke, J. and D. Feldmeyer, *Excitatory signal flow and connectivity in a cortical column: focus on barrel cortex*. Brain Structure and Function, 2007. **212**(1): p. 3-17.
75. Douglas, R.J. and K.A. Martin, *Neuronal circuits of the neocortex*. Annu Rev Neurosci, 2004. **27**: p. 419-51.
76. Lefort, S., et al., *The Excitatory Neuronal Network of the C2 Barrel Column in Mouse Primary Somatosensory Cortex*. Neuron. **61**(2): p. 301-316.

77. Isaacson, J.S. and M. Scanziani, *How Inhibition Shapes Cortical Activity*. Neuron, 2011. **72**(2): p. 231-243.
78. Markram, H., et al., *Interneurons of the neocortical inhibitory system*. Nat Rev Neurosci, 2004. **5**(10): p. 793-807.
79. Zhang, Z. and Q.-Q. Sun, *The Balance Between Excitation And Inhibition And Functional Sensory Processing In The Somatosensory Cortex*, in *International review of neurobiology*, N.K.K.I. Masayuki Kobayashi and L.W. John, Editors. 2011, Academic Press. p. 305-333.
80. Ascoli, G.A.Y., R., *Petilla terminology: nomenclature of features of GABAergic interneurons of the cerebral cortex*. Nat Rev Neurosci, 2008. **9**(7): p. 557-568.
81. Jones, E.G., *Cortical and subcortical contributions to activity-dependent plasticity in primate somatosensory cortex*. Annu Rev Neurosci, 2000. **23**: p. 1-37.
82. Feldman, D.E. and M. Brecht, *Map plasticity in somatosensory cortex*. Science, 2005. **310**(5749): p. 810-5.
83. Griffen, T.C. and A. Maffei, *GABAergic synapses: their plasticity and role in sensory cortex*. Frontiers in Cellular Neuroscience, 2014. **8**: p. 91.
84. Donato, F., S.B. Rompani, and P. Caroni, *Parvalbumin-expressing basket-cell network plasticity induced by experience regulates adult learning*. Nature, 2013. **504**(7479): p. 272-6.
85. Sugiyama, S., et al., *Experience-dependent transfer of Otx2 homeoprotein into the visual cortex activates postnatal plasticity*. Cell, 2008. **134**(3): p. 508-20.
86. Hensch, T.K. and M. Fagiolini, *Excitatory-inhibitory balance and critical period plasticity in developing visual cortex*. Prog Brain Res, 2005. **147**: p. 115-24.
87. Foeller, E. and D.E. Feldman, *Synaptic basis for developmental plasticity in somatosensory cortex*. Curr Opin Neurobiol, 2004. **14**(1): p. 89-95.
88. Hensch, T.K., *Critical period plasticity in local cortical circuits*. Nat Rev Neurosci, 2005. **6**(11): p. 877-888.
89. Fox, K., *A critical period for experience-dependent synaptic plasticity in rat barrel cortex*. J Neurosci, 1992. **12**(5): p. 1826-38.
90. Stern, E.A., M. Maravall, and K. Svoboda, *Rapid Development and Plasticity of Layer 2/3 Maps in Rat Barrel Cortex In Vivo*. Neuron. **31**(2): p. 305-315.
91. Diamond, M.E., M. Armstrong-James, and F.F. Ebner, *Experience-dependent plasticity in adult rat barrel cortex*. Proceedings of the National Academy of Sciences of the United States of America, 1993. **90**(5): p. 2082-6.
92. Trachtenberg, J.T., et al., *Long-term in vivo imaging of experience-dependent synaptic plasticity in adult cortex*. Nature, 2002. **420**(6917): p. 788-794.
93. Kim, S.K. and J. Nabekura, *Rapid synaptic remodeling in the adult somatosensory cortex following peripheral nerve injury and its association with neuropathic pain*. J Neurosci, 2011. **31**(14): p. 5477-82.
94. Komagata, S., et al., *Nociceptive cortical responses during capsaicin-induced tactile allodynia in mice with spinal dorsal column lesioning*. Neurosci Res, 2011. **69**(4): p. 348-51.
95. Fox, K., *Anatomical pathways and molecular mechanisms for plasticity in the barrel cortex*. Neuroscience, 2002. **111**(4): p. 799-814.
96. Carcea, I. and R.C. Froemke, *Cortical Plasticity, Excitatory-Inhibitory Balance, and Sensory Perception*. Prog Brain Res, 2013. **207**: p. 65-90.
97. Feldman, D.E., *Synaptic Mechanisms for Plasticity in Neocortex*. Annual review of neuroscience, 2009. **32**: p. 33-55.
98. Winship, I.R. and T.H. Murphy, *Remapping the somatosensory cortex after stroke: insight from imaging the synapse to network*. The Neuroscientist : a review journal bringing neurobiology, neurology and psychiatry, 2009. **15**(5): p. 507-24.

99. Li, C.X., J.C. Callaway, and R.S. Waters, *Removal of GABAergic inhibition alters subthreshold input in neurons in forepaw barrel subfield (FBS) in rat first somatosensory cortex (SI) after digit stimulation*. Experimental Brain Research, 2002. **145**(4): p. 411-428.
100. Petersen, C.C.H. and B. Sakmann, *Functionally Independent Columns of Rat Somatosensory Barrel Cortex Revealed with Voltage-Sensitive Dye Imaging*. The Journal of Neuroscience, 2001. **21**(21): p. 8435.
101. Moore, C.I. and S.B. Nelson, *Spatio-Temporal Subthreshold Receptive Fields in the Vibrissa Representation of Rat Primary Somatosensory Cortex*. Journal of neurophysiology, 1998. **80**(6): p. 2882.
102. Petersen, C.C.H., A. Grinvald, and B. Sakmann, *Spatiotemporal Dynamics of Sensory Responses in Layer 2/3 of Rat Barrel Cortex Measured &emdash;In Vivo&emdash; by Voltage-Sensitive Dye Imaging Combined with Whole-Cell Voltage Recordings and Neuron Reconstructions*. The Journal of Neuroscience, 2003. **23**(4): p. 1298.
103. Brown, C.E., et al., *In Vivo&emdash; Voltage-Sensitive Dye Imaging in Adult Mice Reveals That Somatosensory Maps Lost to Stroke Are Replaced over Weeks by New Structural and Functional Circuits with Prolonged Modes of Activation within Both the Peri-Infarct Zone and Distant Sites*. The Journal of Neuroscience, 2009. **29**(6): p. 1719.
104. Bushnell, M.C., et al., *Pain perception: Is there a role for primary somatosensory cortex?* Proceedings of the National Academy of Sciences, 1999. **96**(14): p. 7705-7709.
105. Kim, W., S.K. Kim, and J. Nabekura, *Functional and structural plasticity in the primary somatosensory cortex associated with chronic pain*. Journal of neurochemistry, 2017. **141**(4): p. 499-506.
106. Kong, J., et al., *S1 is associated with chronic low back pain: a functional and structural MRI study*. Molecular pain, 2013. **9**: p. 43.
107. Kim, W. and S.K. Kim, *Neural circuit remodeling and structural plasticity in the cortex during chronic pain*. Korean J Physiol Pharmacol, 2016. **20**(1): p. 1-8.
108. DaSilva, A.F., et al., *Thickening in the somatosensory cortex of patients with migraine*. Neurology, 2007. **69**(21): p. 1990-5.
109. Kim, C.E., et al., *Large-scale plastic changes of the brain network in an animal model of neuropathic pain*. NeuroImage, 2014. **98**: p. 203-15.
110. Vierck, C.J., et al., *Role of primary somatosensory cortex in the coding of pain*. Pain, 2013. **154**(3): p. 334-44.
111. Kim, S.K., et al., *Phase-specific plasticity of synaptic structures in the somatosensory cortex of living mice during neuropathic pain*. Molecular pain, 2011. **7**: p. 87.
112. Kim, S.K., K. Eto, and J. Nabekura, *Synaptic structure and function in the mouse somatosensory cortex during chronic pain: in vivo two-photon imaging*. Neural Plast, 2012. **2012**: p. 640259.
113. Komagata, S., et al., *Initial phase of neuropathic pain within a few hours after nerve injury in mice*. J Neurosci, 2011. **31**(13): p. 4896-905.
114. Sharma, N.K., et al., *Primary somatosensory cortex in chronic low back pain - a H-MRS study*. J Pain Res, 2011. **4**: p. 143-50.
115. Christopherson, K.S., et al., *Thrombospondins Are Astrocyte-Secreted Proteins that Promote CNS Synaptogenesis*. Cell, 2005. **120**(3): p. 421-433.
116. Kim, S.K., et al., *Cortical astrocytes rewire somatosensory cortical circuits for peripheral neuropathic pain*. The Journal of clinical investigation, 2016. **126**(5): p. 1983-1997.
117. Vargová, L. and E. Syková, *Astrocytes and extracellular matrix in extrasynaptic volume transmission*. Philosophical Transactions of the Royal Society B: Biological Sciences, 2014. **369**(1654): p. 20130608.
118. Dityatev, A., M. Schachner, and P. Sonderegger, *The dual role of the extracellular matrix in synaptic plasticity and homeostasis*. Nat Rev Neurosci, 2010. **11**(11): p. 735-746.
119. Wang, D. and J. Fawcett, *The perineuronal net and the control of CNS plasticity*. Cell and tissue research, 2012. **349**(1): p. 147-160.

120. Zhuo, M., *Cortical excitation and chronic pain*. Trends in Neurosciences, 2008. **31**(4): p. 199-207.
121. Eto, K., et al., *Enhanced GABAergic Activity in the Mouse Primary Somatosensory Cortex Is Insufficient to Alleviate Chronic Pain Behavior with Reduced Expression of Neuronal Potassium-Chloride Cotransporter*. The Journal of Neuroscience, 2012. **32**(47): p. 16552.
122. Blom, S.M., et al., *Nerve injury-induced neuropathic pain causes disinhibition of the anterior cingulate cortex*. J Neurosci, 2014. **34**(17): p. 5754-64.
123. Kang, S.J., et al., *Bidirectional modulation of hyperalgesia via the specific control of excitatory and inhibitory neuronal activity in the ACC*. Mol Brain, 2015. **8**(1): p. 81.
124. Wrigley, P.J., et al., *Neuropathic pain and primary somatosensory cortex reorganization following spinal cord injury*. Pain, 2009. **141**(1-2): p. 52-9.
125. Yanagisawa, T., et al., *Induced sensorimotor brain plasticity controls pain in phantom limb patients*. Nat Commun, 2016. **7**: p. 13209.
126. Knecht, S., et al., *Cortical reorganization in human amputees and mislocalization of painful stimuli to the phantom limb*. Neuroscience letters, 1995. **201**(3): p. 262-264.
127. Gustin, S.M., et al., *Pain and plasticity: is chronic pain always associated with somatosensory cortex activity and reorganization?* J Neurosci, 2012. **32**(43): p. 14874-84.
128. Moseley, G.L. and H. Flor, *Targeting cortical representations in the treatment of chronic pain: a review*. Neurorehabil Neural Repair, 2012. **26**(6): p. 646-52.
129. Naro, A., et al., *Non-invasive Brain Stimulation, a Tool to Revert Maladaptive Plasticity in Neuropathic Pain*. Front Hum Neurosci, 2016. **10**: p. 376.
130. Fuchs, P.N., et al., *The anterior cingulate cortex and pain processing*. Frontiers in Integrative Neuroscience, 2014. **8**: p. 35.
131. Apkarian, A.V., et al., *Human brain mechanisms of pain perception and regulation in health and disease*. European journal of pain, 2005. **9**(4): p. 463-84.
132. Bliss, T.V., et al., *Synaptic plasticity in the anterior cingulate cortex in acute and chronic pain*. Nat Rev Neurosci, 2016. **17**(8): p. 485-96.
133. Xu, H., et al., *Presynaptic and postsynaptic amplifications of neuropathic pain in the anterior cingulate cortex*. J Neurosci, 2008. **28**(29): p. 7445-53.
134. Toyoda, H., M.G. Zhao, and M. Zhuo, *Enhanced quantal release of excitatory transmitter in anterior cingulate cortex of adult mice with chronic pain*. Molecular pain, 2009. **5**: p. 4.
135. Cao, X.Y., et al., *Characterization of intrinsic properties of cingulate pyramidal neurons in adult mice after nerve injury*. Molecular pain, 2009. **5**: p. 73.
136. Zhuo, M., *A synaptic model for pain: long-term potentiation in the anterior cingulate cortex*. Mol Cells, 2007. **23**(3): p. 259-71.
137. Johansen, J.P., H.L. Fields, and B.H. Manning, *The affective component of pain in rodents: Direct evidence for a contribution of the anterior cingulate cortex*. Proceedings of the National Academy of Sciences, 2001. **98**(14): p. 8077-8082.
138. Tolomeo, S., et al., *A causal role for the anterior mid-cingulate cortex in negative affect and cognitive control*. Brain, 2016. **139**(Pt 6): p. 1844-54.
139. Rainville, P., et al., *Pain Affect Encoded in Human Anterior Cingulate But Not Somatosensory Cortex*. Science, 1997. **277**(5328): p. 968.
140. Craig, A.D., et al., *Functional imaging of an illusion of pain*. Nature, 1996. **384**(6606): p. 258-60.
141. Gu, L., et al., *Pain inhibition by optogenetic activation of specific anterior cingulate cortical neurons*. PLoS ONE, 2015. **10**(2): p. e0117746.
142. Li, X.Y., et al., *Erasing injury-related cortical synaptic potentiation as a new treatment for chronic pain*. J Mol Med (Berl), 2011. **89**(9): p. 847-55.
143. Navratilova, E., et al., *Endogenous opioid activity in the anterior cingulate cortex is required for relief of pain*. J Neurosci, 2015. **35**(18): p. 7264-71.
144. Gorka, S.M., et al., *Opioid modulation of resting-state anterior cingulate cortex functional connectivity*. J Psychopharmacol, 2014. **28**(12): p. 1115-24.

145. Bingel, U., et al., *Mechanisms of placebo analgesia: rACC recruitment of a subcortical antinociceptive network*. Pain, 2006. **120**(1-2): p. 8-15.
146. Vogt, B.A., *Pain and emotion interactions in subregions of the cingulate gyrus*. Nat Rev Neurosci, 2005. **6**(7): p. 533-44.
147. Barthas, F., et al., *The anterior cingulate cortex is a critical hub for pain-induced depression*. Biol Psychiatry, 2015. **77**(3): p. 236-45.
148. Koga, K., et al., *Coexistence of two forms of LTP in ACC provides a synaptic mechanism for the interactions between anxiety and chronic pain*. Neuron, 2015. **85**(2): p. 377-89.
149. Zhuo, M., *Neural Mechanisms Underlying Anxiety-Chronic Pain Interactions*. Trends Neurosci, 2016. **39**(3): p. 136-45.
150. Calejesan, A.A., S.J. Kim, and M. Zhuo, *Descending facilitatory modulation of a behavioral nociceptive response by stimulation in the adult rat anterior cingulate cortex*. European journal of pain, 2000. **4**(1): p. 83-96.
151. Craig, A.D., *How do you feel? Interoception: the sense of the physiological condition of the body*. Nat Rev Neurosci, 2002. **3**(8): p. 655-666.
152. Craig, A.D., *Interoception: the sense of the physiological condition of the body*. Curr Opin Neurobiol, 2003. **13**(4): p. 500-505.
153. Brooks, J.C.W., et al., *Somatotopic organisation of the human insula to painful heat studied with high resolution functional imaging*. NeuroImage, 2005. **27**(1): p. 201-209.
154. Lu, C., et al., *Insular Cortex is Critical for the Perception, Modulation, and Chronification of Pain*. Neuroscience Bulletin, 2016. **32**(2): p. 191-201.
155. Wager, T.D., et al., *An fMRI-Based Neurologic Signature of Physical Pain*. New England Journal of Medicine, 2013. **368**(15): p. 1388-1397.
156. Segerdahl, A.R., et al., *The dorsal posterior insula subserves a fundamental role in human pain*. Nat Neurosci, 2015. **18**(4): p. 499-500.
157. Seifert, F. and C. Maihöfner, *Central mechanisms of experimental and chronic neuropathic pain: Findings from functional imaging studies*. Cellular and Molecular Life Sciences, 2008. **66**(3): p. 375.
158. Ostrowsky, K., et al., *Representation of pain and somatic sensation in the human insula: a study of responses to direct electrical cortical stimulation*. Cereb Cortex, 2002. **12**(4): p. 376-85.
159. Starr, C.J., et al., *Roles of the Insular Cortex in the Modulation of Pain: Insights from Brain Lesions*. J Neurosci, 2009. **29**(9): p. 2684-2694.
160. Watson, C.J., *Insular balance of glutamatergic and GABAergic signaling modulates pain processing*. Pain, 2016. **157**(10): p. 2194-2207.
161. Mutschler, I., et al., *Pain and emotion in the insular cortex: evidence for functional reorganization in major depression*. Neuroscience letters, 2012. **520**(2): p. 204-209.
162. Seminowicz, D.A. and M. Moayed, *The Dorsolateral Prefrontal Cortex in Acute and Chronic Pain*. The Journal of Pain.
163. Mouraux, A., et al., *A multisensory investigation of the functional significance of the "pain matrix"*. NeuroImage, 2011. **54**(3): p. 2237-2249.
164. Compston, A. and A. Coles, *Multiple sclerosis*. Lancet, 2002. **359**(9313): p. 1221-31.
165. Compston, A. and A. Coles, *Multiple sclerosis*. The Lancet. **372**(9648): p. 1502-1517.
166. Murray, T.J., *The history of multiple sclerosis: the changing frame of the disease over the centuries*. J Neurol Sci, 2009. **277** Suppl 1: p. S3-8.
167. Mallucci, G., et al., *The role of immune cells, glia and neurons in white and gray matter pathology in multiple sclerosis*. Progress in neurobiology, 2015. **0**: p. 1-22.
168. Hauser, S.L. and J.R. Oksenberg, *The Neurobiology of Multiple Sclerosis: Genes, Inflammation, and Neurodegeneration*. Neuron. **52**(1): p. 61-76.
169. Browne, P., et al., *Atlas of Multiple Sclerosis 2013: A growing global problem with widespread inequity*. Neurology, 2014. **83**(11): p. 1022-1024.

170. Dendrou, C.A., L. Fugger, and M.A. Friese, *Immunopathology of multiple sclerosis*. Nat Rev Immunol, 2015. **15**(9): p. 545-558.
171. Oksenberg, J.R., et al., *The genetics of multiple sclerosis: SNPs to pathways to pathogenesis*. Nat Rev Genet, 2008. **9**(7): p. 516-526.
172. Belbasis, L., et al., *Environmental risk factors and multiple sclerosis: an umbrella review of systematic reviews and meta-analyses*. The Lancet Neurology. **14**(3): p. 263-273.
173. O’Gorman, C., R. Lucas, and B. Taylor, *Environmental Risk Factors for Multiple Sclerosis: A Review with a Focus on Molecular Mechanisms*. International Journal of Molecular Sciences, 2012. **13**(9): p. 11718-11752.
174. Vollmer, T., *The natural history of relapses in multiple sclerosis*. Journal of the neurological sciences, 2007. **256**, **Supplement 1**: p. S5-S13.
175. Miller, D.H., D.T. Chard, and O. Ciccarelli, *Clinically isolated syndromes*. The Lancet Neurology. **11**(2): p. 157-169.
176. Ciccarelli, O. and A.T. Toosy, *Conversion from clinically isolated syndrome to multiple sclerosis: A large multicentre study*. Multiple Sclerosis Journal, 2015. **21**(8): p. 967-968.
177. Kuhle, J., et al., *Conversion from clinically isolated syndrome to multiple sclerosis: A large multicentre study*. Multiple sclerosis, 2015. **21**(8): p. 1013-24.
178. Fisniku, L.K., et al., *Disability and T2 MRI lesions: a 20-year follow-up of patients with relapse onset of multiple sclerosis*. Brain, 2008. **131**(Pt 3): p. 808-17.
179. Rovaris, M., et al., *Secondary progressive multiple sclerosis: current knowledge and future challenges*. The Lancet Neurology, 2006. **5**(4): p. 343-354.
180. Miller, D.H. and S.M. Leary, *Primary-progressive multiple sclerosis*. The Lancet Neurology, 2007. **6**(10): p. 903-912.
181. Lassmann, H., W. Bruck, and C. Lucchinetti, *Heterogeneity of multiple sclerosis pathogenesis: implications for diagnosis and therapy*. Trends in molecular medicine, 2001. **7**(3): p. 115-21.
182. Disanto, G., et al., *Heterogeneity in Multiple Sclerosis: Scratching the Surface of a Complex Disease*. Autoimmune Diseases, 2011. **2011**.
183. Franklin, R.J., *Why does remyelination fail in multiple sclerosis?* Nat Rev Neurosci, 2002. **3**(9): p. 705-14.
184. Dutta, R. and B.D. Trapp, *Mechanisms of neuronal dysfunction and degeneration in multiple sclerosis*. Progress in neurobiology, 2011. **93**(1): p. 1-12.
185. Stadelmann, C., C. Wegner, and W. Brück, *Inflammation, demyelination, and degeneration — Recent insights from MS pathology*. Biochimica et Biophysica Acta (BBA) - Molecular Basis of Disease, 2011. **1812**(2): p. 275-282.
186. Bar-Or, A., *The immunology of multiple sclerosis*. Semin Neurol, 2008. **28**(1): p. 29-45.
187. Sospedra, M. and R. Martin, *Immunology of multiple sclerosis*. Annu Rev Immunol, 2005. **23**: p. 683-747.
188. Becher, B., S. Spath, and J. Goverman, *Cytokine networks in neuroinflammation*. Nat Rev Immunol, 2017. **17**(1): p. 49-59.
189. Jangi, S., et al., *Alterations of the human gut microbiome in multiple sclerosis*. Nat Commun, 2016. **7**: p. 12015.
190. Geurts, J.J. and F. Barkhof, *Grey matter pathology in multiple sclerosis*. Lancet Neurol, 2008. **7**(9): p. 841-51.
191. Stadelmann, C., C. Wegner, and W. Bruck, *Inflammation, demyelination, and degeneration - recent insights from MS pathology*. Biochimica et biophysica acta, 2011. **1812**(2): p. 275-82.
192. Goverman, J., *Autoimmune T cell responses in the central nervous system*. Nature reviews. Immunology, 2009. **9**(6): p. 393.
193. Stys, P.K., et al., *Will the real multiple sclerosis please stand up?* Nat Rev Neurosci, 2012. **13**(7): p. 507-514.

194. Steinman, M.D.L., *Multiple Sclerosis: A Coordinated Immunological Attack against Myelin in the Central Nervous System*. Cell, 1996. **85**(3): p. 299-302.
195. Steinman, L., *Multiple sclerosis: a two-stage disease*. Nat Immunol, 2001. **2**(9): p. 762-764.
196. Stadelmann, C., *Multiple sclerosis as a neurodegenerative disease: pathology, mechanisms and therapeutic implications*. Curr Opin Neurol, 2011. **24**(3): p. 224-9.
197. Sospedra, M. and R. Martin, *Immunology of Multiple Sclerosis*. Semin Neurol, 2016. **36**(2): p. 115-27.
198. Turner, M.D., et al., *Cytokines and chemokines: At the crossroads of cell signalling and inflammatory disease*. Biochimica et Biophysica Acta (BBA) - Molecular Cell Research, 2014. **1843**(11): p. 2563-2582.
199. Maimone, D., G.C. Guazzi, and P. Annunziata, *IL-6 detection in multiple sclerosis brain*. J Neurol Sci, 1997. **146**(1): p. 59-65.
200. Carpintero, R. and D. Burger, *IFN $\beta$  and glatiramer acetate trigger different signaling pathways to regulate the IL-1 system in multiple sclerosis*. Communicative & integrative biology, 2011. **4**(1): p. 112-114.
201. Guo, H., J.B. Callaway, and J.P.Y. Ting, *Inflammasomes: mechanism of action, role in disease, and therapeutics*. Nat Med, 2015. **21**(7): p. 677-687.
202. Özenci, V., et al., *Multiple sclerosis is associated with an imbalance between tumour necrosis factor-alpha (TNF- $\alpha$ )- and IL-10-secreting blood cells that is corrected by interferon-beta (IFN- $\beta$ ) treatment*. Clinical and experimental immunology, 2000. **120**(1): p. 147-153.
203. Selmaj, K., et al., *Identification of lymphotoxin and tumor necrosis factor in multiple sclerosis lesions*. Journal of Clinical Investigation, 1991. **87**(3): p. 949-954.
204. *TNF neutralization in MS: results of a randomized, placebo-controlled multicenter study. The Lenercept Multiple Sclerosis Study Group and The University of British Columbia MS/MRI Analysis Group*. Neurology, 1999. **53**(3): p. 457-65.
205. Beattie, E.C., et al., *Control of Synaptic Strength by Glial TNF $\alpha$* . Science, 2002. **295**(5563): p. 2282-2285.
206. Mandolesi, G., et al., *IL-1beta dependent cerebellar synaptopathy in a mouse mode of multiple sclerosis*. Cerebellum, 2015. **14**(1): p. 19-22.
207. Yang, G., et al., *Peripheral elevation of TNF-alpha leads to early synaptic abnormalities in the mouse somatosensory cortex in experimental autoimmune encephalomyelitis*. Proc Natl Acad Sci U S A, 2013. **110**(25): p. 10306-11.
208. Kawasaki, Y., et al., *Cytokine Mechanisms of Central Sensitization: Distinct and Overlapping Role of Interleukin-1 $\beta$ , Interleukin-6, and Tumor Necrosis Factor- $\alpha$  in Regulating Synaptic and Neuronal Activity in the Superficial Spinal Cord*. The Journal of Neuroscience, 2008. **28**(20): p. 5189-5194.
209. Khairova, R.A., et al., *A potential role for pro-inflammatory cytokines in regulating synaptic plasticity in major depressive disorder*. International Journal of Neuropsychopharmacology, 2009. **12**(4): p. 561-578.
210. Heesen, C., et al., *Fatigue in multiple sclerosis: an example of cytokine mediated sickness behaviour?* Journal of neurology, neurosurgery, and psychiatry, 2006. **77**(1): p. 34-39.
211. Di Filippo, M., et al., *Neuroinflammation and synaptic plasticity: theoretical basis for a novel, immune-centred, therapeutic approach to neurological disorders*. Trends Pharmacol Sci, 2008. **29**(8): p. 402-412.
212. McAfoose, J. and B.T. Baune, *Evidence for a cytokine model of cognitive function*. Neuroscience & Biobehavioral Reviews, 2009. **33**(3): p. 355-366.
213. Trapp, B.D. and K.A. Nave, *Multiple sclerosis: an immune or neurodegenerative disorder?* Annu Rev Neurosci, 2008. **31**: p. 247-69.
214. Trapp, B.D. and P.K. Stys, *Virtual hypoxia and chronic necrosis of demyelinated axons in multiple sclerosis*. The Lancet Neurology, 2009. **8**(3): p. 280-291.
215. Dutta, R., et al., *Mitochondrial dysfunction as a cause of axonal degeneration in multiple sclerosis patients*. Annals of neurology, 2006. **59**(3): p. 478-489.

216. Stys, P.K., S.G. Waxman, and B.R. Ransom, *Na(+)-Ca2+ exchanger mediates Ca2+ influx during anoxia in mammalian central nervous system white matter*. *Annals of neurology*, 1991. **30**(3): p. 375-80.
217. Stys, P.K., *General mechanisms of axonal damage and its prevention*. *Journal of the neurological sciences*, 2005. **233**(1-2): p. 3-13.
218. Mahad, D.H., B.D. Trapp, and H. Lassmann, *Pathological mechanisms in progressive multiple sclerosis*. *The Lancet Neurology*, 2015. **14**(2): p. 183-193.
219. Mathur, D., et al., *Perturbed Glucose Metabolism: Insights into Multiple Sclerosis Pathogenesis*. *Frontiers in neurology*, 2014. **5**: p. 250.
220. Mandolesi, G., et al., *Synaptopathy connects inflammation and neurodegeneration in multiple sclerosis*. *Nat Rev Neurol*, 2015. **11**(12): p. 711-24.
221. Nisticò, R., et al., *Synaptic plasticity in multiple sclerosis and in experimental autoimmune encephalomyelitis*. *Philosophical Transactions of the Royal Society B: Biological Sciences*, 2014. **369**(1633): p. 20130162.
222. Nistico, R., et al., *Inflammation subverts hippocampal synaptic plasticity in experimental multiple sclerosis*. *PLoS ONE*, 2013. **8**(1): p. e54666.
223. Falco, A., et al., *Reduction in parvalbumin-positive interneurons and inhibitory input in the cortex of mice with experimental autoimmune encephalomyelitis*. *Exp Brain Res*, 2014. **232**(7): p. 2439-49.
224. Ziehn, M.O., et al., *Hippocampal CA1 atrophy and synaptic loss during experimental autoimmune encephalomyelitis, EAE*. *Laboratory investigation; a journal of technical methods and pathology*, 2010. **90**(5): p. 774-786.
225. Rossi, S., et al., *Inflammation inhibits GABA transmission in multiple sclerosis*. *Multiple Sclerosis Journal*, 2012. **18**(11): p. 1633-1635.
226. Kettenmann, H., F. Kirchhoff, and A. Verkhratsky, *Microglia: New Roles for the Synaptic Stripper*. *Neuron*, 2013. **77**(1): p. 10-18.
227. Stephan, A.H., B.A. Barres, and B. Stevens, *The complement system: an unexpected role in synaptic pruning during development and disease*. *Annu Rev Neurosci*, 2012. **35**: p. 369-89.
228. Audoin, B., et al., *Compensatory cortical activation observed by fMRI during a cognitive task at the earliest stage of multiple sclerosis*. *Human Brain Mapping*, 2003. **20**(2): p. 51-58.
229. Rocca, M.A. and M. Filippi, *Functional MRI in Multiple Sclerosis*. *Journal of Neuroimaging*, 2007. **17**: p. 36S-41S.
230. Pantano, P., C. Mainero, and F. Caramia, *Functional Brain Reorganization in Multiple Sclerosis: Evidence from fMRI Studies*. *Journal of Neuroimaging*, 2006. **16**(2): p. 104-114.
231. Potter, L.E., et al., *Altered excitatory-inhibitory balance within somatosensory cortex is associated with enhanced plasticity and pain sensitivity in a mouse model of multiple sclerosis*. *Journal of neuroinflammation*, 2016. **13**(1): p. 142.
232. Cifelli, A. and P.M. Matthews, *Cerebral plasticity in multiple sclerosis: insights from fMRI*. *Multiple Sclerosis Journal*, 2002. **8**(3): p. 193-199.
233. Goldenberg, M.M., *Multiple Sclerosis Review*. *Pharmacy and Therapeutics*, 2012. **37**(3): p. 175-184.
234. Fox, E.J., *Management of worsening multiple sclerosis with mitoxantrone: a review*. *Clin Ther*, 2006. **28**(4): p. 461-74.
235. Atkins, H.L., et al., *Immunoablation and autologous haemopoietic stem-cell transplantation for aggressive multiple sclerosis: a multicentre single-group phase 2 trial*. *The Lancet*, 2016. **388**(10044): p. 576-585.
236. Branas, P., et al., *Treatments for fatigue in multiple sclerosis: a rapid and systematic review*. *Health Technol Assess*, 2000. **4**(27): p. 1-61.
237. Rizzo, M.A., et al., *Prevalence and treatment of spasticity reported by multiple sclerosis patients*. *Multiple Sclerosis Journal*, 2004. **10**(5): p. 589-595.
238. O'Carroll, C.B., et al., *Is donepezil effective for multiple sclerosis-related cognitive dysfunction? A critically appraised topic*. *The neurologist*, 2012. **18**(1): p. 51-4.

239. Canada, M.S.o. *Symptom Management (Treatments - Medications)*. [website] 2017 [cited 2017 6/12/2017]; Available from: <https://mssociety.ca/managing-ms/treatments/medications/symptom-management>.
240. Baxter, A.G., *The origin and application of experimental autoimmune encephalomyelitis*. Nat Rev Immunol, 2007. **7**(11): p. 904-912.
241. Constantinescu, C.S., et al., *Experimental autoimmune encephalomyelitis (EAE) as a model for multiple sclerosis (MS)*. British Journal of Pharmacology, 2011. **164**(4): p. 1079-1106.
242. Höftberger, R., et al., *Autoimmune encephalitis in humans: how closely does it reflect multiple sclerosis ?* Acta Neuropathologica Communications, 2015. **3**(1): p. 80.
243. Rivers, T.M., D.H. Sprunt, and G.P. Berry, *OBSERVATIONS ON ATTEMPTS TO PRODUCE ACUTE DISSEMINATED ENCEPHALOMYELITIS IN MONKEYS*. The Journal of experimental medicine, 1933. **58**(1): p. 39-53.
244. Rivers, T.M. and F.F. Schwentker, *ENCEPHALOMYELITIS ACCOMPANIED BY MYELIN DESTRUCTION EXPERIMENTALLY PRODUCED IN MONKEYS*. The Journal of experimental medicine, 1935. **61**(5): p. 689-702.
245. Gold, R., C. Linington, and H. Lassmann, *Understanding pathogenesis and therapy of multiple sclerosis via animal models: 70 years of merits and culprits in experimental autoimmune encephalomyelitis research*. Brain, 2006. **129**(8): p. 1953-1971.
246. Ransohoff, R.M., *Animal models of multiple sclerosis: the good, the bad and the bottom line*. Nat Neurosci, 2012. **15**(8): p. 1074-1077.
247. Robinson, A.P., et al., *The experimental autoimmune encephalomyelitis (EAE) model of MS: utility for understanding disease pathophysiology and treatment*. Handbook of clinical neurology, 2014. **122**: p. 173-189.
248. Furlan, R., C. Cuomo, and G. Martino, *Animal models of multiple sclerosis*. Methods in molecular biology, 2009. **549**: p. 157-73.
249. Croxford, A.L., F.C. Kurschus, and A. Waisman, *Mouse models for multiple sclerosis: Historical facts and future implications*. Biochimica et Biophysica Acta (BBA) - Molecular Basis of Disease, 2011. **1812**(2): p. 177-183.
250. Fletcher, J.M., et al., *T cells in multiple sclerosis and experimental autoimmune encephalomyelitis*. Clinical & Experimental Immunology, 2010. **162**(1): p. 1-11.
251. t Hart, B.A., B. Gran, and R. Weissert, *EAE: imperfect but useful models of multiple sclerosis*. Trends in molecular medicine, 2011. **17**(3): p. 119-25.
252. Yong, T., G.A. Meininger, and D.S. Linthicum, *Enhancement of histamine-induced vascular leakage by pertussis toxin in SJL/J mice but not BALB/c mice*. Journal of neuroimmunology, 1993. **45**(1-2): p. 47-52.
253. Linthicum, D.S., J.J. Munoz, and A. Blaskett, *Acute experimental autoimmune encephalomyelitis in mice. I. Adjuvant action of Bordetella pertussis is due to vasoactive amine sensitization and increased vascular permeability of the central nervous system*. Cell Immunol, 1982. **73**(2): p. 299-310.
254. Hofstetter, H.H., C.L. Shive, and T.G. Forsthuber, *Pertussis toxin modulates the immune response to neuroantigens injected in incomplete Freund's adjuvant: induction of Th1 cells and experimental autoimmune encephalomyelitis in the presence of high frequencies of Th2 cells*. Journal of immunology, 2002. **169**(1): p. 117-25.
255. Greter, M., et al., *Dendritic cells permit immune invasion of the CNS in an animal model of multiple sclerosis*. Nat Med, 2005. **11**(3): p. 328-334.
256. The Lenercept Multiple Sclerosis Study, G. and M.S.M.R.I.A.G. The University of British Columbia, *TNF neutralization in MS: Results of a randomized, placebo-controlled multicenter study*. Neurology, 1999. **53**(3): p. 457-457.
257. Burger, D., et al., *Glatiramer acetate increases IL-1 receptor antagonist but decreases T cell-induced IL-1beta in human monocytes and multiple sclerosis*. Proceedings of the National Academy of Sciences of the United States of America, 2009. **106**(11): p. 4355-9.

258. Glabinski, A.R. and R.M. Ransohoff, *The Chemokine System in Experimental Autoimmune Encephalomyelitis*, in *Experimental Models of Multiple Sclerosis*, E. Lavi and C.S. Constantinescu, Editors. 2005, Springer US: Boston, MA. p. 363-377.
259. Archelos, J.J., S.C. Previtali, and H.-P. Hartung, *The role of integrins in immune-mediated diseases of the nervous system*. Trends in Neurosciences. **22**(1): p. 30-38.
260. Sunnemark, D., et al., *CX3CL1 (fractalkine) and CX3CR1 expression in myelin oligodendrocyte glycoprotein-induced experimental autoimmune encephalomyelitis: kinetics and cellular origin*. Journal of neuroinflammation, 2005. **2**: p. 17.
261. Yong, V.W., et al., *Elevation of matrix metalloproteinases (MMPs) in multiple sclerosis and impact of immunomodulators*. Journal of the neurological sciences, 2007. **259**(1-2): p. 79-84.
262. MacKenzie-Graham, A., et al., *Cortical atrophy in experimental autoimmune encephalomyelitis: in vivo imaging*. NeuroImage, 2012. **60**(1): p. 95-104.
263. Musella, A., et al., *Linking synaptopathy and gray matter damage in multiple sclerosis*. Mult Scler, 2015.
264. Centonze, D., et al., *Inflammation Triggers Synaptic Alteration and Degeneration in Experimental Autoimmune Encephalomyelitis*. The Journal of Neuroscience, 2009. **29**(11): p. 3442.
265. Tambalo, S., et al., *Functional Magnetic Resonance Imaging of Rats with Experimental Autoimmune Encephalomyelitis Reveals Brain Cortex Remodeling*. J Neurosci, 2015. **35**(27): p. 10088-100.
266. Rossi, S., et al., *Impaired striatal GABA transmission in experimental autoimmune encephalomyelitis*. Brain, Behavior, and Immunity, 2011. **25**(5): p. 947-956.
267. Smith, T., et al., *Autoimmune encephalomyelitis ameliorated by AMPA antagonists*. Nat Med, 2000. **6**(1): p. 62-6.
268. Pitt, D., P. Werner, and C.S. Raine, *Glutamate excitotoxicity in a model of multiple sclerosis*. Nat Med, 2000. **6**(1): p. 67-70.
269. Rossi, S., et al., *Abnormal activity of the Na/Ca exchanger enhances glutamate transmission in experimental autoimmune encephalomyelitis*. Brain, Behavior, and Immunity, 2010. **24**(8): p. 1379-1385.
270. Mandolesi, G., et al., *Cognitive deficits in experimental autoimmune encephalomyelitis: neuroinflammation and synaptic degeneration*. Neurological Sciences, 2010. **31**(2): p. 255-259.
271. Acharjee, S., et al., *Altered cognitive-emotional behavior in early experimental autoimmune encephalitis – Cytokine and hormonal correlates*. Brain, Behavior, and Immunity, 2013. **33**: p. 164-172.
272. Pollak, Y., et al., *Experimental autoimmune encephalomyelitis-associated behavioral syndrome as a model of 'depression due to multiple sclerosis'*. Brain, Behavior, and Immunity, 2002. **16**(5): p. 533-543.
273. Olechowski, C.J., J.J. Truong, and B.J. Kerr, *Neuropathic pain behaviours in a chronic-relapsing model of experimental autoimmune encephalomyelitis (EAE)*. Pain, 2009. **141**(1-2): p. 156-64.
274. Olechowski, C.J., et al., *Changes in nociceptive sensitivity and object recognition in experimental autoimmune encephalomyelitis (EAE)*. Experimental neurology, 2013. **241**(0): p. 113-121.
275. Musgrave, T., C.J. Olechowski, and B.J. Kerr, *Learning new tricks from an old dog: using experimental autoimmune encephalomyelitis to study comorbid symptoms in multiple sclerosis*. Pain Management, 2011. **1**(6): p. 571-576.
276. O'Connor, A.B., et al., *Pain associated with multiple sclerosis: systematic review and proposed classification*. Pain, 2008. **137**(1): p. 96-111.
277. Foley, P.L., et al., *Prevalence and natural history of pain in adults with multiple sclerosis: Systematic review and meta-analysis*. PAIN®, 2013. **154**(5): p. 632-642.
278. Svendsen, K.B., et al., *Sensory function and quality of life in patients with multiple sclerosis and pain*. Pain, 2005. **114**(3): p. 473-81.
279. Martinelli Boneschi, F., et al., *Lifetime and actual prevalence of pain and headache in multiple sclerosis*. Multiple Sclerosis Journal, 2008. **14**(4): p. 514-521.

280. Bermejo, P.E., C. Oreja-Guevara, and E. Diez-Tejedor, [*Pain in multiple sclerosis: prevalence, mechanisms, types and treatment*]. *Revista de neurologia*, 2010. **50**(2): p. 101-8.
281. Stenager, E., L. Knudsen, and K. Jensen, *Acute and chronic pain syndromes in multiple sclerosis*. *Acta neurologica Scandinavica*, 1991. **84**(3): p. 197-200.
282. Broła, W., K. Mitosek-Szewczyk, and J. Opara, *Symptomatology and pathogenesis of different types of pain in multiple sclerosis*. *Neurol Neurochir Pol*, 2014. **48**(4): p. 272-9.
283. Österberg, A. and J. Boivie, *Central pain in multiple sclerosis – Sensory abnormalities*. *European journal of pain*, 2010. **14**(1): p. 104-110.
284. Osterberg, A., J. Boivie, and K.A. Thuomas, *Central pain in multiple sclerosis--prevalence and clinical characteristics*. *European journal of pain*, 2005. **9**(5): p. 531-42.
285. Seixas, D., et al., *Pain in multiple sclerosis: A systematic review of neuroimaging studies*. *NeuroImage: Clinical*, 2014. **5**: p. 322-331.
286. Nurmikko, T.J., S. Gupta, and K. MacIver, *Multiple sclerosis-related central pain disorders*. *Curr Pain Headache Rep*, 2010. **14**(3): p. 189-95.
287. Nick, S.T., et al., *Multiple sclerosis and pain*. *Neurological research*, 2012.
288. Truini, A., et al., *Mechanisms of pain in multiple sclerosis: a combined clinical and neurophysiological study*. *Pain*, 2012. **153**(10): p. 2048-54.
289. Scherder, E., et al., *Pain in Parkinson's disease and multiple sclerosis: Its relation to the medial and lateral pain systems*. *Neuroscience & Biobehavioral Reviews*, 2005. **29**(7): p. 1047-1056.
290. Khan, N. and M.T. Smith, *Multiple sclerosis-induced neuropathic pain: pharmacological management and pathophysiological insights from rodent EAE models*. *Inflammopharmacology*, 2014. **22**(1): p. 1-22.
291. Solaro, C. and M. Messmer Uccelli, *Pharmacological management of pain in patients with multiple sclerosis*. *Drugs*, 2010. **70**(10): p. 1245-54.
292. Solaro, C. and M.M. Uccelli, *Management of pain in multiple sclerosis: a pharmacological approach*. *Nat Rev Neurol*, 2011. **7**(9): p. 519-27.
293. Grau-López, L., et al., *Analysis of the pain in multiple sclerosis patients*. *Neurología (English Edition)*, 2011. **26**(4): p. 208-213.
294. Lu, J., et al., *Pain in experimental autoimmune encephalitis: a comparative study between different mouse models*. *Journal of neuroinflammation*, 2012. **9**(1): p. 233.
295. Thibault, K., B. Calvino, and S. Pezet, *Characterisation of sensory abnormalities observed in an animal model of multiple sclerosis: a behavioural and pharmacological study*. *Eur J Pain*, 2011. **15**(3): p. 231 e1-16.
296. Steinman, L. and S.S. Zamvil, *Virtues and pitfalls of EAE for the development of therapies for multiple sclerosis*. *Trends in Immunology*. **26**(11): p. 565-571.
297. Aicher, S.A., et al., *Hyperalgesia in an animal model of multiple sclerosis*. *Pain*, 2004. **110**(3): p. 560-70.
298. Thorburn, K.C., et al., *Facial hypersensitivity and trigeminal pathology in mice with experimental autoimmune encephalomyelitis*. *Pain*, 2016. **157**(3): p. 627-42.
299. Fu, W. and B.K. Taylor, *Activation of cannabinoid CB2 receptors reduces hyperalgesia in an experimental autoimmune encephalomyelitis mouse model of multiple sclerosis*. *Neuroscience letters*, 2015. **595**: p. 1-6.
300. Yuan, S., Y. Shi, and S.J. Tang, *Wnt signaling in the pathogenesis of multiple sclerosis-associated chronic pain*. *Journal of neuroimmune pharmacology : the official journal of the Society on NeuroImmune Pharmacology*, 2012. **7**(4): p. 904-13.
301. Campbell, A.M., I.S. Zagon, and P.J. McLaughlin, *Opioid growth factor arrests the progression of clinical disease and spinal cord pathology in established experimental autoimmune encephalomyelitis*. *Brain Res*, 2012. **1472**: p. 138-48.

302. Lisi, L., et al., *Rapamycin reduces clinical signs and neuropathic pain in a chronic model of experimental autoimmune encephalomyelitis*. Journal of neuroimmunology, 2012. **243**(1-2): p. 43-51.
303. Dutra, R.C., et al., *The role of kinin B1 and B2 receptors in the persistent pain induced by experimental autoimmune encephalomyelitis (EAE) in mice: evidence for the involvement of astrocytes*. Neurobiology of disease, 2013. **54**: p. 82-93.
304. Rodrigues, D.H., et al., *IL-1 $\beta$  Is Involved with the Generation of Pain in Experimental Autoimmune Encephalomyelitis*. Molecular neurobiology, 2016. **53**(9): p. 6540-6547.
305. Grace, P.M., et al., *Behavioral assessment of neuropathic pain, fatigue, and anxiety in experimental autoimmune encephalomyelitis (EAE) and attenuation by interleukin-10 gene therapy*. Brain, Behavior, and Immunity, 2017. **59**: p. 49-54.
306. Lu, J., et al., *Pain in experimental autoimmune encephalitis: a comparative study between different mouse models*. Journal of neuroinflammation, 2012. **9**: p. 233-233.
307. Khan, N., et al., *Antiallodynic effects of alpha lipoic acid in an optimized RR-EAE mouse model of MS-neuropathic pain are accompanied by attenuation of upregulated BDNF-TrkB-ERK signaling in the dorsal horn of the spinal cord*. Pharmacology Research & Perspectives, 2015. **3**(3): p. e00137.
308. Schmitz, K., et al., *Dichotomy of CCL21 and CXCR3 in nerve injury-evoked and autoimmunity-evoked hyperalgesia*. Brain Behav Immun, 2013. **32**: p. 186-200.
309. Pender, M.P. and T.A. Sears, *Involvement of the dorsal root ganglion in acute experimental allergic encephalomyelitis in the Lewis rat. A histological and electrophysiological study*. J Neurol Sci, 1986. **72**(2-3): p. 231-42.
310. Pender, M.P. and T.A. Sears, *Vulnerability of the dorsal root ganglion in experimental allergic encephalomyelitis*. Clin Exp Neurol, 1985. **21**: p. 211-23.
311. Pender, M.P. and T.A. Sears, *The pathophysiology of acute experimental allergic encephalomyelitis in the rabbit*. Brain, 1984. **107 ( Pt 3)**: p. 699-726.
312. Xu, Z.-Z., et al., *Inhibition of mechanical allodynia in neuropathic pain by TLR5-mediated A-fiber blockade*. Nature medicine, 2015. **21**(11): p. 1326-1331.
313. Duffy, S.S., et al., *Peripheral and Central Neuroinflammatory Changes and Pain Behaviors in an Animal Model of Multiple Sclerosis*. Frontiers in Immunology, 2016. **7**: p. 369.
314. Wang, I.C., et al., *Peripheral sensory neuron injury contributes to neuropathic pain in experimental autoimmune encephalomyelitis*. 2017. **7**: p. 42304.
315. Gritsch, S., et al., *Oligodendrocyte ablation triggers central pain independently of innate or adaptive immune responses in mice*. Nat Commun, 2014. **5**: p. 5472.
316. Moalem, G. and D.J. Tracey, *Immune and inflammatory mechanisms in neuropathic pain*. Brain Research Reviews, 2006. **51**(2): p. 240-264.
317. Duffy, S.S., J.G. Lees, and G. Moalem-Taylor, *The Contribution of Immune and Glial Cell Types in Experimental Autoimmune Encephalomyelitis and Multiple Sclerosis*. Multiple sclerosis international, 2014. **2014**: p. 285245.
318. Olechowski, C.J., et al., *A diminished response to formalin stimulation reveals a role for the glutamate transporters in the altered pain sensitivity of mice with experimental autoimmune encephalomyelitis (EAE)*. Pain, 2010. **149**(3): p. 565-72.
319. Musgrave, T., et al., *Tissue concentration changes of amino acids and biogenic amines in the central nervous system of mice with experimental autoimmune encephalomyelitis (EAE)*. Neurochemistry international, 2011. **59**(1): p. 28-38.
320. Marte, A., et al., *Alterations of glutamate release in the spinal cord of mice with experimental autoimmune encephalomyelitis*. Journal of neurochemistry, 2010. **115**(2): p. 343-52.
321. Doolen, S., et al., *Peripheral nerve injury increases glutamate-evoked calcium mobilization in adult spinal cord neurons*. Molecular pain, 2012. **8**: p. 56.

322. Sung, B., G. Lim, and J. Mao, *Altered expression and uptake activity of spinal glutamate transporters after nerve injury contribute to the pathogenesis of neuropathic pain in rats*. The Journal of neuroscience : the official journal of the Society for Neuroscience, 2003. **23**(7): p. 2899-910.
323. Aicher, S.A., et al., *Hyperalgesia in an animal model of multiple sclerosis*. Pain, 2004. **110**(3): p. 560-570.
324. Melanson, M., et al., *Experimental autoimmune encephalomyelitis-induced upregulation of tumor necrosis factor-alpha in the dorsal root ganglia*. Multiple sclerosis, 2009. **15**(10): p. 1135-45.
325. Begum, F., et al., *Elevation of tumor necrosis factor alpha in dorsal root ganglia and spinal cord is associated with neuroimmune modulation of pain in an animal model of multiple sclerosis*. Journal of neuroimmune pharmacology : the official journal of the Society on NeuroImmune Pharmacology, 2013. **8**(3): p. 677-90.
326. Zhu, W., et al., *Elevated expression of fractalkine (CX3CL1) and fractalkine receptor (CX3CR1) in the dorsal root ganglia and spinal cord in experimental autoimmune encephalomyelitis: implications in multiple sclerosis-induced neuropathic pain*. Biomed Res Int, 2013. **2013**: p. 480702.
327. Sloane, E., et al., *Anti-inflammatory cytokine gene therapy decreases sensory and motor dysfunction in experimental Multiple Sclerosis: MOG-EAE behavioral and anatomical symptom treatment with cytokine gene therapy*. Brain Behav Immun, 2009. **23**(1): p. 92-100.
328. Mahad, D.J. and R.M. Ransohoff, *The role of MCP-1 (CCL2) and CCR2 in multiple sclerosis and experimental autoimmune encephalomyelitis (EAE)*. Semin Immunol, 2003. **15**(1): p. 23-32.
329. Ji, R.-R., et al., *MMP regulation of neuropathic pain*. Trends Pharmacol Sci, 2009. **30**(7): p. 336-340.
330. Ji, R.-R., Z.-Z. Xu, and Y.-J. Gao, *Emerging targets in neuroinflammation-driven chronic pain*. Nat Rev Drug Discov, 2014. **13**(7): p. 533-548.
331. Sun, J.H., et al., *MCP-1 enhances excitability of nociceptive neurons in chronically compressed dorsal root ganglia*. Journal of neurophysiology, 2006. **96**(5): p. 2189-99.
332. Tsuda, M., et al., *Neuronal and microglial mechanisms for neuropathic pain in the spinal dorsal horn and anterior cingulate cortex*. Journal of neurochemistry, 2017. **141**(4): p. 486-498.
333. Schomberg, D. and J.K. Olson, *Immune responses of microglia in the spinal cord: contribution to pain states*. Experimental neurology, 2012. **234**(2): p. 262-70.
334. Ramesh, G., A.G. MacLean, and M.T. Philipp, *Cytokines and Chemokines at the Crossroads of Neuroinflammation, Neurodegeneration, and Neuropathic Pain*. Mediators of Inflammation, 2013. **2013**: p. 20.
335. Nessler, S., et al., *Effect of minocycline in experimental autoimmune encephalomyelitis*. Annals of neurology, 2002. **52**(5): p. 689-690.
336. Benson, C., et al., *Voluntary wheel running delays disease onset and reduces pain hypersensitivity in early experimental autoimmune encephalomyelitis (EAE)*. Experimental neurology, 2015. **271**: p. 279-290.
337. MacKenzie, E.M., et al., *Phenelzine: An Old Drug That May Hold Clues to The Development of New Neuroprotective Agents*. Klinik Psikofarmakoloji Bülteni-Bulletin of Clinical Psychopharmacology, 2010. **20**(2): p. 179-186.
338. Parent, M.B., M.K. Habib, and G.B. Baker, *Time-dependent changes in brain monoamine oxidase activity and in brain levels of monoamines and amino acids following acute administration of the antidepressant/antipanic drug phenelzine*. Biochem Pharmacol, 2000. **59**(10): p. 1253-63.
339. McManus, D.J., et al., *Effects of the antidepressant/antipanic drug phenelzine on GABA concentrations and GABA-transaminase activity in rat brain*. Biochemical pharmacology, 1992. **43**(11): p. 2486-2489.
340. Baker, G.B., et al., *Effects of the antidepressant phenelzine on brain levels of gamma-aminobutyric acid (GABA)*. J Affect Disord, 1991. **21**(3): p. 207-11.
341. Parent, M.B., et al., *Effects of the antidepressant/antipanic drug phenelzine and its putative metabolite phenylethylidenehydrazine on extracellular gamma-aminobutyric acid levels in the striatum*. Biochem Pharmacol, 2002. **63**(1): p. 57-64.

342. Baker, G.B., et al., *Insights into the mechanisms of action of the MAO inhibitors phenelzine and tranylcypromine: a review*. J Psychiatry Neurosci, 1992. **17**(5): p. 206-14.
343. Michael-Titus, A.T., et al., *Imipramine and phenelzine decrease glutamate overflow in the prefrontal cortex--a possible mechanism of neuroprotection in major depression?* Neuroscience, 2000. **100**(4): p. 681-4.
344. Yang, J. and J. Shen, *In vivo evidence for reduced cortical glutamate-glutamine cycling in rats treated with the antidepressant/antipanic drug phenelzine*. Neuroscience, 2005. **135**(3): p. 927-37.
345. Song, M.-S., et al., *The antidepressant phenelzine protects neurons and astrocytes against formaldehyde-induced toxicity*. Journal of neurochemistry, 2010. **114**(5): p. 1405-1413.
346. Mifflin, K.A., et al., *Manipulation of Neurotransmitter Levels Has Differential Effects on Formalin-Evoked Nociceptive Behavior in Male and Female Mice*. The Journal of Pain, 2016. **17**(4): p. 483-498.
347. Musgrave, T., et al., *The MAO inhibitor phenelzine improves functional outcomes in mice with experimental autoimmune encephalomyelitis (EAE)*. Brain, behavior, and immunity, 2011. **25**(8): p. 1677-88.
348. Benson, C.A., et al., *The MAO inhibitor phenelzine can improve functional outcomes in mice with established clinical signs in experimental autoimmune encephalomyelitis (EAE)*. Behav Brain Res, 2013. **252**: p. 302-11.

# Chapter 2

Acute antinociceptive effects of the antidepressant phenelzine are mediated by context-dependent inhibition of neuronal responses in the dorsal horn

Unpublished

Potter LE, Doolen SD, Mifflin K, Tenorio G, Baker G, Taylor BK, Kerr BJ.

**Note:** LP did the experimental work, analysis, figures, and wrote the paper. SD designed the calcium imaging methods / experiments, did surgeries for imaging, and assisted with analysis. Imaging was done in the lab of BKT. KM and GT did formalin injections. Behavioral/IHC work was done in the lab of BJK. BJK helped with formulating the experiments / paper. GB/BJK postulated the use of PLZ. BJK, SD, and my examining committee members helped edit the paper.

## 2.1 - Abstract

Recent studies have suggested that the antidepressant phenelzine (PLZ) possesses anti-allodynic properties. PLZ is a monoamine-oxidase inhibitor, which elevates CNS concentrations of the monoamine neurotransmitters (serotonin-5-HT, and noradrenalin-NA) by inhibiting their degradation. PLZ also increases CNS GABA content by inhibiting the enzyme GABA-transaminase through an active metabolite. We confirmed an effect of PLZ in female C57/BL6 mice on nociceptive behaviors evoked by intraplantar formalin. Pretreating with PLZ 3h prior to formalin injection reduced nociceptive responding in the second phase of the assay, compared to vehicle (VEH). PLZ had no effect on the first phase of the formalin response, or on basal mechanical and thermal nociceptive sensitivity. PLZ also reduced formalin-evoked c-Fos, and increased 5-HT+ immunoreactivity in the superficial dorsal horn. We also tested the effects of bath-applied PLZ on glutamate-evoked intracellular calcium rises in an acute *ex vivo* spinal cord slice preparation. Pretreating lumbar slices with PLZ at 100-300 $\mu$ M concentrations produced a 20-40% inhibition of intracellular calcium responses to a 1mM, but not 0.3mM, bath-applied glutamate stimulus. Pretreating the slices with the 5HT1A-receptor antagonist WAY-100,635, but not the adrenergic antagonist idazoxan, prior to and during PLZ application, blocked the inhibition of responses to 1mM glutamate. These findings confirm that acute PLZ is anti-allodynic in female C57/BL6 mice, while not affecting basal nociceptive sensitivity. This anti-allodynic action likely involves a 5-HT/5HT1AR-dependent inhibition of neuronal responses within nociceptive circuits of the dorsal horn.

## 2.2 - Introduction

The monoamine oxidase inhibitor (MAOI) phenelzine (PLZ) was once commonly prescribed for the treatment of depression [1]. Concerns over the potential for precipitating a hypertensive crisis when used in the presence of dietary tyramine, through the so called 'cheese reaction', led to the eventual

supplanting of PLZ and other MAOIs by newer drugs, such as the selective-serotonin reuptake inhibitors (SSRIs) [1]. Critical reviews of the literature ultimately found that these fears were overstated, and suggested that the MAOIs were widely underutilized [1-3]. Today, PLZ is occasionally prescribed as a second- or third-line option in depressed patients who do not respond to the more commonly used SSRIs/SNRIs (serotonin/norepinephrine-reuptake inhibitors) [1, 3].

PLZ is unique amongst the MAOIs in that, apart from producing an elevation in CNS levels of the monoamine neurotransmitters through irreversible inhibition of both isoforms of their major degradative enzyme (MAO-A/B), it also reversibly inhibits GABA transaminase, leading to an elevation in CNS GABA content [4, 5]. This secondary action, mediated through the active metabolite phenylethylidenehydrazine (PEH), gives PLZ an additional anxiolytic effect in animal models [6, 7]. PLZ may also possess several other unique pharmacological characteristics, including an effect on glutamate release from CNS neurons [8], and neuroprotective effects mediated through the direct chemical 'scrubbing' of reactive aldehyde molecules and the inhibition of reactive-oxygen species (ROS) production by MAO [9, 10]. This broad range of biological activities has led to a renewed interest in the possibility of novel therapeutic uses for PLZ [11].

Recent publications have highlighted a potential application for PLZ, and its derivatives PEH and N<sub>2</sub>-Acetyl-PLZ, in the treatment of pain. Mifflin et al. 2016 [14] described the effects of acutely administered PLZ (and its derivatives) in male and female C57/BL6 mice in the formalin model of subacute chemogenic pain. In the current study, we further examined the effects of acute PLZ treatment on nociceptive sensitivity in female C57/BL6 mice, both in the basal condition and again in the formalin model.

We also investigated the central mechanisms of PLZ's antinociceptive effects by examining functional changes in the dorsal horn of the spinal cord (SCDH), both in post-mortem tissues and in an *ex vivo*

adult spinal cord (SC) slice preparation. We employed methods developed by Doolen and Taylor (first published in Doolen et al. 2012, [15]) for the imaging of intracellular calcium responses in live lumbar SC slices for these experiments. This involved bulk-loading lumbar slices with the ratiometric calcium dye fura-2, allowing us to image intracellular calcium responses in (putative) neurons within the SCDH in real time, following stimulation with extracellular bath-applied glutamate. We imaged responses both before and after superfusing the slices with PLZ at multiple concentrations, allowing us to identify a 'direct' (local) inhibitory effect of PLZ in the isolated SCDH. We also pretreated slices with specific monoamine receptor antagonists - idazoxan for adrenergic alpha receptors, and WAY-100,635 for 5HT1A receptors - alongside PLZ, in order to determine the separate contributions of these neurotransmitter/receptor systems to the overall inhibitory effect. These experiments help to establish a mechanistic basis for the observed effects of PLZ on nociceptive behaviors in the EAE and formalin models.

## **2.3 - Methods**

### **2.3.1 - Animals and Ethics**

A total of 40, 8–12-week-old, female C57/BL6 mice (Charles River–Saint Constant, Quebec, Canada / Indianapolis, IN, USA) were used in these experiments. Mice were housed 5 per cage, in standard cages, and fed *ad libitum*. Behavioral/immunohistochemistry experiments were conducted in accordance with the Canadian Council on Animal Care's Guidelines and Policies, and with protocols approved by the University of Alberta Health Sciences Animal Care and Use Committee. Calcium imaging experiments were conducted in accordance with protocols approved by the Institutional Animal Care and Use Committee of the University of Kentucky.

### **2.3.2 - Drug Treatments**

For behavioral and immunohistochemistry experiments, mice were divided into two groups (1 cages each /  $n=5$  for VFH, 2 cages each /  $n=10$  for hotplate/formalin,) which received an I.P. injection of either vehicle (VEH, bacteriostatic water, 10mL / kg body weight) or phenelzine (PLZ, 15 mg/kg body weight, Sigma-Aldrich—Oakville, ON, Canada). The injections were administered on the day of the testing, 1h before the first Von Frey / hotplate test, or 3h before the formalin assay.

### **2.3.3 - Behavioral Pain Assays**

#### **2.3.3.1 - Von Frey Hairs**

The Von Frey hair (VF/VFH) assay was used to assess the effects of acute PLZ treatment on basal mechanical (tactile/punctate pressure) sensitivity. Animals were placed in transparent plexiglass boxes over a screen that allowed access to the paws. Prior to the start of testing, all mice underwent a period of habituation to the boxes (5–10 min/day, for 3 days before baseline testing began). Mice were also given 5–10 min of habituation time in the testing boxes at the start of each test day. After this period, the plantar surface of each hindpaw was stimulated five times with a weighted VFH monofilament. An observer blinded to the experimental/treatment groups monitored and recorded behavioral responses to stimulation. “Noxious responding” (i.e., shaking, licking, or guarding of the paw) was noted. Hindpaw stimulation was repeated through a progressive series of filament weights (0.04–2.0 g), until a stimulus produced a “noxious response”  $\geq 60\%$  of the time—the weight at which this occurred was taken to be the withdrawal threshold for that paw at that time point. Left and right paw responses were averaged within each animal to provide a combined threshold for each test day, and these combined thresholds were used for subsequent analysis. VFH testing was conducted at 1h and 3h post injection.

#### **2.3.3.2 - Hot Plate**

The hot plate assay was used to assess the effects of acute PLZ treatment on noxious thermal (heat) sensitivity. The plate was warmed to 52<sup>0</sup>C (a temperature at which nociceptive C fibres are activated [16]). Mice were placed onto the plate, and an observer blinded to the treatment groups monitored and

recorded the time to the first 'noxious' response (usually a flick of the hindpaw), and the time to a 'lick' response. This assay was repeated twice per animal to obtain an average withdrawal latency for each time point. Hot plate testing was conducted prior to injections and then again at 3h post injection.

### **2.3.3.3 - Formalin Assay**

The formalin assay was used to test the effects of acute PLZ treatment in a model of subacute inflammatory/neuropathic pain. Animals were given drug injections 3h prior to the beginning of the assay. On three previous days for 10 min. each, and for 10 min. prior to the start of the assay, each animal was placed into the clear-walled plexiglass observation chamber, in order to allow for habituation to the surroundings. A solution of 1% formalin was made daily by diluting 37% into 0.9% w/v saline. 30 $\mu$ L of this solution was injected subcutaneously into the plantar surface of the left hindpaw, and the animal was returned to the observation chamber. An observer blinded to the treatment groups observed and recorded the time (in seconds) spent 'noxiously' responding, independently recording the time spent lifting/shaking the paw, and the time spent licking the paw. A period of 30 min. post-formalin injection was binned into six 5 min. intervals for recording purposes. Subsequently, the first two bins (0-10 min. post formalin) and the last four bins (10-30 min. post formalin) were defined as 'phase one' and 'phase two' of the assay (respectively). Times spent licking/lifting/shaking were added together and reported as 'nociceptive response time'. A 'nociception score' was also calculated / reported from the response times for each bin by the formula  $(((\text{Lick time}) * 2) + (\text{Lift time})) / 300$ .

## **2.3.4 - Immunohistochemistry/Immunocytochemistry**

### **2.3.4.1 - Tissue Collection / Preparation**

Following the formalin assay, a period of 1h was allowed to elapse before sacrificing the animal for tissue collection, in order to allow for full expression of the c-Fos protein. Animals underwent transcardiac exsanguination / perfusion with saline (0.9% w/v) followed by fixation with 4% paraformaldehyde (PFA) / 1% glutaraldehyde (GA) in 0.1M PB. Lumbar (L1-L5) spinal cord was

removed and post-fixed overnight in PFA/GA. Tissues were then cryoprotected by immersion in sucrose 30% solution for 48h, followed by embedding in TissueTek OCT and freezing over liquid N<sub>2</sub>. Frozen tissues were stored at -80°C until they could be sectioned on a cryostat (20µm sections) and mounted directly onto slides.

#### **2.3.4.2 - Immunohistochemistry Staining**

Tissues were stained using standard immunohistochemistry (IHC) / immunofluorescence protocols as described below. The following reagents/antibodies were used:

##### **2.3.4.3 - c-Fos / DAB:**

Tissues were incubated with rabbit anti-c-Fos (1:1000, Cell Signalling, Danvers, MA, USA) primary antibody overnight, followed by goat anti-rabbit biotin (1:400, 2h RT, Vector Labs, Burlingame, CA, USA), and avidin-biotin complex (ABC 1:200, 1.5h RT, "VectaStain Elite™ ABC/HRP Kit", Vector Labs), before visualization with 3,3'-diaminobenzidine (DAB, Vector Labs) (plus nickel). Slides were coverslipped using Permount.

##### **2.3.4.4 - Immunofluorescence:**

Tissues were incubated overnight with the following primary antibodies: rabbit anti-5-HT (1:1000, Sigma-Aldrich, Oakville, ON, Canada). Primary antibodies were then visualized with the following secondary antibodies: goat anti-rabbit AlexaFluor 488 (1:200, 1h RT, Invitrogen Life Technologies Inc., Burlington, ON, Canada). Slides were coverslipped using Vectashield™ with DAPI (Vector Labs).

##### **2.3.4.5 - IHC Image Acquisition and Quantification**

Slides were imaged using a Zeiss AxioCam MRm camera on a Zeiss Observer Z.1 inverted fluorescence microscope equipped with a 20x objective lens. Images of both ipsilateral and contralateral (to stimulus) dorsal horn at the L4-L5 level were captured for quantification, from 2

sections per slide / 2 slides per animal. Exposure levels were maintained at a consistent setting for each tissue set. Sections were quantified using NIH ImageJ/FIJI and Adobe Photoshop. Manual cell counting for c-Fos was performed by an observer blinded to treatment groups. Only the dorsal horn ipsilateral to stimulus was quantified for c-Fos analysis. 5-HT was quantified by integrated density, performed using template regions of interest (ROIs) manually adjusted to fit the individual section (but with consistent overall area  $\sim\pm 2\%$ ). Ipsi-/contralateral dorsal horns were averaged together for the 5-HT analysis.

All quantitative IHC image analyses were performed on either the original unmodified images, or on images processed in a consistently applied manner as described elsewhere in the methods.

Representative photomicrographs used in figures were additionally adjusted for brightness, contrast, color balance, and histogram scaling in order to improve the overall visibility of the images. These adjustments were performed only on whole images and were applied in a consistent a manner such that the figures accurately reflect the entire contents and relative intensities of the original images.

### **2.3.5 - Calcium Imaging (Adapted From Doolen et al. 2012)**

#### **2.3.5.1 - Preparation of Adult Mouse Spinal Cord Slices:**

Mice were anesthetized with 5% isoflurane and quickly perfused transcardially with 10 mL of ice-cold sucrose-containing artificial cerebrospinal fluid (aCSF) (sucrose-aCSF) that contained (in mM): NaCl 95, KCl 1.8,  $\text{KH}_2\text{PO}_4$  1.2,  $\text{CaCl}_2$  0.5,  $\text{MgSO}_4$  7,  $\text{NaHCO}_3$  26, glucose 15, sucrose 50, kynurenic acid 1, oxygenated with 95%  $\text{O}_2$ , 5%  $\text{CO}_2$ ; pH 7.4. The lumbar spinal cord was rapidly (within 90s) isolated by laminectomy from the cervical enlargement to the cauda equina, placed in oxygenated ice-cold sucrose-aCSF, cleaned of dura mater and ventral roots, and super-glued vertically to a block of 4% agar (Fisher Scientific, Pittsburgh, PA) on the stage of a Campden 5000mz vibratome (Lafayette, IN). Transverse slices (300–450  $\mu\text{m}$ ) from lumbar segments L3-L4 were cut in ice-cold sucrose-aCSF using

minimum forward speed ranging from 0.03 to 1 mm/s and using maximum vibration. The ideal total dissection and slicing time to ensure slice viability was 22 minutes or less.

### **2.3.5.2 - Ratiometric Ca<sup>2+</sup> Measurements:**

Lumber slices were incubated for 30 min. at room temperature (37<sup>o</sup> C) with Fura-2 AM (10 μM), pluronic acid (0.1%) in oxygenated aCSF containing (in mM): NaCl 127, KCl 1.8, KH<sub>2</sub>PO<sub>4</sub> 1.2, CaCl<sub>2</sub> 2.4, MgSO<sub>4</sub> 1.3, NaHCO<sub>3</sub> 26, glucose 15, followed by a 20 min. de-esterification period in normal aCSF. Prior to recording, slices were kept at RT in a chamber containing approximately 150 mL of oxygenated aCSF. Slices were perfused at 1–2 mL/min with normal aCSF in an RC-25 recording chamber (Warner Instruments, Hamden, CT) mounted on a Nikon FN-1 upright microscope fitted with a 79000 ET FURA2 Hybrid filter set (Nikon Instruments, Melville, NY) and a Photometrics CoolSNAP HQ<sub>2</sub> camera (Tucson, AZ). Relative intracellular Ca<sup>2+</sup> levels were determined by measuring the change in ratio of fluorescence emission at 510 nm in response to excitation at 340 and 380 nm (200 ms exposure). Paired images were collected at 1–1.5 seconds/frame. Relative changes in Ca<sup>2+</sup> levels were evaluated using Nikon Elements software by creating a region of interest over the cell body and calculating the peak change in ratio. Approximately 10 cells were analyzed in each slice/treatment condition. The peak magnitude of Ca<sup>2+</sup> transients were expressed as the difference in ratio following exposure to exogenous glutamate compared to baseline before glutamate. The criterion for a Ca<sup>2+</sup> response to be considered was a 10% increase above the baseline 340/380nm ratio. Ca<sup>2+</sup> transients were in response to a 10s exposure to 0.3mM or 1mM glutamate in aCSF in the initial PLZ(-only) study. Only the 1mM glutamate stimulus was used in the PLZ plus antagonists study. For the PLZ-only study, each slice was stimulated twice with each glutamate concentration (with several min. between stimuli to allow calcium levels to return to baseline), prior to perfusion with oxygenated aCSF/PLZ at the given concentration (1 slice per PLZ concentration for 0, 10, 30, 100, and 300μM) for 30 min. Following PLZ perfusion, the slice was re-stimulated two times with each glutamate concentration. For each PLZ concentration, the 'raw' ΔF<sub>340/380</sub> magnitudes of the calcium response before and after PLZ exposure were reported, as well

as the change in magnitude by calculating the *post*-PLZ magnitude as a percentage of the *pre*-PLZ response (to each glutamate concentration / average of two stimuli). This change was also expressed as a 'percent inhibition' of the *pre*-PLZ response. For antagonist studies, the slice was stimulated twice with 1mM glutamate, then perfused with the antagonist (30 $\mu$ M idazoxan for adrenergic alpha-2 receptor antagonism, 10 $\mu$ M WAY-100,635 for 5HT1A receptor antagonism) in oxygenated aCSF for 10 min. prior to and during 2 additional glutamate stimuli. This was done to assess the effect of each antagonist on intracellular calcium responses in the absence of PLZ. Following the antagonist exposure, the slice was perfused with 200 $\mu$ M PLZ plus antagonist in oxygenated aCSF for 30 min., and then re-stimulated twice with 1mM glutamate. Magnitudes of the calcium responses were expressed as the 'raw'  $\Delta F_{340/380}$  values, and as a percentage of the *pre*-antagonist/PLZ 1mM glutamate response.

### 2.3.6 - Statistics

For behavioral/immunohistochemistry experiments, statistical analyses were performed with Student's t-test, or by the Mann-Whitney rank sum test for non-parametric data sets - or by two-way RMANOVA, with post-hoc testing by the Holm-Sidak method. For the calcium imaging experiments, a repeated measures/within-animal design was used. Statistical analyses were performed by within subject t-tests, or Wilcoxon signed rank-test for non-parametric data. Significance was set at  $P < 0.05$ .

## 2.4 - Results

### 2.4.1 - *Acute PLZ pretreatment (in vivo) does not affect basal mechanical or thermal nociceptive sensitivity.*

We first sought to determine the effects of acute PLZ treatment on basal nociceptive behavioral responses / sensitivity. To this end, we measured the mechanical withdrawal thresholds of VEH (**n=5**) and PLZ (**n=5**) pretreated animals using the Von Frey hair (VFH) assay. Sources in the literature indicated that a single I.P. dose of PLZ produces significant elevation of monoamine neurotransmitters

(5-HT/NA/dopamine) and GABA by T+1-4h (following injection), with maximal elevation by 6h, followed by a slow return to basal concentrations over hours to days due to irreversible MAOI inhibition [4, 14, 17, 18]. We therefore assessed VF thresholds in the animals at baseline (prior to VEH/PLZ injection), and at T+1h and T+4h following VEH/PLZ injection. No effect on VF threshold was noted at either time point when the PLZ-treated group was compared to the VEH-treated group. Responses were analyzed as raw thresholds. (**FIG. 2.1A**; 2-way *RmANOVA*, effect of treatment NS  $p=0.500$ )

We also measured the effect of acute PLZ pretreatment on the response to noxious heat (52°C) using the hot plate assay. For the hotplate assay, we only examined responses in the baseline condition (ie. prior to VEH/PLZ injection), and at T+3h post VEH/PLZ injection (**n=10**), in order to minimize sensitizing the animals through over-testing. In both treatment groups, the time to initially detect/respond to the hot plate (ie. to the first lick/lift/flick of the hindpaw, withdrawal latency) was slightly reduced at the T+3h time point. However, the VEH and PLZ groups did not significantly differ from one another in terms of their average withdrawal latency at T+3h post-treatment. (**FIG. 2.1B**; 2-way *RmANOVA*, effect of treatment NS  $p=0.130$ )

#### **2.4.2 - Acute PLZ pretreatment (in vivo) inhibits the second phase of the response to intraplantar formalin.**

As our initial assays indicated no effect of acutely administered PLZ on basal mechanical and thermal nociceptive sensitivity, we next sought to determine if there was any effect of acute PLZ pretreatment on nociceptive responses in a model of subacute chemogenic pain. To this end, we examined responses to intraplantar injection of formalin in acute VEH/PLZ- (**n=10**) pretreated animals. For this experiment, formalin was administered at the T+3h time point post VEH/PLZ injection. Our lab previously reported on the effects of acute PLZ pretreatment on formalin evoked nociceptive behaviors in Mifflin et al. 2016 [14]. That paper reached the conclusion that acute PLZ did not significantly inhibit responses to intraplantar formalin in female C57/BL6 mice, despite a strong trend (~40% reduction) in

the duration of the second phase of the response. Mifflin et al. 2016 noted an apparent biphasic distribution in female mice treated with PLZ, with approximately half of the mice responding to the drug, and half exhibiting responses similar to those of the VEH treated animals. In the current experiment, we again observed that several (2-3) individual animals in the treated group did not respond strongly to PLZ – however this small proportion of apparent ‘non-responders’ may merely be due to off-target treatment injections. Nevertheless, across the group there was a statistically significant (~50%) reduction in the second (*‘delayed’, 10-30 min. post-formalin, t-test, \*p=0.033, FIG. 2.2B*), but not the first (*‘acute’, 0-10 min. post-formalin, t-test, NS p=0.301 FIG. 2.2B*) phase of the formalin response. (Also analyzed as *‘nociception score’: 2-way RMANOVA, \*p=0.046 overall effect of treatment, all-pairwise post-hoc comparisons by Holm-Sidak, \*p<0.05 effect of treatment within time bins: 15-20 min., 20-25 min., 25-30 min., p>0.05/NS NO effect of treatment within time bins: 0-5 min., 5-10 min., 10-15 min. FIG. 2.2A*).

#### **2.4.3 - Acute PLZ pretreatment (in vivo) reduces c-Fos+ immunoreactivity in the ipsilateral superficial dorsal horn following intraplantar formalin.**

c-Fos is a nuclear transcription factor that is commonly used as an immunohistochemical marker for neuronal activation [19]. Noxious stimulation of the hindpaw with intraplantar formalin is known to reliably evoke a strong c-Fos signal in the ipsilateral superficial dorsal horn of the lumbar SC [20]. We therefore stained for c-Fos in the lumbar SCDH of the VEH/PLZ plus formalin-treated animals (**n=5** ea.), with the intent of examining the effect of acute PLZ pretreatment on formalin-evoked cellular activation/responses within the nociceptive circuitry of the SCDH (**FIG. 2.3A**). Because acute PLZ pretreatment inhibited the second phase of the behavioral response to formalin, we predicted that PLZ would also reduce the number of c-Fos+ neurons within the ipsilateral DH. Our analysis confirmed that PLZ pretreatment led to a reduction in formalin-evoked c-Fos+ cells in the ipsilateral superficial DH (laminae I-II) (**FIG. 2.3B; t-test, \*p=0.018**), but not in the deeper laminae of the DH (III-VI) (*not shown*;

*t*-test, NS  $p=0.151$ ). The contralateral DH did not exhibit strong c-Fos staining in either treatment group, and was not quantified.

#### **2.4.4 - Acute PLZ treatment (*in vivo*) increases 5-HT+ immunoreactivity in the superficial dorsal horn.**

Although sources in the literature, and experiments in our own lab using high-performance liquid chromatography (HPLC) on SC homogenate from naïve, formalin-treated, and EAE animals, have established that acute PLZ treatment produces an increase in the concentration of monoamine neurotransmitters (5-HT, NA, dopamine) and GABA [4, 14, 17, 18] in the spinal cord, we wanted to ascertain if these differences could be localized specifically to the dorsal horn. To this end, we employed immunohistochemical staining with antibodies directly targeting the small molecules (5-HT/GABA). IHC for GABA, however, requires non-trivial alternative tissue processing and staining methods (see [21]) to be reliable. Indeed, the quality and specificity of the staining we accomplished using our standard protocol was deemed unsatisfactory for analysis. We therefore focused our reporting toward 5-HT only.

We identified a statistically significant elevation in 5-HT+ immunoreactivity within the superficial (laminae I-III) DH (**FIG. 2.4A,B**) in the PLZ-treated group ( $n=5$ ) compared to VEH, ( $n=5$ ) (**FIG. 2.4C**; *t*-test,  $*p=0.018$ ). There was no statistically significant difference in 5-HT+ immunoreactivity within the ventral horn (VH) in the PLZ-treated group compared to VEH (**FIG. 2.4D-F**; *t*-test, NS  $p=0.209$ ).

#### **2.4.5 - PLZ produces a dose-dependent inhibition of glutamate-evoked calcium responses in *ex vivo* lumbar slices.**

After determining the effects of acute PLZ pretreatment on nociceptive behavioral responses and cellular activation/neurotransmission in the SCDH *in vivo*, we sought to further investigate the precise mechanism of PLZ's actions in an *ex vivo* spinal cord slice preparation. Acutely prepared lumbar spinal

cord slices from adult female C57/BL6 mice were bulk-loaded with the ratiometric calcium dye fura-2, in order to allow us to measure intracellular calcium responses in dorsal horn neurons, evoked by bath application of glutamate. We used a 10s superfusion of 0.3mM glutamate in aCSF for a low glutamate stimulus, and also a 1mM high glutamate stimulus (**FIG. 2.5A,B**). Slices were stimulated twice with each glutamate concentration, before being perfused with oxygenated aCSF + PLZ for 30 min. at 0, 10, 30, 100, and 300 $\mu$ M concentrations (1 slice per concentration/animal, **n=3-5** animals per [PLZ]), and then re-stimulated. By comparing the post-PLZ intracellular calcium response with the pre-PLZ response, we were able to determine whether bath-applied PLZ directly inhibited cellular (neuronal) responses within the SCDH. We determined that there was a dose-dependent inhibitory effect of PLZ treatment on intracellular calcium responses to the 1mM (high) (**FIG. 2.5F-H**), but not the 0.3mM (low) (**FIG. 2.5C-E**), glutamate stimulus. This inhibition of responses to the 1mM stimulus was significant at the 100 and 300 $\mu$ M concentrations of PLZ (**FIG. 2.5F**; *peak ( $\Delta$ )F340/F380, paired t-test, within slice control, \***p=0.019** at 100 $\mu$ M PLZ, \***p=0.002** at 300 $\mu$ M PLZ). We also analyzed the post-PLZ response as a percentage of the pre-PLZ response (*paired t-test, within slice control, \***p=0.042** at 300 $\mu$ M PLZ, FIG. 2.5G*). The mean magnitude of inhibition produced was 24.8 $\pm$  4.4% for 100 $\mu$ M PLZ, to 36.5 $\pm$  6.2% for 300 $\mu$ M PLZ, of the peak response intensity following 1mM glutamate. No significant effects were observed at any tested concentration of PLZ for the 0.3mM glutamate stimulus, **FIG. 2.5C-E**. Of note, a gradual upward drift in the baseline F340/380 ratio (ie. in the absence of stimulation) was observed over the course of the experiments (~40 min. each) in the slices treated with 300 $\mu$ M, but not 100 $\mu$ M, PLZ. This could be indicative of a general toxic or detrimental effect upon the slice of PLZ superfusion at the highest (300 $\mu$ M) concentration. For this reason, we used the slightly lower concentration of 200 $\mu$ M PLZ in subsequent experiments.*

**2.4.6 - Pretreatment with the 5HT1AR antagonist WAY-100,635, but not the adrenergic antagonist idazoxan, blocks the inhibition of glutamate-evoked calcium responses in the DH by PLZ.**

After confirming an inhibitory effect of PLZ within the SCDH in isolated spinal cord slices, we next assessed the role of specific neurotransmitter/receptor systems in the SCDH through the addition of specific receptor antagonists to the *ex vivo* design. Literature sources and experiments in our lab ([14]) indicated that 5-HT may be inhibitory in the SCDH by its action at the 5HT1A receptor (5HT1AR) [22-26]), while NA may be inhibitory in the SCDH through the alpha-2(A/C) receptor [27, 28] (or indirectly through alpha-1 [29]). For this reason, we decided to test the effect of pretreating the *ex vivo* SC slices with the 5HT1AR antagonist WAY-100,635 (at 10 $\mu$ M), or the alpha-2 antagonist idazoxan (at 30 $\mu$ M), prior to and during superfusion with PLZ at 200 $\mu$ M in aCSF. Literature K<sub>s</sub> and reported working concentrations suggested that these would be effective concentrations for the antagonists [23, 30, 31]. For this experiment, we used only the 1mM glutamate stimulus, as no effect of PLZ was apparent with the 0.3mM glutamate stimulus. We stimulated the slice (2x) prior to application of the antagonist, and again after 10 min. superfusion of the antagonist (in oxygenated aCSF), and after 30 min. superfusion of antagonist + PLZ (at 200 $\mu$ M, in oxygenated aCSF). This design allowed us to detect any effect of the antagonist in the absence of PLZ. We confirmed that treatment of the slices with 200 $\mu$ M PLZ (in oxygenated aCSF, no antagonist, **n=5**) for 30 min. produced a ~20% inhibition of intracellular calcium responses to 1mM glutamate (**FIG. 2.6A**, peak ( $\Delta$ )F340/380, paired *t*-test, \***p=0.030**). No baseline drift over the course of the experiment, as had been observed with 300 $\mu$ M PLZ, was observed at this concentration of PLZ. Pretreatment of the slices with 30 $\mu$ M idazoxan (**n=4**) or 10 $\mu$ M WAY-100,635 (**n=3**) for 10 min. did not have any significant effects on the response to 1mM glutamate (*idazoxan*: Wilcoxon signed rank-test, post-idazoxan vs. pre, NS *p*=0.125; WAY: paired-test, post-WAY vs. pre, NS *p*=0.742) (**FIG. 2.6B/C**). Treatment with 30 $\mu$ M idazoxan + 200 $\mu$ M PLZ did not prevent the expected inhibition of responses to the 1mM glutamate stimulus (paired *t*-test post-PLZ + idazoxan vs. pre-PLZ + idazoxan, \***p=0.007**) (**FIG. 2.6B**). Treatment with 10 $\mu$ M WAY-100,635 + 200 $\mu$ M PLZ fully prevented PLZ-induced inhibition of responses to the 1mM glutamate stimulus (paired *t*-test post-PLZ + WAY vs. pre-PLZ + WAY, NS *p*=0.830). (**FIG. 2.6C**)

## 2.5 - Discussion

Antidepressants, such as the selective serotonin-/serotonin norepinephrine-reuptake inhibitors (SS/SNRIs), and the tricyclics (TCAs), are commonly employed as first-line treatments for chronic/neuropathic pain conditions [32]. These drugs elevate synaptic concentrations of the monoamine neurotransmitters (5-HT/NA) by inhibiting the function of membrane transporters responsible for their reuptake into the nerve terminal. This leads to enhanced signalling through pre/post-synaptic monoamine receptors, producing a variety of downstream effects on cellular/neuronal function. In the SCDH, the monoamine neurotransmitters generally act to inhibit neuronal activity, which may explain the efficacy of antidepressants in treating pain conditions [23, 27, 33]. The other major class of first-line treatments for chronic neuropathic pain (CNP) are the gabapentinoids - gabapentin and pregabalin [32]. The precise mechanism of action of the gabapentinoids is complex and has not been fully elucidated; however, they are known to act (partially) in a manner similar to certain anticonvulsants [34, 35]. Neither class of treatments is fully effective in the majority of cases of CNP, creating an urgent need for improved treatment options [36].

As an “atypical” MAOI, PLZ shares properties of both these treatment classes. As mentioned, PLZ raises CNS levels of the monoamine neurotransmitters (5-HT, NA, and dopamine) by irreversibly inhibiting MAO-A/B [10]. PLZ also enhances central inhibitory signalling - the net effect of which is similar to anticonvulsant/anxiolytic therapies - by elevating GABA in the CNS through the inhibitory action of the active metabolite PEH upon the enzyme GABA transaminase [7]. All of these neurotransmitters have been implicated in (anti-)nociception, and this combined activity makes PLZ a potentially useful investigatory drug for CNP. At least one early study regarding its effect on nociception found that PLZ suppressed responses in the tail-flick assay [37], a widely used behavioral test of thermal nociceptive sensitivity. More recently, Mifflin et al. (2016) [14] studied PLZ and its derivatives, PEH and N<sup>2</sup>-Acetyl-PLZ, in the context of the formalin model of subacute chemogenic pain in both male

and female C57/BL6 mice. Notably, the authors found that PLZ produced less reliable antinociceptive effects in females compared to males – although a roughly 40% reduction in the duration of the second phase of the formalin response was apparent in females in that study. However, due to the fact that the female cohort split roughly equally between animals which responded strongly to PLZ, and animals in which PLZ produced little to no antinociceptive effect, the authors of Mifflin et al. (2016) ultimately concluded that there was no statistically significant behavioral effect of PLZ in the formalin assay in females. Male mice, on the other hand, responded reliably to PLZ and its N<sub>2</sub>-acetyl derivative, with a reduced response to formalin in the second phase. Furthermore, the authors found that the antinociceptive effects of N<sub>2</sub>-acetyl-PLZ in male mice could be blocked by pretreating the animals with intrathecal WAY-100,635 [14].

In the current study, we re-examined the possibility that PLZ possesses acute antinociceptive effects in female C57/BL6 mice - both on basal mechanical and thermal nociceptive sensitivity, and in the intraplantar formalin assay. Our updated findings confirm the effect which was first observed in Mifflin et al. (2016) [14], but which failed to reach statistical significance in that study. Specifically, we also found that pretreatment with PLZ produced a mean 40-50% reduction in the second phase of the formalin response in female mice. In contrast to what was described in the earlier tail-flick assays, we found no effect of acute PLZ treatment in naïve (non-allodynic) females on mechanical withdrawal thresholds, or on withdrawal latencies in the hot plate assay. This suggests that PLZ lacks a classical ‘analgesic’ effect – ie. a broadly ‘numbing’/anesthetic effect, or a generalized motor-inhibitory effect - such as might be produced by opioids, anesthetic agents, or sedatives/depressants [38].

As described above, in the formalin assay, the majority of female mice in the current study were responsive to PLZ treatment. Only 2 out of 10 animals in the PLZ group did not respond strongly to the drug. The effect of PLZ was primarily on the second phase of the formalin response - ie. the ‘delayed’ pain response, from 10-30 min post-formalin injection. The first (acute, 0-10 min.) phase of the

response was not significantly inhibited by PLZ treatment compared to VEH. This temporal distinction may hold mechanistic relevance: whereas the first phase of the formalin response is thought to be primarily mediated by peripheral C-fibre volleys, the second phase of the formalin response is thought to involve glutamate dependent central sensitization and peripheral inflammation [39, 40]. Furthermore, these findings support the conclusion that PLZ has an anti-allodynic/anti-hyperalgesic action, while acute nociceptive sensitivity remains unchanged.

Intraplantar formalin reliably evokes c-Fos expression in neurons of the ipsilateral superficial dorsal horn, making it a useful marker of neuronal activation in this assay [20]. IHC for c-Fos in the formalin-treated animals revealed that PLZ pretreatment significantly reduced c-Fos+ cells in the ipsilateral superficial DH. This finding demonstrates that PLZ has an overall inhibitory action on neurons within the central nociceptive circuitry of the DH *in vivo*. Although the precise cellular/circuit mechanisms cannot be revealed by c-Fos IHC alone, it is likely that this inhibition of neuronal activation within the superficial DH underlies the reduced behavioral response to formalin in the PLZ treated animals [41].

We also assessed 5-HT levels in the SCDH using IHC in these mice, but were unable to stain for GABA/NA. IHC for 5-HT confirmed that a single injection of PLZ produced a detectable increase in 5-HT+ immunoreactivity in the superficial SCDH. This finding extends an additional degree of anatomical specificity to what was previously reported in Mifflin et al. (2016) [14] using HPLC – namely, that a single injection of PLZ in female C57/BL6s produces a significant elevation of 5-HT in the whole lumbar SC [14]. The experiments by Mifflin et al. [14] also found that an injection of PLZ prior to formalin in female C57/BL6 mice produced a significant elevation of GABA (and NA) content in the lumbar SC. The possibility that PLZ's antinociceptive effects involve the enhancement of GABA- (or NA-) mediated inhibition in the SCDH should therefore not be discounted. Indeed, Mifflin et al. [14] also found that pretreatment with the active metabolite PEH – which acts only through GABA, and not through the monoamines – reduced responses in the second phase of the formalin assay in both sexes [14].

In order to further study the central actions of acute PLZ in the SCDH in isolation, we moved from *in vivo* testing and *post-mortem* tissue assays into an *ex vivo* lumbar spinal cord slice preparation. As described, we measured the effect of pretreating the lumbar slices with bath-applied PLZ, on intracellular calcium responses to bath-applied glutamate at 0.3mM (low [glu]) and 1mM (high [glu]). Doolen et al. (2012) [15] demonstrated that the ED<sub>50</sub> for Ca<sup>2+</sup> responses in this preparation was 0.64mM glutamate. Our use of a simple within-subjects design allowed us to directly measure the inhibition produced by PLZ at each concentration in each individual. We found that at the two highest concentrations used (100μM and 300μM), PLZ pretreatment inhibited responses to the 1mM glutamate stimulus (~25% for 100μM to ~36% for 300μM), but did not inhibit responses to the weaker 0.3mM glutamate stimulus. This divergence in the response to differing concentrations of extracellular glutamate is noteworthy for several reasons. First, it bears analogy to the divergent behavioral effects of PLZ – namely, lacking an effect on basal nociception and the first phase of the formalin response, yet conversely inhibiting the ‘sensitized’ / delayed pain response in the second phase of the formalin assay. Indeed, our behavioral, histological, and imaging results all suggest that PLZ has an inhibitory effect only for specific conditions and stimuli (ie. it is truly anti-allodynic/anti-hyperalgesic) - becoming ‘active’ in the ‘sensitized’/high-threshold condition, without altering basal nociception and responses to low-threshold stimuli. Mechanistically, this ‘thresholded’ or dichotomous action raises the possibility that PLZ is inhibitory in the 1mM glutamate condition, but not the 0.3mM glutamate condition, because the higher concentration of glutamate is perhaps able to engage specific neural circuits and mechanisms within the DH which are not activated by the lower glutamate concentration.

Both 5-HT and NA are involved in descending antinociceptive/inhibitory control circuits, in which monoaminergic neurons originating in the brainstem project into the DH, and modulate spinal nociceptive activity primarily through volume neurotransmission [33]. Neuronal receptors for 5-HT (5HT1AR – but also 5HT1B/D/F, 5HT2C, 5HT3/5HT5A, 5HT7Rs) and NA (alpha-1/2 receptors) are

found throughout the SCDH, and are particularly abundant in the superficial laminae of the DH, including on inhibitory and excitatory interneurons in the *substantia gelatinosa* [33]. As mentioned, activation of these receptors generally produces a net inhibition of central nociceptive/functional responses, either by directly binding to the responsive cells, or by acting trans-synaptically / indirectly through interneurons [23, 24, 27, 42]. Monoamine receptors are also found on peripheral afferent terminals in the DH, where they can elicit presynaptic inhibition [42]. In order to further elucidate the role of the monoamine neurotransmitters, and their receptors, in the inhibitory effect of PLZ in the isolated SCDH, we pretreated the lumbar slices with specific receptor antagonists prior to and during the application of PLZ. We did not attempt to isolate any GABA-mediated effects of PLZ in this experiment because we were not confident that a 'silent' GABA antagonist – ie. one which would not independently alter neuronal responses - could be found. We tested the effects of the adrenergic alpha-2 receptor antagonist idazoxan, and the 5HT1AR-specific antagonist WAY-100,635. Neither antagonist altered responses to 1mM glutamate in the absence of PLZ. Pretreatment of the slices with WAY-100,635, but not with idazoxan, was found to negate the inhibitory effects of 200µM PLZ on intracellular calcium responses to 1mM glutamate. This result indicates that the inhibition produced by PLZ in this paradigm is 5HT1AR-dependent, but does not require adrenergic alpha-2 receptor activation. It should be emphasized that this result does not suggest that 5HT1AR activation is sufficient for PLZ's effect in this paradigm - merely, that it is necessary - especially as the role of GABA remains unknown.

Furthermore, it is unclear how monoamine release and signalling are altered by isolating the transverse spinal cord slices – as descending monoaminergic axons are undoubtedly severed in this preparation. While the mechanisms that act in the intact animal may differ in substantial ways from what is observed in isolated SC tissues, by combining both *in vivo/post-mortem* and *ex vivo* approaches, we can better assert that PLZ's antinociceptive effects are likely mediated by the inhibition of neuronal activity within the central nociceptive circuitry of the SCDH.

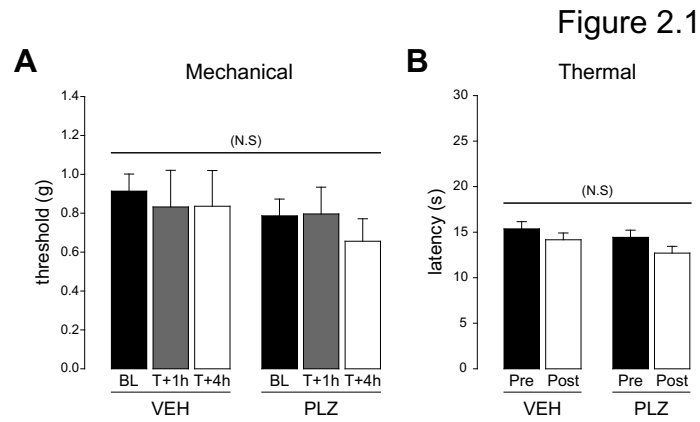


**Figure 2.1** Acute effects of PLZ treatment on basal mechanical and thermal nociceptive sensitivity.

(A) Mean mechanical withdrawal thresholds (Von Frey Hairs) before and (1h/4h) after acute VEH (**n=5**) and PLZ (**n=5**) treatment. (2-way *RmANOVA*, effect of treatment *NS*  $p=0.500$ ) (B) Mean nociceptive thermal withdrawal latency (hotplate @ 52°C), time to first detection (hindpaw flick/lift/lick), before and (3h) after acute VEH (**n=10**) and PLZ (**n=10**) treatment. (2-way *RmANOVA*, effect of treatment *NS*  $p=0.130$ )

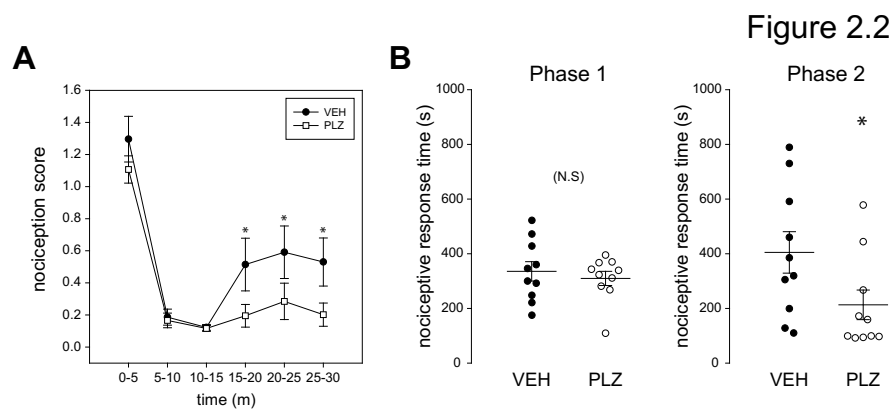


**Figure 2.2** Acute effects of PLZ treatment on formalin-evoked nociceptive behavior.

(A) Mean 'nociception score' for 30 min. (5 min. bins) following intraplantar formalin injection 3h after acute VEH ( $n=10$ ) and PLZ ( $n=10$ ) treatment (two-way RMANOVA,  $*p=0.046$  effect of treatment,  $*p<0.05$  at 15-20, 20-25, and 25-30 min., NS at other bins). (B) Dot plot / mean total nociceptive response times (licking + lifting and shaking) for phase 1 (0-10 min. post-formalin,  $t$ -test, NS  $p=0.301$ ) and phase 2 (10-30 min. post-formalin,  $t$ -test,  $*p=0.033$ ) of the formalin response in acute VEH- and PLZ-treated animals.

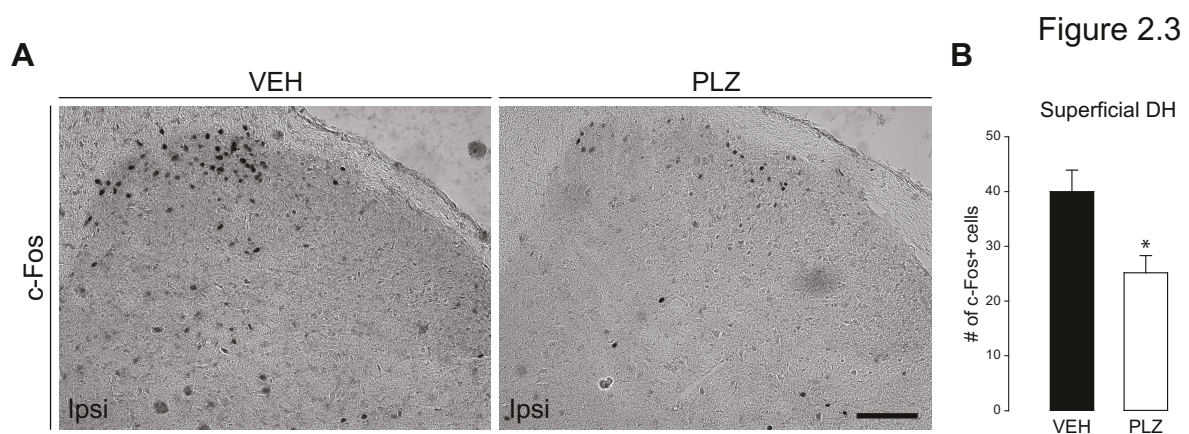


**Figure 2.3** Effect of PLZ treatment on formalin-evoked c-Fos in the dorsal horn.

(A) Representative photomicrographs of c-Fos immunostaining in the ipsilateral (to formalin injection) lumbar dorsal horn in acute VEH- and PLZ-treated animals. Scale bar = 100 $\mu$ m, applies throughout. (B) Quantification of the number of c-Fos+ cells in the ipsilateral superficial (laminae I-III) dorsal horn (post-formalin) in acute VEH- (n=5) and PLZ-treated (n=5) animals (*t*-test, \**p*=0.018).

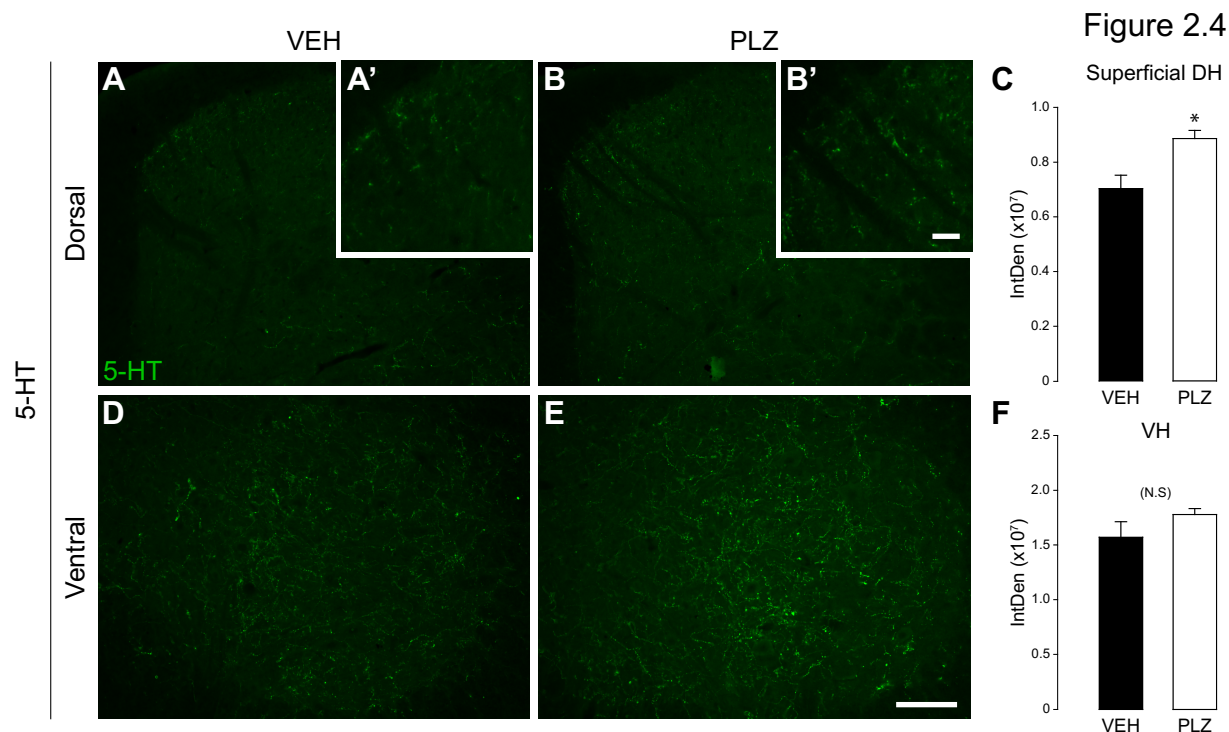


**Figure 2.4** Effect of PLZ treatment on 5-HT+ immunoreactivity in the dorsal horn.

(A,B) Representative photomicrographs of 5-HT immunostaining in the lumbar dorsal horn in acute VEH- (n=5) and PLZ-treated (n=5) animals. Scale bar in E = 100 $\mu$ m, applies A-E. (A',B' inset) Higher magnification of superficial dorsal horn 5-HT staining. Scale bar in B' = 20 $\mu$ m. (C) Quantification (integrated density) of 5-HT+ immunoreactivity in the superficial (laminae I-III) of the (bilaterally averaged) dorsal horn (*t*-test, \**p*=0.013). (D,E) Representative photomicrographs of 5-HT immunostaining in the lumbar ventral horn. (F) Quantification (integrated density) of 5-HT+ immunoreactivity in the (bilaterally averaged) ventral horn. (*t*-test, NS *p*=0.209)

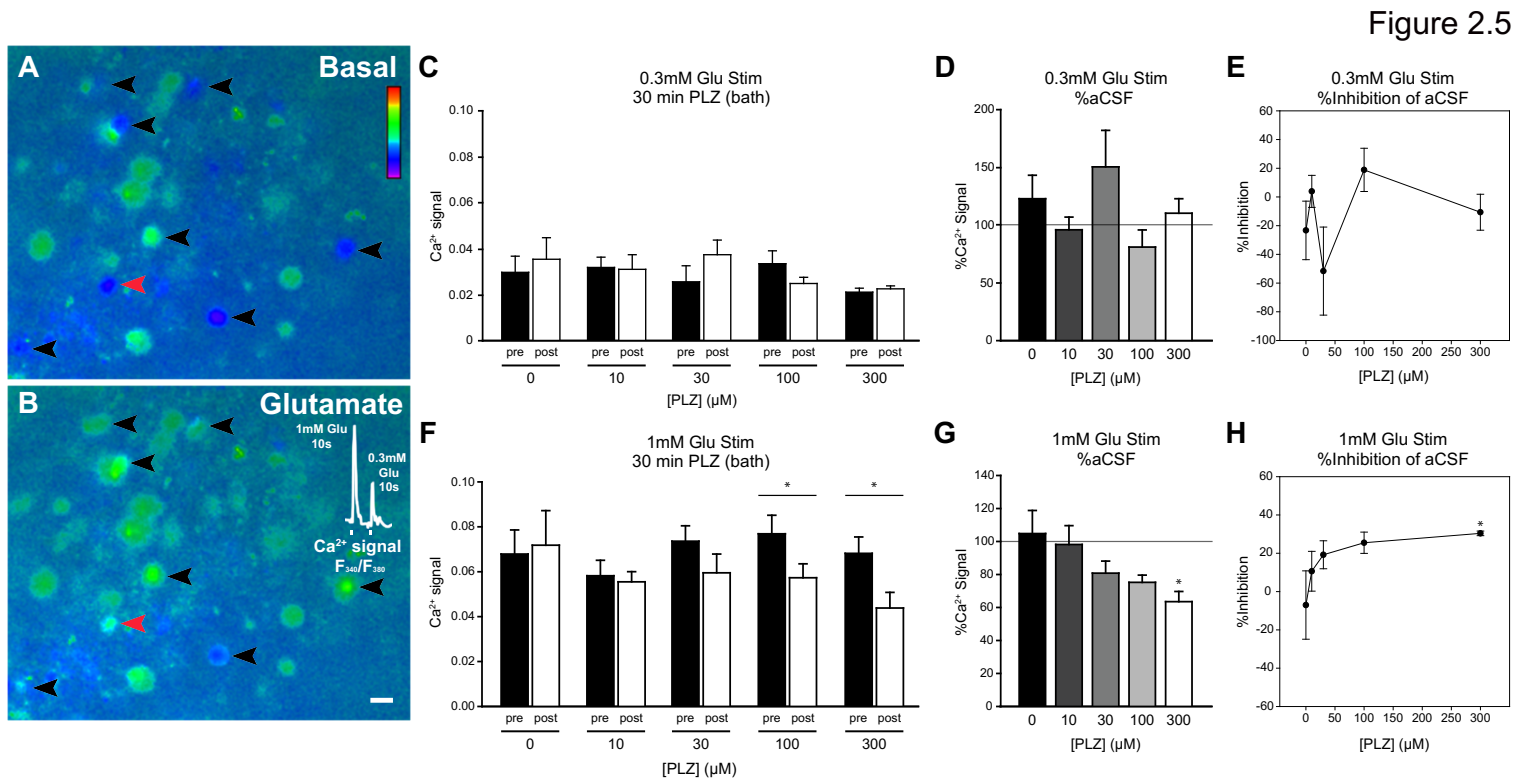


**Figure 2.5** Dose-dependent inhibition of high-molar glutamate-evoked intracellular calcium responses in the dorsal horn by bath-applied PLZ.

(**A,B**) Representative pseudocolor images depicting the F340/380 ratio in dorsal horn neurons in an *ex vivo* lumbar slice (**A**) before 1mM glutamate stimulus, and (**B**) during exposure to glutamate (1mM, 10s). Black arrowheads indicate glutamate-responsive cells. Calcium traces from the cell indicated by the red arrowhead are shown in the inlay upon exposure to glutamate at 1 and then 0.3mM (10s each). Pseudocolor scale represents F340/380 ratio where blue indicates lower and green/red indicates higher relative  $\text{Ca}^{2+}$  levels. Scale bar = 10 $\mu\text{m}$ , applies throughout. (**C**) Group mean peak (ratiometric) fluorescence intensity ( $\Delta\text{F}_{340/380}$ ) following 0.3mM glutamate stimulus (*avg. of 2 stims/slice*) prior to bath application of PLZ (**pre**) (at 0, 10, 30, 100, 300 $\mu\text{M}$  concentrations, ( $n=3-5$ /[PLZ])), and following 30 min. PLZ superfusion (**post**). (**D**) Group mean calcium response ( $\Delta\text{F}_{340/380}$ ) to 0.3mM glutamate *post*-PLZ superfusion (at each concentration), as a percentage of the (*within slice*) response *pre*-PLZ superfusion. (**E**) Curve depicting the average (%) calcium signal inhibition of the *pre*-PLZ response to 0.3mM glutamate at each PLZ concentration. (**F**) Group mean peak (ratiometric) fluorescence intensity following 1mM glutamate stimulus prior to bath application of PLZ (**pre**) (at 0, 10, 30, 100, 300 $\mu\text{M}$  concentrations), and following 30 min. PLZ superfusion (**post**). (**G**) Group mean calcium response to 1mM glutamate *post*-PLZ superfusion (at each concentration), as a percentage of the *pre*-PLZ response. (**H**) Curve depicting the average (%) calcium signal inhibition of the *pre*-PLZ response to 1mM glutamate at each PLZ concentration.

Paired *t*-test on 'raw' peak  $\Delta\text{F}_{340/380}$ , within slice control (vs. *pre*-PLZ glu stim), 1mM glu stim  $*p=0.019$  at 100 $\mu\text{M}$  PLZ,  $*p=0.002$  at 300 $\mu\text{M}$  PLZ. As a percentage (of *pre*-PLZ response),  $*p=0.042$  at 300 $\mu\text{M}$  PLZ (1mM glu). All [PLZ] NS for 0.3mM glu stim.

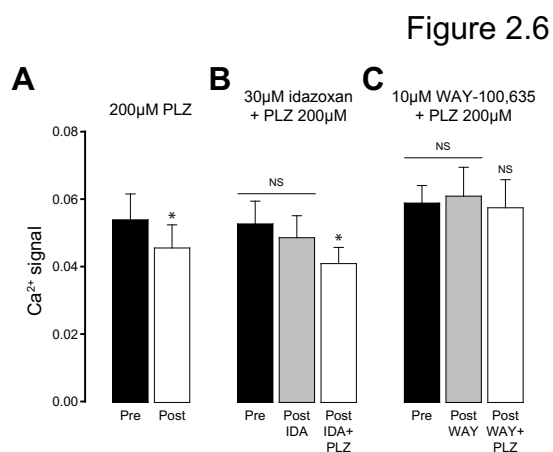


**Figure 2.6** Pretreatment with the 5HT<sub>1A</sub>R antagonist WAY-100,635, but not the adrenergic antagonist idazoxan, blocks the inhibition of intracellular calcium responses in the DH by PLZ.

(A) Group mean peak (ratiometric) fluorescence intensity ( $\Delta F_{340/380}$ ), in *ex vivo* lumbar slices, following 1mM glutamate stimulus (avg. of 2 stims/slice) prior to bath application of 200µM PLZ (**pre**) (**n=6**), and following 30 min. PLZ superfusion (**post**). (B) Group mean peak calcium response to 1mM glutamate prior to bath application of 30µM idazoxan (**pre**) (**n=4**), following 10 min. 30µM idazoxan superfusion (**post IDA**), and following 30 min. bath-applied 200µM PLZ + 30µM idazoxan (**post IDA+PLZ**). (C) Group mean peak calcium response to 1mM glutamate prior to bath application of 10µM WAY-100,635 (**pre**) (**n=3**), following 10 min. 10µM WAY-100,635 superfusion (**post WAY**), and following 30 min. bath-applied 200µM PLZ + 10µM WAY-100,635 (**post WAY+PLZ**).

Paired *t*-test for 200µM PLZ (no antagonist, pre vs. post-PLZ), \***p=0.041**.

Paired *t*-test for 200µM PLZ + 30µM idazoxan (pre vs. post-PLZ/ida), \***p=0.007**.

Paired *t*-test for 200µM PLZ + 10µM WAY-100,635 (pre vs. post-PLZ/WAY), NS. **p=0.830**.

## 2.7 - REFERENCES

1. Fiedorowicz, J.G. and K.L. Swartz, *The Role of Monoamine Oxidase Inhibitors in Current Psychiatric Practice*. Journal of psychiatric practice, 2004. **10**(4): p. 239-248.
2. Rapaport, M.H., *Dietary restrictions and drug interactions with monoamine oxidase inhibitors: the state of the art*. J Clin Psychiatry, 2007. **68 Suppl 8**: p. 42-6.
3. Shulman, K.I., et al., *Current prescription patterns and safety profile of irreversible monoamine oxidase inhibitors: a population-based cohort study of older adults*. J Clin Psychiatry, 2009. **70**(12): p. 1681-6.
4. Parent, M.B., M.K. Habib, and G.B. Baker, *Time-dependent changes in brain monoamine oxidase activity and in brain levels of monoamines and amino acids following acute administration of the antidepressant/antipanic drug phenelzine*. Biochem Pharmacol, 2000. **59**(10): p. 1253-63.
5. McManus, D.J., et al., *Effects of the antidepressant/antipanic drug phenelzine on GABA concentrations and GABA-transaminase activity in rat brain*. Biochemical pharmacology, 1992. **43**(11): p. 2486-2489.
6. Paslawski, T., et al., *The antidepressant drug phenelzine produces antianxiety effects in the plus-maze and increases in rat brain GABA*. Psychopharmacology (Berl), 1996. **127**(1): p. 19-24.
7. Parent, M.B., et al., *Effects of the antidepressant/antipanic drug phenelzine and its putative metabolite phenylethylenedihydrazine on extracellular gamma-aminobutyric acid levels in the striatum*. Biochem Pharmacol, 2002. **63**(1): p. 57-64.
8. Michael-Titus, A.T., et al., *Imipramine and phenelzine decrease glutamate overflow in the prefrontal cortex--a possible mechanism of neuroprotection in major depression?* Neuroscience, 2000. **100**(4): p. 681-4.
9. Song, M.-S., et al., *The antidepressant phenelzine protects neurons and astrocytes against formaldehyde-induced toxicity*. Journal of neurochemistry, 2010. **114**(5): p. 1405-1413.
10. MacKenzie, E.M., et al., *Phenelzine: An Old Drug That May Hold Clues to The Development of New Neuroprotective Agents*. Klinik Psikofarmakoloji Bülteni-Bulletin of Clinical Psychopharmacology, 2010. **20**(2): p. 179-186.
11. Song, M.-S., et al., *An update on amine oxidase inhibitors: Multifaceted drugs*. Progress in Neuro-Psychopharmacology and Biological Psychiatry, 2013. **44**: p. 118-124.
12. Potter, L.E., et al., *Altered excitatory-inhibitory balance within somatosensory cortex is associated with enhanced plasticity and pain sensitivity in a mouse model of multiple sclerosis*. Journal of neuroinflammation, 2016. **13**(1): p. 142.
13. Ransohoff, R.M., *Animal models of multiple sclerosis: the good, the bad and the bottom line*. Nat Neurosci, 2012. **15**(8): p. 1074-1077.
14. Mifflin, K.A., et al., *Manipulation of Neurotransmitter Levels Has Differential Effects on Formalin-Evoked Nociceptive Behavior in Male and Female Mice*. The Journal of Pain, 2016. **17**(4): p. 483-498.
15. Doolen, S., et al., *Peripheral nerve injury increases glutamate-evoked calcium mobilization in adult spinal cord neurons*. Molecular pain, 2012. **8**: p. 56.
16. Dubin, A.E. and A. Patapoutian, *Nociceptors: the sensors of the pain pathway*. The Journal of clinical investigation, 2010. **120**(11): p. 3760-3772.
17. Griebel, G., et al., *Behavioral effects of phenelzine in an experimental model for screening anxiolytic and anti-panic drugs: correlation with changes in monoamine-oxidase activity and monoamine levels*. Neuropharmacology, 1998. **37**(7): p. 927-935.
18. Musgrave, T., et al., *The MAO inhibitor phenelzine improves functional outcomes in mice with experimental autoimmune encephalomyelitis (EAE)*. Brain, Behavior, and Immunity, 2011. **25**(8): p. 1677-1688.
19. Gao, Y.J. and R.R. Ji, *c-Fos and pERK, which is a better marker for neuronal activation and central sensitization after noxious stimulation and tissue injury?* Open Pain J, 2009. **2**: p. 11-17.

20. Abbadie, C., et al., *Differential contribution of the two phases of the formalin test to the pattern of c-fos expression in the rat spinal cord: studies with remifentanyl and lidocaine*. Pain, 1997. **69**(1-2): p. 101-110.
21. Polgár, E., et al., *A Quantitative Study of Inhibitory Interneurons in Laminae I-III of the Mouse Spinal Dorsal Horn*. PLoS ONE, 2013. **8**(10): p. e78309.
22. Bardin, L., et al., *In the formalin model of tonic nociceptive pain, 8-OH-DPAT produces 5-HT<sub>1A</sub> receptor-mediated, behaviorally specific analgesia*. European Journal of Pharmacology, 2001. **421**(2): p. 109-114.
23. Abe, K., et al., *Responses to 5-HT in morphologically identified neurons in the rat substantia gelatinosa in vitro*. Neuroscience, 2009. **159**(1): p. 316-324.
24. Xie, D.J., et al., *Identification of 5-HT receptor subtypes enhancing inhibitory transmission in the rat spinal dorsal horn in vitro*. Molecular pain, 2012. **8**: p. 58.
25. Jeong, C.Y., J.I. Choi, and M.H. Yoon, *Roles of serotonin receptor subtypes for the antinociception of 5-HT in the spinal cord of rats*. European Journal of Pharmacology, 2004. **502**(3): p. 205-211.
26. Bardin, L., J. Lavarenne, and A. Eschalier, *Serotonin receptor subtypes involved in the spinal antinociceptive effect of 5-HT in rats*. Pain, 2000. **86**(1-2): p. 11-18.
27. Sonohata, M., et al., *Actions of noradrenaline on substantia gelatinosa neurones in the rat spinal cord revealed by in vivo patch recording*. The Journal of physiology, 2004. **555**(2): p. 515-526.
28. Fairbanks, C.A., L.S. Stone, and G.L. Wilcox, *Pharmacological Profiles of Alpha 2 Adrenergic Receptor Agonists Identified Using Genetically Altered Mice and Isobolographic Analysis*. Pharmacology & Therapeutics, 2009. **123**(2): p. 224-238.
29. Pertovaara, A., *Noradrenergic pain modulation*. Progress in neurobiology, 2006. **80**(2): p. 53-83.
30. Bourgoin, S., et al., *Monoaminergic control of the release of calcitonin gene-related peptide- and substance P-like materials from rat spinal cord slices*. Neuropharmacology, 1993. **32**(7): p. 633-640.
31. Hirono, M., et al., *Developmental enhancement of  $\alpha$ 2-adrenoceptor-mediated suppression of inhibitory synaptic transmission onto mouse cerebellar Purkinje cells*. Neuroscience, 2008. **156**(1): p. 143-154.
32. Dworkin, R.H., et al., *Pharmacologic management of neuropathic pain: evidence-based recommendations*. Pain, 2007. **132**(3): p. 237-51.
33. Millan, M.J., *Descending control of pain*. Progress in neurobiology, 2002. **66**(6): p. 355-474.
34. Patel, R. and A.H. Dickenson, *Mechanisms of the gabapentinoids and  $\alpha$ 2 $\delta$ -1 calcium channel subunit in neuropathic pain*. Pharmacology Research & Perspectives, 2016. **4**(2): p. n/a-n/a.
35. Dickenson, A.H., E.A. Matthews, and R. Suzuki, *Neurobiology of neuropathic pain: mode of action of anticonvulsants*. European journal of pain, 2002. **6**(SA): p. 51-60.
36. Finnerup, N.B., et al., *Pharmacotherapy for neuropathic pain in adults: a systematic review and meta-analysis*. The Lancet Neurology, 2015. **14**(2): p. 162-173.
37. Lee, I., et al., *Analgesic properties of meperidine, amitriptyline and phenelzine in mice*. Canadian Anaesthetists' Society Journal, 1983. **30**(5): p. 501-505.
38. Carter, R.B., *Differentiating analgesic and non-analgesic drug activities on rat hot plate: effect of behavioral endpoint*. Pain, 1991. **47**(2): p. 211-220.
- 39.Coderre, T.J., A.L. Vaccarino, and R. Melzack, *Central nervous system plasticity in the tonic pain response to subcutaneous formalin injection*. Brain Research, 1990. **535**(1): p. 155-158.
40. Coderre, T.J. and R. Melzack, *The contribution of excitatory amino acids to central sensitization and persistent nociception after formalin-induced tissue injury*. The Journal of Neuroscience, 1992. **12**(9): p. 3665.
41. Gogas, K.R., et al., *The antinociceptive action of supraspinal opioids results from an increase in descending inhibitory control: Correlation of nociceptive behavior and c-fos expression*. Neuroscience, 1991. **42**(3): p. 617-628.
42. Lu, Y. and E.R. Perl, *Selective action of noradrenaline and serotonin on neurones of the spinal superficial dorsal horn in the rat*. The Journal of physiology, 2007. **582**(Pt 1): p. 127-36.

# Chapter 3

Functional and structural plasticity in the dorsal horn associated with allodynia in EAE, and the effects of the antidepressant phenelzine

Unpublished

Potter LE, Doolen SD, Suh J, Tenorio G, Winship I, Baker G, Taylor BK, Kerr BJ.

**Note:** LP did the experimental work, analysis, figures, and wrote the paper. SD designed the calcium imaging methods / experiments, did surgeries for imaging, and assisted with analysis. Imaging was done in the lab of BKT. JS did some of the IHC/analysis. GT assisted with IHC. BJK and GT did the EAE induction. Behavioral/IHC work was done in the lab of BJK. Stimulation for Fos was done in IW's lab. BJK/LP formulated the experiments / paper. GB/BJK postulated the use of PLZ in EAE. BJK and my examining committee members helped edit the paper.

### 3.1 - Abstract

We examined functional and structural plasticity within the dorsal horn related to allodynia in early female C57/BL6/MOG<sub>35-55</sub> EAE. This was accomplished using post-mortem c-Fos immunohistochemistry following repeated innocuous vibromechanical stimulation of the hindlimb. Vehicle-treated EAE animals assessed at clinical onset exhibited an increase in the overall number of c-Fos+ neurons in the dorsal horn compared to CFA controls. c-Fos+ staining was also specifically enhanced in the ipsilateral (to stimulus) superficial dorsal horn relative to the contralateral side in VEH-treated EAE animals, but not in CFA controls. Treatment with the anti-depressant monoamine oxidase inhibitor phenelzine (PLZ) reversed mechanical and cold allodynia in EAE animals assessed at clinical onset. PLZ pretreatment also reduced the stimulus-related c-Fos signal in the ipsilateral dorsal horn, but did not affect the overall number of c-Fos+ neurons. We also assessed glutamate-evoked intracellular calcium responses in *ex vivo* spinal cord slices from EAE and CFA animals. Calcium responses following a 0.3mM or 1.0mM bath-applied glutamate stimulus were intensified in the dorsal horn of EAE animals. Bath application of PLZ normalized the intensity of responses in EAE slices, and also reduced the intensity of responses in CFA slices. PLZ treatment did not alter cellular inflammation and gliosis, but did normalize 5-HT+ immunoreactivity in the dorsal horn of EAE animals. EAE animals also exhibited increased vGlut1+ immunoreactivity in the deep dorsal horn laminae indicative of synaptic plasticity at low-threshold afferent terminals, which was not normalized by PLZ treatment. These experiments indicate that functional plasticity in the dorsal horn, as well as structural plasticity in deep laminae dorsal horn components, likely participate in allodynia in EAE. The anti-allodynic treatment PLZ primarily modifies evoked functional responses in the dorsal horn, likely through a mechanism involving monoaminergic neurotransmission, and possibly GABA.

### 3.2 - Introduction

Multiple sclerosis (MS) is a chronic, progressive neurological disease characterized by demyelination, inflammation, and damage within the central nervous system (CNS), leading to a wide range of cognitive, motor, and sensory impairments [1]. Pain, which may arise by a variety of mechanisms, is increasingly recognized as one of the most common and debilitating symptoms of MS [2-4]. At present, pain in MS is also widely undertreated and poorly understood. There is an apparent need for an improved scientific understanding of the underlying processes which establish and maintain pathological pain in MS, and for the development of more effective treatment options [5-8].

Pain of central neuropathic origin (CNP), resulting from either direct neuronal damage or aberrant neuronal plasticity and function within the CNS, affects roughly 30-40% of MS patients with pain [2, 9]. This may manifest in a variety of ways, including as allodynia, a condition in which previously non-noxious or painful stimuli become painful [5, 10, 11]. CNP in MS has recently been investigated scientifically using the disease model experimental autoimmune encephalomyelitis (EAE) [12-15]. EAE has long been considered useful for the study of MS, owing to substantial similarities in both the underlying pathology and symptomatology of the diseases [16, 17], including the “secondary symptoms” such as pain [18, 19]. Female C57/BL6 mice in the early stages of MOG<sub>35-55</sub> EAE are particularly useful for studying CNP in MS, as they reliably develop robust mechanical and thermal (cold) allodynia, which may be assessed behaviorally prior to the onset of paralytic symptoms [15].

Earlier studies that characterized altered nociception in the MOG<sub>35-55</sub> (female C57/BL6) EAE model identified elevated basal expression of c-Fos protein, a commonly used histological marker for neuronal activity, within the dorsal horn of the spinal cord (SCDH) [15]. This provided evidence of ongoing neuronal activity in the DH – indicative of central sensitization [20] - arising in the early stages of EAE. This elevated c-Fos expression coincides temporally with several other pathological developments in

the model, including increased nociceptive behavioral sensitivity / allodynia. Reduced GABA and monoamine neurotransmitter content throughout the CNS, including in the SC, has also been reported in EAE [21]. In this chapter, we investigate the effect of chronic pre-treatment with the monoamine oxidase inhibitor (MAOI) phenelzine (PLZ) on mechanical withdrawal thresholds, and cold sensitivity in animals at the onset of clinical (ie. paralytic) symptoms of EAE. PLZ acts to increase GABA and monoamine content in the CNS by interfering with the degradation of these neurotransmitters through irreversible inhibition of both isoforms of the enzyme monoamine oxidase (A/B), and through reversible inhibition of the enzyme GABA-transaminase (GABA-T) by PLZ's active metabolite phenethylidenehydrazine (PEH) [22-24]. Musgrave/Benson et al. (2011) [25] previously confirmed this action in EAE, and identified an effect on the number of days to disease onset in EAE animals pretreated with PLZ. Here, we find that PLZ pretreatment also normalizes behavioral measures of mechanical and cold sensitivity, reversing allodynia in early (onset) EAE.

Most research on the neurobiology of altered nociception in EAE to date has relied on correlating behavioral measures with ongoing changes in the nervous system, and has not directly examined responses in the CNS/PNS to nociceptive (or non-nociceptive) stimuli. One study that has addressed the question of the stimulus-evoked response in EAE is Olechowski et al. 2010 [26], in which the authors examined the neuronal response in the SCDH to intraplantar injection of formalin using c-Fos immunohistochemistry (IHC). Formalin is a noxious chemical stimulus that commonly evokes a strong c-Fos signal in the SCDH of naïve animals, but was paradoxically found to reduce the overall number of Fos+ cells in the SCDH of EAE animals [26-28]. While this approach (ie. the use of a noxious stimulus) yielded several mechanistic insights into the altered pain response in EAE, it did not specifically address the issue of allodynia in EAE/MS. In this study, we examined the neuronal response within the SCDH to a vibromechanical stimulus which is normally not noxious, but which may become noxious in EAE, using c-Fos IHC. We also examined neuronal responses to bath-applied glutamate in live adult

spinal cord slices from EAE animals and CFA-treated controls using fura 2-dye ratiometric intracellular calcium imaging.

In addition to investigating altered functional responses within the SCDH, we identified structural neuronal/synaptic plasticity in the SCDH, which may contribute to allodynia in the disease.

Furthermore, we evaluated how the novel anti-allodynic treatment PLZ alters neuronal responses and plasticity within the SCDH in the EAE. Additionally, we investigated the possibility that PLZ's effects in EAE are mediated by a modification or suppression of cell-mediated immune/inflammatory responses. Lastly, we further characterized the contribution of individual neurotransmitters within the SCDH to PLZ's effects.

### **3.3 - Methods**

#### **3.3.1 - Animals and Ethics**

A total of 106, 8–12-week-old, female C57/BL6 mice (Charles River–Saint Constant, Quebec, Canada) were used in the behavioral and IHC experiments. Mice were housed 5 per cage, in standard cages, and fed *ad libitum*. For behavioral and IHC experiments, all procedures were conducted in accordance with the Canadian Council on Animal Care's Guidelines and Policies and with protocols approved by the University of Alberta Health Sciences Animal Care and Use Committee. A total of 16, 8-12-week old, female C57/BL6 mice (Charles River–Indianapolis, IN, USA) were used in the calcium imaging experiments. Calcium imaging experiments were conducted in accordance with protocols approved by the Institutional Animal Care and Use Committee of the University of Kentucky.

#### **3.3.2 - EAE Induction**

For behavioral/IHC experiments, EAE was induced in mice by subcutaneous (S.C.) injection into the hindquarters of 50 µg of myelin oligodendrocyte glycoprotein (MOG<sub>35–55</sub>) - obtained from the Peptide

Synthesis Facility at the University of Calgary (Calgary, Alberta, Canada - and emulsified in Complete Freund's Adjuvant (CFA, 1.5 mg/mL) containing additional heat-killed *Mycobacterium tuberculosis* H37Ra (Difco Laboratories/BD Biosciences—Franklin Lakes, NJ, USA). Immunized mice also received two intraperitoneal (I.P.) injections of pertussis toxin (*Bordetella pertussis*) (PT, List Biological Labs—Campbell, CA, USA)—first, on the day of the induction and again 48h later. Control mice received identical CFA with added *M. tuberculosis* H37Ra (S.C./hindquarters), but without MOG<sub>35-55</sub>. CFA mice also received PT injections on the same days.

For calcium imaging experiments, induction was identical, except MOG<sub>35-55</sub> was obtained from AnaSpec Inc., Fremont, CA, USA. CFA was made by adding 5.5mg/mL *Mycobacterium tuberculosis* (Voigt Global Distribution, Lawrence, KS, USA) into incomplete Freund's adjuvant (IFA, Sigma-Aldrich, St. Louis, MO, USA). MOG<sub>35-55</sub> emulsified in CFA was injected at 150 µg S.C. per flank. A booster injection of MOG<sub>35-55</sub> (150 µg, S.C. per flank) was administered on day 6. As in the behavioral/IHC experiments, PT (List Biological Labs) was injected (200 ng/200 µL, I.P.) on the day of induction and again 48h later.

### 3.3.3 - Disease Scoring

Mice were monitored for clinical symptoms daily, and were taken for c-Fos induction / histology when they reached clinical onset, ie. a score of 1 or greater in the standard five point scale (grades 0–4) which is defined as follows [32]: grade 0—*normal mouse, no loss of motor function*; grade 1—*flaccid tail, paralyzed in ≥50 % of the tail's length, or partial paralysis of the tail with visible weakness in one or more of the limbs*; grade 2—*completely paralyzed tail, some hindlimb weakness, preserved righting reflex*; grade 3—*severe hindlimb weakness, slowed righting reflex*; grade 4—*complete paralysis of one or both of the hindlimbs*. CFA mice were taken at roughly contemporaneous time-points (from 7 to 12 days post-induction, dpi.). Mice used for calcium imaging were between the grades of 1-3, and were

taken between (10 and 21 dpi.); with CFA/EAE mice being (roughly) alternated such that they were at approximately equivalent post-induction time-points.

### **3.3.4 - Drug Treatments**

For behavioral experiments, mice were divided into groups that, starting at 7 dpi., received daily I.P. injections of either vehicle (VEH, bacteriostatic water, 10mL/kg body weight), or phenelzine (PLZ, 15mg/kg body weight, Sigma-Aldrich – Oakville, ON, Canada). For EAE animals receiving PLZ, drug was given on alternate days with injections of VEH given on the ‘off’ day. This design was intended to control for multiple I.P. injections, as previous experiments showed that for longer experiments (some of these mice were carried past onset for use in other experiments), the effectiveness of GABA-T inhibition is better maintained by this injection schedule [29]. For immunohistochemistry experiments, the same design was used, except that drug (PLZ) injections were given daily (rather than alternating PLZ with VEH). For calcium imaging experiments, treatments were applied acutely to the isolated slices as described in subsequent methods.

### **3.3.5 - Pain Testing**

#### **3.3.5.1 - Von Frey Hair Assay**

The Von Frey hair (VF/VFH) assay was used to assess mechanical (tactile/punctate pressure) sensitivity and allodynia [30]. Animals were placed in transparent plexiglass boxes over a screen that allowed access to the paws. Prior to the start of testing, all mice underwent a period of habituation to the boxes (5-10min/day, for 3 days before baseline testing began). Mice were also given 5-10 min. of habituation time in the testing boxes at the start of each test day. After this period, the plantar surface of each hindpaw was stimulated 5x with a weighted Von Frey hair monofilament. An observer blinded to the experimental/ treatment groups monitored and recorded behavioral responses to stimulation. “Noxious-responding” (i.e. shaking, licking or guarding of the paw) was noted. Hindpaw stimulation was repeated through a progressive series of filament-weights (*0.04g-2.0g*), until a stimulus produced a

“noxious response”  $\geq 60\%$  of the time – the weight at which this occurred was taken to be the withdrawal threshold for that paw on that day. Left and right paw responses were averaged within each animal to provide a combined threshold for each test day, and these combined thresholds were used for subsequent analysis. Prior to disease induction, all animals underwent VFH testing on 3 separate days to establish baseline mechanical thresholds. After induction, mice were tested on days 3, 7, 9 and 12 post-induction, and at clinical-onset. CFA animals from 7-12 days post-induction (dpi.) were used in the ‘onset’ analysis:  $n=5$  from each of days 7, 9, and 12 for the VEH group. PLZ-treated CFAs were taken at day 12, following 7 daily drug injections.

#### **3.3.5.2 - Acetone Assay**

The acetone assay was used to test for cold allodynia. A single drop of acetone was placed onto the ventral surface of one hindpaw, and the duration of “noxious responding” (ie. shaking, raising the paw) immediately after was measured. The alternate paw was tested at least 5 min. apart from the initial paw, but only responsive paws ( $>1s$  duration) were included in the analysis for EAE groups (only a subset of animals exhibit responses in this assay). In the CFA group, shorter responses were included, as only 2 animals in the group exhibited responses greater than 1s. The CFA responses included in the analysis were those measured on 7 dpi. The acetone assay was administered on the same days as the VFH test.

#### **3.3.5.3 - Rotorod**

To confirm that there was no confounding influence of motor impairment in EAE mice at this stage of the disease, the Rotorod assay (Harvard Apparatus, Holliston, MA, USA) was also administered alongside the VFH assay. Any animals with a clinical grade of  $\geq 2$ , or that could not successfully complete the Rotorod task, remaining on the Rotorod for the full duration of 180s in at least one of three attempts - and additionally failed to respond in the VFH (obtained a 2.0g threshold, the maximum) were

excluded from the behavioral analysis ( $n=3$ ). After excluding these animals, none of the groups differed in terms of their (mean) duration spent on the Rotorod.

### **3.3.6 - Additional Assays**

In addition to the assays described here, all animals underwent behavioral testing as described above – including animals only used for IHC/calcium imaging. Animals used for histological experiments also underwent *in vivo* functional imaging simultaneous to c-Fos induction as described and reported in *Chapter 4*.

### **3.3.7- c-Fos Induction**

A separate cohort of EAE/CFA animals was used for the histology experiments. In order to induce c-Fos in the SCDH, animals received a repeated vibromechanical stimulus, applied to their left hindpaw (LHP). Animals under urethane anesthesia (1.25g/kg I.P.) at normothermia and under heat control, were stimulated on the LHP 40x using a computer triggered piezoceramic element (Piezo Systems, Woburn, MA, USA) (1s stimulus duration, 100Hz, 1mm deflection, 20s interstimulus interval). After an interval of 1h to allow for full expression of the c-Fos protein, animals were checked for depth of anesthesia, with additional isoflurane anesthesia applied when necessary, and then sacrificed for histology. For the c-Fos double-label experiment - and for 2 additional animals used only in the 5-HT stain - no stimulus was applied, but VEH / PLZ-treated EAE animals at clinical onset were used (**n=2-5** per group).

### **3.3.8 - Tissue Collection / Preparation**

Animals underwent transcardiac exsanguination / perfusion with saline (0.9% w/v) followed by fixation with paraformaldehyde (PFA) 4% in 0.1M PB. Lumbar (L1-L5) spinal cord was removed and post-fixed overnight in PFA. Tissues were then cryoprotected by immersion in sucrose 30% solution for 48h,

followed by embedding in TissueTek OCT and freezing over liquid N<sub>2</sub>. Frozen tissues were stored at -80°C until they could be sectioned on a cryostat (20µm sections) and mounted directly onto slides.

### **3.3.9 - Immunohistochemistry / Immunocytochemistry**

Tissues were stained using standard immunohistochemistry (IHC) / immunofluorescence protocols as described below. The following reagents/antibodies were used:

#### **3.3.9.1 - c-Fos / DAB:**

Tissues were incubated with rabbit anti-c-Fos (1:1000, Cell Signalling, Danvers, MA, USA) primary antibody overnight, followed by goat anti-rabbit biotin (1:400, 2h RT, Vector Labs), and avidin-biotin complex (ABC 1:200, 1.5h RT, "VectaStain Elite™ ABC/HRP Kit", Vector Labs), before visualization with 3,3'-diaminobenzidine (DAB, Vector Labs) (plus nickel). Slides were coverslipped using Permount.

#### **3.3.9.2 - Immunofluorescence / Double-Labeling:**

Tissues were incubated overnight with the following primary antibodies: rabbit anti-c-Fos (1:1000, Cell Signalling), rat anti-cd3 (1:200, AbD Serotec®—BioRad Laboratories Canada Ltd., Mississauga, ON, Canada), rabbit anti-Iba-1 (1:500, Wako Chemicals USA Inc., Richmond, VA, USA), rabbit anti-GFAP (1:1000, Dako, Mississauga, ON, Canada), rat anti-Mac-1 (1:200, AbD Serotec®), AlexaFluor 488-conjugated mouse anti-NeuN (1:500, Chemicon/Millipore, Temecula, CA, USA), rabbit anti-VGLUT1 (1:1000, Cell Signalling), rabbit anti-5-HT (1:1000, Sigma-Aldrich, Oakville, ON, Canada). Primary antibodies were then visualized with the following secondary antibodies: goat anti-rabbit/rat AlexaFluor 488 / 594 (1:200, 1h RT, Invitrogen Life Technologies Inc., Burlington, ON, Canada). Slides were coverslipped using Vectashield with DAPI.

#### **3.3.9.3 - IHC Image Acquisition and Quantification**

Slides were imaged using a Zeiss AxioCam MRm camera on a Zeiss Observer Z.1 inverted fluorescence microscope equipped with a 20x objective lens. Images of both ipsilateral and contralateral (to stimulus) dorsal horn at the L4-L5 level were captured for quantification, 2 sections from each of 2 slides per animal (*only 1 slide/animal was used for CD3 quantification*). Exposure levels were maintained at a consistent setting for each tissue set. Sections were quantified using NIH ImageJ/FIJI and Adobe Photoshop. Manual cell counting for c-Fos was performed by an observer blinded to treatment groups, with ipsilateral and contralateral dorsal horns being added (before being averaged) for 'total' c-Fos, or subtracted (for 'superficial/stim no-stim.' c-Fos). For 'deep' c-Fos, the ipsi/contra sides were averaged together. Other quantifications (integrated density / thresholded area) were made using template regions of interest (ROIs) manually adjusted to fit the individual section (but with consistent overall area  $\sim\pm 2\%$ ). Thresholding was performed automatically using FIJI's "default" automatic thresholding algorithm (with minor manual adjustments of  $\sim\pm 5\%$  in cases where poor foreground/background separation resulted). GABA+ cells were also counted manually. In some instances, individual replicates or animals / outliers were excluded from the final analysis based on the presence of major unavoidable artifacts or poor staining and tissue quality (ie. folds/damaged tissues, or lack of reactivity towards any of the antibodies tested).

All quantitative IHC image analyses were performed either on the original unmodified images, or on images processed in a consistently applied manner as described elsewhere in the methods.

Representative photomicrographs used in figures were additionally adjusted for brightness, contrast, color balance, and histogram scaling in order to improve the overall visibility of the images. These adjustments were performed only on whole images and were applied in a consistent manner such that the figures accurately reflect the entire contents and relative intensities of the original images.

### **3.3.10 - Calcium Imaging (Adapted From Doolen et al. 2012)**

#### **3.3.10.1 - Preparation of Adult Mouse Spinal Cord Slices:**

Mice were anesthetized with 5% isoflurane and quickly perfused transcardially with 10 ml of ice-cold sucrose-containing artificial cerebrospinal fluid (aCSF) (sucrose-aCSF) that contained (in mM): NaCl 95, KCl 1.8,  $\text{KH}_2\text{PO}_4$  1.2,  $\text{CaCl}_2$  0.5,  $\text{MgSO}_4$  7,  $\text{NaHCO}_3$  26, glucose 15, sucrose 50, kynurenic acid 1, oxygenated with 95%  $\text{O}_2$ , 5%  $\text{CO}_2$ ; pH 7.4. The lumbar spinal cord was rapidly (within 90s) isolated by laminectomy from the cervical enlargement to the cauda equina, placed in oxygenated ice-cold sucrose-aCSF, cleaned of dura mater and ventral roots, and super-glued vertically to a block of 4% agar (Fisher Scientific, Pittsburgh, PA) on the stage of a Campden 5000mz vibratome (Lafayette, IN). Transverse slices (300–450  $\mu\text{m}$ ) from lumbar segments L4-L5 were cut in ice-cold sucrose-aCSF using minimum forward speed ranging from 0.03 to 1 mm/s and using maximum vibration. The ideal total dissection and slicing time to ensure slice viability was 22 minutes or less.

### **3.3.10.2 - Ratiometric $\text{Ca}^{2+}$ Measurements:**

Lumber slices were incubated for 30 min. at 37<sup>0</sup>C with fura-2 AM (10  $\mu\text{M}$ ), pluronic acid (0.1%) in oxygenated aCSF containing (in mM): NaCl 127, KCl 1.8,  $\text{KH}_2\text{PO}_4$  1.2,  $\text{CaCl}_2$  2.4,  $\text{MgSO}_4$  1.3,  $\text{NaHCO}_3$  26, glucose 15, followed by a 20 min de-esterification period in normal aCSF. Prior to recording, slices were kept at RT in a chamber containing approximately 150 ml of oxygenated aCSF. Slices were perfused at 1–2 ml/min with normal aCSF in an RC-25 recording chamber (Warner Instruments, Hamden, CT) mounted on a Nikon FN-1 upright microscope fitted with a 79000 ET FURA2 Hybrid filter set (Nikon Instruments, Melville, NY) and a Photometrics CoolSNAP HQ<sub>2</sub> camera (Tucson, AZ). Relative intracellular  $\text{Ca}^{2+}$  levels were determined by measuring the change in ratio of fluorescence emission at 510 nm in response to excitation at 340 and 380 nm (200 ms exposure). Paired images were collected at 1–1.5 seconds/frame. Relative changes in  $\text{Ca}^{2+}$  levels were evaluated using Nikon Elements software by creating a region of interest over the cell body and calculating the peak change in ratio. Approximately 10-15 cells were analyzed in each slice/treatment condition. The peak magnitude of the  $\text{Ca}^{2+}$  transient was expressed as the difference in F340/380nm ratio following exposure to exogenous glutamate compared to baseline before glutamate.  $\text{Ca}^{2+}$  transients were in

response to a 10s exposure to 0.3mM or 1mM glutamate in aCSF. The criterion for a responsive cell to be considered was a 0.02 increase in the F340/380 ratio with the 1mM glutamate stimulus.

For the PLZ studies, each slice was stimulated twice (with several minutes between stimuli to allow calcium levels to return to baseline), prior to perfusion with oxygenated aCSF/PLZ at 200 $\mu$ M for 30 min. This concentration of PLZ was chosen based on the experiments in Chapter 2. Following PLZ perfusion, the slice was re-stimulated two times with each glutamate concentration. The raw F340/380 magnitudes of the calcium response before and after PLZ exposure were calculated, as well as the change in response magnitude by calculating the *post*-PLZ magnitude as a percentage of the *pre*-PLZ response (to each glutamate concentration). This change was expressed as a 'percent inhibition' (ie. % change, subtracted from 100%) of the *pre*-PLZ response.

### 3.3.11 - Statistics

Statistical analyses were carried out by standard methods (one-way ANOVA, with either the Holm–Sidak method for pairwise post-hoc testing, or Dunnett's method for post-hoc testing vs. control only). Kruskal–Wallis ANOVA on ranks was used for non-parametric data sets, along with the Dunn's method for post-hoc testing (multi or vs. control). For calcium imaging experiments, within subjects (paired) t-tests were used. Significance was set at  $P < 0.05$ .

## 3.4 - Results

### 3.4.1 - *Pretreatment with PLZ normalizes nociceptive sensitivity in EAE animals at clinical onset.*

We initially confirmed the previously reported effect of PLZ treatment on time to clinical onset. As in earlier experiments, PLZ treatment delayed the time to clinical onset by several days (*t-test*,  $*p=0.041$ ; VEH  $n=26$ , PLZ  $n=27$ ) (FIG. 3.1A). In order to assess the effects of PLZ treatment on (behavioral measures of) nociception in EAE, we also characterized the response to punctate mechanical (ie. VFH)

stimulation. For this analysis, a cohort of CFA-only and EAE mice were treated with either VEH or PLZ from 7 dpi., and assessed with VF hairs on the day of clinical-onset (CFA mice were assessed at matched time-points as described in methods). As demonstrated previously [15, 18] mice with EAE (treated with VEH, **n=14**) exhibit significantly decreased mechanical withdrawal thresholds at clinical-onset compared to CFA-treated controls (**n=15**) (**FIG. 3.1B**). In contrast, mechanical withdrawal thresholds were normalized in EAE mice treated with PLZ (**n=17**), and were not significantly different from CFA controls. PLZ-treated CFA mice (**n=5**) did not differ significantly from VEH-treated CFA, or PLZ-treated EAE animals (*Kruskal-Wallis one-way ANOVA on Ranks, \* $p=0.005$ ; all post-hoc comparisons vs. CFA by Dunn's method; only EAE-VEH vs. CFA-VEH \* $p<0.05$* ) (**FIG. 3.1B**).

Performance on the Rotorod assay was not impaired in any group at this disease time point (*group-means, avg. of 3 attempts / 95% C.I. of mean: CFA 173.6s /  $\pm 6.1$ s; EAE-VEH 126.7s /  $\pm 68.6$ s; EAE-PLZ 157.8s /  $\pm 39.8$ s - Kruskal-Wallis one-way ANOVA on Ranks not significant,  $p=0.242$* ) (**FIG. 3.1C**).

We also examined the effects of PLZ treatment on thermal (cold) allodynia using the acetone assay. Response durations following cold (acetone) stimulation were prolonged in the VEH treated EAE animals (**n=8**) tested at clinical onset, compared to CFA controls (**n=10**), indicative of cold allodynia (**FIG. 3.1D**). This effect was, however, observed only in a proportion of the animals tested – only single responsive paws (1 paw per responsive animal) which were greater than 1s in duration were included in the EAE groups for the analysis. For CFA controls, only 2 responses exceeded 1s, so this criterion was not applied to that group. PLZ pretreatment normalized response durations in EAE animals (**n=10**), ie. responses in the PLZ-treated group were not significantly different from those seen in CFA controls. (*Kruskal-Wallis one-way ANOVA on Ranks, \* $p<0.001$ ; all pairwise post-hoc comparisons by Dunn's method, VEH vs. CFA \* $p<0.05$ , PLZ vs. CFA NS., VEH vs. PLZ NS.*) (**FIG. 3.1D**)

**3.4.2 - Vibromechanical stimulation evokes additional c-Fos+ neurons in the superficial dorsal horn of VEH-treated EAE, but not PLZ-treated EAE animals or CFA controls.**

In order to investigate the role of functional plasticity within spinal nociceptive networks in allodynia in EAE, we assessed neuronal activation in the SCDH with c-Fos IHC following repeated vibromechanical stimulation of the LHP. As reported by Olechowski et al. (2009) [15], EAE animals (VEH/PLZ **n=10**) were found to have dramatically elevated numbers of Fos+ cells throughout the superficial and deep laminae of the lumbar (L3-L5) dorsal horn (DH) on both the ipsi- / contralateral sides, compared to CFA controls (**n=8**) (in which few Fos+ neurons are found) (*Kruskal–Wallis ANOVA on Ranks, \*p=0.015, post-hoc comparisons vs. control (CFA) by Dunn’s method. (VEH vs. CFA \*p<0.05, PLZ vs. CFA \*p<0.05)*). PLZ-treated EAE mice showed no attenuation of total Fos+ cell numbers in the DH (**FIG. 3.2A-G**). This was also true when just the deeper laminae (IV-VI) of the DH were considered (*Kruskal–Wallis ANOVA on Ranks, \*p=0.022, post-hoc comparisons vs. control (CFA) by Dunn’s method. (VEH vs. CFA \*p<0.05, PLZ vs. CFA \*p<0.05)*, \*(VEH **n=9**) (**FIG. 3.2H**). Lateralized clusters of Fos+ cells were, however, observed in the superficial laminae (I-III) of many of the VEH-treated EAE animals (**FIG. 3.2D**), which were not present in either the CFA controls or PLZ-treated EAE animals (**FIG. 3.2A-F**). This was confirmed by comparing the differences in the number of Fos+ cells between the ipsilateral (to stimulus) and contralateral superficial dorsal horns in the three treatment groups. Only in the VEH treated EAE animals was there a significant difference between the two sides, presumably attributable to the stimulus (*Kruskal–Wallis ANOVA on Ranks, \*p=0.002, all pairwise post-hoc comparisons by Dunn’s method. (VEH vs. PLZ \*p<0.05, CFA vs. VEH \*p<0.05, CFA vs. PLZ NS.)*) (**FIG. 3.2I**). While there were laterally disparate cell-counts for individual sections in all treatment groups, these tended to be smaller and occurring on either side in the CFA and EAE-PLZ groups, leading to those differences being cancelled out upon averaging. Although we included laminae I to III in this analysis, dense/lateralized Fos staining was mainly apparent in laminae I and II.

In order to confirm the neuronal identity of the Fos+ cells in the EAE tissue, we conducted IHC co-localization experiments. We co-labelled for c-Fos alongside markers for each of the major inflammatory/glial cell types which are upregulated in the DH in EAE: CD3 was used for infiltrating T-

cells (**FIG. 3.3A-C**), GFAP for astrocytes (**FIG. 3.3D-F**), and Mac-1 for reactive microglia/macrophages (**FIG. 3.3G-I**), as well as with NeuN for neurons (**FIG. 3.3J-L**). c-Fos was found to only co-register with NeuN (**FIG. 3.3L**), confirming its specificity and usefulness as a marker of neuronal activation in EAE.

### **3.4.3 - PLZ's actions in EAE are not mediated by a reduction of inflammatory cells in the dorsal horn.**

Several groups have reported on the central inflammatory (ie. immune/glial cell-mediated inflammation) response in the DH in EAE [15, 31, 32], which is thought to play a major role in the establishment and maintenance of central sensitization and nociceptive hypersensitivity in the disease. In the early disease (ie. presymptomatic / onset stages), infiltrating T-cells are detectable in the DH, followed quickly by central glial activation, including upregulation of Iba-1+ reactive microglia/macrophages and astrocytic GFAP - both of which are detectable/elevated in the DH by clinical onset [15]. Because these cellular responses may be either directly or indirectly modulated by PLZ (ie. through 5-HT, NA, DA etc., or by neuronal activity-dependent effects), we stained for these cells (CD3+ T-cells, GFAP+ astrocytes, Iba-1+ microglia/macrophages) in the various treatment groups. However, none of these cell-types were reduced in the DH of EAE animals following treatment with PLZ versus VEH. All three cell-types were elevated in both EAE (-VEH/PLZ) groups compared to CFA controls. (**FIG. 3.4**) (*n's reported as CFA, VEH, PLZ*)

**CD3:** *Kruskal-Wallis ANOVA on Ranks, \*p=0.024, all pairwise post-hoc comparisons by Dunn's method. (VEH vs. CFA \*p<0.05, PLZ vs. CFA \*p<0.05, VEH vs. PLZ NS.). (n=4,6,9) (FIG. 3.4A-D)*

**GFAP:** *One-way ANOVA, \*p=0.003, all pairwise post-hoc comparisons by Holm-Sidak method. (VEH vs. CFA \*p<0.05, PLZ vs. CFA \*p<0.05, VEH vs. PLZ NS.). (n=5,10,10) (FIG. 3.4E-H)*

**Iba-1:** *One-way ANOVA, \*p=0.007, all pairwise post-hoc comparisons by Holm-Sidak method. (VEH vs. CFA \*p<0.05, PLZ vs. CFA \*p<0.05, VEH vs. PLZ NS.). (n=9,10,10) (FIG. 3.4I-L)*

#### **3.4.4 - Intracellular calcium responses to glutamate are enhanced within the dorsal horn in EAE, and are normalized by bath-applied PLZ.**

While c-Fos staining showed what appears to be a stimulus-related increase in neuronal activation within the dorsal horn in EAE, the indirect and post-mortem nature of c-Fos IHC limits the direct causal attribution of any observed differences in staining to a specific stimulus or event. In order to examine stimulus-evoked neuronal responses in the dorsal horn – and the effect and mechanism of PLZ - more directly, we performed calcium imaging in *ex vivo* spinal cord slices from CFA and EAE animals. For these experiments, we incubated freshly extracted transverse lumbar slices in the ratiometric calcium-sensitive dye fura 2. We previously made use of this approach to investigate the effects of bath-applied PLZ on glutamate-evoked intracellular calcium responses in dorsal horn neurons within isolated lumbar slices from naïve adult female C57/BL6 mice (*see Chapter 1*). Here, we assessed glutamate-evoked calcium responses in dorsal horn neurons within lumbar slices isolated from CFA and EAE animals near the time of disease onset/peak (between 10 and 21 dpi.). We also assessed the effects of bath-applied PLZ on calcium responses in both groups.

On average, the magnitude of intracellular calcium rises following bath application of either 0.3mM glutamate (10s duration in aCSF) or 1.0mM glutamate was greater in slices from EAE (**n=8**) animals than in those from CFA (**n=7**) animals (*t-test “pre-PLZ” vs. “pre-PLZ”, 0.3mM glutamate: \*p=0.040; 1.0mM glutamate: \*p=0.012*) (**FIG. 3.5A,B**). In both CFA and EAE groups, bath application of 200µM PLZ (in oxygenated aCSF) for 30 minutes produced a modest inhibition of responses to either 0.3mM or 1.0mM glutamate (for 0.3mM glutamate: ~29% in CFAs, ~24% in EAEs; for 1.0mM glutamate: ~11% in CFAs, ~21% in EAEs) (*paired t-tests “pre-PLZ” vs. “post-PLZ”: CFA 0.3mM glutamate \*p=0.005, 1.0mM glutamate \*p=0.044; EAE 0.3mM glutamate \*p=0.017, 1.0mM glutamate \*p=0.001*) (**FIG. 3.5B,C**). The magnitudes of the calcium responses to 0.3mM and 1.0mM glutamate in EAE slices following acute PLZ treatment were similar to the magnitudes of responses in CFAs prior to PLZ treatment (ie. PLZ normalized responses).

### **3.4.5 - Plasticity of excitatory synaptic terminals within the deeper laminae (III to VI) of the dorsal horn in EAE.**

Sensitization of central nociceptive pathways may occur by many mechanisms [20]. In addition to purely functional changes in neuronal excitability/responsiveness, sensitization may involve structural alterations to neurons in the form of addition and deletion of synaptic contacts [33, 34]. Generally, an increase in the number of synaptic contacts between two neurons tends to strengthen their (excitatory or inhibitory) connection. This type of mechanism is known to play a role in the induction and maintenance of chronic/neuropathic pain states [35, 36]. Aberrant synaptic plasticity (ie. synaptopathy) has also been found to play an important role in many aspects of EAE/MS, including “secondary symptoms” such as cognitive/sensory dysfunction [37-40].

In the spinal cord, anti-VGLUT1 primarily labels the central glutamatergic terminals of low-threshold primary afferent (ie. peripheral A $\beta$ ) fibres, which occur primarily in the deeper laminae of the DH (III-VI) [42] – although some local DH neurons and descending afferents may also express VGLUT1 [43]. Excitatory neuronal processes (interneurons) which link the deep and superficial laminae tend to express VGLUT2 as opposed to VGLUT1, as do high-threshold nociceptive peripheral afferents (ie. C-fibres) – which may also be labelled with a variety of markers that distinguish specific subpopulations [42, 44]. Previous work by Olechowski et al. (2009) [15] demonstrated that CGRP+ and galanin+ central (C-fibre) terminals within the superficial DH were unchanged in EAE. Duffy et al. (2017) [32] also reported that, within the trigeminal ganglion, early EAE is associated with inflammatory damage to myelinated A-class fibres, but not IB4+ or CGRP+ C-fibres – which may drive facial allodynia in the model. Here, we stained for VGLUT1 in the same CFA (n=6), EAE-VEH (n=10), and EAE-PLZ (n=10) animals to determine whether structural/synaptic plasticity was present in the deeper laminae of the SCDH (where low-threshold afferent fibres terminate), and to determine whether PLZ had any effect on these synapses. (**FIG. 3.6**)

Both VEH- and PLZ-treated EAE animals were found to have elevated VGLUT1+ reactivity (ie. increased density of excitatory presynaptic terminals) in the deeper laminae (III-VI) of the DH compared to CFA controls (**FIG. 3.6A-C,D**). VGLUT1 staining was largely confined to these deeper laminae (ie. did not extend into the superficial layers) in all groups (**FIG. 3.6A-C**). PLZ treatment in EAE did not attenuate these increases (**FIG. 3.6C,D**). As no lateralized difference in VGLUT1 density was expected (or was naively apparent), both sides of the SC were considered together for this analysis. (*One-way ANOVA, \*p=0.033, all pairwise post hoc comparisons by Holm-Sidak method. (CFA vs. VEH \*p<0.05, CFA vs. PLZ \*p<0.05, PLZ vs. VEH NS.)*)

#### **3.4.6 - 5-HT+ immunoreactivity is reduced in the dorsal horn in EAE, and is normalized by pretreatment with PLZ.**

In order to further investigate the spinal mechanisms of PLZ's anti-allodynic effects in EAE, we sought to confirm the effect of PLZ on monoamine concentrations within the DH. Musgrave/Benson et al. (2011/2013) [21, 25, 45] previously reported that, as quantitatively determined by HPLC on whole SC homogenate (as well as on brain and brainstem), acute and chronic PLZ treatment increased or restored monoamine and GABA concentrations in the later stages of EAE. In animals at clinical onset, monoamines (5-HT/NA/DA) were disrupted compared to CFA controls [21]; however, GABA levels were not significantly reduced until the peak/chronic stage of the disease [21]. Because those HPLC experiments lacked anatomical specificity (ie. neurotransmitter promoting effects could not specifically be localized to the lumbar DH), and did not specifically measure the effects of chronic PLZ at clinical onset, we performed immunostaining for 5-HT/GABA in these animals. While immunostaining for GABA in the DH of these animals was not conclusive (*not shown*), immunostaining for 5-HT provided more definitive results. Benson/Musgrave [45] also previously found that 5-HT immunoreactivity in the lumbar ventral horn was reduced in EAE, and was normalized by PLZ treatment. Here, we found a similar pattern in the DH (**FIG. 3.7A-C**). VEH treated EAE animals (**n=10**) exhibited reduced 5-HT

immunoreactivity in the total DH (quantified by integrated density), compared to CFA controls (**n=9**). 5-HT immunoreactivity was normalized/enhanced (ie. to equal *or greater* than CFA levels) in the group pretreated with PLZ (**n=10**) (*One-way ANOVA,  $p<0.001$ , all pairwise post hoc comparisons by Holm-Sidak method. (CFA vs. PLZ NS., CFA vs. VEH  $*p<0.05$ , VEH vs. PLZ  $*p<0.05$ ).*) (FIG. 3.7D)

### 3.5 - Discussion

Mechanical allodynia is detectable in the early stages of (female C57/BL6) EAE by the VFH assay. Allodynia is also commonly described in the clinical MS population, and may be diagnosed using a variety of simple tests and inventories [10]. In this chapter, we first established that chronic PLZ pretreatment, initiated at a time point when behavioral sensitization is frequently present (7 dpi.) [15], normalizes mechanical and thermal sensitivity (ie. reverses allodynia) in EAE animals assessed at clinical onset. This represents a novel use for this compound, and provides new evidence that normalizing monoamine (and possibly GABA) concentrations in the dorsal horn is a useful strategy to treating pain in EAE/MS. We next examined the functional neuronal response in the SCDH to a (normally) non-noxious vibromechanical stimulus in early EAE, using c-Fos IHC. This builds on the previous work of Olechowski et al. 2009 [15], which reported on basally elevated c-Fos+ cells in the SCDH - and Olechowski et al. 2010 [26], which investigated the SCDH (c-Fos) response to intraplantar formalin injection in EAE. Those studies provided key early insights into altered neuronal activation and central sensitization in the SCDH in EAE. In the current study, the use of a non-noxious vibromechanical stimulus to evoke c-Fos provides additional behaviorally relevant insights into the central mechanisms of allodynia in EAE. We also find that PLZ treatment modifies the functional (c-Fos) response in the SCDH to this non-noxious vibromechanical stimulus. In addition to examining functional neuronal responses in the SCDH using post-mortem c-Fos IHC, we also looked at neuronal responses to glutamate in live *ex vivo* spinal cord slices from EAE and CFA animals using ratiometric calcium imaging. We confirmed that, in this complementary modality, functional responses in the dorsal

horn of EAE animals are intensified. As in chapter 1, we also find that acute bath-applied PLZ inhibits glutamate-evoked responses in the SCDH in slices from EAE (and CFA) animals.

In order to examine neuronal activation in the SCDH, we first made use of c-Fos IHC. c-Fos is a nuclear transcription factor which is encoded by the *C-Fos* gene, one of several so-called 'immediate early genes' (IEGs) which are rapidly transduced following exposure to certain stimuli [46, 47]. c-Fos is widely expressed in neurons within the SCDH, and is transduced in response to strong neuronal activation (ie. repeated depolarizations) [48, 49]. Many studies have demonstrated that c-Fos is robustly activated in neurons of the DH following the application of noxious stimuli, making it a useful marker for neuronal functional activity in pain studies [27, 50]. For this study, in order to rule out any *de novo* expression of c-Fos in cell types other than neurons (ie. in inflammatory cells), and ensure its usefulness as a neuronal activity marker in our model, we performed double-labelling in (EAE-VEH/PLZ) SCDH tissues. These experiments confirmed that c-Fos is expressed in neurons, and not in inflammatory/glia cells (T-cells, microglia/macrophages, astrocytes), in EAE.

The use of noxious stimuli such as intraplantar formalin injection to evoke a c-Fos signal in the SCDH of EAE animals yields an apparently paradoxical reduction in c-Fos+ neurons [26]. This effect was explained in Olechowski et al. 2010 [26] by the induction of mGluR-mediated diffuse noxious inhibitory controls (DNIC). The additive effect of formalin-evoked glutamate, alongside basally elevated extracellular glutamate in EAE, was believed to exceed the threshold of activation for the inhibitory (group 2/3) mGluR-mediated response. In the case of non-noxious stimulation (ie. low-weight VFHs or vibromechanical stimulation), there is an exaggerated behavioral, and central functional (in S1 [41], and the DH), response in EAE animals – both of which are indicative of an allodynic state. In the current experiment, the novel finding that repeated vibromechanical stimulation of the LHP also induces additional c-Fos+ neurons within the ipsilateral superficial DH in EAE, supports the conclusion that sensitization of the spinal nociceptive circuitry contributes to allodynia in the disease. Fos+ neurons

were also elevated in EAE animals in the contralateral and deep DH (compared to CFA controls), replicating previous findings [15], and indicating that neuronal activity is altered throughout the DH laminae/circuitry. This conclusion is also supported by the *ex vivo* calcium imaging experiments, which involved labelling and recording from neurons distributed throughout the superficial and deep laminae of the dorsal horn.

We initially hypothesized that PLZ pretreatment would reduce the total number of c-Fos+ neurons in the DH in EAE, however, our data here refute this hypothesis. Overall c-Fos levels remained elevated throughout the DH in PLZ-treated EAE animals, indicating that PLZ does not normalize basal/ongoing neuronal activity in the DH – although active neuronal populations may differ. PLZ treatment in EAE did, however, reduce or eliminate the stimulus-related c-Fos signal in the ipsilateral superficial DH. This finding suggests the possibility of a stimulus- or activity-dependent effect of PLZ; however, additional experiments would be required to verify such a mechanism.

We also examined neuronal function in the EAE SCDH with fura 2 ratiometric calcium imaging in isolated (live) lumbar slices. This complementary technique measures intracellular calcium content – which transiently rises following neuronal depolarizations/discharges – allowing us to measure stimulus-evoked responses in dorsal horn neurons directly and in real-time. The exaggerated intracellular calcium responses / hyperexcitability we observed in DH neurons in EAE slices provide further evidence of the sensitization of DH nociceptive networks in the disease. This hyperexcitability may be due to intrinsic neuronal changes, or to a pro-excitatory shift in the network balance of excitation and inhibition within the DH [33] (or both). Such a pro-excitatory shift could, in turn, be due to a gain in network excitability, a loss of inhibition, or both.

In addition to these functional changes, staining for VGLUT1 in the SC indicated the presence of structural neuronal plasticity within the deep laminae components of the DH in EAE. Increased density

of VGLUT1+ presynaptic excitatory terminals in these DH laminae mirrors our findings in S1 (Chapter 3 / Potter et al. 2016 [41]), and may be a consequence of the ongoing functional activity, excess glutamate concentrations, and inflammation found in the SCDH in EAE [18, 21, 26]. Another possibility is that increased VGLUT1+ staining may result from ectopic discharges and ongoing excitatory drive from myelinated low-threshold peripheral afferents (ie. peripheral sensitization) [31, 32] [56]. An increase in the number of excitatory synaptic connections and peripheral terminals within the SCDH might serve to maintain and contribute to central sensitization and allodynia in EAE [20, 33-35]. Other factors which may contribute to aberrant and excessive synaptic plasticity in the DH in EAE include the presence of circulating cytokines such as TNF $\alpha$  and IL-1 $\beta$  [18, 51, 52], other cell-mediated inflammatory effects [53-56], and/or altered matrix-metalloproteinase activity and extracellular matrix composition (Paylor/Benson unpublished findings) [57-61].

The apparent disparity between the findings of altered neuronal responses in the *superficial* laminae of the DH following vibromechanical stimulation, and altered synaptic density and ongoing neuronal activation in the *deeper* laminae of the DH in EAE, may be resolved by considering the functional anatomy of the DH circuits which are thought to underlie allodynia – a subject on which the scientific understanding has advanced considerably in recent years [62-64]. In general, allodynia is thought to involve a functional and/or anatomical ‘cross-wiring’ of low-threshold peripheral afferent inputs onto nociceptive (high threshold) ascending circuits [33, 65]. This ‘cross-wiring’ may arise through a variety of mechanisms [34, 62, 64]. The projection neurons that participate in the ascending nociceptive circuits (eg. neurokinin-1 receptor+ neurons) are preferentially located within the superficial laminae of the DH [42, 62]. The pattern of c-Fos/VGLUT1+ reactivity observed here supports the hypothesis that, in EAE, neuronal plasticity and sensitization within the deeper laminae of the SCDH (and possibly the superficial DH as well) results in normally non-noxious peripheral inputs eliciting activity in the nociceptive superficial DH neurons. The detailed cellular mechanism is unknown, but would be an ideal subject for future studies.

The finding that PLZ treatment did not reduce or reverse changes in VGLUT1+ synapse density in the SCDH may reflect the fact that PLZ treatment also did not reduce 'basal'/ongoing neuronal activity (ie. total c-Fos expression) in EAE. If synaptic plasticity in the deep DH is primarily reflective of ongoing functional activity – or if inflammation is the primary driver - these findings would appear to be consistent. Indeed, we also find that PLZ treatment has no apparent effect on cellular inflammation and gliosis within the SCDH in EAE, suggesting that the effects of PLZ in the DH in EAE are primarily upon neuronal function and neurotransmission.

Musgrave/Benson et al. [25, 45] confirmed the effects of PLZ on CNS concentrations of monoamines and GABA in EAE using HPLC. In the current study, we build upon those findings by establishing with IHC that 5-HT is specifically reduced in the SCDH in EAE at clinical onset, and is normalized or enhanced by PLZ pretreatment. We did not stain for NA (or DA) in the current study because we were unaware of any reliable antibodies targeting the small-molecules; however, the previous HPLC studies did confirm that NA is reduced in the SC in EAE, and is normalized by PLZ treatment. The monoamine neurotransmitters are generally inhibitory in the DH – although they may exert a facilitatory influence as well – and act primarily in a volume transmission / neuromodulatory manner [33, 66]. Loss of monoamines in the SCDH – leading to disinhibition - is thus one possible factor that may contribute to the overall sensitization of nociceptive networks in EAE. GABA is also generally inhibitory in the SCDH, and is diminished in the EAE CNS/SC at later stages of the disease [21]. However, we were unable to use IHC to confirm or refute an effect of PLZ on GABA within the SCDH in EAE at clinical onset. Nevertheless, a contribution to the effects of PLZ from the PEH metabolite, acting to augment GABAergic transmission in the SCDH through GABA-T inhibition, is conceivable. The earlier HPLC studies showed that a single I.P. dose of PLZ at disease peak, or chronic PLZ treatment in the established disease produced an increase in spinal GABA content [25, 45]. Overall, the evidence to date supports a mechanism wherein PLZ acts to boost or restore both monoamine and GABA content

in the SCDH, and thereby to bolster inhibition in dorsal horn nociceptive networks. Additional experiments which may further clarify the precise mechanisms of PLZ in EAE are ongoing in our lab.

### **3.5.1 - Conclusions**

The findings of this study help to clarify the role of functional/structural plasticity in the SCDH in allodynia in EAE, and elucidate the spinal mechanisms underlying the anti-allodynic effects of treatment with the MAOI PLZ. These findings may have implications for the treatment of CNP in MS, which may result from similar underlying neurobiological changes. Although the precise mechanisms of PLZ and allodynia in EAE require further investigation, treatments which mirror aspects of PLZ's actions (or, perhaps, even PLZ itself) may prove to be effective against CNP in MS, as they are for allodynia in EAE.

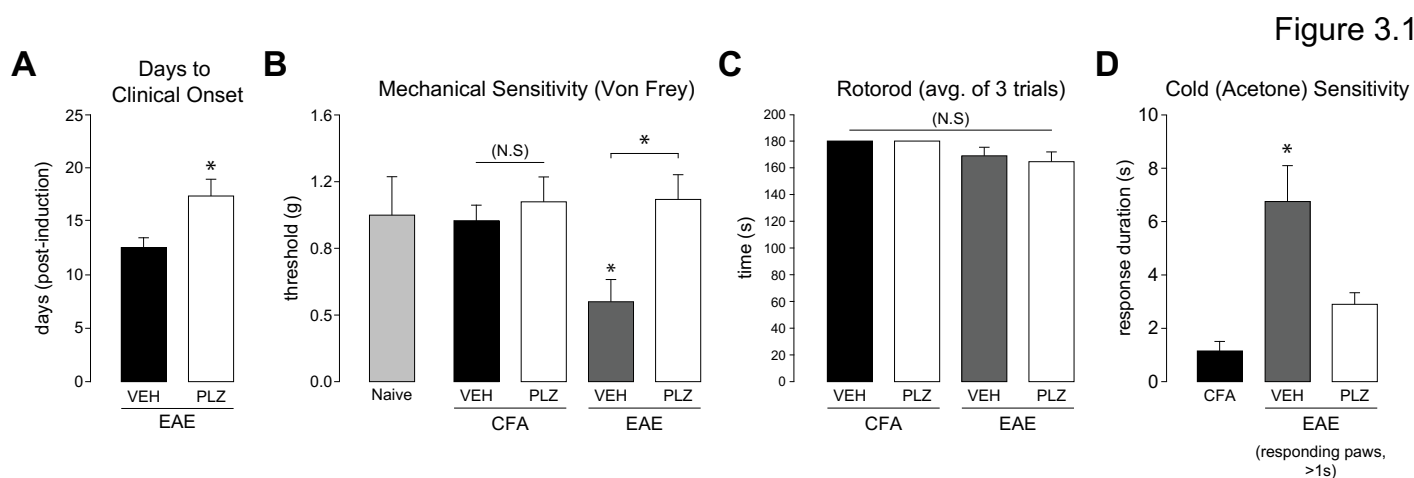


**Figure 3.1** Effects of chronic pretreatment with PLZ on clinical score and nociceptive behaviors in EAE animals at onset.

(A) Mean number of days (post-induction) to clinical onset (grade > 0) in animals treated with vehicle (VEH,  $n=26$ ) or phenelzine (PLZ,  $n=27$ ) since day 7 dpi. PLZ delayed the clinical onset of EAE by several days (t-test,  $*p=0.041$ ). (B) Group-mean ( $\pm$ S.E.) response thresholds to punctate mechanical stimulation of the hindpaws (Von Frey hairs) for CFA-VEH (7-12 dpi  $n=15$ ), CFA-PLZ (12 dpi  $n=5$ ), EAE-VEH ( $n=14$ ), and EAE-PLZ ( $n=17$ ) mice at clinical-onset. EAE-VEH mice exhibited significantly reduced mechanical thresholds compared to CFA-VEH controls. Chronic treatment with PLZ from 7 dpi normalized mechanical thresholds in EAE at onset, but did not affect thresholds in CFA mice (Kruskal-Wallis ANOVA on ranks,  $*p=0.005$ ; post-hoc comparisons vs. CFA-VEH by Dunn's method). Naives (pictured,  $n=3$ ) were not included in the analysis. (C) Mean time spent on the rotarod (average of three trials per animal) in each treatment group at clinical onset. (D) Mean duration of response to a drop of acetone, applied to the ventral surface of the paw (cold sensitivity) in CFA controls, and VEH and PLZ treated EAE animals at clinical onset (Kruskal-Wallis one-way ANOVA on Ranks,  $*p<0.001$ ; all pairwise post-hoc comparisons by Dunn's method, VEH vs. CFA  $*p<0.05$ , PLZ vs. CFA NS., VEH vs. PLZ NS.).

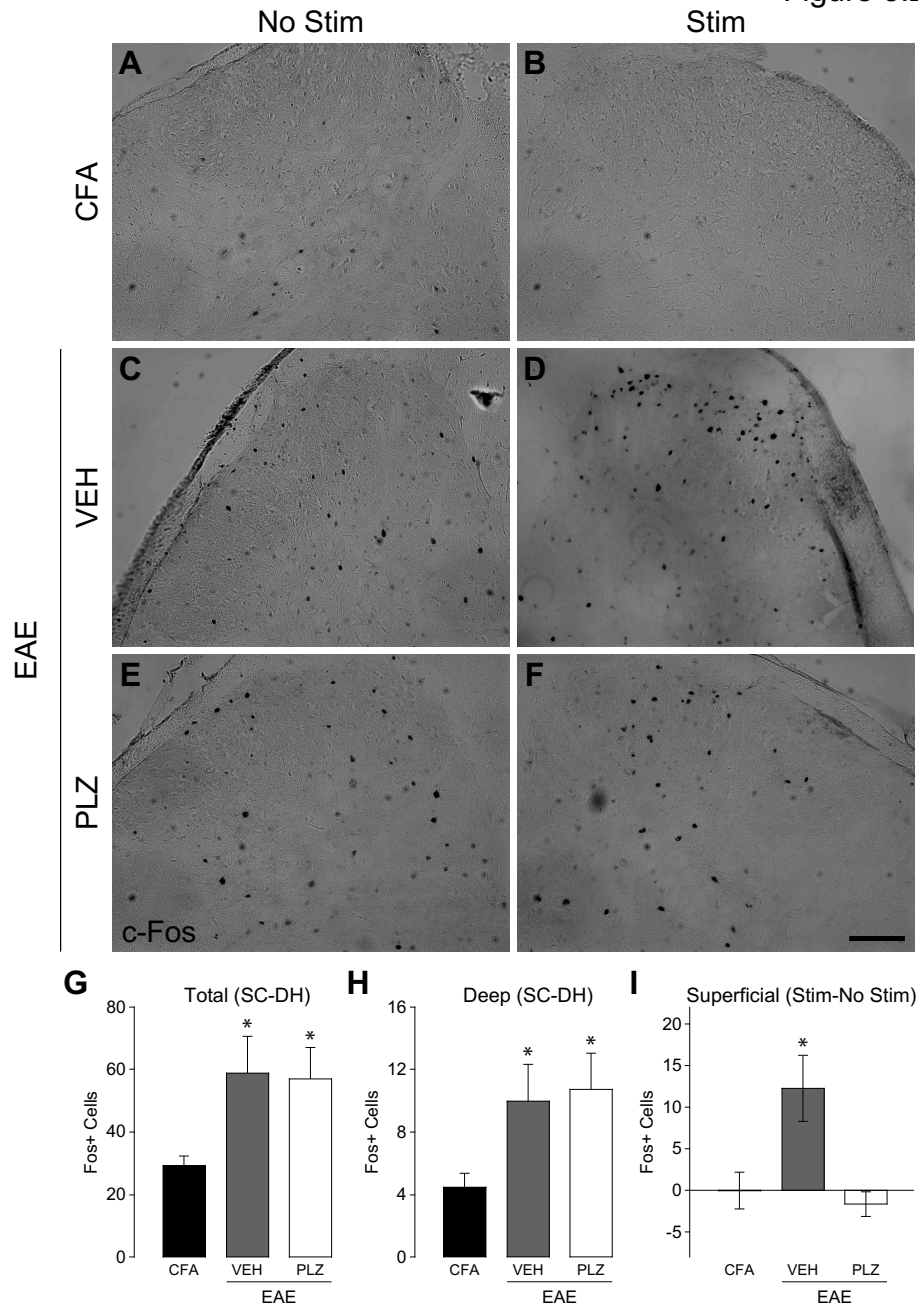
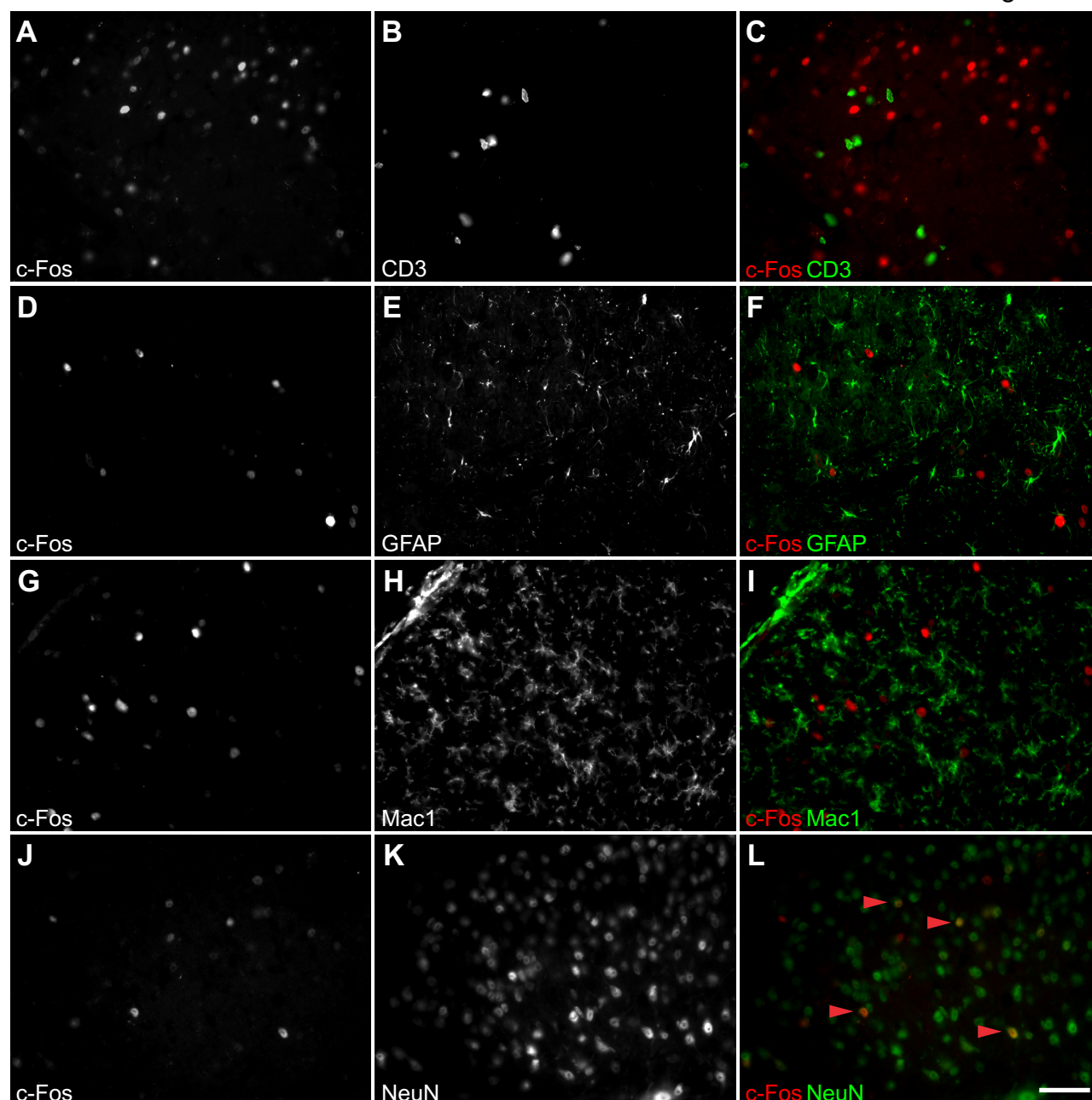


**Figure 3.2** Vibromechanically evoked *c-Fos* in the dorsal horn in (onset) EAE is normalized by pretreatment with PLZ.

(A-F) Representative photomicrographs of *c-Fos* expression in the ipsilateral and contralateral dorsal horns following vibromechanical stimulation of the LHP in CFA controls (A,B), VEH treated EAE (C,D), PLZ treated EAE (E,F), at clinical onset. Scale bar in F=100 $\mu$ m, applies throughout. (G) Quantification of the mean total number of *c-Fos*+ cells in the ipsi- and contralateral dorsal horns (post-stimulation) in CFA controls (n=8), VEH treated EAE (n=10), and PLZ treated EAE. (n=10) (H) Quantification of the mean number of *c-Fos*+ cells in the deeper laminae (IV-VI) of the dorsal horn (sides averaged). (VEH, n=9\*) (I) Quantification of the mean difference in *c-Fos*+ cells between the ipsi- and contralateral superficial (laminae I-III) dorsal horns following vibromechanical stimulation.

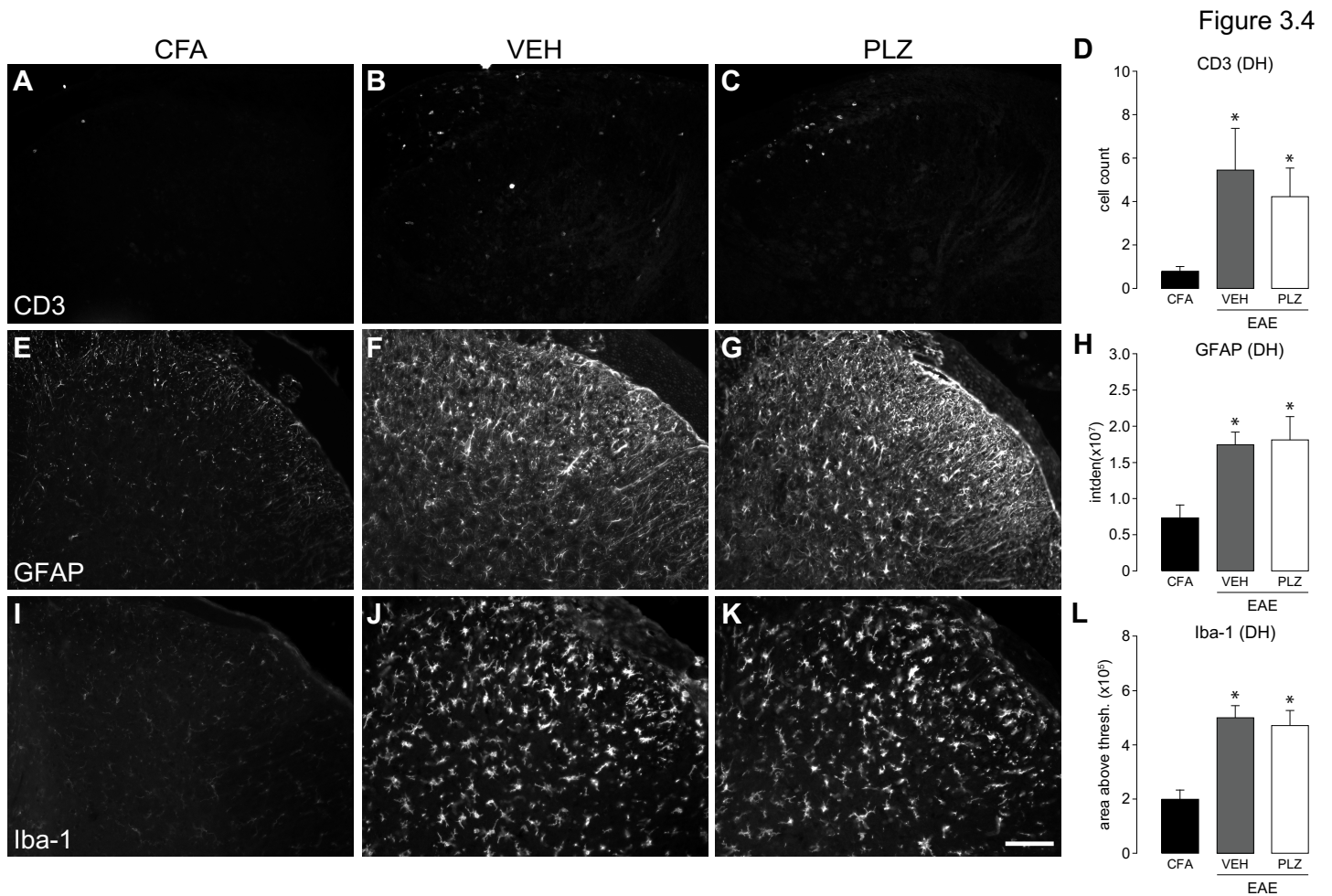
**Total:** Kruskal–Wallis ANOVA on Ranks, \* $p=0.015$ , post-hoc comparisons vs. control (CFA) by Dunn's method. (VEH vs. CFA \* $p<0.05$ , PLZ vs. CFA \* $p<0.05$ ). **Deep:** Kruskal–Wallis ANOVA on Ranks, \* $p=0.022$ , post-hoc comparisons vs. control (CFA) by Dunn's method. (VEH vs. CFA \* $p<0.05$ , PLZ vs. CFA \* $p<0.05$ ). **Superficial (Difference):** Kruskal–Wallis ANOVA on Ranks, \* $p=0.002$ , all pairwise post-hoc comparisons by Dunn's method. (VEH vs. PLZ \* $p<0.05$ , CFA vs. VEH \* $p<0.05$ , CFA vs. PLZ NS.).

Figure 3.3



**Figure 3.3** *c-Fos* co-localizes with neurons, and not with inflammatory cell types, in the dorsal horn in VEH and PLZ treated EAE.

(A-C) Representative photomicrographs of *c-Fos* staining (A) alongside CD3<sup>+</sup> infiltrating T-cells (B) in the dorsal horn of VEH treated EAE animals (PLZ treated EAE not shown). Merge in (C). Scale bar in L=100 $\mu$ m, applies throughout. (D-F) Representative photomicrographs of *c-Fos* staining (D) alongside GFAP staining (astrocytes, E) in the dorsal horn of VEH treated EAE animals (PLZ treated EAE not shown). Merge in (F). (G-I) Representative photomicrographs of *c-Fos* staining (G) alongside Mac-1 reactive microglia (H) in the dorsal horn of VEH treated EAE animals (PLZ treated EAE not shown). Merge in (I). (J-L) Representative photomicrographs of *c-Fos* staining (J) alongside neuronal nuclei (NeuN, K) in the dorsal horn of VEH treated EAE animals (PLZ treated EAE not shown). Merge in (L), co-labelled *c-Fos*<sup>+</sup> neurons indicated by red arrowheads.



**Figure 3.4** PLZ's actions in EAE are not mediated by a reduction of inflammatory cells in the dorsal horn.

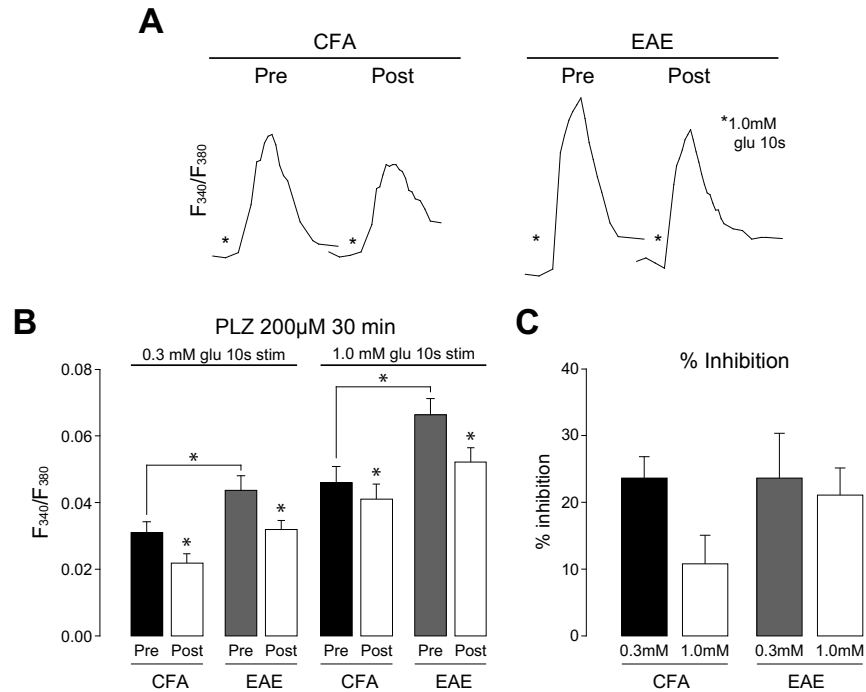
(A-C) Representative photomicrographs of CD3<sup>+</sup> infiltrating T-cells in the dorsal horn of CFA controls (A, n=4), VEH treated EAE (B, n=6), and PLZ treated EAE (C, n=9). Scale bar in K=100 $\mu$ m, applies throughout. (D) Quantification of the number of CD3<sup>+</sup> cells in the dorsal horn. (E-G) Representative photomicrographs of GFAP staining (astrocytes) in the dorsal horn of CFA controls (E, n=5), VEH treated EAE (F, n=10), and PLZ treated EAE (G, n=10). (H) Quantification (integrated density) of GFAP immunoreactivity in the superficial laminae (I-III) of the dorsal horn. (I-K) Representative photomicrographs of Iba-1<sup>+</sup> reactive microglia in the dorsal horn of CFA controls (I, n=9), VEH treated EAE (J, n=10), and PLZ treated EAE (K, n=10). (L) Quantification (area above threshold) of Iba-1<sup>+</sup> immunoreactivity in the superficial laminae (I-III) of the dorsal horn.

**CD3:** Kruskal-Wallis ANOVA on Ranks, \* $p=0.024$ , all pairwise post-hoc comparisons by Dunn's method. (VEH vs. CFA \* $p<0.05$ , PLZ vs. CFA \* $p<0.05$ , VEH vs. PLZ NS.).

**GFAP:** One-way ANOVA, \* $p=0.003$ , all pairwise post-hoc comparisons by Holm-Sidak method. (VEH vs. CFA \* $p<0.05$ , PLZ vs. CFA \* $p<0.05$ , VEH vs. PLZ NS.).

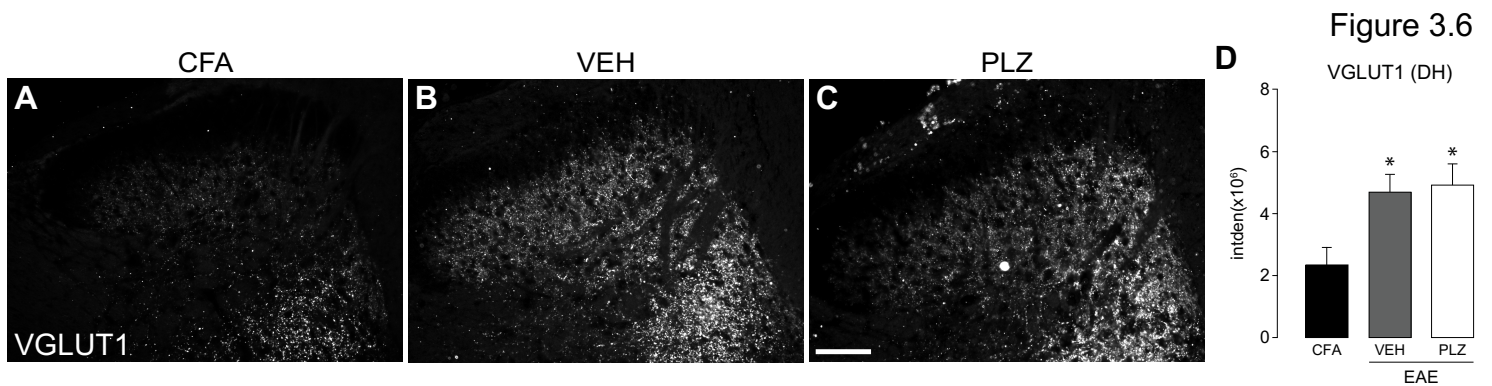
**Iba-1:** One-way ANOVA, \* $p=0.007$ , all pairwise post hoc comparisons by Holm-Sidak method. (VEH vs. CFA \* $p<0.05$ , PLZ vs. CFA \* $p<0.05$ , VEH vs. PLZ NS.).

Figure 3.5



**Figure 3.5** Intracellular calcium responses are enhanced within the dorsal horn in EAE, and are normalized by bath- applied PLZ.

(A) Representative F340/380 traces of a single neuron post-1mM glutamate stimulus, before (Pre) and after (Post) 30 min. PLZ superfusion, in EAE/CFA slices. (B) Group mean peak (ratiometric) fluorescence intensity (F340/F380) following 0.3mM and 1.0mM glutamate stimulus (avg. of 2 stims/slice) prior to bath application of 200 $\mu$ M PLZ (pre) and following 30 min. PLZ superfusion (post). (CFA n=7, EAE n=8) (paired *t*-tests “pre-PLZ” vs. “post-PLZ”: CFA 0.3mM glutamate \**p*=0.005, 1.0mM glutamate \**p*=0.044; EAE 0.3mM glutamate \**p*=0.017, 1.0mM glutamate \**p*=0.001), (*t*-test “pre-PLZ” vs. “pre-PLZ”, 0.3mM glutamate: \**p*=0.040; 1.0mM glutamate: \**p*=0.012) (C) Group mean calcium response (%F340/F380) to 0.3mM and 1.0mM glutamate post-PLZ superfusion, as a percentage of the (within slice) response pre-PLZ superfusion.



**Figure 3.6** Increased density of VGLUT1+ presynaptic terminals in the deeper laminae (III-VI) of the dorsal horn in EAE.

(A-C) Representative photomicrographs of VGLUT1 (presynaptic excitatory terminals / low-threshold primary afferent terminals) staining in the dorsal horn in CFA controls (A, n=6), VEH treated EAE (B, n=10), and PLZ treated EAE (C, n=10). Scale bar in C=100 $\mu$ m, applies throughout. (D) Quantification (integrated density) of VGLUT1 immunoreactivity in the deeper laminae (III-VI) of the (bilaterally averaged) dorsal horn. (One-way ANOVA, \* $p=0.033$ , all pairwise post-hoc comparisons by Holm-Sidak method. (CFA vs. VEH \* $p<0.05$ , CFA vs. PLZ \* $p<0.05$ , PLZ vs. VEH NS.)

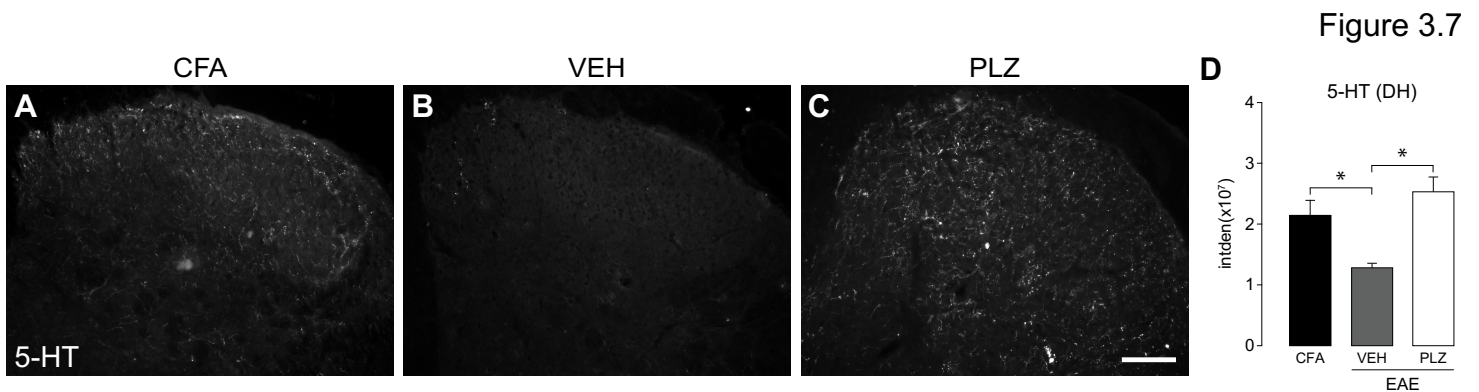


**Figure 3.7** 5-HT<sup>+</sup> immunoreactivity is reduced in the dorsal horn in EAE, and is normalized by pretreatment with PLZ.

(A-C) Representative photomicrographs of 5-HT staining in the dorsal horn of CFA controls (A, n=9), VEH treated EAE (B, n=10), and PLZ treated EAE (C, n=10). Scale bar in C=100 $\mu$ m, applies throughout. (D) Quantification (integrated density) of 5-HT immunoreactivity in the total dorsal horn (laminae I-VI). (One-way ANOVA, \* $p$ <0.001, all pairwise post-hoc comparisons by Holm-Sidak method. (CFA vs. PLZ NS., CFA vs. VEH \* $p$ <0.05, VEH vs. PLZ \* $p$ <0.05).

### 3.7 - REFERENCES

1. Compston, A. and A. Coles, *Multiple sclerosis*. Lancet, 2002. 359(9313): p. 1221-31.
2. Svendsen, K.B., et al., *Sensory function and quality of life in patients with multiple sclerosis and pain*. Pain, 2005. 114(3): p. 473-81.
3. Svendsen, K.B., et al., *Pain in patients with multiple sclerosis: a population-based study*. Archives of neurology, 2003. 60(8): p. 1089-94.
4. O'Connor, A.B., et al., *Pain associated with multiple sclerosis: systematic review and proposed classification*. Pain, 2008. 137(1): p. 96-111.
5. Iannitti, T., B.J. Kerr, and B.K. Taylor, *Mechanisms and Pharmacology of Neuropathic Pain in Multiple Sclerosis*. Current topics in behavioral neurosciences, 2014. 20: p. 75-97.
6. Grau-López, L., et al., *Analysis of the pain in multiple sclerosis patients*. Neurología (English Edition), 2011. 26(4): p. 208-213.
7. Solaro, C. and M. Messmer Uccelli, *Pharmacological management of pain in patients with multiple sclerosis*. Drugs, 2010. 70(10): p. 1245-54.
8. Solaro, C. and M.M. Uccelli, *Management of pain in multiple sclerosis: a pharmacological approach*. Nat Rev Neurol, 2011. 7(9): p. 519-27.
9. Osterberg, A., J. Boivie, and K.A. Thuomas, *Central pain in multiple sclerosis--prevalence and clinical characteristics*. European journal of pain, 2005. 9(5): p. 531-42.
10. Österberg, A. and J. Boivie, *Central pain in multiple sclerosis – Sensory abnormalities*. European journal of pain, 2010. 14(1): p. 104-110.
11. Khan, F. and J. Pallant, *Chronic Pain in Multiple Sclerosis: Prevalence, Characteristics, and Impact on Quality of Life in an Australian Community Cohort*. The Journal of Pain, 2007. 8(8): p. 614-623.
12. Thibault, K., B. Calvino, and S. Pezet, *Characterisation of sensory abnormalities observed in an animal model of multiple sclerosis: a behavioural and pharmacological study*. Eur J Pain, 2011. 15(3): p. 231 e1-16.
13. Aicher, S.A., et al., *Hyperalgesia in an animal model of multiple sclerosis*. Pain, 2004. 110(3): p. 560-70.
14. Khan, N. and M.T. Smith, *Multiple sclerosis-induced neuropathic pain: pharmacological management and pathophysiological insights from rodent EAE models*. Inflammopharmacology, 2014. 22(1): p. 1-22.
15. Olechowski, C.J., J.J. Truong, and B.J. Kerr, *Neuropathic pain behaviours in a chronic-relapsing model of experimental autoimmune encephalomyelitis (EAE)*. Pain, 2009. 141(1-2): p. 156-64.
16. Croxford, A.L., F.C. Kurschus, and A. Waisman, *Mouse models for multiple sclerosis: Historical facts and future implications*. Biochimica et Biophysica Acta (BBA) - Molecular Basis of Disease, 2011. 1812(2): p. 177-183.
17. Ransohoff, R.M., *Animal models of multiple sclerosis: the good, the bad and the bottom line*. Nat Neurosci, 2012. 15(8): p. 1074-1077.
18. Olechowski, C.J., et al., *Changes in nociceptive sensitivity and object recognition in experimental autoimmune encephalomyelitis (EAE)*. Experimental neurology, 2013. 241(0): p. 113-121.
19. Aicher, S.A., et al., *Hyperalgesia in an animal model of multiple sclerosis*. Pain, 2004. 110(3): p. 560-570.
20. Latremoliere, A. and C.J. Woolf, *Central Sensitization: A Generator of Pain Hypersensitivity by Central Neural Plasticity*. The journal of pain : official journal of the American Pain Society, 2009. 10(9): p. 895-926.
21. Musgrave, T., et al., *Tissue concentration changes of amino acids and biogenic amines in the central nervous system of mice with experimental autoimmune encephalomyelitis (EAE)*. Neurochemistry international, 2011. 59(1): p. 28-38.

22. Parent, M.B., et al., *Effects of the antidepressant/antipanic drug phenelzine and its putative metabolite phenylethylidenehydrazine on extracellular gamma-aminobutyric acid levels in the striatum*. *Biochem Pharmacol*, 2002. 63(1): p. 57-64.
23. Parent, M.B., M.K. Habib, and G.B. Baker, *Time-dependent changes in brain monoamine oxidase activity and in brain levels of monoamines and amino acids following acute administration of the antidepressant/antipanic drug phenelzine*. *Biochem Pharmacol*, 2000. 59(10): p. 1253-63.
24. McManus, D.J., et al., *Effects of the antidepressant/antipanic drug phenelzine on GABA concentrations and GABA-transaminase activity in rat brain*. *Biochem Pharmacol*, 1992. 43(11): p. 2486-9.
25. Musgrave, T., et al., *The MAO inhibitor phenelzine improves functional outcomes in mice with experimental autoimmune encephalomyelitis (EAE)*. *Brain, Behavior, and Immunity*, 2011. 25(8): p. 1677-1688.
26. Olechowski, C.J., et al., *A diminished response to formalin stimulation reveals a role for the glutamate transporters in the altered pain sensitivity of mice with experimental autoimmune encephalomyelitis (EAE)*. *Pain*, 2010. 149(3): p. 565-72.
27. Abbadie, C., et al., *Differential contribution of the two phases of the formalin test to the pattern of c-fos expression in the rat spinal cord: studies with remifentanyl and lidocaine*. *Pain*, 1997. 69(1-2): p. 101-110.
28. Coderre, T.J., A.L. Vaccarino, and R. Melzack, *Central nervous system plasticity in the tonic pain response to subcutaneous formalin injection*. *Brain Research*, 1990. 535(1): p. 155-158.
29. Benson, C.A., et al., *The MAO inhibitor phenelzine can improve functional outcomes in mice with established clinical signs in experimental autoimmune encephalomyelitis (EAE)*. *Behavioural brain research*, 2013. 252: p. 302-11.
30. Barrot, M., *Tests and models of nociception and pain in rodents*. *Neuroscience*, 2012. 211: p. 39-50.
31. Lu, J., et al., *Pain in experimental autoimmune encephalitis: a comparative study between different mouse models*. *Journal of neuroinflammation*, 2012. 9(1): p. 233.
32. Duffy, S.S., et al., *Peripheral and Central Neuroinflammatory Changes and Pain Behaviors in an Animal Model of Multiple Sclerosis*. *Frontiers in Immunology*, 2016. 7: p. 369.
33. Sandkühler, J., *Models and Mechanisms of Hyperalgesia and Allodynia*. *Physiological Reviews*, 2009. 89(2): p. 707.
34. Kuner, R. and H. Flor, *Structural plasticity and reorganisation in chronic pain*. *Nat Rev Neurosci*, 2017. 18(1): p. 20-30.
35. Ji, R.-R., et al., *Central sensitization and LTP: do pain and memory share similar mechanisms?* *Trends in Neurosciences*, 2003. 26(12): p. 696-705.
36. Woolf, C.J. and M.W. Salter, *Neuronal plasticity: increasing the gain in pain*. *Science*, 2000. 288(5472): p. 1765-9.
37. Mandolesi, G., et al., *IL-1beta dependent cerebellar synaptopathy in a mouse model of multiple sclerosis*. *Cerebellum*, 2015. 14(1): p. 19-22.
38. Mandolesi, G., et al., *Synaptopathy connects inflammation and neurodegeneration in multiple sclerosis*. *Nat Rev Neurol*, 2015. 11(12): p. 711-24.
39. Nisticò, R., et al., *Synaptic plasticity in multiple sclerosis and in experimental autoimmune encephalomyelitis*. *Philosophical Transactions of the Royal Society B: Biological Sciences*, 2014. 369(1633): p. 20130162.
40. Centonze, D., et al., *Inflammation Triggers Synaptic Alteration and Degeneration in Experimental Autoimmune Encephalomyelitis*. *The Journal of Neuroscience*, 2009. 29(11): p. 3442.
41. Potter, L.E., et al., *Altered excitatory-inhibitory balance within somatosensory cortex is associated with enhanced plasticity and pain sensitivity in a mouse model of multiple sclerosis*. *Journal of neuroinflammation*, 2016. 13(1): p. 142.
42. Todd, A.J., *Neuronal circuitry for pain processing in the dorsal horn*. *Nature reviews. Neuroscience*, 2010. 11(12): p. 823-836.

43. Brumovsky, P.R., *VGLUTs in Peripheral Neurons and the Spinal Cord: Time for a Review*. ISRN Neurology, 2013. 2013: p. 28.
44. Todd, A.J., et al., *The expression of vesicular glutamate transporters VGLUT1 and VGLUT2 in neurochemically defined axonal populations in the rat spinal cord with emphasis on the dorsal horn*. European Journal of Neuroscience, 2003. 17(1): p. 13-27.
45. Benson, C.A., et al., *The MAO inhibitor phenelzine can improve functional outcomes in mice with established clinical signs in experimental autoimmune encephalomyelitis (EAE)*. Behav Brain Res, 2013. 252: p. 302-11.
46. Gao, Y.-J. and R.-R. Ji, *c-Fos and pERK, which is a better marker for neuronal activation and central sensitization after noxious stimulation and tissue injury?* Open Pain J, 2009. 2: p. 11-17.
47. Sheng, M. and M.E. Greenberg, *The regulation and function of c-fos and other immediate early genes in the nervous system*. Neuron, 1990. 4(4): p. 477-485.
48. Bullitt, E., *Expression of C-fos-like protein as a marker for neuronal activity following noxious stimulation in the rat*. The Journal of comparative neurology, 1990. 296(4): p. 517-530.
49. Sheng, M., G. McFadden, and M.E. Greenberg, *Membrane depolarization and calcium induce c-fos transcription via phosphorylation of transcription factor CREB*. Neuron, 1990. 4(4): p. 571-582.
50. Gao, Y.J. and R.R. Ji, *c-Fos and pERK, which is a better marker for neuronal activation and central sensitization after noxious stimulation and tissue injury?* Open Pain J, 2009. 2: p. 11-17.
51. Rodrigues, D.H., et al., *IL-1 $\beta$  Is Involved with the Generation of Pain in Experimental Autoimmune Encephalomyelitis*. Molecular neurobiology, 2016. 53(9): p. 6540-6547.
52. Yang, G., et al., *Peripheral elevation of TNF-alpha leads to early synaptic abnormalities in the mouse somatosensory cortex in experimental autoimmune encephalomyelitis*. Proc Natl Acad Sci U S A, 2013. 110(25): p. 10306-11.
53. Kim, H., et al., *Increased phosphorylation of cyclic AMP response element-binding protein in the spinal cord of Lewis rats with experimental autoimmune encephalomyelitis*. Brain Research, 2007. 1162: p. 113-120.
54. Moalem, G. and D.J. Tracey, *Immune and inflammatory mechanisms in neuropathic pain*. Brain Research Reviews, 2006. 51(2): p. 240-264.
55. Scholz, J. and C.J. Woolf, *The neuropathic pain triad: neurons, immune cells and glia*. Nature Neuroscience, 2007. 10(11): p. 1361-1368.
56. Ji, R.-R., Z.-Z. Xu, and Y.-J. Gao, *Emerging targets in neuroinflammation-driven chronic pain*. Nat Rev Drug Discov, 2014. 13(7): p. 533-548.
57. Yong, V.W., et al., *Elevation of matrix metalloproteinases (MMPs) in multiple sclerosis and impact of immunomodulators*. Journal of the neurological sciences, 2007. 259(1-2): p. 79-84.
58. Ji, R.-R., et al., *MMP regulation of neuropathic pain*. Trends Pharmacol Sci, 2009. 30(7): p. 336-340.
59. Szklarczyk, A. and K. Conant, *Matrix Metalloproteinases, Synaptic Injury, and Multiple Sclerosis*. Frontiers in Psychiatry, 2010. 1(130).
60. Lakhan, S.E. and M. Avramut, *Matrix Metalloproteinases in Neuropathic Pain and Migraine: Friends, Enemies, and Therapeutic Targets*. Pain Research and Treatment, 2012. 2012: p. 10.
61. Huntley, G.W., *Synaptic circuit remodelling by matrix metalloproteinases in health and disease*. Nat Rev Neurosci, 2012. 13(11): p. 743-757.
62. Peirs, C. and R.P. Seal, *Neural circuits for pain: Recent advances and current views*. Science, 2016. 354(6312): p. 578.
63. Peirs, C., et al., *Dorsal Horn Circuits for Persistent Mechanical Pain*. Neuron, 2015. 87(4): p. 797-812.
64. Gangadharan, V. and R. Kuner, *Unravelling Spinal Circuits of Pain and Mechanical Allodynia*. Neuron, 2015. 87(4): p. 673-675.
65. Braz, J., et al., *Transmitting pain and itch messages: A contemporary view of the spinal cord circuits that generate Gate Control*. Neuron, 2014. 82(3): p. 522-536.
66. Millan, M.J., *Descending control of pain*. Progress in neurobiology, 2002. 66(6): p. 355-474.

67. Polgár, E., et al., *A Quantitative Study of Inhibitory Interneurons in Laminae I-III of the Mouse Spinal Dorsal Horn*. PLoS ONE, 2013. 8(10): p. e78309.

# Chapter 4

Altered excitatory-inhibitory balance within somatosensory cortex  
is associated with enhanced plasticity and pain sensitivity  
in a mouse model of multiple sclerosis

Published as: *Altered excitatory-inhibitory balance within somatosensory cortex is associated with enhanced plasticity and pain sensitivity in a mouse model of multiple sclerosis.*

Potter LE, Paylor JW, Suh J, Tenorio G, Caliaperumal J, Colbourne F, Baker G, Winship I, Kerr BJ.

Journal of Neuroinflammation, 2016. 13(1): p. 142.

**Note:** LP did most of the experimental work and analysis, designed all figures, and wrote the paper. JS/LP did the Golgi Cox/VGLUT1 staining/analysis. JWP did the WFA, Iba-1, and PV (nuclei) analyses. GT assisted with IHC/tissue preparation. Kasia Zubkow also assisted with IHC. JC/FC instructed on Golgi Cox. Golgi Cox tissues were cut in FC's lab. Dr. Majid Mohajeranni / Campus Alberta Neuroscience assisted LP with designing the perisomatic PV analysis. IW instructed on FAI/confocal imaging/analysis, and imaging was done in IW's lab. BJK and GT did the EAE induction. IHC work was done in the lab of BJK. BJK/LP/IW formulated the experiments / paper. GB/BJK postulated the use of PLZ in EAE. BJK, IW, GB, FC and my examining committee members helped edit the paper.

## 4.1 - Abstract

**Background:** Chronic neuropathic pain is a common symptom of multiple sclerosis (MS). MOG<sub>35-55</sub><sup>-</sup> induced experimental autoimmune encephalomyelitis (EAE) has been used as an animal model to investigate the mechanisms of pain in MS. Previous studies have implicated sensitization of spinal nociceptive networks in the pathogenesis of pain in EAE. However, the involvement of supraspinal sites of nociceptive integration, such as the primary somatosensory cortex (S1), has not been defined. We therefore examined functional, structural, and immunological alterations in S1 during the early stages of EAE, when pain behaviors first appear.

We also assessed the effects of the antidepressant/antiallodynic treatment phenelzine (PLZ) on S1 alterations in early EAE. PLZ has been shown to restore central nervous system (CNS) tissue-concentrations of GABA and the monoamines (5-HT, NA), and normalize nociceptive behaviors and evoked neuronal responses in the dorsal horn in EAE. We hypothesized that PLZ treatment also contributes to the normalization of nociceptive sensitivity in EAE by restoring the balance of excitation and inhibition (E-I) in the CNS.

**Methods:** We used *in vivo* flavoprotein autofluorescence imaging (FAI) to assess neural ensemble responses in S1 to vibrotactile stimulation of the limbs in early EAE. We also used immunohistochemistry (IHC), and Golgi-Cox staining, to examine synaptic changes and neuroinflammation in S1.

**Results:** Mice with early EAE exhibited significantly intensified and expanded FAI responses in S1 compared to controls. IHC revealed increased VGLUT1 expression and disrupted parvalbumin+ (PV+) interneuron connectivity in S1 of EAE mice. Furthermore, peri-neuronal nets (PNNs) were significantly reduced in S1. Morphological analysis of excitatory neurons in S1 revealed increased dendritic spine densities. Iba-1+ cortical microglia were significantly elevated early in the disease. Chronic PLZ treatment normalized S1 FAI responses, neuronal morphologies, and cortical microglia numbers, and attenuated VGLUT1 reactivity - but did not significantly attenuate the loss of PNNs – in EAE mice. PLZ did not effect S1 responses in control (CFA) mice.

**Conclusions:** These findings implicate a pro-excitatory shift in the E-I balance of the somatosensory CNS, arising early in the pathogenesis EAE, and leading to large-scale functional and structural plasticity in S1. This plasticity may contribute to nociceptive hypersensitivity in EAE. Our findings also suggest that cortical mechanisms contribute to the antiallodynic effect of PLZ in EAE.

## 4.2 – Introduction

In addition to progressive paralysis and the formation of white matter plaques, multiple sclerosis (MS) is often associated with prominent secondary symptoms [1]. Sensory alterations, including pain and dysaesthesia, are frequently reported in the clinical MS population [2, 3]. A substantial proportion of those affected (up to 40%) suffer from pain of central neuropathic origin (CNP) [4, 5]. An increasing awareness of these issues has developed in parallel with an increased focus on the importance of grey matter alterations in the pathobiology of MS [6]. Furthermore, a connection between maladaptive plasticity within pain-associated grey matter regions of the brain – such as the primary somatosensory cortex (S1) – and CNP has been established in the literature [7-9].

Several recent studies have shown that the disease model, experimental autoimmune encephalomyelitis (EAE), includes aspects of both cortical and sensory dysfunction. EAE shares many pathobiological characteristics with MS, and these studies provide an experimental foundation for investigations into the connections between these phenomena in diseases like MS/EAE. Specifically, earlier studies by Olechowski et al. [10-12] and others [13-15] established the suitability of the female C57/BL6 mouse model of EAE for the study of the underlying mechanisms of CNP in MS. These studies revealed that mice with EAE develop robust mechanical and thermal allodynia prior to the onset of paralytic symptoms. They also found evidence of hyperexcitability within the dorsal horn of the spinal cord (SC-DH), a form of central sensitization [10, 16]. While a few previous reports have highlighted the existence of altered neuronal structure and function in the neocortex of animals with EAE [17-19], no study to date has directly examined changes in neuronal activity and structure in higher sensory cortex in connection with altered pain behaviors in the early stages of the disease.

In the current study, we quantified synaptic densities and neuronal morphologies in S1 of female C57/BL6 mice with EAE using histological methods. This involved immunostaining for VGLUT1+ presynaptic excitatory terminals and parvalbumin+ (PV+) inhibitory networks, and reflectance-mode confocal microscopy of Golgi-Cox-stained cortical neurons. We also quantified sensory-evoked

functional neuronal responses in S1 of EAE mice using *in vivo* flavoprotein autofluorescence imaging (FAI). FAI has recently been employed in several studies of cortical (S1) responses to noxious and non-noxious peripheral stimuli in rodents under acute urethane-induced anesthesia. This technique measures increases in endogenous green fluorescence, produced by oxidized flavoproteins within the mitochondrial respiratory chain, as a quantitative and non-hemodynamic index of neuronal energy metabolism and activity [20]. The FAI signal has been shown to exhibit a roughly linear correspondence with local-field potentials and intracellular calcium-rises, and with stimulus amplitude, frequency and duration [21]. These features make FAI an ideal technique for investigating cortical nociceptive responses in EAE, and for the assessment of novel antinociceptive treatments.

The antidepressant phenelzine (PLZ) is an atypical monoamine oxidase inhibitor (MAOI). We have previously demonstrated that EAE is associated with a reduction in CNS-tissue concentrations of the monoamine neurotransmitters serotonin (5-HT), noradrenaline (NA), and dopamine (DA), as well as gamma-amino butyric acid (GABA) [22]. PLZ can restore CNS-tissue concentrations of all of these neurotransmitters when given chronically to mice with EAE [23]. PLZ therefore combines the features of both an anticonvulsant and an antidepressant – the net effect of which, we predicted, would be a promotion of neuronal inhibition within the CNS. As both pain and neocortical plasticity are thought to be regulated by a precise balance of excitation and inhibition (E-I) in the CNS [24],[25], we hypothesized that a disruption of this E-I balance might underlie both of these conditions in EAE. We also hypothesized that restoring this balance, by bolstering CNS inhibition with PLZ, would be an effective approach to treatment for these symptoms of the disease. In the previous chapter, we tested this hypothesis with respect to dorsal horn function, and confirmed the antiallodynic behavioral effects of chronic PLZ treatment in EAE. In the current chapter, we focused on PLZ's effects on neuronal function and structure in EAE at the supraspinal level, in S1.

## 4.3 – Methods

### 4.3.1 – Animals and Ethics

A total of 86, 8-12 week old, female C57/BL6 mice (Charles River – Saint Constant, Quebec, Canada) were used in these experiments. Mice were housed 5 per cage, in standard cages, and fed *ad libitum*. All animal experiments and procedures were conducted in accordance with the Canadian Council on Animal Care's Guidelines and Policies, and with protocols approved by the University of Alberta Health Sciences Animal Care and Use Committee.

### 4.3.2 – EAE Induction

EAE was induced in mice by subcutaneous (S.C.) injection into the hindquarters of 50µg of myelin oligodendrocyte glycoprotein (MOG<sub>35-55</sub>), obtained from the Peptide Synthesis Facility at the University of Calgary (Calgary, Alberta, Canada) and emulsified in Complete Freund's Adjuvant (CFA, 1.5mg/mL) containing additional heat-killed *Mycobacterium tuberculosis* H37Ra (Difco Laboratories/BD Biosciences – Franklin Lakes, NJ, USA). Immunized mice also received two intraperitoneal (I.P.) injections of pertussis toxin (*Bordetella pertussis*) (PTX, List Biological Labs – Campbell, CA, USA) - first, on the day of the induction, and again 48h later. Control mice received identical CFA with added *Mycobacterium tuberculosis* H37Ra (S.C./hindquarters), but without MOG<sub>35-55</sub>. CFA mice also received PTX injections on the same days.

### 4.3.3 – Disease Scoring

Mice were scored daily for clinical disease severity by an observer blinded to the treatment groups, using a standard 5 point scale (grades 0-4) defined as follows [26]: Grade 0 – *Normal mouse, no loss of motor function*; Grade 1 – *Flaccid tail, paralyzed in ≥50% of the tail's length, or partial paralysis of the tail with visible weakness in one or more of the limbs*; Grade 2 – *Completely paralyzed tail, some hindlimb weakness, preserved righting reflex*; Grade 3 – *Severe hindlimb weakness, slowed righting*

*reflex*; Grade 4 – *Complete paralysis of one or both of the hindlimbs*. “Clinical-onset” or “disease-onset” was defined as the first day an animal scored a clinical grade of 1 or higher. Except in the “pre-symptomatic” experiments (and excluding CFA/naïve controls), only mice that developed clinical signs of EAE were included in the analyses.

#### **4.3.4 – Drug Treatments**

For the “established histology” cohort, mice were divided into groups that, starting at 7 dpi., received daily I.P. injections of either vehicle (VEH, bacteriostatic water, 10mL/kg body weight), or phenelzine (PLZ, 15mg/kg body weight, Sigma-Aldrich – Oakville, ON, Canada). For EAE animals receiving PLZ, drug was given on alternate days with injections of VEH given on the ‘off’ day. This design was intended to control for multiple IP injections, as previous experiments showed that for longer experiments (a 21 dpi. fixed endpoint was selected for cohort), the effectiveness of GABA-T inhibition is better maintained by this injection schedule [27]. For the “onset” FAI/histology (Golgi-Cox) experiment, treatment was conducted in identical fashion; except animals in the (EAE- and CFA-) PLZ groups received the drug daily, rather than having the drug alternated with injections of VEH. No drug treatments were given for the “presymptomatic” imaging and histology experiments.

#### **4.3.5 – Pain testing / Von Frey hair assay**

Although the results are not reported in this chapter (see Chapter 2), all animals underwent behavioral habituation and pain testing by the Von Frey hair assay and Rotorod, as previously described, prior to other assays.

#### **4.3.6 – *In Vivo* Flavoprotein Autofluorescence Imaging (FAI) of S1**

FAI through a thinned-skull window has several methodological advantages over other functional imaging techniques. It is minimally invasive to the animal, and avoids certain experimental pitfalls common to more invasive methods, which frequently involve at minimum a craniotomy

(electrophysiology, calcium imaging). By imaging through a thin window, we minimized the risk of exposing the brain to inadvertent physical trauma and/or periods of hypoxia/tissue exposure, and avoided inducing excess inflammation/infection at the site of the cranial window. Furthermore, since the FAI signal is endogenous, no additional (and potentially disruptive or toxic) extrinsic compounds had to be applied to the brain. [20, 28]

#### **4.3.6.1 – Animal Preparation (Thin Window)**

Mice at 7-9 dpi. (“pre-symptomatic”) (n=4 EAE mice, n=5 CFA mice) or clinical-onset (n=8 VEH-treated CFA mice at matched time-points, n=4 PLZ-treated CFA mice at 14-17 dpi., n=8 VEH-treated EAE mice, n=10 PLZ-treated EAE mice) were imaged acutely through a thinned-skull window [29], before being euthanized for histological analysis. Animals did not receive any treatment injections on the day of the procedure. Prior to surgery, mice were lightly anesthetized with urethane (1.25g/kg body weight I.P., plus supplemental doses as required, dissolved at 20% w/v in 0.9% saline). Urethane was chosen as it provides stable and long-lasting anesthesia, and does not uncouple mitochondrial respiration in neurons (unlike volatile anesthetics [30]), making it suitable for FAI [31]. Relative to other anesthetics (such as pentobarbital, or ketamine), urethane also does not strongly or preferentially modulate CNS GABA or glutamate function, and does not significantly interfere with evoked neuronal-ensemble responses, provided the dosage is appropriate and the achieved depth of anesthesia consistent [32, 33]. Anesthetized mice were placed in a modified stereotaxic apparatus, with body temperature continuously monitored and maintained at 37°C by a rectal thermometer and heating pad. The hair of the scalp was grazed, and a local anaesthetic (bupivacaine, 0.1 mg S.C.) was administered to the incision area. A rostrocaudal incision (approximately 1 cm in length) was made at the midline, and the overlying skin was pulled back to expose the dorsal surface of the skull. Any underlying connective tissue was cleared away to reveal the underlying bone. Under a dissecting microscope, bregma was located and used as a reference to locate the region-of-interest (ROI) above the right primary somatosensory cortex (S1HL/FL, centered 2mm lateral from midline, 0.5mm caudal to bregma) [34]. A

circle, 3mm in diameter, was traced over the ROI to demarcate the boundaries of the window. Using a high-speed dental drill, the skull was progressively thinned to the point where the underlying vasculature was clearly visible (approximately 30% of the original thickness). During this process, physiological saline was periodically dripped onto the skull to aid with visualizing the region, and to prevent frictional heating. Particular attention was paid to ensuring that excessive mechanical pressure, which can cause blood to pool beneath the window, was not applied during the thinning process. This is necessary because blood absorbs light and scatters both the excitation and emission wavelengths for FA imaging. Once a smooth cranial surface was obtained at the appropriate depth, the animal was transferred to the imaging setup.

#### **4.3.6.2 – FA Imaging**

After preparation, animals in the stereotaxic frame and held at normothermia were positioned into the imaging setup. The imaging setup consists of a binocular epifluorescence microscope (TCS SP5 MP – Leica Microsystems, Wetzlar, Germany) equipped with 2.5x objective lens. Under blue excitation light (450-490nm, I3 filter-cube – Leica) generated by a 120W metal-halide lamp (Leica EL6000), images of the brain's endogenous green (>515nm) fluorescence were captured from a software-controlled frame-grabber (EPIX PIXCI™ EL1 – EPIX Inc., Buffalo Grove, IL, USA) connected to a 12-bit CCD camera (DALSA Pantera™ DS-21-01M60 – Teledyne Dalsa, Waterloo, ON, Canada). This setup employs a dichroic mirror (510nm) to accommodate separate light paths for excitation and emission wavelengths, preventing contamination and dilution of the relatively weak fluorescence signal by the much larger blue-green reflectance signal [21]. In order to improve detection of the weak fluorescence signal and enhance the signal-to-noise ratio, the camera was also set to 4x4 spatial binning. The animal's left fore- and hindlimb were positioned into computer-triggered vibromechanical stimulators incorporating piezoceramic actuators (Piezo Systems, Woburn, MA, USA) [35]. All external light sources were removed by dimming the light in the room and covering the imaging setup with an opaque black curtain. Extraneous vibrational sources were controlled for by the use of an air table. Imaging trials involved the

continuous capture of frames for 7.5s at 4hz (250ms exposure, 31 frames) for “pre-symptomatic” imaging, or for 6s at 5hz (200ms exposure, 31 frames) for “onset” imaging, with the stimulus (1mm deflection, 100hz, 1s stimulus duration) being delivered after the first second. These relatively long exposure times were necessary to reliably detect the weak fluorescence signal; however, the temporal resolution we obtained was adequate, as the time-course of the *in vivo* sensory evoked FA signal in mouse S1 is relatively slow (in the order of seconds). In order to obtain a consistent and accurately quantifiable FA response, each imaging session was comprised of 40 repeated trials per limb (alternating fore- and hind-), with a 20s interstimulus interval to allow activity to return to baseline. All images were stored as uncompressed 256x256 pixel grayscale TIFF stacks.

#### **4.3.6.3 – FA Image Processing and Data Analysis**

Data analysis was performed using NIH ImageJ 1.43/FIJI software equipped with the Intrinsic Signal and VSD Processor plugin (v1.0.8, written by Albrecht Sigler) obtained from the website of Dr. Timothy Murphy [36]. Briefly – in order to obtain representative response and improve signal-to-noise ratio, all trials from a given limb and session were averaged to provide a mean time-series. Prior to averaging, all trials were manually inspected for any obvious motion, light, or equipment artifacts that might obscure the signal (due to their much larger relative magnitudes). The plugin’s automated data quality algorithm was also used to detect trials that deviated strongly from the mean response (i.e.  $\geq 10\%$  frame-by-frame deviation in the average gray value from the mean z-stack). Any trials contaminated by artifacts, or with a highly deviating response profile, were excluded from the analysis. A Gaussian filter ( $r=1.0$  pixel) was applied to all images in the x,y directions to reduce high frequency noise. In order to control for global differences in basal cortical activity, tissue autofluorescence, and ambient light levels, all responses were normalized to a percent change in fluorescence versus baseline ( $\% \Delta F/F$ ). A “baseline” image was calculated from the mean time-series as the (pixel-by-pixel gray value) average of the frames immediately preceding the onset of stimulation. A “response” frame was defined for each session as the frames that, following the onset of stimulation, comprised the primary FA response (i.e.

from the initial upward inflection point or signal onset - to the zero intercept, or signal offset), as determined from the intensity-versus-time plot of the mean time-series. The baseline image was subtracted from all images in the series to create a “difference-series”. All images in the response-frame (of the difference-series) were then divided by the baseline image (and multiplied by 100), to yield a time-series of images in which the intensity of each pixel indicated the % change in intensity versus baseline ( $\% \Delta F/F$ ) [37].

This ( $\% \Delta F/F$ ) time-series was then quantified along the following parameters: time of signal onset, time to peak-response, duration of the attack phase, duration of the decay phase, and total response duration (only decay-duration data shown – although total response-duration differed between treatment groups, this was accounted for by changes in decay-duration). In the spatial domain, the areal extent of the “cortical map” (i.e. response area) was quantified. This “cortical map” was defined as the area where the  $\% \Delta F/F$  was  $>50\%$  of its maximal value in a (mean) z-projected image of the response frame. An ROI was drawn around this “map” area, and the (ROI-wide) mean intensity ( $\% \Delta F/F$ ) was plotted versus time, in order to determine the intensity at peak-response. For the “surround-inhibitory” FA signal analysis, an ROI was drawn manually around the darkened regions adjacent to the “cortical map”, and the peak (negative)  $\% \Delta F/F$  intensity value was thereby attained.

#### **4.3.7 – Histology**

Histological analysis was performed on brain tissues extracted from CFA controls and EAE (untreated, VEH-treated, PLZ-treated) mice at the various experimental end-points: “pre-symptomatic” (7-9 dpi. / post-FAI), “clinical-onset” (the day a mouse first presented as clinical grade 1 or higher, post-FAI; CFA endpoints matched), and at the “established disease” endpoint of 21 dpi. In order to improve certain group sizes and obtain greater statistical power, “additional onset” brains (referred to in the subsequent text) were obtained from a separate cohort of CFA/EAE mice that received no drug treatments, but did receive similar behavioral habituation and baseline assessments, were fixed at clinical-onset (7-9 dpi.

for CFA animals) for tissues. Statistical comparisons confirmed that these mice did not differ significantly from the initial cohorts on the applicable measures.

#### **4.3.7.1 – Tissue Extraction and Fixation**

For “pre-symptomatic” and “clinical-onset” cohorts, depth of anesthesia was assessed immediately after FAI. Any animals that required additional anesthesia were put into a chamber supplied with isoflurane/O<sub>2</sub> mixture at 5% w/v, 3L/min @ 14.7psi for approximately 1min. For behavioural/histology cohorts (“additional onset” and “established disease” immunohistochemistry - IHC), mice were anesthetized with sodium pentobarbital (1.7g/kg I.P.). Fully anesthetized mice underwent exsanguination and fixation by transcardiac perfusion with 4% w/v paraformaldehyde (PFA) in 0.1M phosphate buffer (PB). For Golgi-Cox staining, extracted tissues (whole brains from the “clinical-onset” FAI experiment) were briefly immersed in ddH<sub>2</sub>O, and then placed immediately into Golgi-Cox solution (*see below*). For IHC, extracted tissues were post-fixed in 4% w/v PFA/0.1M PB for at least 24h, and then immersed in 30% w/v sucrose solution in 0.1M PB overnight, before being snap frozen with isopentane on solid carbon dioxide. Frozen tissues were stored at -80°C prior to sectioning on a cryostat (50µm) as free-floating sections (*see below*, “established disease” cohort only), or immediately mounted onto slides (“pre-symptomatic” and “onset” histology).

#### **4.3.7.2 – Free-Floating Sections**

For “established disease” histology, free-floating sections were stored in phosphate-buffered saline solution (PBS) at 4°C until they could be stained. After staining with a standard IHC protocol (*see below*), sections were mounted onto slides and coverslipped with Vectashield® Mounting Medium with DAPI (Vector Laboratories Inc., Burlingame, CA, USA).

#### **4.3.7.3 – Golgi-Cox Staining**

We performed Rapid Golgi-Cox staining, combined with reflectance-mode laser-scanning confocal microscopy, on tissue-sections incorporating S1 from CFA, VEH-treated EAE, and PLZ-treated EAE mice at clinical-onset. Immediately after FAI, extracted brains were immersed in Rapid Golgi-Cox solution ("*Solutions A/B*", FD Rapid GolgiStain Kit™, FD Neurotechnologies – Columbia, MD, USA) for 14 days (changing the solution once after 24h) at RT/low ambient light, before being transferred into cutting solution ("*Solution C*"). Brains were sectioned on a vibratome (Leica VT1200S) at 200μm to ensure that whole (untransected) neuronal arbors could be accommodated [38], and then mounted on gelatin-coated slides. Slides were further developed and processed according to the manufacturer's instructions, before being coverslipped with Permount™ Mounting Medium (Fisher Scientific Co., Waltham, MA, USA).

Spiny (excitatory/glutamatergic) neurons in cortical layers 2/3 and of S1 – mainly pyramidal cells in layers 2/3, or stellate/star-pyramid (principal) cells in layer 4 [39, 40] – were located by reference to a stereotaxic atlas [34], and identified by their cytoarchitectonic/morphological characteristics. This step was performed under bright-field illumination on a Leica TCS SP-5 MP microscope by an unbiased observer. Three-dimensional z-stacks of these neurons were then acquired from the same microscope in confocal reflectance mode (488nm argon laser, 30/70 R/T filter), equipped with a 20x objective water-immersion lens (1.0 NA). Only neurons that were completely stained and unbroken were selected for acquisition to ensure that accurate quantifications could be obtained. Whenever staining permitted, at least 2 neurons from each layer were chosen from each animal for analysis. Z-stacks of the neurons' entire dendritic arbors were acquired (2048x2048 pixels, pixel-size 240x240nm, z-length: 0.54μm, 2x line/frame-averaging) using Leica's LAS-AF™ software suite. The observer then manually selected representative dendritic segments, and manually counted the total number of spines (protruding in all 3 planes) along their lengths using FIJI/ImageJ [41]. Only protrusions with a distinctly formed neck and head were considered to be dendritic spines ("stubs" and filipodia were not included in the counts). For each neuron, a minimum of 3 and a maximum of 9 dendritic segments were analyzed, with an effort made to sample equally from proximal and distal branches, and from the apical and basilar tufts (when

staining permitted). This resulted in a total of n=42 neurites from 8 layer 2/3 neurons, and n=47 neurites from 10 layer 4 neurons (5 mice) for the CFA group. For the EAE-VEH group, n=66 neurites from 14 layer 2/3 neurons, and n=76 neurites from 14 layer 4 neurons (8 mice) were obtained; and for the EAE-PLZ group, n=79 neurites from 18 layer 2/3 (9 mice), and n=83 neurites from 20 layer 4 neurons (10 mice). Dendritic segment lengths were determined using the Simple Neurite Tracer plugin for FIJI/ImageJ [42], and the spine density of each segment was calculated by dividing the total number of spines by the length the corresponding segment.

#### **4.3.7.4 – Immunohistochemistry**

##### **4.3.7.4.1 – Antibodies/Reagents**

Tissues were stained using a standard IHC protocol with the following commercially available antibodies: rat anti-CD3 (1:200 concentration, AbD Serotec® - BioRad Laboratories Canada Ltd., Mississauga, ON, Canada), rat anti-CD45 (1:200, AbD Serotec®, rabbit anti-Iba1 (1:500, Wako Chemicals USA Inc., Richmond, VA, USA), mouse anti-PV (1:2000, Cedar Lane, Burlington, ON, Canada), rabbit anti-VGLUT1 (1:1000, Cell Signaling Technology, Danvers, MA, USA), and *Wisteria floribunda* lectin (WFA, 1:1000, Vector Laboratories). Primary antibodies were visualized with the following fluorescent secondary antibodies: goat anti-rabbit Alexa Fluor®488 (1:200, Invitrogen™ – Life Technologies Inc., Burlington, ON, Canada), donkey anti-rat 488 Alexa Fluor®488 (1:200), Alexa Fluor® 647 streptavidin (1:200), goat anti-rabbit Alexa Fluor®594 (1:200). Selected PV-stained slides that were used in the “perisomatic” analysis were counterstained with NeuroTrace® 530/615 Red Fluorescent Nissl Stain (“fluoronissl” - ThermoFisher Scientific, Waltham, MA, USA) according to the manufacturer’s instructions. All slides were coverslipped using Vectashield® with DAPI.

##### **4.3.7.4.2 IHC: Image Acquisition**

Low-power images were captured on a Leica DMI 6000B microscope equipped with a 5x objective lens (50x total magnification). Higher magnification images required for the VGLUT1 analysis were acquired

on a Zeiss Observer Z.1 inverted microscope equipped with a 40x objective lens (400x total magnification). For the “perisomatic” PV analysis, 3-dimensional high-resolution (2048x2048 pixels, 0.301µm x 0.301µm pixel size, 0.615µm optical slice thickness, ~30 slices) confocal fluorescence z-stack images were acquired (focused on L2/3 in S1HL, 1 image per section, 2 sections per slide, 2 slides per animal) with a Leica TCS SP-5 MP microscope equipped with a 20x objective water-immersion lens (1.0 NA). For VGLUT1 analysis, 4 images from (S1HL) layer 2/3 and 4 images from layer 4/5 were taken from at least 2 sections per slide, 1 or 2 slides per animal. All other measurements (Iba-1, WFA, and PV) were taken as the average of 3 sections per slide, 1 slide per animal (**see Table 1 for histology sample-sizes**). Image acquisition parameters remained consistent within each analysis. All quantitative IHC image analyses were performed on either the original unmodified images, or on images processed in a consistently-applied manner as described elsewhere in the methods. Representative photomicrographs used in figures were additionally adjusted for brightness, contrast, color-balance, and histogram-scaling in order to improve the overall visibility of the images. These adjustments were performed only on whole-images, and were applied in a consistent a manner such that the figures accurately reflect the entire contents and relative-intensities of the original images.

**Table 1: Immunohistochemistry Group Sizes (n’s):**

<b>Marker:</b> <b>Group</b>	<b>CD3/CD4</b> <b>5</b> <i>(Early/Est .)</i>	<b>PV (Cell</b> <b>Counts)</b> <i>(Pre/Ons/Est.)</i>	<b>Perisomatic</b> <b>PV</b> <i>(Pre/Est.)</i>	<b>VGLUT</b> <b>1</b> <i>(Pre/Est .)</i>	<b>WFA</b> <i>(Pre/Ons/E st.)</i>	<b>Iba-1</b> <i>(Pre/Ons/E st.)</i>
CFA	4/4	8/8/6	8/8	8/5	11/11/6	13/13/6
EAE (VEH)	4/4	4/4/7	4/4	4/5	4/8/7	4/8/7
EAE (PLZ)	4/4	-/-/4	-/4	-/4	-/-/4	-/-/4

#### 4.3.7.4.3 - IHC: Analysis

CD3/CD45 staining was not quantified, as no infiltrating cells were present in any of the slides. For all other stains, images were quantified by an unbiased observer blind to treatment groups. Apart from the “perisomatic” PV analysis (*see below*), images were quantified with NIH ImageJ/FIJI. S1 hindlimb region (S1HL), and individual cortical layers therein, were identified visually by inspecting cytoarchitectonic features and by making reference to stereotaxic atlases [34], [43]. An ROI over S1HL was manually drawn, and the total area of this ROI measured to ensure it remained consistent across all images and animals (the standard deviation for ROI area remained below 5% at all times). Within this ROI, quantifications of parvalbumin-positive (PV+) and Iba-1+ cells were performed using the ITCN automated cell-counting plugin for ImageJ (by Thomas Kuo et al. [44]). PV+ cell quantifications were performed for 7-9 dpi. CFA control mice, “pre-symptomatic” EAE, and “additional onset” EAE groups; as well as for all “established” (21 dpi.) groups (CFA, EAE-VEH, EAE-PLZ). Quantification of WFA staining was performed by manually counting peri-neuronal nets (PNNs) in the ROI. For VGLUT1 analysis, a custom Fiji macro was used to create an ROI of consistent dimensions/area in each image and subsequently return the integrated density within that ROI.

#### 4.3.7.4.4 - IHC: Analysis (“Perisomatic” PV)

Perisomatic PV staining was quantified using a custom Matlab application (created by Liam Potter, using elements of code and guidance from Dr. Majid Mohajerani, University of Lethbridge, Canada). This program was designed to operate on confocal images that had been “pre-processed” with a custom FIJI script, the purpose of which was to produce images of manageable file-size, reduce image “noise”, and achieve better separation of the relevant foreground pixels from image background. Briefly - a 1-pixel-radius median filter was applied to each z-stack. Filtered stacks were group z-projected (by max intensity; 5 slices to 1 slice), followed by the manual selection of 2 or 3 consecutive “in-plane” (properly gained and artifact/distortion-free) z-projected images from each stack. These images were

concatenated to form a new “compressed” z-stack. Compressed z-stacks were binarized using an automatic local thresholding function (Bernsen algorithm, 15-pixel radius). Following this pre-processing, a final “control” image was added at the end of the binarized stack by performing a watershed transform on a single “guide” image chosen from the stack. This “guide” image was selected to be one that contained many basket-cell outlines (ie. “perisomatic” staining surrounding a putative pyramidal cell shadow). These shadows were later confirmed as pyramidal neurons by examining the fluoronissl counterstain. The watershed transform applied to the “guide” image served to close-off the spatial boundaries of these shadows so a region-growing algorithm could be applied.

Final processed/binarized stacks were loaded into the Matlab viewer, and an unbiased operator was then able to “click” inside these cell “shadows”, triggering the region-growing algorithm in the “control” image, followed by morphological dilation, to define the “perisomatic” ROI for that neuron. This ROI was then used as a Boolean mask to obtain the total number of “above-threshold” (white) pixels captured therein from each image in the stack (excluding the “control image”). After adding up the areas from each image in the stack (yielding a “pseudo-volume”), the resulting sum was normalized to the cross-sectional area of the “shadow neuron” (the initial undilated area of the ROI), and divided by the number of images in the (compressed) z-stack (excluding the “control image”). The final quantity obtained for each neuron was therefore a stack- (or “volume-”) averaged ratio of total stained area (adjacent the neuron) to the neuronal cross-sectional area. Approximately 25 “shadows” were analyzed per confocal stack (ie. approx. 100 neurons per animal). The program operator was able to avoid inadvertently capturing any PV+ somas, confounding tissue-artifacts, non-neuronal hypo/hyperintensities, and poorly binarized areas in the images by constant visual comparison with the unprocessed original confocal stacks during the analysis.

#### **4.3.8 - Statistics**

Statistical analyses were carried out using (the two-tailed) Student's t-test, or by one-way ANOVA with additional post-hoc tests. The Holm-Sidak method was generally used for all pairwise post-hoc

comparisons (SNK method was used for layer 4 2<sup>o</sup> branches Golgi-Cox analysis), whereas Dunnett's method was used when only post-hoc comparisons against the control group were required. For non-parametric data, or cases where assumptions of normality/homogeneity of variances were not met, the Mann–Whitney Rank Sum test, or the Kruskal-Wallis one-way ANOVA (with post-hoc comparisons against the control group by Dunn's method) were used. Significance ( $\alpha$ ) was set at  $p < 0.05$ .

## 4.4 – Results

### 4.4.1 – *Mice with EAE exhibit enhanced neuronal responses to tactile stimulation within S1 pre-symptomatically.*

S1 plays a critical role in processing “sensory-discriminative” aspects of both painful and non-painful touch. Within S1, the body-centric locations of external stimuli are encoded as a spatially organized “somatotopic map” comprised by distinct regions of cortical activation. The intensity (or perceived intensity) of an external stimulus is encoded as the magnitude (rate, extent, and duration of neuronal spiking activity, within an ensemble) of cortical activation in S1. Painful stimuli, which are generally perceived as being more intense, are associated with greater magnitudes of activation in S1 [45]. Allodynia, such as in EAE/MS with CNP, involves non-noxious stimuli being perceived as painful – and is thought to involve intense activation (hyperexcitability) in S1 and connected “pain-associated” brain regions [46-48]. Indeed, plasticity and enhanced activation in S1 has been shown to enhance activation in other “pain regions”, such as the anterior cingulate cortex, and to enhance chronic pain states. [7, 46]

To examine whether EAE involves changes in the functional (neuronal) activation of S1, we used FAI to measure responses in the forelimb (FL) and hindlimb (HL) cortex regions (S1FL/HL), evoked by a “non-noxious” vibrotactile (mechanical) stimulus. We first imaged naïve and CFA-only controls, along with EAE animals at a “pre-symptomatic” time-point (7-9 dpi.) - prior to any clinical signs of the disease, but when mechanical allodynia has been observed [12]. Vibrotactile-evoked FAI responses in S1HL were significantly more intense in the EAE group than in CFA-only controls, or

“naïve” animals (*one-way ANOVA*,  $*p=0.012$ ; *all pairwise post-hoc comparisons by Holm-Sidak method*) (**FIG. 4.1A,B**). The area of cortical activation elicited by this stimulus was also significantly larger in the EAE group compared to naïve animals or mice treated with CFA only (*one-way ANOVA*,  $*p=0.009$ ; *all pairwise post-hoc comparisons by Holm-Sidak method*). (**FIG. 4.1C**)

When the HL-evoked FAI signal was analyzed in the temporal domain, we found that the overall signal duration - the time between stimulus onset and signal-offset - was prolonged in the EAE group when compared to CFA-only or naïve animals. Specifically, the duration of the decay phase, or the time between signal-peak and signal-offset, was significantly prolonged, and accounted for most of the overall increase in signal duration (*one-way ANOVA*,  $*p=0.013$ ; *all pairwise post-hoc comparisons by Holm-Sidak method*) (**FIG. 4.1D**). As CFA-only mice and naïve mice did not differ in terms of evoked functional activation of S1, CFA-only mice were used as the control group in subsequent analyses.

#### **4.4.2 – Early EAE is associated with changes in the density of inhibitory and excitatory synaptic markers within S1.**

We next examined the possibility of a specific intracortical synaptic basis for the functional plasticity that we observed with FAI in S1 in EAE mice. To this end, we employed IHC on brain-tissues collected post-FAI from CFA-only and pre-symptomatic EAE mice, and examined the density of excitatory and inhibitory synaptic contacts in S1HL.

We found no significant difference in the number of parvalbumin-positive (PV+) inhibitory interneuron cell bodies in S1 from EAE or CFA control mice (*see FIG. 4.8A*). However, we did observe a significant reduction in perisomatic PV-immunoreactivity around putative pyramidal neurons residing in cortical layers 2/3 of S1 at the earliest time-point (*two-tailed t-test ‘pre’ vs. CFA*,  $*p=0.042$ ) (**FIG. 4.2A-C**). Hypo-intense regions or “shadows” in the dense PV-staining, targeted in this analysis, were visually confirmed to correspond with neuronal (mostly pyramidal) cell bodies using fluoronissl counterstaining. (**FIG. 4.2A’**)

The vesicular glutamate transporter VGLUT1 is commonly used as a presynaptic marker of excitatory synapses. VGLUT1 is expressed at both thalamocortical and corticocortical glutamatergic terminals throughout S1. In contrast to PV, we found a significant increase in VGLUT1 density in layers 2/3 and 4/5 of S1 in pre-symptomatic EAE animals, compared to CFA controls (*two-tailed t-tests*, L2/3: **\*p=0.041**, L4/5: **\*p=0.047**). (FIG. 4.2D-I)

#### **4.4.3 – Chronic treatment with the antidepressant PLZ normalizes vibrotactile-evoked FAI responses in S1 of mice with EAE at clinical-onset.**

Our next experiment characterized the effects of PLZ treatment on vibrotactile-evoked FAI responses in S1 of CFA/EAE mice at the clinical-onset of the disease, the time-point when behaviorally measured allodynia is most prominent in EAE mice [12]. CFA-only controls and mice with EAE were treated with either vehicle (VEH) or PLZ, beginning at 7 dpi. S1 responses to vibrotactile stimulation of the limbs were imaged on the day when a mouse first presented with clinical signs of the disease (clinical-onset/grade 1, flaccid paralyzed tail). As observed in pre-symptomatic animals, VEH-treated EAE mice exhibited significantly intensified HL-evoked S1 FAI responses at clinical-onset, compared to control mice treated with CFA alone. Chronic PLZ treatment in EAE animals normalized the intensity of HL-evoked responses to levels similar to (VEH-treated) CFA controls. PLZ-treated CFA animals did not significantly differ from VEH-treated CFA or PLZ-treated EAE animals (*one-way ANOVA*, **\*p<0.001**; *all post-hoc comparisons by Holm-Sidak method*). (FIG. 4.3A,B)

Similar to what we observed at the pre-symptomatic stage, the area of the HL-evoked S1 FAI response remained significantly expanded at clinical-onset in EAE mice treated with vehicle. This functional “map” expansion in S1 of EAE animals was normalized by PLZ treatment. PLZ treatment did not significantly affect HL-evoked response area in CFA animals (*one-way ANOVA*, **\*p=0.003**; *all-pairwise post-hoc comparisons by Holm-Sidak method*) (FIG. 4.3C). EAE animals at clinical-onset also exhibited increased HL-evoked FAI signal duration, which was mainly the result of a significantly prolonged decay phase. Treatment with PLZ normalized HL-evoked response/decay-durations in EAE

animals at clinical-onset, but did not alter response durations in CFA animals (*one-way ANOVA, \*p=0.012, all pairwise post-hoc comparisons by Holm-Sidak method*) (**FIG. 4.3D**). VEH-treated EAE mice also displayed significantly more intense FAI responses in S1FL to forelimb stimulation at clinical-onset. PLZ treatment in mice with EAE normalized the intensity of FL-evoked responses to CFA levels. Again, PLZ-treated CFA animals did not significantly differ from VEH-treated CFA mice or PLZ-treated EAE animals for FL parameters (*Kruskal-Wallis one-way ANOVA on ranks, \*p<0.001 post-hoc comparisons vs. CFA by Dunn's method*). (**FIG. 4.4**)

To determine whether measurable changes in functional inhibition might contribute to the altered patterns of activation observed in S1 of EAE animals [49-51], we also quantified the magnitude of the early/adjacent “surround-inhibitory/off-map” FAI signal. This signal component indicates reduced neuronal spiking and oxidative metabolism, and has been shown to be GABA-A receptor-mediated [52-54]. There was no significant difference in the magnitude of this negative signal component between CFA control mice treated with either VEH or PLZ, nor did we find any differences between VEH-treated CFA controls and VEH-treated EAE mice (*post-hoc comparisons not significant, p>0.05*). However, we found that the magnitude of this negative signal was significantly greater in PLZ-treated EAE mice compared to EAE mice treated with VEH (*one-way ANOVA, \*p=0.007, all pairwise post-hoc comparisons by Holm-Sidak method*). (**FIG. 4.3A,E**)

#### **4.4.4 – EAE is associated with morphological changes to excitatory neurons of cortical layers 2/3 and 4 of S1, which are prevented or reversed by PLZ treatment.**

Altered functional responses in the neocortex are often a consequence of structural plasticity and modified connectivity amongst excitatory pyramidal/principal neurons [50]. Moreover, neuropathic pain states are associated with the rapid remodeling of dendritic spines, where the excitatory post-synaptic density is localized [55], in excitatory neurons of S1. We therefore investigated whether we could detect alterations in the density of dendritic spines along the processes of spiny excitatory (principal and pyramidal) neurons in cortical layer 4 and layers 2/3 of S1. Layer 2/3 and layer 4 spiny (excitatory)

neurons were found to exhibit greater overall spine densities along the examined dendrites from the EAE-VEH group (*Kruskal-Wallis one-way ANOVA on ranks, layers 2/3: \*p=0.032, layer 4: \*p<0.001, all post-hoc comparisons vs. CFA by Dunn's method*). This effect was normalized to CFA levels in the EAE-PLZ group (*post-hoc comparison between EAE-PLZ and CFA not significant, p>0.05*). (**FIG. 4.5A,B,C**)

We next examined spine-densities in the same set of neurons, grouping dendritic segments according to their relative position within their associated neuronal arbor. We classified dendritic segments as either apical or basilar branches, and as primary, secondary and tertiary branches. We then analyzed all possible permutations of these categories (primary apical, primary basilar, secondary apical, etc.). This “grouped” analysis allowed us to determine that the increased spine density we observed at the neurites of layer 2/3 neurons from the EAE-VEH group was almost completely localized to the tertiary (i.e. the most distal dendrites, in this classification) basilar branches. PLZ treatment prevented or reversed these changes, as spine-densities at tertiary-basilar neurites were normalized to CFA levels (*Kruskal-Wallis one-way ANOVA on ranks, \*p=0.007, all post-hoc comparisons vs. CFA by Dunn's method*) (**FIG. 4.5B**). The distribution of layer 4-neuronal dendrites exhibiting elevated spine densities (i.e. from the EAE-VEH group) was less-specifically localized within the arbor. These increases did not occur exclusively in either the apical or basilar tufts, or in the most proximal or distal dendrites. Rather, layer 4-neuronal dendrites from the EAE-VEH group exhibited a significant increase in spine density specifically when considering second-order branches. Again, we found that PLZ treatment normalized these densities to CFA levels (*one way ANOVA, \*p<0.001, all pairwise post-hoc comparisons by SNK method*). (**FIG. 4.5C**)

#### **4.4.5 – Chronic PLZ treatment partially normalizes pre-synaptic excitatory synaptic densities in S1 of mice with established EAE.**

To investigate the long-term consequences of EAE on cortical plasticity and how PLZ can affect these processes, we assessed the effects of chronic PLZ treatment on cortical pre-synaptic alterations in

tissue taken at the fixed endpoint of 21 dpi. This is a time past the 'clinical-onset' phase, when the disease has been fully established in the majority of animals. At this later stage of the disease, perisomatic PV-staining within S1 was not significantly different between CFA controls and VEH- or PLZ- treated EAE animals (*one-way ANOVA not significant,  $p=0.661$* ), (**FIG. 4.6A,B**). In contrast, VGLUT1 staining in S1 remained significantly denser in the VEH treated EAE animals at 21 dpi. compared to CFA controls. This elevated VGLUT1 density was partially diminished in the PLZ treated EAE group, but not completely normalized to CFA levels (*one-way ANOVA, layers 2/3:  $*p=0.014$ , layers 4/5:  $*p=0.007$ , all pairwise post-hoc comparisons by Holm-Sidak method*). (**FIG. 4.6C,D**)

#### **4.4.6 – EAE is associated with a progressive loss of peri-neuronal nets and microgliosis in S1.**

PV+ interneurons are often surrounded by organized components of the extracellular matrix (ECMCs) known as peri-neuronal nets (PNNs) [56]. Intact PNNs are essential to maintaining the fast-inhibitory activity of PV+-interneurons [57]. They are also known to be important regulators of plasticity [58], and may be disrupted in disease states [59]. We next assessed if PNNs were disrupted in the EAE somatosensory cortex by staining with *Wisteria floribunda* agglutinin (WFA) lectin [60]. The number of intact PNNs was significantly diminished in S1 of EAE animals beginning at clinical-onset (*one-way ANOVA,  $*p=0.008$ , post-hoc comparisons vs. CFA by Dunnett's Method*) (**FIG. 4.7C,D**). This reduction in PNN numbers was persistent, and was also observed in S1 of EAE animals at the later 21 dpi. time-point. Chronic PLZ treatment from 7 dpi. did not restore or prevent the decline of PNN numbers in EAE animals assessed at the 21 dpi. time-point (*one-way ANOVA,  $*p=0.021$ , post-hoc comparisons vs. CFA by Dunnett's method*). (**FIG. 4.8A,B**)

We next sought to identify the potential disease-related mechanism that leads to PNN loss and concurrent synaptic remodeling in EAE. As inflammation and immune-mediated mechanisms have been implicated in synaptic plasticity in EAE [18],[61, 62], and in the loss of PNNs in MS [63], we examined the state of neuroinflammation in S1. We first performed immunostaining for CD3 or CD45 expressing CNS-infiltrating leukocytes and T-cells. CD3+ T-cells and CD45+ leukocytes were not

present in S1 at either the pre-symptomatic or clinical-onset time-points (**FIG. 4.9**). We did, however, observe significantly increased numbers of Iba-1+ microglia at both of these early disease time-points (*one-way ANOVA, \*p=0.012, all post-hoc comparisons vs. CFA by Dunnett's method*) (**FIG. 4.7E,F**). This increase in cortical Iba-1+ microglia was also observed in tissues from late stage EAE animals that were treated with VEH at 21 dpi. Notably, chronic PLZ treatment normalized Iba-1+ cell counts in S1 of EAE animals at 21 dpi. (*one-way ANOVA, \*p=0.009, all post-hoc comparisons vs. CFA by Dunnett's method*). (**FIG. 4.8C,D**)

#### 4.5 – Discussion

This study is the first investigation of functional neocortical plasticity along with persistent neuroanatomical and synaptic changes occurring in S1 in the very early stages of the C57/BL6 MOG<sub>35-55</sub> EAE model. Specifically, we find *in vivo* evidence in early EAE of enhanced intensity and spread of the neuronal activation within S1 that is evoked by vibrotactile stimulation of the fore- or hindlimb. Interestingly, a delay exists between the “pre-symptomatic” and “clinical-onset” time-points in the sensitization of responses to forelimb stimulation. This delay mirrors the caudal-to-rostral progression of spinal inflammation and paralysis in EAE [64], and suggests that ascending sensitization within the SC-DH [10] may precede (or initiate) sensitization of supraspinal sites, as has been observed in other models of neuropathic pain and allodynia [8, 46, 47].

In addition to the observed enhancement of functional responses, we find histological evidence of an increased density of excitatory pre-synaptic (VGLUT1+) terminals and post-synaptic contacts (dendritic spines), in cortical layers 2/3 and 4/5 of S1 in early EAE. These changes are indicative of pro-excitatory remodeling of the major feed-forward circuit through S1 [40], in which layer 4 principal neurons receive thalamocortical inputs [65] and project vertically to pyramidal neurons of layer 2/3 - primarily to the distal/basilar branches. Abundant transcolumnar connections in layer 2/3 mediate the horizontal spread of activation through S1, defining the areal extent of a “functional map” [50, 66].

Synaptic remodeling along this pathway therefore likely contributes to the intensification and expansion of S1 functional responses in early EAE [67]. These alterations occur prior to the onset of major paresis, and temporally coincide with the appearance of prominent pain behaviors in the disease. Moreover, similar functional and synaptic alterations occurring in S1 have been shown to play a causal role in other neuropathic pain models [7, 8].

We also find evidence in EAE of an early, although transient, disruption of basket-forming PV+ inhibitory interneurons in S1. The central role of PV-mediated fast-spiking inhibition in limiting the extent to which large-scale plastic changes may occur in the neocortex, during both adulthood and the perinatal critical period, is well documented in the literature [68, 69]. Even a transient loss of PV-mediated perisomatic inhibition in early EAE might therefore have profound and lasting consequences, leading to a dysregulated E-I balance and maladaptive cortical plasticity [70]. Moreover, we find that PV+ interneurons are affected in EAE by an early-appearing and persistent loss of their associated PNN structures. PNNs serve multiple supportive and protective functions for PV+ neurons, including sequestering cations (i.e.  $\text{Ca}^{2+}$ ) to support fast-spiking activity, limiting synaptic modifications and alterations of connectivity, and protecting the neurons against chemical insults such as reactive-oxygen species (ROS) [56]. The loss of PNNs may therefore be a key precipitating factor in the aberrant structural and synaptic plasticity we find in both the inhibitory and excitatory circuitry of S1 in early EAE. Loss of PNNs may additionally contribute to the unique susceptibility of PV+-interneurons to degeneration in the later stages of EAE/MS, which has been reported by several groups [19, 71, 72]. Collectively with our previous findings [10, 22], the multiple functional and synaptic changes in S1 evidenced in this study provide support for the hypothesis that EAE involves a profound, pro-excitatory, shift in the E-I balance of the entire somatosensory CNS, beginning very early in the disease-course. This disrupted E-I balance promotes functional and structural plasticity within S1 [24, 68], leading to amplified cortical responses to peripheral stimuli, and likely contributing to pain behaviors (i.e. allodynia) in the disease [7, 25, 46].

While we are the first group to find an increase in both pre- and post-synaptic glutamatergic markers and a concurrent reduction in perisomatic PV+ immunoreactivity in S1 in early EAE, several other groups have found similar or complementary changes in the EAE/MS brain [19, 71, 72]. A report by Yang et al. (2014) demonstrated enhanced turnover of dendritic spines and axonal boutons in layer 5 pyramidal neurons within S1 in early MOG<sub>35-55</sub> EAE [17]. As mentioned, loss of PV+ interneurons in EAE has also been demonstrated by several groups in multiple brain regions, including primary motor cortex [19, 61, 73]. A single report by Tambalo et al. (2015) also suggested, based on *fMRI*-CBV data, that the later stages (30-60 dpi.) of the dark agouti rat model of EAE involve functional expansion of the vibromechanically-evoked S1 forelimb representation [18]. This study also found dendritic spine loss in layer 2/3 and 4 neurons of S1. While some of the findings and interpretations offered in Tambalo et al. [18] appear to contrast with our observations, it is worth noting that there are significant methodological differences between the studies. Furthermore, inferences about neural activation based strictly on the *fMRI*-CBV signal may potentially be confounded by hemodynamic changes in the disease state. Nevertheless, much agreement exists between these various reports. Indeed, a substantial body of evidence is emerging that early synaptopathy in EAE and MS brains leads progressively to neuronal hyperexcitability, excitotoxicity, and eventual dysfunction and degeneration [19, 62, 74]. In the majority of these studies, inflammation and circulating pro-inflammatory cytokines have been proposed as the proximal causative factors.

In our examination of the role that inflammation plays in initiating or promoting cortical alterations in EAE, we first examined tissues for infiltrating CD3+ T-cells and CD45+ leukocytes. As noted, brain-penetrating T-cells were absent from S1 at these early stages in our model. However, intracortical Iba-1-reactive microglia were found to be significantly more abundant in EAE compared to CFA controls, both pre-symptomatically (7 dpi.), and in the established disease (21 dpi.). Microglia are capable of modifying neuronal connectivity through multiple mechanisms, including the secretion of diffusible factors such as matrix metalloproteases (i.e. MMP-2, MMP-9), which digest ECMs such as PNNs, and are known to be elevated in the brain in EAE/MS [75]. Reactive microglia also secrete

cytokines, such as sTNF $\alpha$  and IL-1 $\beta$  [76, 77] which have been shown to promote synaptic plasticity and neuronal hyperexcitability in EAE [17]. Microglia are furthermore responsive to many activity-dependent signals, such as extracellular glutamate and ATP [78]. The pro-excitatory state found in early EAE cortex therefore likely acts to promote microglial reactivity in a feed-forward manner.

In addition to characterizing cortical changes in early EAE, we also demonstrated novel cortical effects of the antinociceptive/antiallodynic treatment PLZ in the disease. We previously demonstrated that chronic treatment with PLZ from 7 dpi., when early cortical and behavioral alterations are already established, fully normalized mechanical withdrawal thresholds in EAE mice at clinical-onset (*see Chapter 3*). PLZ treatment does not induce a generalized analgesic or sedative effect, as it produced no significant changes in basal mechanical sensitivity or motor function in control/naive animals in the previous experiments (*see Chapter 2 / Chapter 3*). We also previously demonstrated that chronic PLZ treatment reduced vibromechanically-evoked c-Fos in the ipsilateral dorsal horn in EAE mice at onset (*see Chapter 3*). Furthermore, we demonstrated that bath-applied PLZ inhibited glutamate-evoked intracellular calcium responses in dorsal horn neurons within *ex vivo* lumbar spinal cord slices taken from naïve (*see Chapter 2*), CFA, and EAE animals (*see Chapter 3*). Significantly, we also now demonstrated that PLZ treatment normalizes S1 functional responses in EAE at onset, but did not affect evoked S1 functional responses in control (CFA) animals. Furthermore, PLZ treatment attenuated S1 structural and synaptic abnormalities – normalizing dendritic spine densities at clinical-onset, and attenuating VGLUT1+ immunoreactivity in the established disease (21 dpi.). Conversely, we previously found (*see Chapter 3*) that PLZ treatment from 7 dpi. did not attenuate the augmented VGLUT1+ immunoreactivity in the DH in EAE. This difference in effect may suggest that ascending drive from the DH – which is likely inhibited by PLZ – partially or primarily drives downstream S1 presynaptic plasticity; whereas presynaptic plasticity in the DH might be fully established earlier than the alterations in S1, and may result from peripheral drive which may not (yet, or ever) be affected by PLZ-treatment started at 7 dpi. Indeed, in S1, anti-VGLUT1 stains both thalamocortical (TC) afferent terminals and the axon terminals of excitatory intracortical interneurons - although VGLUT2 is more

conventionally associated with TC terminals, VGLUT1 has been shown to co-express in TC terminals innervating layer 4 of S1, particularly while they are undergoing plasticity or in post-natal development [79-81]. In the DH, however, anti-VGLUT1 mainly stains low-threshold peripheral afferent terminals [82, 83].

PLZ restores CNS levels of GABA in EAE through the inhibition of GABA-transaminase (GABA-T) by its active metabolite PEH, and restores monoamine levels by the irreversible inhibition of MAO-A and B [23]. PLZ has previously been shown to enhance functional intracortical GABA release [84-86]. The enhancement of the GABA-AR-mediated [52, 53] surround-inhibitory S1 FAI signal we find in PLZ-treated EAE mice supports this proposed mechanism of action, and suggest that the effects of PLZ-treatment in S1 may not merely be a downstream expression of PLZ's inhibitory effects in the DH. Musgrave/Benson (2011, 2013) [23, 87] also demonstrated that CNS levels of the monoamine neurotransmitters (ie. 5-HT, NA, and DA), which are reduced in the brain in EAE [22], are normalized by PLZ treatment. Thus, additional cortical inhibition in the PLZ-treated animals may result from monoaminergic effects. In this manner PLZ may act to modulate the excitability of PV+-interneurons, which are known to express 5-HT<sub>1</sub> and -2 receptors, and  $\alpha$ 2 and  $\beta$ -adrenoceptors [88, 89]. Activation of cortical NA receptors is also associated with enhanced GABA release [89], and enhanced somatic inhibition of excitatory neurons in layer 2/3 neocortex [90]. The neocortex also contains a large and diverse population of 5-HT<sub>3R</sub>-expressing inhibitory interneurons [91]. Another mechanism through which PLZ might normalize the cortical E-I balance is by decreasing the excitatory output of cortical pyramidal neurons. Cortical pyramidal neurons express a variety of monoaminergic GPCRs, including  $\alpha$ 1Rs and 5-HT<sub>1</sub>Rs, and the actions of 5-HT and NA at these sites are generally inhibitory [92]. Other groups have suggested that PLZ may also attenuate excessive cortical glutamate release by affecting glutamate-glutamine (neuron-astrocyte) shuttling and interconversion [93, 94].

While PLZ treatment in EAE did not rescue disrupted PNNs, it significantly reduced Iba-1+ cells within S1 – again, contrary to the effect in the DH described in Chapter 2. Just as excitatory signaling can promote microglial reactivity, inhibitory signaling through G protein-coupled receptors, such as

GABA-BRs [95] and adrenergic receptors [96], can reduce microglial motility and reactivity.

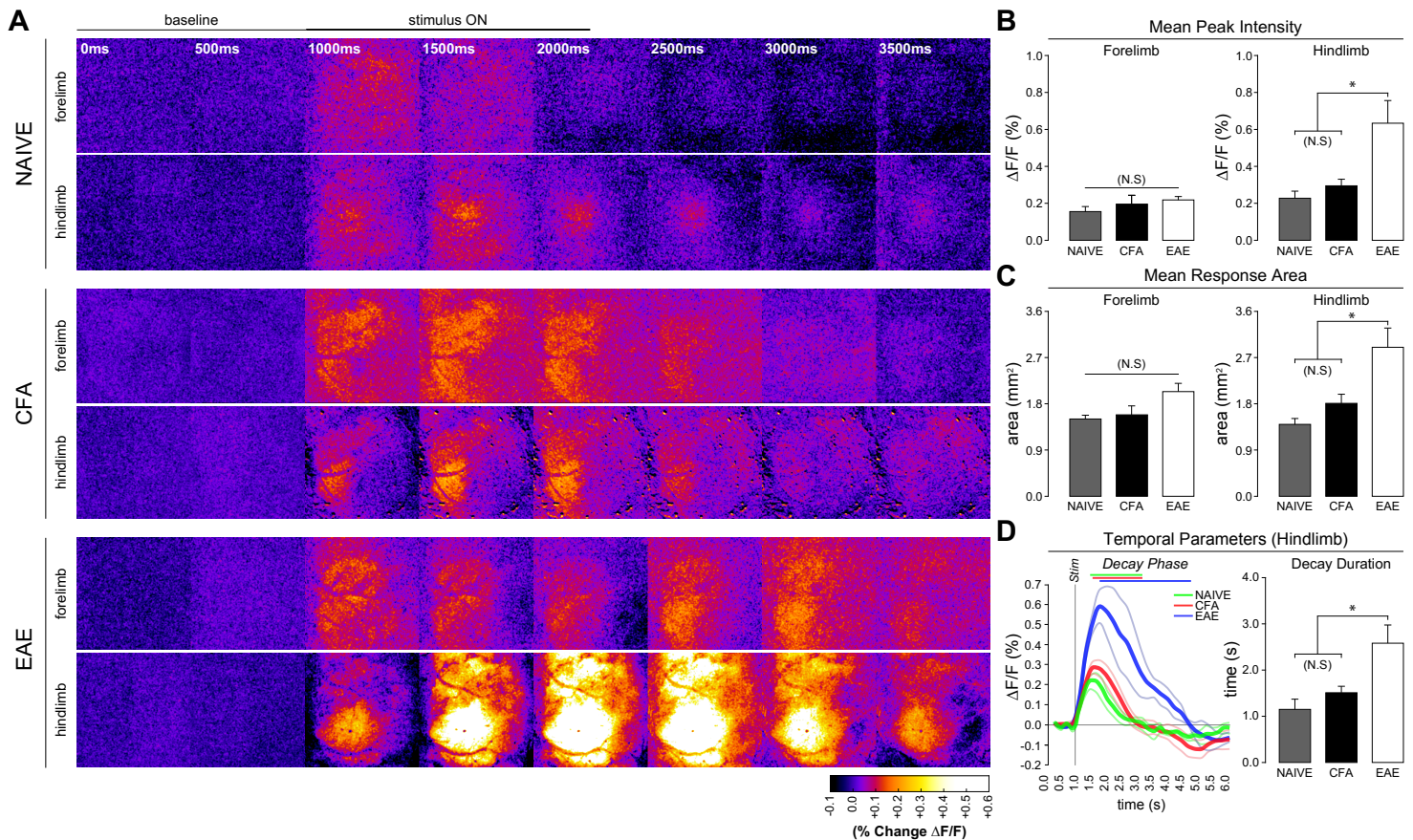
Enhancement of GABAergic/monoaminergic neurotransmission and the concomitant reduction of excitatory signaling may therefore be the means by which PLZ treatment reduces cortical microgliosis in EAE. Why this effect is not observed in the DH is unclear, but may again have to do with timing effects, or local differences in the cell-specific impacts of PLZ. Nevertheless, this synergistic neuro-glia action in the cortex likely aids in the restoration of normal constraints on plasticity within the somatosensory CNS, and contributes to the normalization of pain behaviors in EAE.

Although the current experiments did not involve direct manipulation of the sensory cortex in a way that might conclusively establish an immediate causal link between altered S1 structure/function and altered pain behaviors in EAE, the complete dissociation of responses to PLZ treatment in non-disease controls (ie. the lack of a behavioral response to PLZ in CFA animals, described in Chapter 3; and the lack of effect of PLZ in CFA animals in S1) and EAE animals, supports the hypothesis that maladaptive cortical plasticity within S1 directly contributes to pain in the disease.

#### **4.5.1 - Conclusions**

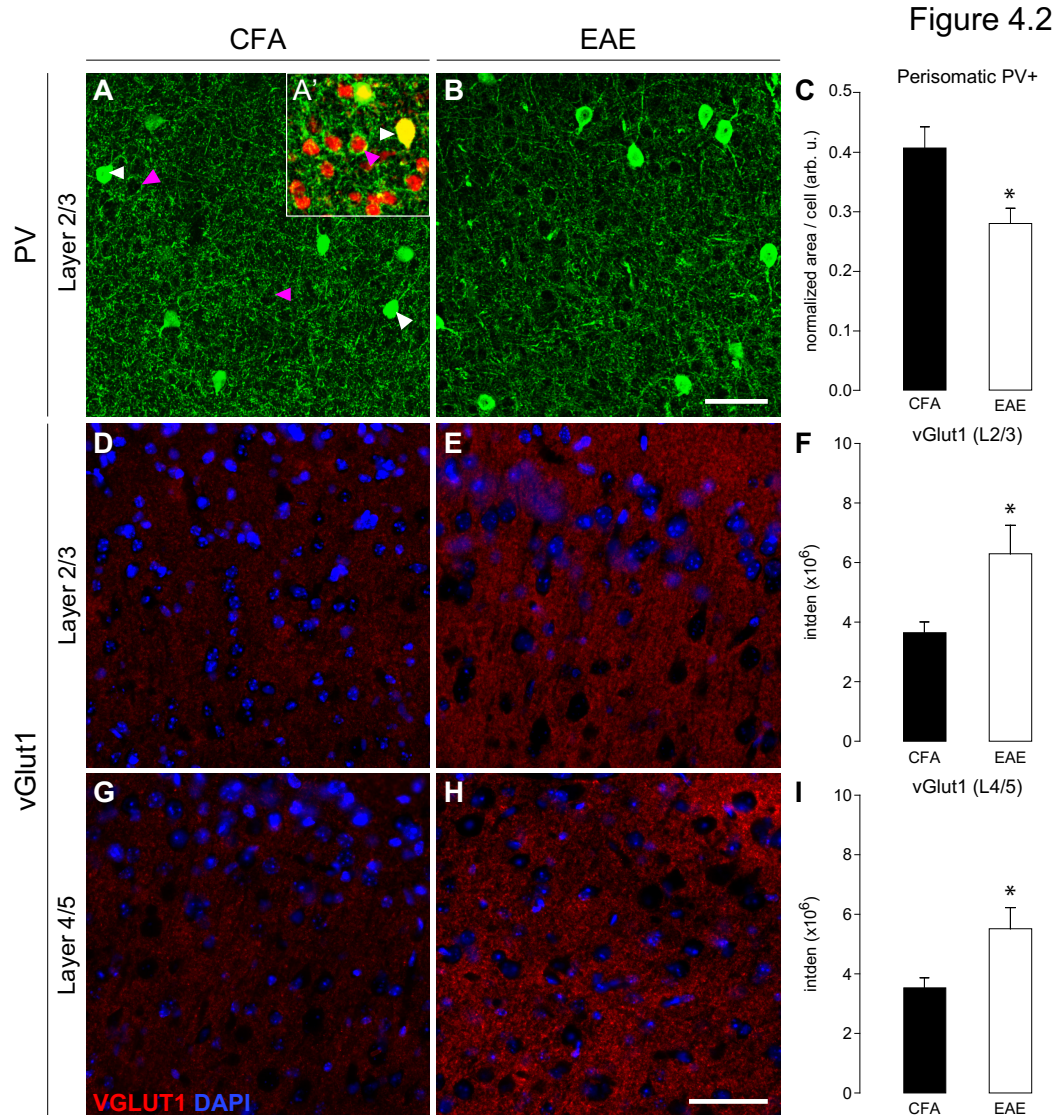
The evidence presented here supports a link between altered central E-I balance, maladaptive functional and structural plasticity in S1, and increased pain behaviors in early EAE. The PLZ experiments demonstrate, in principle, that a treatment which acts to restore lost CNS inhibitory function can normalize pain behaviors and S1 synaptic structure and function in EAE. By focusing our investigation on the early stages of EAE - when pain is first becoming established, and when initiating pathogenic changes occur - we hope to highlight the possibility that early therapeutic intervention, perhaps with a “combined-action” agent similar to PLZ, may be invaluable for preventing the development of CNP states in MS patients.

Figure 4.1



**Figure 4.1** *In vivo* FA imaging of vibrotactile-evoked responses in S1 at the pre-symptomatic stage of EAE.

(A) Balanced-contrast pseudocoloured ( $\% \Delta F/F$ ) montages of representative hindlimb and forelimb responses in S1 of naïve, CFA and pre-symptomatic EAE (7-9 dpi) animals. (B) Group-mean ( $\pm$ S.E.) signal intensities at peak FA response, calculated from the “cortical map” area as a percent change in fluorescence vs. baseline ( $\% \Delta F/F$ ). Pre-symptomatic EAE animals ( $n=4$ ) exhibited significantly intensified responses to vibrotactile stimulation of the hindlimb, but not the forelimb, compared to naïve ( $n=3$ ) and CFA controls ( $n=5$ ). Naïve and CFA responses did not significantly differ from each other (*one-way ANOVA*,  $*p=0.012$ ; *all-pairwise post-hoc comparisons by Holm-Sidak method*). (C) Group-mean ( $\pm$ S.E.) areas of the FAI response, calculated from (grey-value averaged) z-projections of the response phase; and defined as the region exhibiting a  $\geq 50\%$ -of-maximal increase in fluorescence vs. baseline ( $\% \Delta F/F$ ). Pre-symptomatic EAE animals exhibited significantly expanded hindlimb, but not forelimb, responses compared to naïve and CFA-controls. Naïve and CFA responses did not significantly differ from each other (*one-way ANOVA*,  $*p=0.009$ ; *all-pairwise post-hoc comparisons by Holm-Sidak method*). (D) Grand-average FA signal traces (thick traces;  $\pm$ S.E. thin traces) of hindlimb responses in naïve (green trace), CFA (red trace), and pre-symptomatic EAE (blue trace) animals. Grey vertical bar shows time of stimulus onset. Overlying bars indicate signal decay phase (time from peak signal intensity to x-axis intercept). At right, group mean ( $\pm$ S.E.) decay phase durations as bar plot. Pre-symptomatic EAE animals exhibited significantly prolonged FAI decay phase durations vs. naïve and CFA A animals. Naïve and CFA responses did not differ significantly from each other (*one-way ANOVA*,  $*p=0.013$ ; *all-pairwise post-hoc comparisons by Holm-Sidak method*)





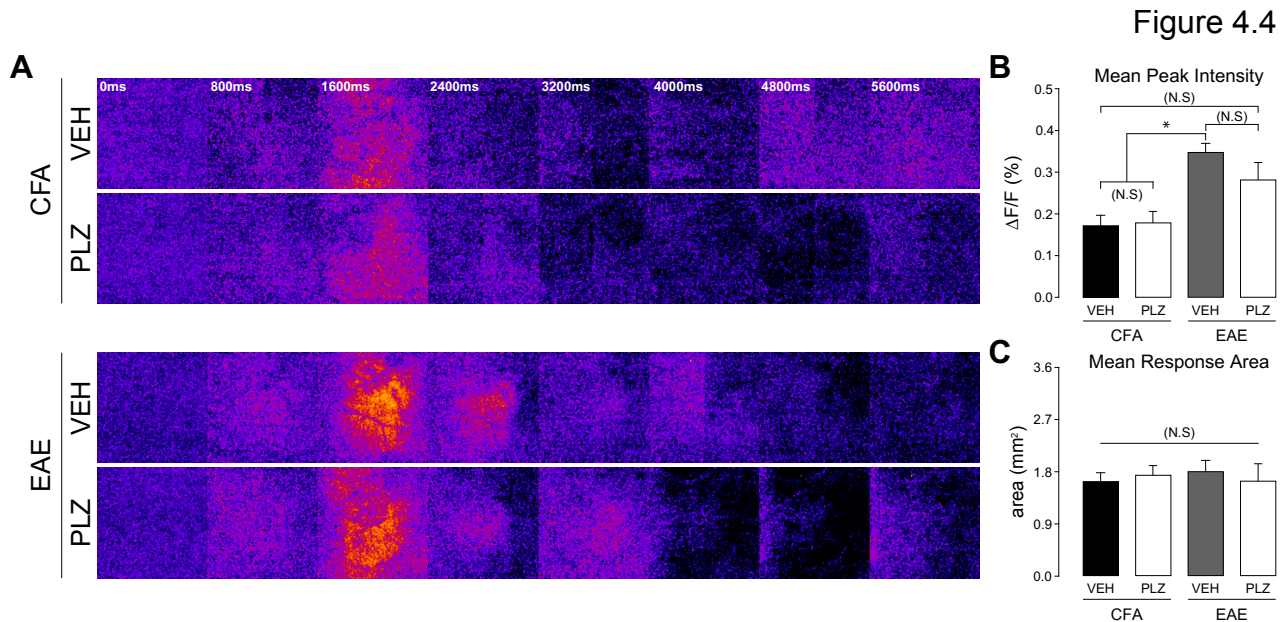


**Figure 4.4** *In vivo* FAI of forelimb vibrotactile-evoked responses in S1 of EAE, and PLZ-treated EAE animals at clinical onset.

**(A)** Balanced-contrast pseudocoloured montages of representative S1 hindlimb responses from VEH/PLZ-treated CFA/EAE animals at clinical-onset. **(B)** Group-mean ( $\pm$ S.E.) forelimb intensities at peak FA response, calculated from the “cortical map” area as a percent change in fluorescence vs. baseline ( $\% \Delta F/F$ ). VEH-treated EAE animals at clinical-onset ( $n=7$ ) exhibited significantly intensified responses to vibrotactile stimulation of the forelimb, compared to CFA controls ( $n=8$ ). PLZ-treated EAE ( $n=9$ ) and PLZ-treated CFA ( $n=4$ ) animals did not significantly differ from CFA (*Kruskall-Wallis one-way ANOVA on ranks*,  $*p<0.001$ ; all post-hoc comparisons vs. CFA-VEH controls by *Dunn’s method*). **(C)** Group-mean ( $\pm$ S.E.) forelimb FA response-areas. EAE-VEH animals at onset exhibited significant expansion of hindlimb responses compared to CFA-VEH controls, CFA-PLZ, and EAE-PLZ animals. CFA-VEH, CFA-PLZ, and EAE-PLZ groups did not significantly differ (*Kruskall-Wallis one-way ANOVA on ranks* not significant,  $p=0.912$ ).

Figure 4.5

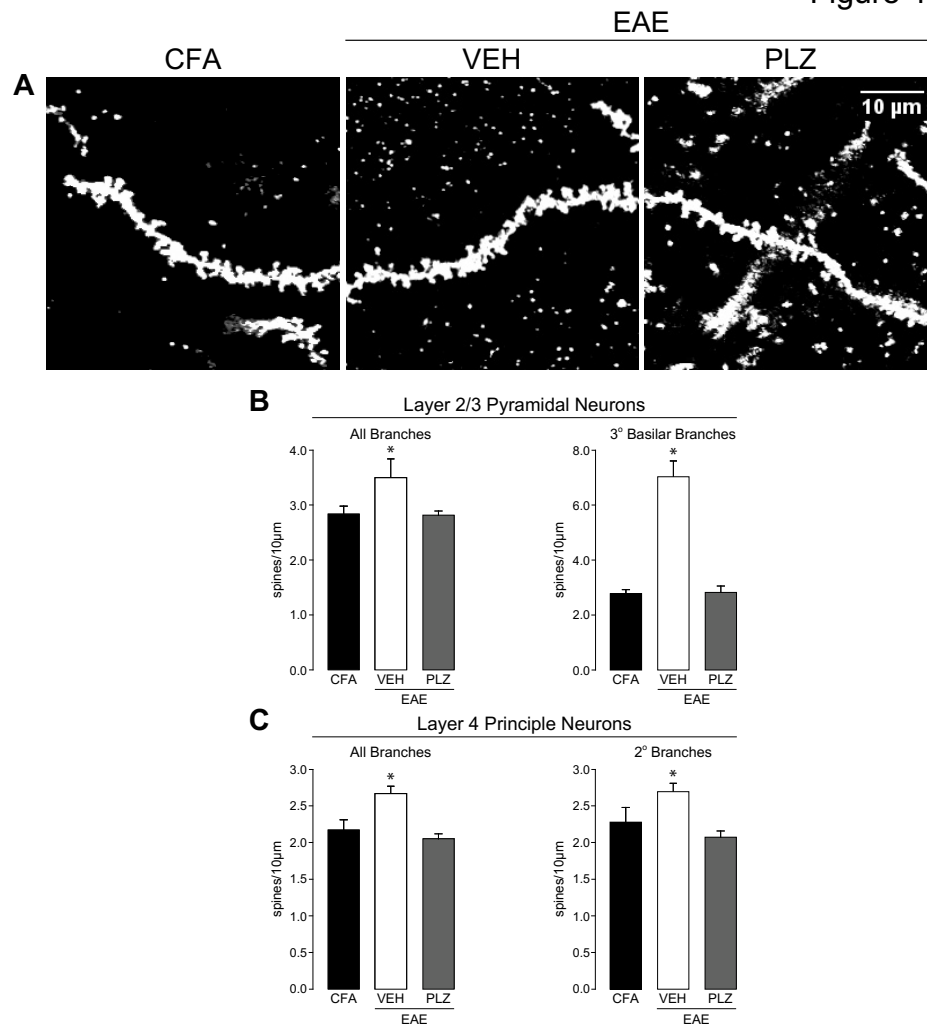


**Figure 4.5** Morphological changes in spiny excitatory neurons of S1 in EAE, and PLZ-treated EAE, at clinical-onset.

(A) Representative maximum z-projected images showing appearance and density of spines on dendritic segments from spiny excitatory neurons in S1. Spines were visualized by reflectance-mode (488nm) laser-scanning confocal microscopy on Golgi-Cox stained brains from VEH-treated CFA (CFA), VEH-treated EAE (VEH), and PLZ-treated EAE (PLZ) animals at clinical-onset. (B) Mean ( $\pm$ S.E.) dendritic-spine densities assessed from the branches of spiny neurons in layers 2/3 of S1 from CFA-VEH ( $n=42$  dendritic segments, 4 animals), EAE-VEH ( $n=66$  dendritic segments, 8 animals), and EAE-PLZ mice ( $n=78$  dendritic segments, 9 animals). Dendritic segments from EAE-VEH animals exhibited significantly increased spine-densities compared to segments from CFA-VEH mice. This increase was localized almost exclusively to the tertiary basilar branches (CFA-VEH  $n=12$ , EAE-VEH  $n=13$ , EAE-PLZ  $n=14$  dendritic segments). Daily treatment with PLZ from 7 dpi prevented or reversed this increase - mean spine-densities along segments from EAE-PLZ animals did not significantly differ from CFA controls (*Kruskal-Wallis one-way ANOVA on ranks*; “all-branches”  $*p=0.032$ ; tertiary-basilar-branches  $*p=0.007$ , all post-hoc comparisons vs. CFA controls by *Dunn’s method*). (C) Mean ( $\pm$ S.E.) dendritic-spine densities assessed from the branches of spiny neurons in layer 4 of S1 from CFA-VEH ( $n=36$  dendritic segments, 4 animals), EAE-VEH ( $n=58$  dendritic segments, 8 animals), and EAE-PLZ mice ( $n=83$  dendritic segments, 10 animals). Dendritic segments from EAE-VEH animals exhibited significantly increased spine-densities compared to segments from CFA-VEH mice. This increase was also specifically significant for second-order branches (CFA-VEH  $n=23$ , EAE-VEH  $n=43$ , EAE-PLZ  $n=54$  dendritic segments). Daily treatment with PLZ prevented or reversed this increase - mean spine-densities along segments from EAE-PLZ animals did not significantly differ from CFA-controls, but were significantly reduced vs. the EAE-VEH group (“all-branches” analyzed by *Kruskal-Wallis one-way ANOVA on ranks*,  $*p<0.001$ ; post-hoc comparisons vs. CFA controls by *Dunn’s method*. Secondary-branches analyzed by *one-way ANOVA*,  $*p<0.001$ , all-pairwise post-hoc comparisons by *SNK test*).

Figure 4.6

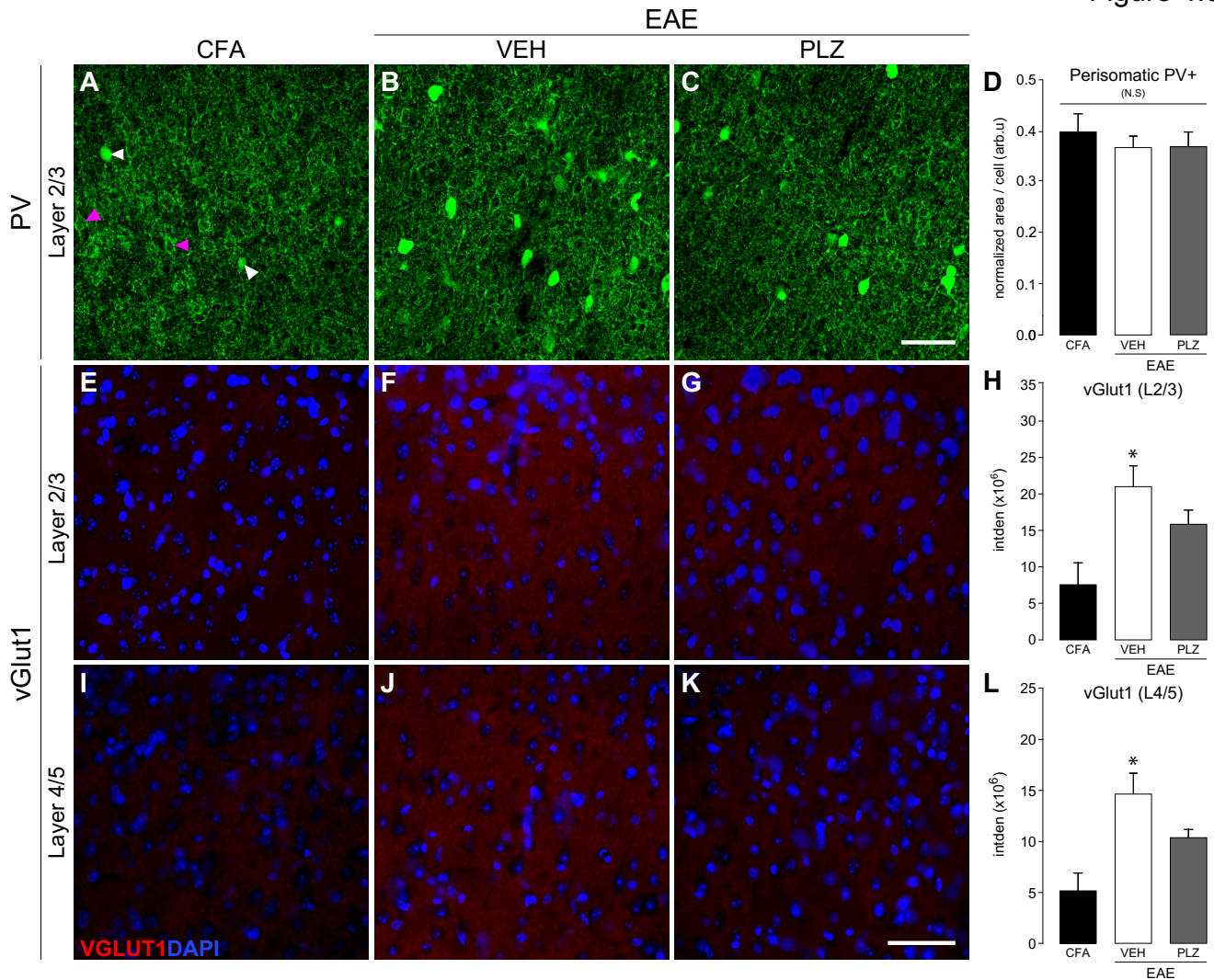


**Figure 4.6** Perisomatic PV+ and VGLUT1+ reactivity and the effects of PLZ treatment in established EAE.

(A-C) Representative confocal z-projections of PV+ somas and terminals (green) in layers 2/3 of S1, in control (CFA), VEH-treated EAE (21 dpi., VEH), and PLZ-treated EAE (21 dpi., PLZ) animals (treated from 7 dpi.). White arrowheads indicate PV+ somas, magenta arrowheads indicate putative pyramidal-neuron “shadows” targeted for quantification. Scale bar in C = 50 $\mu$ m applies in A-C. (D) Group-mean ( $\pm$ S.E.) normalized density values corresponding to perisomatic PV+ staining surrounding layer 2/3 neurons in S1. Control (CFA) (n=8), VEH-treated EAE (n=4), and PLZ-treated EAE (n=4) animals did not differ from each other at this time-point. (*one-way ANOVA not significant, p=0.661*). (E-G) Representative fluorescence photomicrographs of VGLUT1+ staining (red) in layers 2/3 of S1; in control (CFA), VEH-treated EAE (21 dpi, VEH), and PLZ-treated EAE (21 dpi, PLZ) animals (treated from 7 dpi). DAPI (cell-nuclei) counter-stain is shown in blue. Scale bar in K = 50 $\mu$ m applies in E-K. (H) Group-mean ( $\pm$ S.E.) integrated densities of VGLUT1+ stained CFA (n=5), EAE-VEH (n=5), and EAE-PLZ (n=4) animals. VEH-treated EAE animals retained strongly increased VGLUT1+ density in layer 2/3 S1 vs. CFA controls. PLZ treatment from 7 dpi. significantly reduced VGLUT1+ density in EAE animals, but did not normalize to CFA-levels (*one-way ANOVA, \*p=0.014, all-pairwise post-hoc comparisons performed by Holm-Sidak method*). (I-K) Representative fluorescence photomicrographs of VGLUT1+ staining (red) in layers 4/5 of S1; in control (CFA), VEH-treated EAE (21 dpi., VEH), and PLZ-treated EAE (21 dpi., PLZ) animals (treated from 7 dpi.). DAPI (cell-nuclei) counter-stain is shown in blue. (L) Group-mean ( $\pm$ S.E.) integrated densities of VGLUT1+ stained CFA (n=5), EAE-VEH (n=5), and EAE-PLZ (n=4) animals. VEH-treated EAE animals retained strongly increased VGLUT1+ density in layers 4/5 of S1 vs. CFA controls. PLZ treatment from 7 dpi. significantly reduced VGLUT1+ density in EAE animals, but did not normalize to CFA-levels (*one-way ANOVA, \*p=0.007, all-pairwise post-hoc comparisons performed by Holm-Sidak method*).

Figure 4.7

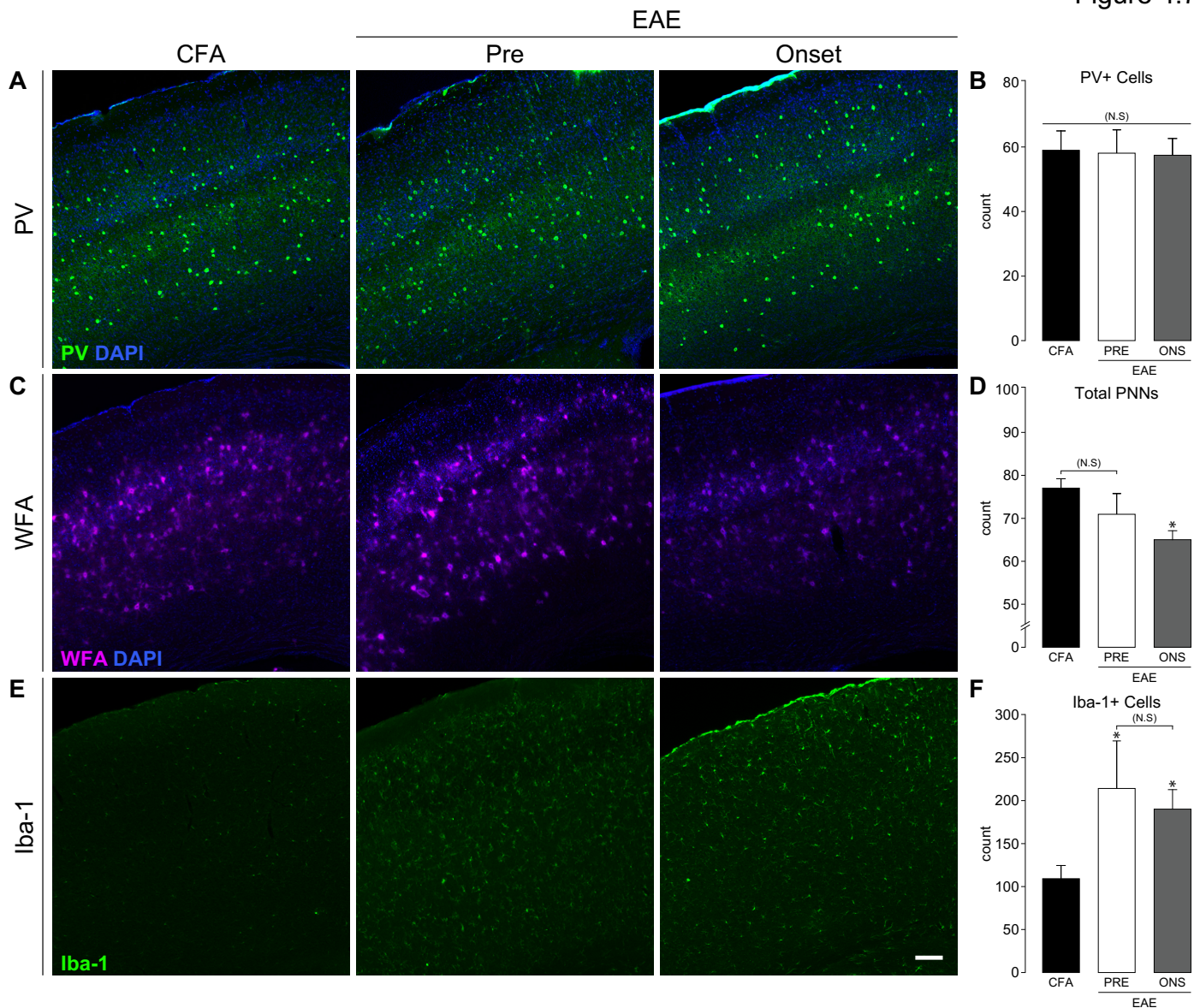


**Figure 4.7** S1 IHC in pre-symptomatic and clinical-onset EAE: PV+ cell counts, PNN counts, and Iba-1+ microglia counts.

(A) Representative fluorescence photomicrographs of PV+ staining (low-mag) in S1 from control (CFA) and EAE animals at the pre-symptomatic stage (7-9 dpi. PRE) or clinical-onset (ONS). Scale bar in E = 100 $\mu$ m applies throughout. (B) Group-mean ( $\pm$ S.E.) total PV+ cell counts from S1HL of CFA (n=8), PRE (n=4), and ONS (n=4) EAE animals. No significant differences were observed between groups (*one-way ANOVA N.S.*) (C) Representative fluorescence photomicrographs of WFA+ staining (PNNs) in S1 from control (CFA) and EAE animals at the pre-symptomatic stage (7-9 dpi. PRE) or clinical-onset (ONS). (D) Group-mean ( $\pm$ S.E.) total PNN counts from S1HL of CFA (n=11), PRE (n=4), and ONS (n=8) EAE animals. EAE animals exhibited significantly reduced PNN-counts versus CFA-controls at clinical-onset (*one-way ANOVA, \*p=0.007, post-hoc comparisons vs. CFA-controls by Dunnett's Method*). (E) Representative fluorescence photomicrographs of Iba-1+ staining (PNNs) in S1 from control (CFA) and EAE animals at the pre-symptomatic stage (7-9 dpi. PRE) or clinical-onset (ONS). (F) Group-mean ( $\pm$ S.E.) total Iba-1+ counts from S1HL of CFA (n=13), PRE (n=4), and ONS (n=8) EAE animals. EAE animals exhibited significantly increased numbers of Iba-1+ cells (microglial activation) in S1HL versus CFA-controls at all time-points (*one-way ANOVA, \*p=0.012, post-hoc comparisons vs. CFA-controls by Dunnett's Method*).

Figure 4.8

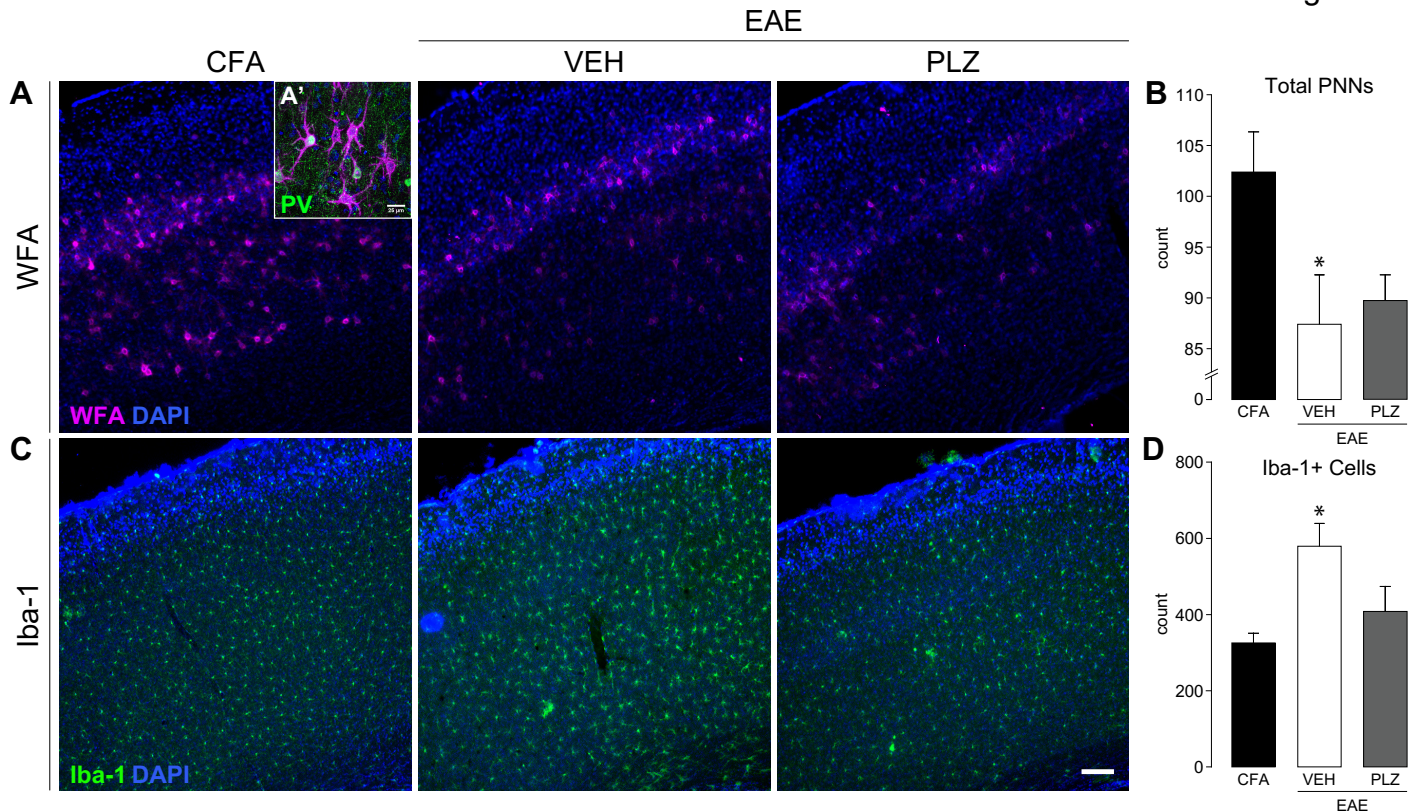


**Figure 4.8** Microglial activation and peri-neuronal net integrity in S1, and the effects of PLZ, in established EAE.

(A) Representative fluorescence photomicrographs of WFA+ staining (PNNs) in S1 from control (CFA) animals, and EAE animals treated from 7 dpi with either (VEH) or (PLZ). Scale bar in C = 100 $\mu$ m applies throughout. (A') (inset) High-magnification confocal photomicrograph depicting PNNs (WFA+, magenta) surrounding PV+ interneurons (green) in S1HL. DAPI (cell-nuclei) counter-stain is shown in blue. (B) Group-mean ( $\pm$ S.E.) total PNN counts from WFA+ stained S1HL of CFA ( $n=6$ ), VEH-treated EAE ( $n=7$ ), and PLZ-treated ( $n=4$ ) EAE animals (21 dpi). VEH-treated EAE animals exhibited significantly reduced PNN-counts in S1HL vs. CFA controls. PNN counts from the PLZ-treated EAE mice were also significantly reduced compared to CFA. PNN counts were approximately equivalent (*not significant*,  $p > 0.05$ ) between both the VEH-treated and PLZ-treated EAE groups (*one-way ANOVA*,  $*p=0.021$ , *post-hoc comparisons vs. CFA controls by Dunnett's method*). (C) Representative fluorescence photomicrographs of Iba-1+ staining (activated microglia/macrophages) in S1HL of CFA animals, and EAE animals treated chronically from 7 dpi with either (VEH) or (PLZ). (D) Group-mean ( $\pm$ S.E.) counts of Iba-1+ cells in S1HL of CFA ( $n=6$ ), VEH-treated EAE ( $n=7$ ), or PLZ-treated EAE ( $n=4$ ) animals. VEH-treated EAE animals exhibited significantly increased numbers of Iba-1+ cells in S1HL vs. CFA controls. Chronic treatment of EAE mice with PLZ from 7 dpi reduced the number of Iba-1+ cells in S1HL - EAE-PLZ animals did not differ significantly from CFA controls (*one-way ANOVA*,  $*p=0.009$ , *post-hoc comparisons vs. CFA controls by Dunnett's method*).

Figure 4.9

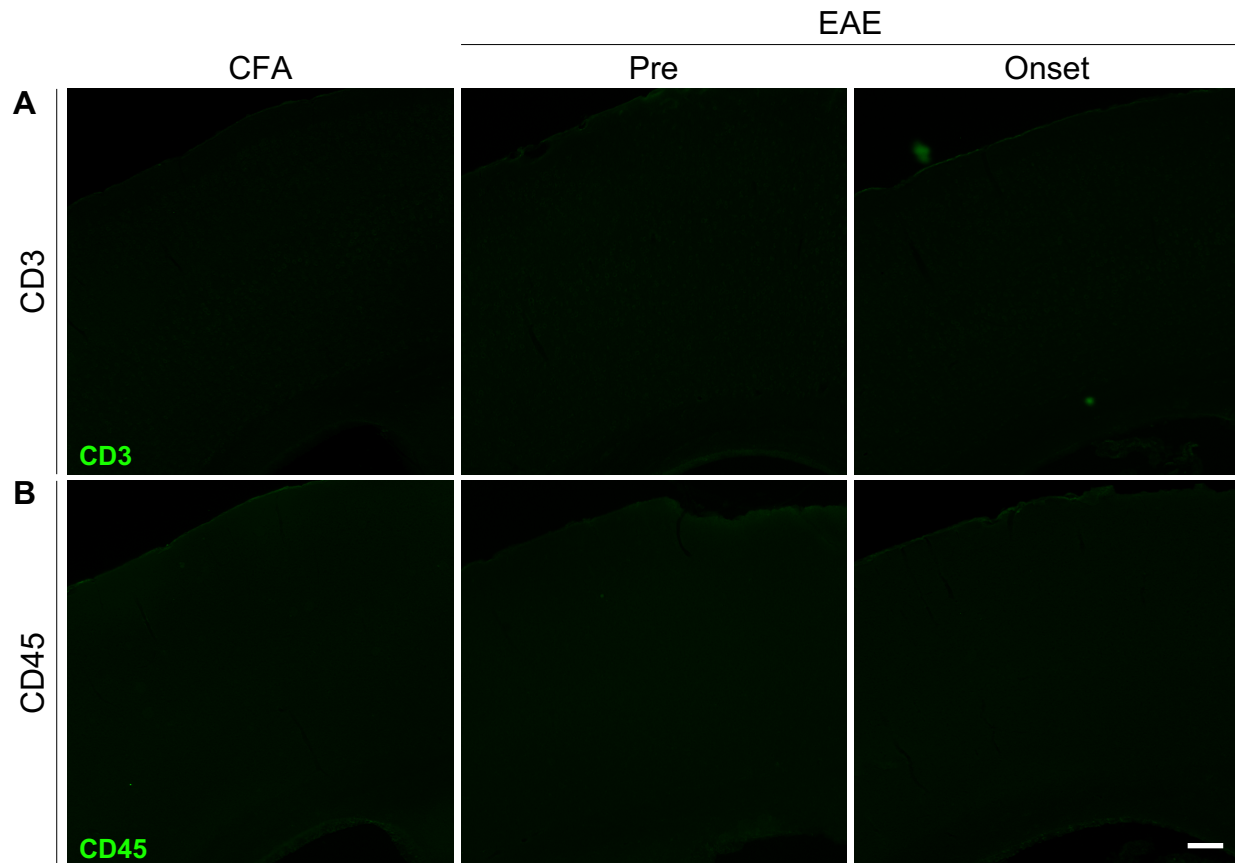


**Figure 4.9** S1 IHC in pre-symptomatic and clinical-onset EAE: Absence of cortical-infiltrating CD3<sup>+</sup> and/or CD45<sup>+</sup> T-cells.

**(A)** Representative fluorescence photomicrographs of CD3<sup>+</sup> staining in S1 from control (CFA) and EAE animals at the pre-symptomatic stage (7-9 dpi. PRE) or clinical-onset (ONS). No infiltrating T-cells were apparent. Scale bar in B = 100 $\mu$ m applies throughout. **(B)** Representative fluorescence photomicrographs of CD45<sup>+</sup> staining in S1 from control (CFA) and EAE animals at the pre-symptomatic stage (7-9 dpi. PRE) or clinical-onset (ONS). No infiltrating T-cells were apparent.

#### 4.7 - REFERENCES

1. Demaree, H.A., E. Gaudino, and J. DeLuca, *The relationship between depressive symptoms and cognitive dysfunction in multiple sclerosis*. Cognitive neuropsychiatry, 2003. **8**(3): p. 161-71.
2. Svendsen, K.B., et al., *Sensory function and quality of life in patients with multiple sclerosis and pain*. Pain, 2005. **114**(3): p. 473-81.
3. Svendsen, K.B., et al., *Pain in patients with multiple sclerosis: a population-based study*. Archives of neurology, 2003. **60**(8): p. 1089-94.
4. O'Connor, A.B., et al., *Pain associated with multiple sclerosis: systematic review and proposed classification*. Pain, 2008. **137**(1): p. 96-111.
5. Osterberg, A., J. Boivie, and K.A. Thuomas, *Central pain in multiple sclerosis--prevalence and clinical characteristics*. European journal of pain, 2005. **9**(5): p. 531-42.
6. Geurts, J.J.G., et al., *Measurement and clinical effect of grey matter pathology in multiple sclerosis*. The Lancet Neurology. **11**(12): p. 1082-1092.
7. Eto, K., et al., *Inter-regional contribution of enhanced activity of the primary somatosensory cortex to the anterior cingulate cortex accelerates chronic pain behavior*. J Neurosci, 2011. **31**(21): p. 7631-6.
8. Kim, S.K. and J. Nabekura, *Rapid synaptic remodeling in the adult somatosensory cortex following peripheral nerve injury and its association with neuropathic pain*. J Neurosci, 2011. **31**(14): p. 5477-82.
9. Gustin, S.M., et al., *Pain and plasticity: is chronic pain always associated with somatosensory cortex activity and reorganization?* J Neurosci, 2012. **32**(43): p. 14874-84.
10. Olechowski, C.J., et al., *A diminished response to formalin stimulation reveals a role for the glutamate transporters in the altered pain sensitivity of mice with experimental autoimmune encephalomyelitis (EAE)*. Pain, 2010. **149**(3): p. 565-72.
11. Olechowski, C.J., et al., *Changes in nociceptive sensitivity and object recognition in experimental autoimmune encephalomyelitis (EAE)*. Experimental neurology, 2013. **241**(0): p. 113-121.
12. Olechowski, C.J., J.J. Truong, and B.J. Kerr, *Neuropathic pain behaviours in a chronic-relapsing model of experimental autoimmune encephalomyelitis (EAE)*. Pain, 2009. **141**(1-2): p. 156-64.
13. Rahn, E.J., et al., *Sex differences in a mouse model of multiple sclerosis: neuropathic pain behavior in females but not males and protection from neurological deficits during proestrus*. Biol Sex Differ, 2014. **5**(1): p. 4.
14. Thibault, K., B. Calvino, and S. Pezet, *Characterisation of sensory abnormalities observed in an animal model of multiple sclerosis: a behavioural and pharmacological study*. European journal of pain, 2011. **15**(3): p. 231 e1-16.
15. Khan, N. and M.T. Smith, *Multiple sclerosis-induced neuropathic pain: pharmacological management and pathophysiological insights from rodent EAE models*. Inflammopharmacology, 2014. **22**(1): p. 1-22.
16. Gao, Y.J. and R.R. Ji, *c-Fos and pERK, which is a better marker for neuronal activation and central sensitization after noxious stimulation and tissue injury?* Open Pain J, 2009. **2**: p. 11-17.
17. Yang, G., et al., *Peripheral elevation of TNF-alpha leads to early synaptic abnormalities in the mouse somatosensory cortex in experimental autoimmune encephalomyelitis*. Proceedings of the National Academy of Sciences of the United States of America, 2013. **110**(25): p. 10306-11.
18. Tambalo, S., et al., *Functional Magnetic Resonance Imaging of Rats with Experimental Autoimmune Encephalomyelitis Reveals Brain Cortex Remodeling*. J Neurosci, 2015. **35**(27): p. 10088-100.
19. Falco, A., et al., *Reduction in parvalbumin-positive interneurons and inhibitory input in the cortex of mice with experimental autoimmune encephalomyelitis*. Experimental brain research. Experimentelle Hirnforschung. Experimentation cerebrale, 2014. **232**(7): p. 2439-49.
20. Shibuki K, H.R., Tohmi M, et al. Frostig RD, editor. , *Flavoprotein Fluorescence Imaging of Experience-Dependent Cortical Plasticity in Rodents*. In: *In Vivo Optical Imaging of Brain Function*. 2nd edition. Chapter 7.

21. Shibuki, K., et al., *Dynamic imaging of somatosensory cortical activity in the rat visualized by flavoprotein autofluorescence*. The Journal of physiology, 2003. **549**(Pt 3): p. 919-27.
22. Musgrave, T., et al., *Tissue concentration changes of amino acids and biogenic amines in the central nervous system of mice with experimental autoimmune encephalomyelitis (EAE)*. Neurochemistry international, 2011. **59**(1): p. 28-38.
23. Musgrave, T., et al., *The MAO inhibitor phenelzine improves functional outcomes in mice with experimental autoimmune encephalomyelitis (EAE)*. Brain, behavior, and immunity, 2011. **25**(8): p. 1677-88.
24. Hensch, T.K. and M. Fagiolini, *Excitatory-inhibitory balance and critical period plasticity in developing visual cortex*. Prog Brain Res, 2005. **147**: p. 115-24.
25. Woolf, C.J. and M.W. Salter, *Neuronal plasticity: increasing the gain in pain*. Science, 2000. **288**(5472): p. 1765-9.
26. Kalyvas, A.e.a. and S. David, *Cytosolic phospholipase A2 plays a key role in the pathogenesis of multiple sclerosis-like disease*. Neuron, 2004. **41**(3): p. 323-35.
27. Benson, C.A., et al., *The MAO inhibitor phenelzine can improve functional outcomes in mice with established clinical signs in experimental autoimmune encephalomyelitis (EAE)*. Behavioural brain research, 2013. **252**: p. 302-11.
28. Tohmi, M., et al., *Transcranial flavoprotein fluorescence imaging of mouse cortical activity and plasticity*. Journal of neurochemistry, 2009. **109 Suppl 1**: p. 3-9.
29. Drew, P.J., et al., *Chronic optical access through a polished and reinforced thinned skull*. Nature Methods, 2010. **7**(12): p. 981-984.
30. Bains, R., et al., *Volatile anaesthetics depolarize neural mitochondria by inhibition of the electron transport chain*. Acta Anaesthesiol Scand, 2006. **50**(5): p. 572-9.
31. T. Robert Husson and Naoum P. Issa. et al. Frostig RD, e., *Functional Imaging with Mitochondrial Flavoprotein Autofluorescence: Theory, Practice, and Applications*. In: *In Vivo Optical Imaging of Brain Function*. 2nd edition. Chapter 8.
32. Maggi, C.A. and A. Meli, *Suitability of urethane anesthesia for physiopharmacological investigations in various systems. Part 1: General considerations*. Experientia, 1986. **42**(2): p. 109-14.
33. Hara, K. and R.A. Harris, *The anesthetic mechanism of urethane: the effects on neurotransmitter-gated ion channels*. Anesthesia and analgesia, 2002. **94**(2): p. 313-8, table of contents.
34. Paxinos, G. and K.B.J. Franklin, *The mouse brain in stereotaxic coordinates*. Compact 2nd ed2004, Amsterdam ; Boston: Elsevier Academic Press.
35. Winship, I.R. and T.H. Murphy, *In Vivo Calcium Imaging Reveals Functional Rewiring of Single Somatosensory Neurons after Stroke*. Journal of Neuroscience, 2008. **28**(26): p. 6592-6606.
36. Sigler, A.a.M., T. IO and VSD Signal Processor. 2012; Available from: [http://www.neuroscience.ubc.ca/faculty/murphy\\_software.html](http://www.neuroscience.ubc.ca/faculty/murphy_software.html).
37. Harrison, T.C., A. Sigler, and T.H. Murphy, *Simple and cost-effective hardware and software for functional brain mapping using intrinsic optical signal imaging*. J Neurosci Methods, 2009. **182**(2): p. 211-8.
38. Gibb, R. and B. Kolb, *A method for vibratome sectioning of Golgi-Cox stained whole rat brain*. J Neurosci Methods, 1998. **79**(1): p. 1-4.
39. Frostig, R.D., *Functional organization and plasticity in the adult rat barrel cortex: moving out-of-the-box*. Curr Opin Neurobiol, 2006. **16**(4): p. 445-50.
40. Lefort, S., et al., *The excitatory neuronal network of the C2 barrel column in mouse primary somatosensory cortex*. Neuron, 2009. **61**(2): p. 301-16.
41. Schindelin, J., et al., *Fiji: an open-source platform for biological-image analysis*. Nat Methods, 2012. **9**(7): p. 676-82.
42. Longair, M.H., D.A. Baker, and J.D. Armstrong, *Simple Neurite Tracer: open source software for reconstruction, visualization and analysis of neuronal processes*. Bioinformatics, 2011. **27**(17): p. 2453-4.

43. Lein, E.S., et al., *Genome-wide atlas of gene expression in the adult mouse brain*. Nature, 2007. **445**(7124): p. 168-76.
44. Kuo, T.e.a. *ITCN Cell Counter*. Available from: <http://rsb.info.nih.gov/ij/plugins/itcn.html>.
45. Komagata, S., et al., *Nociceptive cortical responses during capsaicin-induced tactile allodynia in mice with spinal dorsal column lesioning*. Neuroscience Research, 2011. **69**(4): p. 348-351.
46. Kim, S.K., K. Eto, and J. Nabekura, *Synaptic structure and function in the mouse somatosensory cortex during chronic pain: in vivo two-photon imaging*. Neural Plast, 2012. **2012**: p. 640259.
47. Watanabe, T., et al., *Spinal mechanisms underlying potentiation of hindpaw responses observed after transient hindpaw ischemia in mice*. Sci Rep, 2015. **5**: p. 11191.
48. Komagata, S., et al., *Initial phase of neuropathic pain within a few hours after nerve injury in mice*. J Neurosci, 2011. **31**(13): p. 4896-905.
49. Sachdev, R.N., M.R. Krause, and J.A. Mazer, *Surround suppression and sparse coding in visual and barrel cortices*. Front Neural Circuits, 2012. **6**: p. 43.
50. Margolis, D.J., H. Lutcke, and F. Helmchen, *Microcircuit dynamics of map plasticity in barrel cortex*. Curr Opin Neurobiol, 2014. **24**(1): p. 76-81.
51. Zhang, G., et al., *Upregulation of excitatory neurons and downregulation of inhibitory neurons in barrel cortex are associated with loss of whisker inputs*. Mol Brain, 2013. **6**: p. 2.
52. Reinert, K.C., et al., *Flavoprotein autofluorescence imaging of neuronal activation in the cerebellar cortex in vivo*. Journal of neurophysiology, 2004. **92**(1): p. 199-211.
53. Reinert, K.C., et al., *Flavoprotein autofluorescence imaging in the cerebellar cortex in vivo*. J Neurosci Res, 2007. **85**(15): p. 3221-32.
54. Reinert, K.C., et al., *Cellular and metabolic origins of flavoprotein autofluorescence in the cerebellar cortex in vivo*. Cerebellum, 2011. **10**(3): p. 585-99.
55. Holtmaat, A. and K. Svoboda, *Experience-dependent structural synaptic plasticity in the mammalian brain*. Nat Rev Neurosci, 2009. **10**(9): p. 647-58.
56. Karetko, M. and J. Skangiel-Kramska, *Diverse functions of perineuronal nets*. Acta Neurobiol Exp (Wars), 2009. **69**(4): p. 564-77.
57. Hartig, W., et al., *Cortical neurons immunoreactive for the potassium channel Kv3.1b subunit are predominantly surrounded by perineuronal nets presumed as a buffering system for cations*. Brain Res, 1999. **842**(1): p. 15-29.
58. Levy, A.D., M.H. Omar, and A.J. Koleske, *Extracellular matrix control of dendritic spine and synapse structure and plasticity in adulthood*. Front Neuroanat, 2014. **8**: p. 116.
59. Soleman, S., et al., *Targeting the neural extracellular matrix in neurological disorders*. Neuroscience, 2013. **253**: p. 194-213.
60. Ye, Q. and Q.L. Miao, *Experience-dependent development of perineuronal nets and chondroitin sulfate proteoglycan receptors in mouse visual cortex*. Matrix Biol, 2013. **32**(6): p. 352-63.
61. Centonze, D., et al., *Inflammation triggers synaptic alteration and degeneration in experimental autoimmune encephalomyelitis*. J Neurosci, 2009. **29**(11): p. 3442-52.
62. Mandolesi, G., et al., *Cognitive deficits in experimental autoimmune encephalomyelitis: neuroinflammation and synaptic degeneration*. Neurological sciences : official journal of the Italian Neurological Society and of the Italian Society of Clinical Neurophysiology, 2010. **31**(Suppl 2): p. S255-9.
63. Gray, E., et al., *Elevated matrix metalloproteinase-9 and degradation of perineuronal nets in cerebrocortical multiple sclerosis plaques*. J Neuropathol Exp Neurol, 2008. **67**(9): p. 888-99.
64. Berard, J.L., et al., *Characterization of relapsing-remitting and chronic forms of experimental autoimmune encephalomyelitis in C57BL/6 mice*. Glia, 2010. **58**(4): p. 434-45.
65. Ahissar et al., S., *S1 laminar specialization*. Scholarpedia, 2010. **5**(8).
66. Murakami, H., et al., *Short-term plasticity visualized with flavoprotein autofluorescence in the somatosensory cortex of anaesthetized rats*. The European journal of neuroscience, 2004. **19**(5): p. 1352-60.

67. Feldman, D.E. and M. Brecht, *Map plasticity in somatosensory cortex*. Science, 2005. **310**(5749): p. 810-5.
68. Hensch, T.K., *Critical period regulation*. Annu Rev Neurosci, 2004. **27**: p. 549-79.
69. Donato, F., S.B. Rompani, and P. Caroni, *Parvalbumin-expressing basket-cell network plasticity induced by experience regulates adult learning*. Nature, 2013. **504**(7479): p. 272-6.
70. Toyozumi, T., et al., *A theory of the transition to critical period plasticity: inhibition selectively suppresses spontaneous activity*. Neuron, 2013. **80**(1): p. 51-63.
71. Mandolesi, G., et al., *IL-1beta dependent cerebellar synaptopathy in a mouse model of multiple sclerosis*. Cerebellum, 2015. **14**(1): p. 19-22.
72. Rossi, S., et al., *Impaired striatal GABA transmission in experimental autoimmune encephalomyelitis*. Brain, Behavior, and Immunity, 2011. **25**(5): p. 947-56.
73. Nistico, R., et al., *Synaptic plasticity in multiple sclerosis and in experimental autoimmune encephalomyelitis*. Philos Trans R Soc Lond B Biol Sci, 2014. **369**(1633): p. 20130162.
74. Pitt, D., P. Werner, and C.S. Raine, *Glutamate excitotoxicity in a model of multiple sclerosis*. Nat Med, 2000. **6**(1): p. 67-70.
75. Bar-Or, A., et al., *Analyses of all matrix metalloproteinase members in leukocytes emphasize monocytes as major inflammatory mediators in multiple sclerosis*. Brain, 2003. **126**(Pt 12): p. 2738-49.
76. Schafer, D.P., E.K. Lehrman, and B. Stevens, *The "quad-partite" synapse: microglia-synapse interactions in the developing and mature CNS*. Glia, 2013. **61**(1): p. 24-36.
77. Ramesh, G., A.G. MacLean, and M.T. Philipp, *Cytokines and chemokines at the crossroads of neuroinflammation, neurodegeneration, and neuropathic pain*. Mediators Inflamm, 2013. **2013**: p. 480739.
78. Eyo, U.B. and L.J. Wu, *Bidirectional microglia-neuron communication in the healthy brain*. Neural Plast, 2013. **2013**: p. 456857.
79. Nakamura, K., et al., *Transiently increased colocalization of vesicular glutamate transporters 1 and 2 at single axon terminals during postnatal development of mouse neocortex: a quantitative analysis with correlation coefficient*. The European journal of neuroscience, 2007. **26**(11): p. 3054-67.
80. Nakamura, K., et al., *Postnatal changes of vesicular glutamate transporter (VGLUT)1 and VGLUT2 immunoreactivities and their colocalization in the mouse forebrain*. The Journal of comparative neurology, 2005. **492**(3): p. 263-88.
81. Graziano, A., et al., *Vesicular glutamate transporters define two sets of glutamatergic afferents to the somatosensory thalamus and two thalamocortical projections in the mouse*. The Journal of comparative neurology, 2008. **507**(2): p. 1258-76.
82. Brumovsky, P.R., *VGLUTs in Peripheral Neurons and the Spinal Cord: Time for a Review*. ISRN Neurology, 2013. **2013**: p. 28.
83. Todd, A.J., et al., *The expression of vesicular glutamate transporters VGLUT1 and VGLUT2 in neurochemically defined axonal populations in the rat spinal cord with emphasis on the dorsal horn*. European Journal of Neuroscience, 2003. **17**(1): p. 13-27.
84. Shen, J. and J. Yang, *In Vivo Detection of Altered GABA Levels Following Acute Administration of Antidepressant/Antipanic Drug Phenzelzine*. Proc. Intl. Soc. Mag. Reson. Med., 2005. **13**.
85. Parent, M.B., et al., *Effects of the antidepressant/antipanic drug phenzelzine and its putative metabolite phenylethylidenehydrazine on extracellular gamma-aminobutyric acid levels in the striatum*. Biochemical pharmacology, 2002. **63**(1): p. 57-64.
86. Parent, M.B., M.K. Habib, and G.B. Baker, *Time-dependent changes in brain monoamine oxidase activity and in brain levels of monoamines and amino acids following acute administration of the antidepressant/antipanic drug phenzelzine*. Biochemical pharmacology, 2000. **59**(10): p. 1253-63.
87. Benson, C.A., et al., *The MAO inhibitor phenzelzine can improve functional outcomes in mice with established clinical signs in experimental autoimmune encephalomyelitis (EAE)*. Behav Brain Res, 2013. **252**: p. 302-11.

88. Aznar, S., et al., *The 5-HT<sub>1A</sub> serotonin receptor is located on calbindin- and parvalbumin-containing neurons in the rat brain*. Brain Res, 2003. **959**(1): p. 58-67.
89. Salgado, H., et al., *Pre- and postsynaptic effects of norepinephrine on  $\gamma$ -aminobutyric acid-mediated synaptic transmission in layer 2/3 of the rat auditory cortex*. Synapse, 2012. **66**(1): p. 20-28.
90. Kruglikov, I. and B. Rudy, *Perisomatic GABA release and thalamocortical integration onto neocortical excitatory cells are regulated by neuromodulators*. Neuron, 2008. **58**(6): p. 911-24.
91. Huang, Y., et al., *5-HT<sub>3a</sub> Receptors Modulate Hippocampal Gamma Oscillations by Regulating Synchrony of Parvalbumin-Positive Interneurons*. Cerebral Cortex, 2014.
92. Edeline, J.M., *Beyond traditional approaches to understanding the functional role of neuromodulators in sensory cortices*. Front Behav Neurosci, 2012. **6**: p. 45.
93. Yang, J. and J. Shen, *In vivo evidence for reduced cortical glutamate-glutamine cycling in rats treated with the antidepressant/antipanic drug phenelzine*. Neuroscience, 2005. **135**(3): p. 927-37.
94. Michael-Titus, A.T., et al., *Imipramine and phenelzine decrease glutamate overflow in the prefrontal cortex--a possible mechanism of neuroprotection in major depression?* Neuroscience, 2000. **100**(4): p. 681-4.
95. Kuhn, S.A., et al., *Microglia express GABA(B) receptors to modulate interleukin release*. Mol Cell Neurosci, 2004. **25**(2): p. 312-22.
96. Dello Russo, C., et al., *Inhibition of microglial inflammatory responses by norepinephrine: effects on nitric oxide and interleukin-1beta production*. J Neuroinflammation, 2004. **1**(1): p. 9.

# Chapter 5

Additional Discussion and Conclusions

## 5.1 - Chapter 2 Commentary:

The category of modern psychiatric compounds known as “antidepressants” did not exist as such until the 2<sup>nd</sup> half of the 20<sup>th</sup> century [1]. Although Benzedrine (amphetamine) had been marketed as a decongestant and “psychic energizer” (stimulant), and recommended for use in “mild depression” since 1935 [2]; the term “antidepressant” was not coined until the early 1950s, with the advent of the first monoamine oxidase inhibitors (MAOIs) [3]. Isoniazid, and the closely related compound iproniazid, were the first MAOIs to be identified [3]. Chemically, both drugs belong to the hydrazine class [3]. Isoniazid was originally synthesized in 1912, but it was not until 1951 that it first found use in medicine - not as an antidepressant, but as an antitubercular drug [3]. Despite potentially serious side effects, including liver toxicity, isoniazid is still employed as a first line treatment for tuberculosis today [4]. Iproniazid was first synthesized during the same year (1951), and was also originally investigated as an antitubercular medicine [1]. By 1952, the first indications of psychiatric side effects of isoniazid were noted in patients being treated for tuberculosis [1]. These side effects included euphoria, excitement, convulsions and, in some cases, psychosis [5]. Iproniazid was initially found to have even greater psychiatric side effects; however, subsequent research established that the most prominent negative side effects of both drugs could be minimized with more modest dosages [5]. Also in 1952, *in vitro* studies with iproniazid confirmed that the drug irreversibly inhibited the enzyme monoamine oxidase (MAO) [1], causing tissue levels of noradrenaline (NA) to become elevated [6]. Serotonin (5-HT) was not identified as a neurotransmitter until 1953, while dopamine (DA) was not identified as a neurotransmitter until 1958. Isoniazid turned out to have only weak activity as an inhibitor of MAO, while producing greater proconvulsant side effects compared to iproniazid [3]. By 1957, deliberate studies investigating the use of iproniazid in depressed patients had demonstrated the drug’s effectiveness, and it became the first drug to find clinical approval as an antidepressant in 1958 [3, 7]. Also in 1958, imipramine, the first tricyclic antidepressant (TCA), was starting to be explored clinically [3, 8]. By 1960, it was realized that imipramine acted to inhibit the reuptake of noradrenaline from the synapse [3]. The

introduction of the MAOIs and TCAs soon led to the formulation of the monoamine theory of depression - which postulates that depression is caused by deficient synaptic levels of the monoamine neurotransmitters [8]. Incidences of hepatotoxicity led to the removal of iproniazid from most markets beginning in 1961 [6, 7]. However, by that time, the less toxic MAOIs phenelzine (PLZ) and isocarboxazid - also hydrazine derivatives – had been developed, and quickly replaced iproniazid in clinical practice [6]. Throughout the 1960s and 70s, the various MAOIs and TCAs were used extensively as first line treatments for depression, and were found to be reasonably effective, despite the occasional occurrence of severe side effects with drugs of both classes [3, 6]. By the 1980s, however, the clinical use of MAOIs (especially the earlier irreversible and non-specific compounds) began to rapidly decline, as concerns over the potential for the precipitation of life threatening hypertensive crises through the “cheese effect” grew amongst physicians/psychiatrists [6, 9]. This risk could be mitigated by observing specific dietary restrictions, and later (re)appraisals of the relative safety of the MAOIs generally found these concerns to be overstated [9-11]. Nevertheless, by the late 1980s/1990s, with the introduction of the selective serotonin reuptake inhibitors (SSRIs), and later the SNRIs, both the MAOIs and the TCAs (which are often poorly tolerated due to a wide range of side effects, and can occasionally cause lethal cardiotoxicity) were largely supplanted in clinical practice - relegated to use as third or fourth line treatments in severely depressed or bipolar patients, who are otherwise refractory to treatment [6, 12]. In the 1990s, the only widely approved reversible inhibitor of MAO (RIMA), moclobemide, was introduced into clinical practice [6, 12]. RIMAs are displaced from MAO-A (and lack effect at MAO-B) by tyramine, and so do not produce hypertensive/vasopressive effects when tyramine is consumed [6]. As such, they are considered safer than irreversible MAOIs. However, they are still less commonly prescribed than the various SSRIs/SNRIs, and are not available in the USA [12]. More recent basic animal research on the effects of PLZ (a significant amount of which was carried out under G.A. Baker at the University of Alberta), revealed the synergistic/anxiolytic actions of PLZ's active metabolite PEH, which boosts synaptic and extracellular levels of GABA in the CNS through inhibition of GABA-T [13-15]. Other promising effects of PLZ described in the literature

include an ability to “scrub” (scavenge) reactive oxygen/aldehyde species [13, 16] - a potential neuroprotective mechanism - and reduce glutamate transmission (which could also be neuroprotective, anticonvulsant, antinociceptive etc.) [17, 18]. These various synergistic mechanisms, combined with studies which suggest that the potential for serious side effects with MAOIs has been overemphasized, and perhaps greater/broader efficacy of PLZ (or other MAOIs), have led several observers to point at that this class of compounds (and PLZ in particular [13, 16]) may currently be underutilized in the clinic [6, 9, 12].

While they were once common in psychiatric medicine, MAOIs have not been widely used or explored as treatments for pain. As noted, there were at least one or two studies conducted in the 1960s to 80s on the antinociceptive effects of PLZ [19, 20]. The study cited in Chapter 2 (Lee et al. 1983 [19]) which found an analgesic effect of PLZ in the tail flick assay - a test of acute noxious heat sensitivity - compared PLZ directly with an opioid (meperidine, aka Demerol) and a TCA (amitriptyline). Both are drugs that have been widely used for their analgesic effects. Opioids are generally considered some of the most effective analgesic drugs for acute or short term pain, but are considered much less effective for chronic pain - while TCAs are currently considered as first line treatments for chronic/neuropathic pain. Both drugs exploit descending and local (dorsal horn) nociceptive modulatory (inhibitory) circuits, and have supraspinal effects as well. TCAs, as noted, exploit similar neurotransmitter systems as MAOIs - raising the synaptic/tissue concentrations of the monoamine neurotransmitters, 5-HT and NA, by blocking their synaptic reuptake transporters [3]. TCAs generally have low or no activity at the DA transporter/DAT [21]. TCAs are, however, “dirty drugs”, which also display a variety of other interactions that contribute to a significant side effect profile and reduced tolerability. Many of the side effects of TCAs are due to their strong anticholinergic (antimuscarinic) effects, which produce atropine like symptoms such as dry mouth, nausea, paralytic ileus etc [22, 23]. TCAs also have antihistaminergic (H1 receptor) effects, which can cause drowsiness, and they additionally antagonize 5-HT<sub>2a/c</sub>, 5-HT<sub>3</sub>, 5-HT<sub>6</sub>, 5-HT<sub>7</sub>,  $\alpha$ <sub>1</sub> adrenergic receptors, and various voltage gated ion channels [22, 23]. Other side

effects of TCAs include tachycardia, arrhythmias, heart failure, hypertension, liver toxicity, confusion, dizziness, orthostatic hypotension, and sometimes death [22, 23]. Opioid side effects include tolerance, addiction, withdrawal symptoms, opioid induced hyperalgesia, potentially lethal respiratory depression, constipation, drowsiness and more. So while both classes of drugs (opioids and TCAs) have found wide use in the treatment of acute and/or chronic pain, they are often associated with significant side effects. Notably in Lee et al., acute I.P. PLZ at 1.5mg/kg or 3mg/kg (significantly less than the 15mg/kg I.P. dose we used), PLZ produced the strongest and most sustained analgesic effects (ie. the highest post-injection response temperatures, at T+45/90 min. and 24h). Meperidine was given at 14mg/kg I.P., a very high dosage equivalent to roughly 1g in a 70kg man - although according to the authors, mice are much more tolerant to the effects of opioids than humans. Amitriptyline was given at 6 or 12mg/kg. All three drugs produced statistically significant analgesia, with meperidine producing stronger effects than amitriptyline at the T+45/90 min. time points. The meperidine/amitriptyline effects were no longer present by 24h post-injection. These results clearly suggested that PLZ had good analgesic activity at modest dosages. PLZ may also arguably have a reduced side effect profile compared to the opioids/TCAs, provided the dietary/medication restrictions are observed. Despite this initial promise, PLZ's potential antinociceptive/analgesic effects apparently did not generate significant research interest. The work in this thesis (and by Mifflin et al. [24]) may thus be picking up on a potential missed opportunity.

Contrary to Lee et al. [19], in Chapter 2 (Fig 2.1) we did not find any effect of acutely administered (I.P.) PLZ on basal/acute nociceptive sensitivity in the animals we tested. The assays we used are, of course, not precisely equivalent to the tail flick assay used in Lee et al. The Von Frey hair (VFH) assay was used to test basal mechanical sensitivity, and low weight VF hairs are not necessarily noxious stimuli. The hotplate assay tests the response to noxious heat, and therefore much more closely resembles the tail flick assay - although feet and tails are obviously not directly equivalent. Furthermore, the Lee study used white Swiss Webster mice (presumably males), which surely exhibit

differences from the female C57/BL6 mice we used, in terms of their behavioral profile and pharmacological responses. All of these factors may help to explain the disparity between the two studies in terms of PLZ's effect on acute nociceptive sensitivity.

We also tested the effects of acute (I.P.) PLZ on basal mechanical (VFH) and thermal (Hargreave's) sensitivity in male C57/BL6s, though we did not report on it here. Interestingly, in two separate experiments comparing 10 PLZ treated male mice to 10 VEH treated males, we found that the PLZ-treated group exhibited a transient (24h to 72h duration) sensitizing effect in the VFH assay. The reasons for this are not clear, although we suspect that the apparent sensitization may reflect something more akin to a transient behavioral hyperactivity or hyperreflexivity, owing to the psychostimulant-like NA/DAergic effects of PLZ, as opposed to true nociceptive hypersensitivity. After the period of mechanical hypersensitivity abated, subsequent injections of PLZ did not recapitulate this effect, indicating the males become tolerant to it. In the Hargreave's test of noxious heat sensitivity, in males, there was a modest antinociceptive effect of PLZ (ie. increased withdrawal latency) that did not appear until 24h after the initial dose of PLZ.

A reduction of acute nociceptive sensitivity is not necessarily the desired effect of a pain drug. Of seemingly greater relevance is the action of the drug in the behaviorally and neurobiologically sensitized condition. It is this type of pain which can be burdensome and maladaptive - while acute sensitivity is generally desirable and adaptive. The formalin assay tests this type of sensitized or tonic pain. The first (acute) phase of the formalin response is essentially the result of simple nociceptor activation ( $A\delta$  and C fibres). The second phase, however, involves glutamate-dependent central sensitization of the dorsal horn, and peripheral inflammation [25-28]. It is in this phase where we find PLZ's effect, indicating an antinociceptive / anti-allodynic action. The follow-up experiments - which demonstrated a reduction in c-Fos in the superficial DH following formalin in the PLZ-treated group, and also the inhibition of glutamate-evoked neuronal calcium transients in the isolated SC/DH by bath-

applied PLZ - verify that PLZ acts to inhibit neuronal/network (hyper)excitability in the DH and counteracts central sensitization.

In terms of elucidating the detailed mechanism of PLZ's antinociceptive / anti-allodynic actions, the results presented in Chapter 2 extend beyond the general mechanism described in the preceding paragraph. However, we fell somewhat short of definitively isolating and identifying the contribution from all of the specific cellular and neurochemical components that are involved. We were able to demonstrate the 5-HT elevating effect of PLZ within the DH by IHC - but an effect on NA, GABA, and DA has to be inferred from HPLC experiments reported in Mifflin et al. [24] (and Musgrave/Benson in EAE animals [29, 30]). As noted, these studies demonstrated a concentration-elevating effect of (I.P.) PLZ for 5-HT, NA, DA, and GABA in the spinal cord (and brain/brainstem). This means we cannot explicitly confirm that these elevations specifically occur within the DH. However, it is very likely that they do, based on the known distribution of those transmitters in the SC. Furthermore, the parameters of the experiment in Mifflin et al. were virtually identical to those in Chapter 2 - ie. female (and male) C57/BL6 mice pretreated with 15mg/kg I.P. PLZ 3h prior to formalin administration, as well as identical vendor, animal housing, location etc. - even the same individuals administering the formalin injections. These factors undoubtedly help to validate our inference.

Which of these affected neurotransmitters, acts at which receptors and cells, to produce the overall inhibitory and antinociceptive effects of PLZ? This is another question we cannot fully answer from the experiments and methods in Chapter 2. On one hand, our use of c-Fos IHC has the virtue of allowing the visualization/quantification of the effect of systemically administered PLZ on formalin-induced DH neuronal activation in the intact animal (post-mortem). Additionally, the c-Fos response to formalin is very clear and robust in the ipsilateral superficial DH, providing high signal-to-noise ratio. This is not the case in, for example, the c-Fos experiments in Chapter 3 (in EAE), in which basal c-Fos levels were very high, and specifically attributing any localized or overall differences in the number of c-Fos+

puncta to a specific stimulus or event becomes problematic (due to the post-mortem nature of c-Fos IHC). While it is widely used as such, c-Fos is also not necessarily a specific marker of “nociceptive” neuronal activation. A variety of other stimuli, apart from noxious peripheral stimuli, may evoke c-Fos expression in the CNS - including within the DH [31, 32]. Thus, there are limits on the interpretation of c-Fos IHC. Another clear limitation of c-Fos IHC - as we have conducted it in Chapter 2/3 - is that it does not distinguish specific neuronal populations. Without the use of IHC co-labelling or other identification methods, it is impossible to discern whether the activated (ie. c-Fos+) neurons are excitatory interneurons, projection neurons, or inhibitory interneurons - or non-neuronal cells. Presumably, the majority of c-Fos+ cells in the superficial DH following formalin administration are excitatory interneurons, with projection neurons making up a smaller proportion of the activated cells (due to their inherently fewer numbers), and inhibitory interneurons also making up a subset (ie. fewer than excitatory interneurons). It would be, at the very least, unexpected if the inhibitory cells activated in the DH by formalin outnumbered the (activated) excitatory cells, given the strong behavioral effect. More to the point, it would be instructive to know if the proportion of inhibitory to excitatory cells activated in the DH changed in the PLZ-treated group. One might predict that the overall reduction in c-Fos+ cells in the PLZ-treated group would primarily be due to a reduction in the number of activated excitatory interneurons and projection neurons - and perhaps a large proportion of the remaining c-Fos+ cells would be inhibitory interneurons. Perhaps not only the proportion of c-Fos+ cells that are inhibitory would be enhanced in the PLZ-treated group, but the absolute number of c-Fos+ inhibitory cells might be greater. Such a result would fairly unambiguously indicate that PLZ acts to increase the activity of inhibitory interneurons in the DH. A simple reduction in the number of activated excitatory/projection cells in the DH - in the absence of increased numbers of c-Fos+ inhibitory interneurons - could be interpreted as indicating the “direct” inhibition of excitatory cells (ie. by monoamines or descending GABAergic axons, or other mechanisms) without the intermediate involvement of local inhibitory interneurons. We attempted to co-label for GABA alongside c-Fos in this tissue in order to resolve these questions; however, as noted, we were not able to achieve satisfactory

results with immunostaining for GABA. The few authors who have reported successfully immunostaining for GABA in the SC have employed unconventional, purpose-specific, tissue fixation/ preparation/ staining protocols (ie. by Todd et al. [33, 34]). Although we adopted the use of glutaraldehyde as a fixative (alongside paraformaldehyde) in this experiment - as reported by Todd et al. - we did not adopt their full protocol. Successful application of IHC co-labelling (for c-Fos and cell-type specific markers/antibodies), or c-Fos IHC used in combination with transgenically-encoded indicator mice, could better reveal the circuit level mechanisms of PLZ.

Ratiometric calcium imaging in *ex vivo* spinal cord slices overcomes some of the inherent disadvantages of c-Fos IHC, but also introduces some new considerations and limits on interpretation. The most obvious advantages of ratiometric calcium imaging as a method for measuring neuronal activation are that it is conducted in (essentially) real time, and it is directly representative of the stimulus-evoked activity in the DH. The signal that is measured is directly proportional to the AP firing rate/membrane depolarization of the same specific, individually recorded neurons, immediately following stimulation - both before and after treatment of the tissue with PLZ. There is no intervening need for tissue fixation, preparation, and staining; and no (or much less) need to assume that the observed signal is related to the stimulus. However, the fact that the SCDH is isolated from the rest of the animal carries both advantages and disadvantages. Observing the activity of the DH system in isolation, on one hand, provides the opportunity to see how that system specifically behaves. On the other hand, it makes drawing inferences about the behavior of the DH in the intact animal somewhat problematic. Furthermore, it may modify the activity the treatment, particularly in the case of PLZ's, as its effects are presumably (at least in part) dependent on descending monoaminergic axons originating in the brainstem. How these descending axons and terminals behave in the isolate SC (ie. when they have been severed from their cell bodies) is unknown. It is certainly possible that descending neuron terminals continue to depolarize and physiologically, or non-physiologically, release transmitters into the surrounding tissues even after axon transection. The fact that we were able to antagonize the

effects of PLZ with WAY-100,635 suggests that 5-HT (at least) continues to exert activity in the isolated cord, whether or not this involves continued release from descending axon terminals. Idazoxan did not antagonize the effects of PLZ, which would seem to indicate that PLZ's effects in the isolated cord do not depend on  $\alpha_2$  adrenergic receptors. It is also possible (though unlikely) that insufficient idazoxan was used. Furthermore, the 'n's in the antagonist experiments were low, and the effect being antagonized is fairly small and somewhat inconsistent. Whether these antagonist experiments are directly translatable or applicable to the *in vivo* antinociceptive actions of PLZ is therefore unclear. Naively, it would seem highly likely that NA does in fact play a role in PLZ's *in vivo* antinociceptive effects, based on the large body of literature supporting the analgesic effects of  $\alpha_2$  receptor-mediated descending inhibition in the DH. Another factor which complicates the interpretation of the calcium imaging experiments is the fact that the stimulus we used (ie. bath applied glutamate) is decidedly non-physiological. This stimulus bypasses the peripheral inputs that would be part of a physiological stimulus like formalin. The afferent terminals may still be active in the isolated cord, but if so, it is likely in a non-physiological manner. Bath applied glutamate might, in theory, reduce the outflow of those peripheral afferent terminals, due to the activation of mGluR autoreceptors. These concerns are to some degree mitigated in the current experiment by the fact that, as noted, the second phase of the formalin response is significantly dependent upon central glutamatergic activity and glutamate-dependent central sensitization. The bath-applied glutamate stimulus may therefore be apt in this case. Indeed, peripherally acting analgesics/anesthetics (eg. lidocaine) are known to have only limited effect in the second phase of the formalin assay, while centrally acting drugs are more effective, indicating that ongoing peripheral activity does not significantly contribute to the second phase of the response [26]. Within the DH circuitry, directly activating post- (and pre-) synaptic glutamate receptors by bath application of glutamate is also, of course, not precisely equivalent to what happens in physiological or pathological conditions. How much of the activity measured in these DH neurons with this method is related to direct activation of post-synaptic receptors, and how much involves (mono- or poly-) trans-synaptic activation is unclear. The temporal resolution of fura 2 dye imaging is low ( $\sim 1$  frame/s) so

these phenomena cannot be distinguished - unlike with, for instance, electrophysiology. Also, just as the unmodified c-Fos IHC method cannot distinguish between cell/neuronal types, the same applies to these imaging experiments. Doolen et al. 2012 [35] established that most of the cells labelled in the DH with this method are neurons - a small percentage of labelled cells can also be labelled with sulforhodamine 101, and are therefore likely astrocytes. Also like c-Fos IHC, this method could be combined with genetically encoded indicator mice, to resolve the specific neuronal subtypes being recorded from. As it was deployed, however, we cannot distinguish between inhibitory and excitatory cells with this method. One would predict that if the average magnitude of the response to glutamate goes up in the majority of labelled cells, this would indicate an increase in the excitability of the overall DH circuitry (and vice versa). Of course, it is possible that the method labels a disproportionate number of inhibitory interneurons - in which case the overall effect on the network might be opposite of what it appears. Certainly, it would be useful for future  $\text{Ca}^{2+}$  imaging experiments to attempt to distinguish between inhibitory and excitatory neuronal populations.

The role of GABA in the antinociceptive effect of PLZ would be an open question, given only the data presented in this Chapter. In addition to the technical challenges posed by immunostaining for GABA, experiments that involve antagonizing GABA-A receptors may be subject to the confounding effect of blocking baseline/tonic inhibition. This phenomenon could make it difficult to distinguish between the interaction between the antagonist and the drug of interest (ie. PLZ), and the effects of the antagonist itself. For these reasons we did not attempt to antagonize GABA receptors in the calcium imaging experiments. We did perform several experiments involving bath application of various concentrations of PEH (dissolved in aCSF using 0.01% DMSO) at concentrations of 100, 300, and 500 $\mu\text{M}$ . We did not report on these experiments here, but there appeared to be a modest (more modest than PLZ) inhibitory effect, that did exhibit apparent dose dependency. However, we only recorded from 1 slice for each of 100/500 $\mu\text{M}$ , and 3 slices for the 300 $\mu\text{M}$  concentration, and the effect at 300 $\mu\text{M}$  was below 10% (not significant) inhibition. At this modest level of inhibition, we had some concern that the “apparent”

inhibition was unrelated to the drug, and may have simply represented non-specific decline in the responsiveness or health of the slice, or perhaps a toxic effect of the DMSO. Indeed, the concern over measuring non-specific decline in the health/responsiveness of the slice, versus true inhibition resulting from treatment, was also a concern in our experiments with PLZ. However, the lack of apparent inhibition in the 0 $\mu$ M, 10 $\mu$ M, and 30 $\mu$ M PLZ experiments, and the relatively consistent ~15 to 40% inhibition observed with the higher concentrations (100, 200, and 300 $\mu$ M) helped allay these concerns. Still, there were slices/animals that did not appear to respond (or responded weakly) to even the higher concentrations of PLZ. Similarly, there were animals that did not respond behaviorally (in the formalin assay) to PLZ, in these experiments, and in the initial experiments by Mifflin et al [24]. Why certain animals respond to PLZ while others do not is unclear, although some variability is naturally to be expected. Returning to the subject of GABA, Mifflin et al. also examined the effects of PEH, and N<sub>2</sub>-Ac-PLZ (the PLZ analogue lacking the GABAergic effect) in female and male C57/BL6s in the formalin test and in the SC (with HPLC). From those experiments we know that I.P. PEH does indeed have an antinociceptive effect in the second phase of the formalin assay in both male and female mice, and does work to elevate GABA in the SC. In males, the effects of PLZ and PEH in the 2<sup>nd</sup> phase of the formalin response were equal, although the dosage of PEH used was double the dosage of PLZ (30mg/kg vs. 15mg/kg, respectively). In females, PEH (at 30mg/kg) had a stronger inhibitory effect on the second phase of the formalin assay than PLZ (at 15mg/kg). Indeed, as noted, the effect of PLZ fell short of statistical significance in that experiment. However, the differing dosages used make direct quantitative comparisons between the efficacy of PEH alone and PLZ (which generates PEH at a maximum 1:1 ratio) difficult. When N<sub>2</sub>-Ac-PLZ (at 40mg/kg) was tested, it had a significant effect in the 2<sup>nd</sup> phase of the formalin response in males, but produced only a ~25% (not significant) inhibition of responses in females. In males, pretreatment with intrathecal WAY-100,635, but not idazoxan, or SB-699551 (a 5-HT<sub>4a</sub> antagonist), blocked the effect of N<sub>2</sub>-Ac-PLZ in the formalin assay. In terms of the effect on monoamine levels in the SC, while PLZ produced elevations of both 5-HT and NA in both sexes, it was apparently more effective in the males. Contrarily, both PLZ and PEH had greater GABA

elevating effects in females than males. N<sub>2</sub>-Ac-PLZ elevated NA and 5-HT equivalently in both sexes. The authors concluded from these studies that males utilize monoaminergic mechanisms more efficiently for antinociception, while females appear to utilize GABA more efficiently. Again, with the varying dosages of the 3 compounds, and possibly differing affinities at MAO (between N<sub>2</sub>-Ac-PLZ and PLZ), it is difficult to draw direct quantitative comparisons between the treatments (in either sex, although comparisons between the sexes would not have this issue). It would be reasonable to conclude that both the monoamines and GABA mediate some degree of the inhibition produced by PLZ in both genders. Taken together, the antagonistic effects of WAY-100,635 in the formalin assay in males treated with N<sub>2</sub>-Ac-PLZ, and the antagonistic effect of WAY-100,635 in females (SC slices) treated with PLZ in the calcium imaging experiments, would seem to strengthen the case that the 5-HT<sub>1A</sub> receptor plays a role in the inhibition/antinociceptive produced by PLZ, despite the inequivalence of the experiments. The lack of effect of idazoxan in the same scenarios would seem to refute a role for NA acting at the  $\alpha$ <sub>2</sub> adrenoceptor in PLZ's effects. Interestingly, we also attempted a small number of calcium imaging experiments (females) involving bath application of N<sub>2</sub>-Ac-PLZ, at up to 500 $\mu$ M, although only in 1 or 2 animals. No effect of treatment was observed. Again, we did not report on these experiments here due to insufficient number of animals/slices, but this preliminary result is interesting in view of the behavioral effects reported by Mifflin et al. One might conclude that the monoaminergic effects of PLZ in females are minimal, and that most of the effect of PLZ in females relies on its conversion to PEH. However, the antagonism of the effect of PLZ in slice (females) by WAY-100,635 would seem to contradict that conclusion. One possible interpretation of these various observations could be that, in females, the actions of 5-HT (ie. at 5-HT<sub>1A</sub>R) do little to alter DH activity on their own, but rather potentiate the GABAergic/inhibitory effects of the PEH metabolite. This is an interesting possibility, and could be explained by a depolarizing effect of 5-HT<sub>1A</sub>R activation in a class of inhibitory interneurons with the DH. Ultimately this is, of course, speculation, but the potential for synergism between the monoaminergic and GABAergic effects of PLZ is entirely plausible or even likely.

Another key question we must consider is: what is the clinical relevance of these experiments? Should PLZ be given another look as a “novel” treatment for pain conditions involving central sensitization? Perhaps, although given the obscurity, the negative associations with side effects, and the inability to patent PLZ, it seems unlikely that clinical trials for this use would ever realistically take place. Still, PLZ has already been proven safe to use in humans (again, when dietary and drug restrictions are observed), and could hypothetically be prescribed for off-label use in pain patients. A RIMA such as moclobemide could also be examined, but this agent lacks any potential (direct) contribution from the GABA system. On a more general level, it seems that rationally designed drugs that exploit multiple inhibitory neurotransmitter/receptor systems, potentially in a synergistic manner, could perhaps be more effective than treatments with a more limited spectrum of action. The now-popular analgesic tramadol is a notable example of such a drug, which combines NA reuptake inhibition with mild  $\mu$  opioid agonist effects. The key to effectively realizing this potential is of course, to design drugs that, unlike previous “dirty” drugs (such as the TCAs) are not *overly* “promiscuous”, and burdened by side effects. Potentially, given what we have seen with PLZ/PEH, the combination of activities at the 5-HT<sub>1A</sub> receptor, alongside GABAergic activity, and perhaps NAergic agonist properties could be quite effective. Highly specific drugs which target the 5-HT<sub>1A</sub> (such as F-13640) have already been tested in the formalin assay, and are highly effective - and the analgesic effects of the  $\alpha_2$  agonist clonidine are well documented. GABAergic drugs have also been previously shown to have excellent potential in treating pain; although in the past, the supraspinal sedative and cognitive effects of GABAergic agents (when used at dosages relevant for pain relief) have tended to limit their applicability. Newer GABA-AR-subunit specific positive allosteric modulators have the potential to circumvent these limitations. The GABA-promoting mechanism of PEH (ie. GABA-T inhibition) is also fairly unique and potentially promising, in that PEH/PLZ have not generally been observed to be associated with sedative side effects. One side effect that has been noted with PLZ, which is apparently related to GABA-T inhibition, is a reduction in systemic vitamin B6 (pyridoxal phosphate) levels [36]. This effect has the potential to lead to peripheral neuropathy, but the problem can be mitigated by supplementation with vitamin B6.

## 5.2 - Chapter 3 Commentary:

Pain in EAE is a more complex and long-term phenomenon than formalin induced pain. Ongoing neuroinflammation and gliosis and demyelination/neurodegeneration lead to central sensitization involving both functional/neurochemical and structural/synaptic alterations - and behaviorally to allodynia. The experiments in Chapter 3 build on the earlier work of Olechowski et al. [37, 38], and help to confirm the connections between changes within the dorsal horn, and the observed pain behaviors in the model. They also confirm that PLZ is an effective anti-allodynic treatment in a more complex/chronic model. As in Chapter 2, the experiments in Chapter 3, while building on the previous work/knowledge, fall short of elucidating the complete detailed cellular/circuit mechanisms of allodynia in EAE, or of PLZ's anti-allodynic effects. Many of the same methodological considerations (re: for c-Fos/GABA IHC, as well as  $Ca^{2+}$  imaging), and limitations described for Chapter 2 apply in Chapter 3. In general, there are challenges posed by attempting to link static, post-mortem, observations (ie. IHC) with specific behaviors, stimuli, etc.

As noted in Chapter 3, we were somewhat surprised by the finding that, while PLZ treatment was effective in EAE in terms of normalizing behavioral nociceptive thresholds, it did not reduce the "ongoing" (basal /contralateral/deep DH) numbers of c-Fos+ neurons in the DH. PLZ did, however, reduce the "stimulus related" c-Fos signal, and inhibited glutamate-evoked intracellular calcium signals. This result may imply that the ongoing/basal neuronal activation in the DH perhaps has little causal association with the *evoked* neuronal activity and *evoked* pain behaviors in the model. PLZ's lack of effect on basal c-Fos levels appears to suggest that it relies on a "stimulus dependent" mechanism, as opposed to broadly depressing ongoing activity within the DH. This may suggest that PLZ preferentially engages/enhances phasic inhibition, while having less effect on tonic inhibition. The hypothetical mechanism described in the additional commentary for Chapter 2, or something similar, could fit with

this effect. Compare this with the glutamate reuptake promoting drugs (ie. MS-153/ceftriaxone) studied by Olechowski et al. [38, 39], which reduced ongoing c-Fos levels in the DH. Ceftriaxone was also effectively normalized mechanical sensitivity in the model. These drugs reduced hyperexcitability and ongoing activity in the DH by enhancing (or normalizing) the removal of excess synaptic and extracellular glutamate.

Like the ongoing c-Fos in the DH, the functional relevance of increased vGlut1+ immunoreactivity in the deep DH laminae in EAE is unclear. It is, however, not unreasonable to speculate (as we have) that this result indicates the formation of new synaptic connections and “late phase” LTP/sensitization that contributes to allodynia in the model. Anti-vGlut1 primarily labels low threshold, large diameter, myelinated (ie. A $\beta$ ) afferent terminals within the DH. As previously noted, several groups (and unpublished work by members of the Kerr lab) have pointed to changes in the DRG affecting these (A $\beta$ /myelinated) neurons (ie. increased ATF-3 expression, electrical hyperexcitability) in EAE. In connection with the observation of a vibromechanical stimulus-related c-Fos signal in the superficial DH, it is conceivable to imagine a mechanism in EAE wherein A $\beta$ -mediated excitatory drive is potentiated by functional/synaptic plasticity within the DH, and feeds into novel or latent/unmasked synaptic pathways that link 2<sup>nd</sup> order neurons in the deep DH to ‘nociceptive’ neurons within the superficial DH. Of course, verifying this mechanism would require a substantial amount of additional experimentation. A number of experimental approaches could be taken, including using functional imaging or electrophysiology to characterize activity in specific neuronal types in the DH (ie. *in vivo*, following peripheral low threshold stimulation of the paw/recording of the DH, or *ex vivo* with attached dorsal roots/dorsal root stimulation at A $\beta$  frequencies), but might be technically challenging to accomplish. One could also attempt to identify the DH neurons/circuits that connect the deep and superficial laminae in EAE by looking for synaptic/structural changes in interneuron populations known to bridge the deep and superficial DH. Some candidates for this role include vGlut3+ neurons or PKC $\gamma$ + neurons. Recent studies have demonstrated a key role for DH neurons that (*de novo*) express vGlut3 in

establishing the connection between low threshold afferents and nociceptive projection neurons in the superficial DH in mechanical allodynia [40]. PKC $\gamma$  is also expressed in a population of lamina 2 DH interneurons that have been implicated in allodynia [41]. These interneurons are not grossly altered in the DH in EAE [42], but may be functionally or synaptically altered.

As in Chapter 2, the calcium imaging experiments in Chapter 3 help overcome some of the challenges of relating post-mortem IHC to specific stimuli and/or functional changes in the DH. Neurons throughout the DH are, on average, more excitable (in response to extracellular glutamate) in EAE cords than in CFA cords. Bath-applied PLZ acutely inhibits/normalizes neuronal hyperexcitability in EAE cords, but, notably, also reduces excitability in CFA cords. This result is somewhat divergent from what is seen behaviorally (with VFHs), or with the vibromechanical stimulus in the DH/S1 in the CFA-PLZ group, in that PLZ had no effect in these assays. As previously noted, the *ex vivo* spinal cord preparation and bath-applied glutamate stimulus possess some fundamental differences from these other assays - which involve systemic PLZ administration and physiological peripheral stimulation in the intact animal. Also, unlike in “naïve” spinal cords (Chapter 2), PLZ in the CFA/EAE cords had an effect on responses to both the 1.0mM and 0.3mM glutamate stimulus. The reasons for this are unclear.

We conducted, but did not report on, additional Ca<sup>2+</sup> imaging experiments in EAE/CFA spinal cord slices that involved directly (bath) applying 5-HT and NA (in aCSF, at 300 $\mu$ M each), and measuring the effect on glutamate-evoked stimulation. As predicted, both 5-HT and NA inhibited evoked calcium responses in the DH in both CFA/EAE cords to some degree. Bath applied 5-HT only affected responses to the 1mM glutamate stimulus (and not the 0.3mM stimulus), producing approximately 10% inhibition. NA affected responses to both concentrations of glutamate (0.3/1.0mM), and was generally somewhat more effective than 5-HT, producing ~15 to 25% inhibition. These results confirm that 5-HT/NA are inhibitory in the DH in this experimental paradigm and in EAE. However, we did not report these results because of an unexpected effect in which the difference in response magnitudes between

EAE/CFA was not observed in these cords. The animals used in this experiment were the same animals in which we tested bath application of PLZ, as reported in Chapter 3. We obtained several slices from each animal/lumbar section, permitting several treatments to be tested. PLZ was the first treatment tested in all animals, and a strong difference was observed in the magnitude of responses between CFA/EAE cords. The only apparent difference between the PLZ and 5-HT/NA experiments were that the sections used for 5-HT/NA were therefore “older”, and had been held in oxygenated aCSF while the PLZ experiments were being run. It is possible that, for reasons that are not entirely clear, the excess response magnitudes/hyperexcitability in the EAE group deteriorated over this waiting period.

The 5-HT IHC we reported in Chapter 3, and previous HPLC experiments by Musgrave/Benson, have now demonstrated reduced monoamine and GABA content in the SC/SCDH in EAE, which can be normalized with PLZ treatment. The effects of PLZ in EAE (in the DH/S1, and on behavioral sensitivity) would seem to suggest that this loss of monoamines and/or GABA is a potential cause of DH sensitization and allodynia in the model. Loss of inhibition may therefore play an equally important role in establishing pain/plasticity in EAE as pro-excitatory changes. A potential goal for future investigation could be to confirm that there is a loss of functional inhibition, and/or plasticity or loss of inhibitory interneurons, in the DH in EAE. This (again) could be accomplished with electrophysiology or functional imaging looking at labelled/identified interneuron populations and IPSCs, and by IHC to look for gross/synaptic alterations. It is unclear why inhibitory interneurons are affected in EAE, but some evidence has demonstrated that certain inhibitory neuronal populations are, in fact, preferentially disrupted in the model [43, 44]. This may have to do with the high metabolic requirements of fast-spiking interneurons that mediate phasic inhibition. Similarly, descending monoaminergic (and possibly GABAergic) axons may be disrupted in EAE, particularly if they are affected by demyelination. Another possibility is that transmitter synthesis is disrupted in the DH, leading to depletion of monoamines and GABA. These are all potential subjects for future studies. As previously noted, an effect on phasic

inhibition seems like a likely mechanism for PLZ, given the apparent lack of effect on ongoing c-Fos expression in the DH.

While PLZ had no effect on cellular (IHC) markers of inflammation and gliosis in the DH, and appears to work mainly through affecting functional neuronal inhibition, this does not mean that inflammation and gliosis are not implicated in establishing and/or maintaining central sensitization in EAE. The role of astrocytes in the sensitization of the DH in EAE has already been well established in work by Olechowski et al [37-39]. Pro-inflammatory cytokines may also drive synaptic plasticity and potentiation in the DH. TNF $\alpha$  and IL-1 $\beta$  have previously been shown to be associated with hyperexcitability and synaptic plasticity in EAE, and are known to be elevated in the DH, DRG, and systemic circulation [39, 45-50]. Levels of TNF $\alpha$  and CX3CL1 in the DRG (and TNF $\alpha$  in the DH) have also been correlated with nociceptive hypersensitivity in EAE. Reactive microglia may be a source of pro-inflammatory cytokines in the DH, and other inflammatory mediators such as ROS, complement factors, enzymes such as MMPs, and trophic factors such as BDNF. Targeting microglia in EAE/MS may thus be an effective strategy for relieving pain. One potential challenge in studying these mechanisms in EAE, however, is that it may be difficult to target microglia directly without affecting overall disease progression [51] - which could be a confounding effect if trying to specifically study pain. This experimental challenge could perhaps be overcome by using specifically targeted treatments - as opposed to, for instance, more general glial inhibitors such as minocycline - or by carefully timing the treatments and pain assays.

Whether or not PLZ should (or would) ever be promoted as a treatment for pain in MS is, of course, debatable - as noted in the comments in Chapter 3. Currently, TCAs/SNRIs and various anticonvulsants are considered the front line treatments for pain in MS. It would therefore perhaps have been instructive to directly compare PLZ to some of these treatments in these experiments, although, given that PLZ completely normalizes nociceptive behaviors (to control/CFA levels), there is little

possibility that PLZ would have been outperformed by these other drugs. Perhaps, (again, as noted in the comments for Chapter 3), other drugs that help augment or mimic descending (or local) inhibition through a combination of mechanisms could also be explored in EAE/MS.

### 5.3 - Chapter 4 Commentary:

In Chapter 4 we made use of *in vivo* flavoprotein autofluorescence imaging (FAI) to explore functional plasticity in S1 in EAE. This method enabled us to measure peripherally-evoked activity in neuronal ensembles (ie. cortical maps) within S1. Advantages of this method include a direct, linear correlation between signal intensity and neuronal spiking activity (and with intracellular calcium signals and local field potentials), and lack of reliance on secondary hemodynamic effects (as fMRI and intrinsic signal optical imaging do). Disadvantages of this technique include limited spatial resolution - compared to calcium imaging or electrophysiology - and temporal resolution (compared to calcium imaging, electrophysiology, and voltage-sensitive dye imaging). These limitations meant we were only able to study the local network-level excitability/evoked signal, as opposed to single cell-level changes. A possible argument could also be made that, due to this method's reliance on measuring mitochondrial oxidative metabolism, there could be a potential confounding influence from metabolic/mitochondrial disruption in EAE. However, this argument can be (at least partially) refuted by pointing to the fact that FAI signals in EAE are potentiated, not disrupted as would be expected if mitochondrial oxidative phosphorylation was non-functioning in S1. Agents that uncouple mitochondrial metabolism from neuronal spiking activity, such as volatile anesthetics (eg. isoflurane), abolish the FAI signal. Additionally, the signal being measured is a time/stimulus locked increase in fluorescence, localized over a specific region of cortex, which is the average of 40 individual stimulus-response pairs. This also makes it less likely that differences in the observed signal are related to global (ongoing/background) activity or metabolic changes. That said, there have been reports that lactate metabolism is altered in the cortex in EAE, and extracellular/bath-applied lactate is also known to potentiate FAI signals [52].

This is potentially more of a concern than the possibility of a more general disruption or loss of mitochondrial oxidative phosphorylation - which is effectively ruled out by our data. However, the complementary report by Tambalo et al. [53], which used fMRI to measure evoked forelimb responses in S1 helps to confirm our findings. If one intended to further explore functional changes in S1 in EAE, using a more “direct” and spatially/temporally resolved method such as electrophysiology or  $\text{Ca}^{2+}$  imaging could be advantageous.

The question of whether or not the changes we observe in S1 are causally linked to pain or nociceptive behavioral sensitivity in EAE is worth asking. The aforementioned article by Tambalo et al. [53] took the position that increased area of evoked activation in S1 forelimb cortex was the result of ‘compensation’ for long term neurodegenerative changes in a rat EAE model, and was not the result of sensitization in nociceptive networks. As evidence to support this, they pointed to lack of stimulus-evoked fMRI-CBV signal within the caudate putamen/striatum. A few studies have shown that noxious stimulation in rats is associated with reduced cortical blood flow in this region [54]. Striatal activation or deactivation is, however, not necessarily a robust indicator of nociceptive processing - and there are likely to be differences in the activity evoked by noxious (ie. C fibre frequency) stimulation in naïve animals, and allodynia-associated nociceptive activity evoked by lower frequency stimulation in neuropathic/EAE animals. Notably, they did detect novel activation in the secondary somatosensory cortex, a region which is frequently activated by noxious stimulation/in pain. Nevertheless, the conclusions may be correct in their particular model and at the disease time points which they employed. The Lewis rat model tends to be associated with pain behaviors only over a specific time period in the early disease progression, whereas the measurements in Tambalo et al. [53] were taken at 30 and 60 dpi. (ie. very chronic disease). In our study, we looked at changes in S1 that occurred very early in the disease, when nociceptive behavioral sensitization and central sensitization in the DH are prominent. Furthermore, we observed an increase in dendritic spine density (in pyramidal neuron dendrites) within S1, whereas the Tambalo study found a decrease (supporting the neurodegeneration argument). It is

possible that at later time points, the observed increases in spine density would have reversed in our model, although in one investigation (not reported) we conducted near the 30 dpi. time point, there was still a non-significant trend towards increased spine density in S1 neurons. Additionally, in our model, PLZ, a treatment which blocked or reversed allodynia and boosted inhibition within the DH, also reversed many of the changes in S1. Lastly, there appeared to be a minor correlation (albeit a weak one,  $r^2=0.37$  excluding the PLZ-treated group) between c-Fos expression in the DH and S1 hindlimb signal intensity. As noted, c-Fos measurements in the SC in this model suffer from low signal-to-noise ratio, which may reduce the strength of this relationship. Together, these various points may explain the differing observations between the two studies, and help to support a connection between S1 plasticity and altered nociception/pain in our model. As mentioned in the introductory chapter, the causal nature of the link between S1 plasticity and pain has been investigated/explored in humans and (other) animal models. Most of the evidence to date suggests that plasticity/altered functionality in S1 is indeed causally linked to altered nociceptive behaviors in animal models, and to chronic pain in humans. If one wished to explore this link directly in EAE, the effects of local stimulation or inhibition applied to S1 could be tested - ie. through optogenetics/DREDDs, electric stimulation, and/or the local application of pharmacological agents. No one has examined functional changes in the brain/cortex in association with pain in MS to date, however, this is a promising topic for future studies.

The goal of another possible future study, could be to look for additional evidence of functional changes affecting inhibitory neurons (particularly PV+ interneurons) and disinhibition within S1 in the model. Various results in Chapter 4 point to a loss of phasic / PV+ interneuron-mediated inhibition in S1 (ie. reduced FAI 'surround inhibition', loss of cortical PNNs, and transient reduction in peri-somatic PV+ staining). However, the 'surround inhibition' signal we measured could conceivably represent metabolic undershoot or exhaustion - possibly in astrocytes, which make only a minor contribution to the 'positive/bright' FAI signal, but a larger contribution to the later-phase 'negative/dark' FAI signal - as opposed to GABA-mediated inhibition and reduced spiking activity in S1 neurons. It would therefore be

useful to confirm that there is, in fact, a reduction in functional inhibition (esp. PV+ interneuron mediated/feed-forward phasic inhibition) in S1/in EAE with other methods. As in the DH, this could be accomplished with electrophysiology, or with  $Ca^{2+}$  imaging of labelled neuronal populations.

As noted in the introductory chapter, the establishment or disruption of PV+ interneuron-mediated inhibition and PV-associated PNNs, is known to regulate critical period plasticity in the cortex. It would be interesting to further explore the link between PV interneurons/PNNs and plasticity and pain in S1 in EAE by other methods as well. Perhaps PNNs could be directly targeted and/or restored through some treatment or manipulation. CSPGs, which PNNs are composed from, can be experimentally digested in the cortex by application of the enzyme chondroitinase, however this would arguably be of little value in EAE since PNNs are already mostly disrupted even at early disease time points. As a treatment approach, there may be agents that either protect or stabilize the ECM/PNNs. One possible approach for targeting/inhibiting the degradation of PNNs could be to inhibit the secretion or activity of MMPs in S1, which likely mediate PNN degradation in the model. While there are no treatments (to the author's knowledge) that can specifically restore previously degraded PNNs, it may hypothetically be possible to increase the synthesis and/or secretion of ECM components (ie. CSPGs) by targeting astrocytes. On a functional level, PV+ interneuron-mediated inhibition could be specifically augmented either through optogenetic methods, DREADDs, or pharmacologically with subunit specific GABA-AR positive allosteric modulators - as specific forms of inhibition within the neocortex are mediated by GABA-ARs with specific subunit compositions [55, 56]. Phasic inhibition of cortical pyramidal neurons is, in large part, mediated by GABA-ARs expressing the  $\alpha 1$  subunit [57-59]. Additionally, PV+/fast-spiking interneurons in the cortex are reliant on the potassium channel  $K_v3.1$  (and sometimes  $K_v3.2$ ) in order to express their characteristic fast-spiking behavior [60]. These channels can be experimentally modulated [61], which might help to restore or further disrupt cortical inhibition/plasticity. Lastly, it may be worth investigating the role of the protein Otx2 (orthodenticle homeobox 2) in the model. The experience-dependant/PNN-mediated capture of Otx2, and its continuous internalization/capture within

PV+ interneurons, has been shown to play a crucial role in regulating critical period plasticity in V1 during development, and in experience-dependent plasticity in adults [62-64]. Chondroitinase-mediated digestion of PNNs releases Otx2 from PV+ neurons, and reopens the critical window in V1, as does treatment with a short interfering oligopeptide (RK protein) that disrupts Otx2 localization within PV+ neurons [62]. If Otx2 could be trapped within PV+ neurons, it might hypothetically restrict neocortical plasticity even if PNNs become disrupted. More generally, cortical plasticity in EAE could be investigated and/or targeted by measuring and/or manipulating (inhibiting) various cytokines (ie. sTNF $\alpha$ /IL-1B) that have previously been implicated in cortical plasticity in the model [45, 46, 65]. The acetylcholine (ACh) system is also highly implicated in some forms of cortical plasticity [66, 67], so CNS ACh levels might be worth investigating in EAE. Demyelination/dysmyelination in S1 should be also assessed the model (at early stages), as loss of myelin may play a role in generating sensitization/disinhibition within the cortex.

This study, and other recent studies, provide evidence that refutes the widely held notion that EAE is a “disease of the spinal cord”. In a general sense, this study also helps to validate the view that there is “pain” in the model, as opposed to mere spinal mediated hyperreflexivity. Furthermore, this study (and others) more generally helps to validate EAE as a model for MS, in that it should no longer be argued outright that EAE is confined to the spinal cord (whereas MS is thought of as a “disease of the brain”). Even at early time points, there are extensive functional/synaptic changes within the brain in EAE. Future studies that employ EAE as a model for pain in MS (or studies in MS itself) might do well to examine other cerebral/supraspinal regions of the “pain neuromatrix”. The thalamus, for instance, is one obvious target for investigation. Biochemical changes within the thalamus that may be related to hyperexcitability and/or excitotoxicity and neurodegeneration, have been observed in MS patients [68, 69]. Whether these changes are directly associated with pain in the disease is not known. Electrophysiology or functional imaging could be used to explore the question of hyperexcitability in the thalamus in EAE in future studies. Based on the changes we have observed in S1 and the SCDH, one

would predict that there is sensitization/hyperexcitability within the thalamus as well. Similar studies could be conducted which investigate and/or manipulate the ACC and/or insula, as functional activity and synaptic alterations within these regions are known to be causally linked with both acute and pathological/chronic pain. One other pain-associated brain region that has been explored in the C57/BL6/MOG<sub>35-55</sub> EAE model is the habenula. Olechowski et al. (unpublished findings) previously found increased expression of c-Fos in the lateral habenula(e). As noted, other studies in our lab (by Musgrave/Benson) demonstrated that, in the brain as a whole, there is a reduction in monoamine and GABA content (and elevated glutamate), as measured by HPLC [29, 70, 71]. More targeted measurements of these transmitters (or other transmitters/metabolites) could be made using various approaches, such as HPLC analysis of specifically isolated tissues, *in vivo* microdialysis etc.

#### **5.4 - Conclusions**

Together, these three studies establish the anti-allodynic/antinociceptive properties of PLZ - the effects of which appear to be related to its ability to augment inhibition in the CNS (DH/S1) by a monoamine- and possibly GABA-related mechanism. They also help establish that central sensitization, involving both functional and structural plasticity within the DH and S1, occurs in EAE - and is associated with pain behaviors/allodynia in the model. Treatment with PLZ generally did not affect basal nociceptive sensitivity/responses in control animals, but reduced nociceptive responding/allodynia in EAE and the 2<sup>nd</sup> phase of the formalin assay, both of which involve central sensitization. PLZ, or other treatments that boost inhibition through a synergistic combination of mechanisms, may be useful for treating neuropathic pain in MS. Future experiments should further examine functional and structural/synaptic plasticity, and disrupted E-I balance in the neocortex, in EAE/MS; and should investigate treatment approaches that directly target this plasticity. Potentially, intervening against these forms of plasticity early on in MS disease progression could prevent the establishment of long term CNS changes/plasticity that underlie chronic/neuropathic pain.

## 5.5 - REFERENCES

1. Ban, T.A., *Capsules: History of Psychopharmacology*.
2. Heal, D.J., et al., *Amphetamine, past and present – a pharmacological and clinical perspective*. Journal of Psychopharmacology (Oxford, England), 2013. **27**(6): p. 479-496.
3. Stolerman, I.P., *Encyclopedia of Psychopharmacology*, I.P. Stolerman, Editor 2010, SpringerReference.
4. Nolan, C.M., S.V. Goldberg, and S.E. Buskin, *Hepatotoxicity associated with isoniazid preventive therapy: A 7-year survey from a public health tuberculosis clinic*. JAMA, 1999. **281**(11): p. 1014-1018.
5. Pleasure, H., *Psychiatric and neurological side-effects of isoniazid and iproniazid*. A.M.A. Archives of Neurology & Psychiatry, 1954. **72**(3): p. 313-320.
6. Shulman, K.I., N. Herrmann, and S.E. Walker, *Current Place of Monoamine Oxidase Inhibitors in the Treatment of Depression*. CNS drugs, 2013. **27**(10): p. 789-797.
7. Maxwell, M., *Drug Discovery*. 1990.
8. Ramachandrai, C.T., et al., *Antidepressants: From MAOIs to SSRIs and more*. Indian Journal of Psychiatry, 2011. **53**(2): p. 180-182.
9. Grady, M.M. and S.M. Stahl, *Practical guide for prescribing MAOIs: debunking myths and removing barriers*. CNS spectrums, 2012. **17**(1): p. 2-10.
10. McCabe-Sellers, B.J., C.G. Staggs, and M.L. Bogle, *Tyramine in foods and monoamine oxidase inhibitor drugs: A crossroad where medicine, nutrition, pharmacy, and food industry converge*. Journal of Food Composition and Analysis, 2006. **19**: p. S58-S65.
11. Folks, D.G., *Monoamine oxidase inhibitors: reappraisal of dietary considerations*. J Clin Psychopharmacol, 1983. **3**(4): p. 249-52.
12. Fiedorowicz, J.G. and K.L. Swartz, *The Role of Monoamine Oxidase Inhibitors in Current Psychiatric Practice*. Journal of psychiatric practice, 2004. **10**(4): p. 239-248.
13. Song, M.-S., et al., *An update on amine oxidase inhibitors: Multifaceted drugs*. Progress in Neuro-Psychopharmacology and Biological Psychiatry, 2013. **44**: p. 118-124.
14. Parent, M.B., et al., *Effects of the antidepressant/antipanic drug phenelzine and its putative metabolite phenylethylidenehydrazine on extracellular gamma-aminobutyric acid levels in the striatum*. Biochem Pharmacol, 2002. **63**(1): p. 57-64.
15. McManus, D.J., et al., *Effects of the antidepressant/antipanic drug phenelzine on GABA concentrations and GABA-transaminase activity in rat brain*. Biochem Pharmacol, 1992. **43**(11): p. 2486-9.
16. MacKenzie, E.M., et al., *Phenelzine: An Old Drug That May Hold Clues to The Development of New Neuroprotective Agents*. Klinik Psikofarmakoloji Bülteni-Bulletin of Clinical Psychopharmacology, 2010. **20**(2): p. 179-186.
17. Michael-Titus, A.T., et al., *Imipramine and phenelzine decrease glutamate overflow in the prefrontal cortex--a possible mechanism of neuroprotection in major depression?* Neuroscience, 2000. **100**(4): p. 681-4.
18. Yang, J. and J. Shen, *In vivo evidence for reduced cortical glutamate-glutamine cycling in rats treated with the antidepressant/antipanic drug phenelzine*. Neuroscience, 2005. **135**(3): p. 927-37.
19. Lee, I., et al., *Analgesic properties of meperidine, amitriptyline and phenelzine in mice*. Canadian Anaesthetists' Society Journal, 1983. **30**(5): p. 501-505.
20. EMELE, J.F., J. SHANAMAN, and M.R. WARREN, *THE ANALGESIC ACTIVITY OF PHENELZINE AND OTHER COMPOUNDS*. Journal of Pharmacology and Experimental Therapeutics, 1961. **134**(2): p. 206-209.
21. Schulze, D.R., F.I. Carroll, and L.R. McMahon, *Interactions between dopamine transporter and cannabinoid receptor ligands in rhesus monkeys*. Psychopharmacology (Berl), 2012. **222**(3): p. 425-38.
22. Excellium Pharmaceutical, I., *IMIPRAMINE HYDROCHLORIDE Prescribing Information*.

23. Medicine, N.-U.S.N.L.o. *Imipramine*. [cited 2017; Available from: <https://medlineplus.gov/druginfo/meds/a682389.html>.
24. Mifflin, K.A., et al., *Manipulation of Neurotransmitter Levels Has Differential Effects on Formalin-Evoked Nociceptive Behavior in Male and Female Mice*. *The Journal of Pain*, 2016. **17**(4): p. 483-498.
25. Hunskaar, S. and K. Hole, *The formalin test in mice: dissociation between inflammatory and non-inflammatory pain*. *Pain*, 1987. **30**(1): p. 103-14.
26. Abbadie, C., et al., *Differential contribution of the two phases of the formalin test to the pattern of c-fos expression in the rat spinal cord: studies with remifentanyl and lidocaine*. *Pain*, 1997. **69**(1-2): p. 101-110.
- 27.Coderre, T.J., A.L. Vaccarino, and R. Melzack, *Central nervous system plasticity in the tonic pain response to subcutaneous formalin injection*. *Brain Research*, 1990. **535**(1): p. 155-158.
28. Coderre, T.J. and R. Melzack, *The contribution of excitatory amino acids to central sensitization and persistent nociception after formalin-induced tissue injury*. *The Journal of Neuroscience*, 1992. **12**(9): p. 3665.
29. Benson, C.A., et al., *The MAO inhibitor phenelzine can improve functional outcomes in mice with established clinical signs in experimental autoimmune encephalomyelitis (EAE)*. *Behav Brain Res*, 2013. **252**: p. 302-11.
30. Musgrave, T., et al., *The MAO inhibitor phenelzine improves functional outcomes in mice with experimental autoimmune encephalomyelitis (EAE)*. *Brain, behavior, and immunity*, 2011. **25**(8): p. 1677-88.
31. Bullitt, E., *Expression of C-fos-like protein as a marker for neuronal activity following noxious stimulation in the rat*. *The Journal of comparative neurology*, 1990. **296**(4): p. 517-530.
32. Gao, Y.-J. and R.-R. Ji, *c-Fos and pERK, which is a better marker for neuronal activation and central sensitization after noxious stimulation and tissue injury?* *Open Pain J*, 2009. **2**: p. 11-17.
33. Sardella, T.C., et al., *Dynorphin is expressed primarily by GABAergic neurons that contain galanin in the rat dorsal horn*. *Molecular pain*, 2011. **7**(1): p. 76.
34. Polgár, E., et al., *A Quantitative Study of Inhibitory Interneurons in Laminae I-III of the Mouse Spinal Dorsal Horn*. *PLoS ONE*, 2013. **8**(10): p. e78309.
35. Doolen, S., et al., *Peripheral nerve injury increases glutamate-evoked calcium mobilization in adult spinal cord neurons*. *Molecular pain*, 2012. **8**: p. 56.
36. Malcolm, D.E., et al., *Phenelzine reduces plasma vitamin B6*. *Journal of Psychiatry and Neuroscience*, 1994. **19**(5): p. 332-334.
37. Olechowski, C.J., J.J. Truong, and B.J. Kerr, *Neuropathic pain behaviours in a chronic-relapsing model of experimental autoimmune encephalomyelitis (EAE)*. *Pain*, 2009. **141**(1-2): p. 156-64.
38. Olechowski, C.J., et al., *A diminished response to formalin stimulation reveals a role for the glutamate transporters in the altered pain sensitivity of mice with experimental autoimmune encephalomyelitis (EAE)*. *Pain*, 2010. **149**(3): p. 565-72.
39. Olechowski, C.J., et al., *Changes in nociceptive sensitivity and object recognition in experimental autoimmune encephalomyelitis (EAE)*. *Experimental neurology*, 2013. **241**(0): p. 113-121.
40. Peirs, C., et al., *Dorsal Horn Circuits for Persistent Mechanical Pain*. *Neuron*, 2015. **87**(4): p. 797-812.
41. Peirs, C. and R.P. Seal, *Neural circuits for pain: Recent advances and current views*. *Science*, 2016. **354**(6312): p. 578.
42. Lieu, A., G. Tenorio, and B.J. Kerr, *Protein kinase C gamma (PKC $\gamma$ ) as a novel marker to assess the functional status of the corticospinal tract in experimental autoimmune encephalomyelitis (EAE)*. *Journal of neuroimmunology*, 2013. **256**(1): p. 43-48.
43. Falco, A., et al., *Reduction in parvalbumin-positive interneurons and inhibitory input in the cortex of mice with experimental autoimmune encephalomyelitis*. *Exp Brain Res*, 2014. **232**(7): p. 2439-49.
44. Rossi, S., et al., *Impaired striatal GABA transmission in experimental autoimmune encephalomyelitis*. *Brain, Behavior, and Immunity*, 2011. **25**(5): p. 947-956.

45. Rossi, S., et al., *Tumor necrosis factor is elevated in progressive multiple sclerosis and causes excitotoxic neurodegeneration*. Multiple Sclerosis Journal, 2013. **20**(3): p. 304-312.
46. Mandolesi, G., et al., *IL-1beta dependent cerebellar synaptopathy in a mouse model of multiple sclerosis*. Cerebellum, 2015. **14**(1): p. 19-22.
47. Zhu, W., et al., *Elevated expression of fractalkine (CX3CL1) and fractalkine receptor (CX3CR1) in the dorsal root ganglia and spinal cord in experimental autoimmune encephalomyelitis: implications in multiple sclerosis-induced neuropathic pain*. Biomed Res Int, 2013. **2013**: p. 480702.
48. Begum, F., et al., *Elevation of tumor necrosis factor alpha in dorsal root ganglia and spinal cord is associated with neuroimmune modulation of pain in an animal model of multiple sclerosis*. Journal of neuroimmune pharmacology : the official journal of the Society on NeuroImmune Pharmacology, 2013. **8**(3): p. 677-90.
49. Melanson, M., et al., *Experimental autoimmune encephalomyelitis-induced upregulation of tumor necrosis factor-alpha in the dorsal root ganglia*. Multiple sclerosis, 2009. **15**(10): p. 1135-45.
50. Rodrigues, D.H., et al., *IL-1 $\beta$  Is Involved with the Generation of Pain in Experimental Autoimmune Encephalomyelitis*. Molecular neurobiology, 2016. **53**(9): p. 6540-6547.
51. Nessler, S., et al., *Effect of minocycline in experimental autoimmune encephalomyelitis*. Annals of neurology, 2002. **52**(5): p. 689-690.
52. Reinert, K.C., et al., *Cellular and metabolic origins of flavoprotein autofluorescence in the cerebellar cortex in vivo*. Cerebellum, 2011. **10**(3): p. 585-99.
53. Tambalo, S., et al., *Functional Magnetic Resonance Imaging of Rats with Experimental Autoimmune Encephalomyelitis Reveals Brain Cortex Remodeling*. J Neurosci, 2015. **35**(27): p. 10088-100.
54. Shih, Y.Y., et al., *Striatal and cortical BOLD, blood flow, blood volume, oxygen consumption, and glucose consumption changes in noxious forepaw electrical stimulation*. J Cereb Blood Flow Metab, 2011. **31**(3): p. 832-41.
55. Hiu, T., et al., *Enhanced phasic GABA inhibition during the repair phase of stroke: a novel therapeutic target*. Brain, 2016. **139**(2): p. 468-480.
56. Rudolph, U. and H. Möhler, *GABA(A) Receptor Subtypes: Therapeutic Potential in Down Syndrome, Affective Disorders, Schizophrenia, and Autism*. Annual review of pharmacology and toxicology, 2014. **54**: p. 483-507.
57. Lewis, D.A., et al., *Cortical parvalbumin interneurons and cognitive dysfunction in schizophrenia*. Trends in Neurosciences. **35**(1): p. 57-67.
58. Farrant, M. and Z. Nusser, *Variations on an inhibitory theme: phasic and tonic activation of GABA<sub>A</sub> receptors*. Nat Rev Neurosci, 2005. **6**(3): p. 215-229.
59. Fagiolini, M., et al., *Specific GABA<sub>A</sub> Circuits for Visual Cortical Plasticity*. Science, 2004. **303**(5664): p. 1681-1683.
60. Chow, A., et al., *K(+) channel expression distinguishes subpopulations of parvalbumin- and somatostatin-containing neocortical interneurons*. J Neurosci, 1999. **19**(21): p. 9332-45.
61. Rosato-Siri, M.D., et al., *A Novel Modulator of Kv3 Potassium Channels Regulates the Firing of Parvalbumin-Positive Cortical Interneurons*. The Journal of pharmacology and experimental therapeutics, 2015. **354**(3): p. 251-60.
62. Beurdeley, M., et al., *Otx2 binding to perineuronal nets persistently regulates plasticity in the mature visual cortex*. J Neurosci, 2012. **32**(27): p. 9429-37.
63. Bernard, C. and A. Prochiantz, *Otx2-PNN Interaction to Regulate Cortical Plasticity*. Neural Plast, 2016. **2016**: p. 7931693.
64. Sugiyama, S., et al., *Experience-dependent transfer of Otx2 homeoprotein into the visual cortex activates postnatal plasticity*. Cell, 2008. **134**(3): p. 508-20.
65. Yang, G., et al., *Peripheral elevation of TNF-alpha leads to early synaptic abnormalities in the mouse somatosensory cortex in experimental autoimmune encephalomyelitis*. Proc Natl Acad Sci U S A, 2013. **110**(25): p. 10306-11.

66. Kuo, M.-F., et al., *Focusing Effect of Acetylcholine on Neuroplasticity in the Human Motor Cortex*. The Journal of Neuroscience, 2007. **27**(52): p. 14442.
67. Bear, M.F. and W. Singer, *Modulation of visual cortical plasticity by acetylcholine and noradrenaline*. Nature, 1986. **320**(6058): p. 172-6.
68. Tisell, A., et al., *Increased Concentrations of Glutamate and Glutamine in Normal-Appearing White Matter of Patients with Multiple Sclerosis and Normal MR Imaging Brain Scans*. PLoS ONE, 2013. **8**(4): p. e61817.
69. Geurts, J.J.G., et al., *MR spectroscopic evidence for thalamic and hippocampal, but not cortical, damage in multiple sclerosis*. Magnetic Resonance in Medicine, 2006. **55**(3): p. 478-483.
70. Musgrave, T., et al., *The MAO inhibitor phenelzine improves functional outcomes in mice with experimental autoimmune encephalomyelitis (EAE)*. Brain, Behavior, and Immunity, 2011. **25**(8): p. 1677-1688.
71. Musgrave, T., et al., *Tissue concentration changes of amino acids and biogenic amines in the central nervous system of mice with experimental autoimmune encephalomyelitis (EAE)*. Neurochemistry international, 2011. **59**(1): p. 28-38.

## WORKS CITED

### Chapter 1

1. Sandkühler, J., *Models and Mechanisms of Hyperalgesia and Allodynia*. *Physiological Reviews*, 2009. **89**(2): p. 707.
2. Ji, R.-R., et al., *Central sensitization and LTP: do pain and memory share similar mechanisms?* *Trends in Neurosciences*, 2003. **26**(12): p. 696-705.
3. Julius, D.M., E.W., *Cellular and molecular properties of primary afferent neurons*, in *Melzack & Wall's Textbook of Pain 5th Ed.* 2005, Elsevier.
4. Woolf, C.J., *What is this thing called pain?* *The Journal of clinical investigation*, 2010. **120**(11): p. 3742-3744.
5. Craig, A.D., *Pain mechanisms: labeled lines versus convergence in central processing*. *Annu Rev Neurosci*, 2003. **26**: p. 1-30.
6. Woolf, C.J.S., M. W., *Plasticity and pain: role of the dorsal horn*, in *Wall & Melzack's Textbook of Pain, 5th ed.* 2005, Elsevier.
7. Millan, M.J., *The induction of pain: an integrative review*. *Progress in neurobiology*, 1999. **57**(1): p. 1-164.
8. Todd, A.K., H.R., *Neuroanatomical substrates of spinal nociception*, in *Wall & Melzack's Textbook of Pain, 5th ed.* 2005, Elsevier.
9. Costigan, M., J. Scholz, and C.J. Woolf, *Neuropathic Pain: A Maladaptive Response of the Nervous System to Damage*. *Annual review of neuroscience*, 2009. **32**: p. 1-32.
10. Doleys, D.M., *Chronic Pain as a Hypothetical Construct: A Practical and Philosophical Consideration*. *Frontiers in Psychology*, 2017. **8**: p. 664.
11. Goldberg, D.S. and S.J. McGee, *Pain as a global public health priority*. *BMC Public Health*, 2011. **11**: p. 770.
12. von Hehn, Christian A., R. Baron, and Clifford J. Woolf, *Deconstructing the Neuropathic Pain Phenotype to Reveal Neural Mechanisms*. *Neuron*, 2012. **73**(4): p. 638-652.
13. Campbell, J.N. and R.A. Meyer, *Mechanisms of Neuropathic Pain*. *Neuron*, 2006. **52**(1): p. 77-92.
14. Verma, S., L. Estanislao, and D. Simpson, *HIV-Associated Neuropathic Pain*. *CNS drugs*, 2005. **19**(4): p. 325-334.
15. Khan, F. and J. Pallant, *Chronic Pain in Multiple Sclerosis: Prevalence, Characteristics, and Impact on Quality of Life in an Australian Community Cohort*. *The Journal of Pain*, 2007. **8**(8): p. 614-623.
16. Woolf, C.J., *Central sensitization: Implications for the diagnosis and treatment of pain*. *Pain*, 2011. **152**(3 Suppl): p. S2-15.
17. Treede, R.-D., et al., *A classification of chronic pain for ICD-11*. *Pain*, 2015. **156**(6): p. 1003-1007.
18. Bushnell, C.M.A., A. V., *Representation of pain in the brain*, in *Wall & Melzack's Textbook of Pain, 5th ed.* 2005, Elsevier.
19. Todd, A.J., *Neuronal circuitry for pain processing in the dorsal horn*. *Nature reviews. Neuroscience*, 2010. **11**(12): p. 823-836.
20. Dubin, A.E. and A. Patapoutian, *Nociceptors: the sensors of the pain pathway*. *The Journal of clinical investigation*, 2010. **120**(11): p. 3760-3772.
21. Kuner, R., *Central mechanisms of pathological pain*. *Nat Med*, 2010. **16**(11): p. 1258-66.
22. Woolf, C.J., *Neuronal Plasticity: Increasing the Gain in Pain*. *Science*, 2000. **288**(5472): p. 1765-1768.
23. Peirs, C. and R.P. Seal, *Neural circuits for pain: Recent advances and current views*. *Science*, 2016. **354**(6312): p. 578.
24. Braz, J., et al., *Transmitting pain and itch messages: A contemporary view of the spinal cord circuits that generate Gate Control*. *Neuron*, 2014. **82**(3): p. 522-536.
25. Melzack, R. and P.D. Wall, *Pain mechanisms: a new theory*. *Science*, 1965. **150**(3699): p. 971-9.

26. Kuner, R. and H. Flor, *Structural plasticity and reorganisation in chronic pain*. Nat Rev Neurosci, 2017. **18**(1): p. 20-30.
27. Woolf, C.J., *Evidence for a central component of post-injury pain hypersensitivity*. Nature, 1983. **306**(5944): p. 686-8.
28. Millan, M.J., *Descending control of pain*. Progress in neurobiology, 2002. **66**(6): p. 355-474.
29. Latremoliere, A. and C.J. Woolf, *Central Sensitization: A Generator of Pain Hypersensitivity by Central Neural Plasticity*. The journal of pain : official journal of the American Pain Society, 2009. **10**(9): p. 895-926.
30. Peirs, C., et al., *Dorsal Horn Circuits for Persistent Mechanical Pain*. Neuron, 2015. **87**(4): p. 797-812.
31. Nickel, F.T., et al., *Mechanisms of neuropathic pain*. European Neuropsychopharmacology, 2012. **22**(2): p. 81-91.
32. Hunskaar, S. and K. Hole, *The formalin test in mice: dissociation between inflammatory and non-inflammatory pain*. Pain, 1987. **30**(1): p. 103-14.
33. Scholz, J. and C.J. Woolf, *The neuropathic pain triad: neurons, immune cells and glia*. Nat Neurosci, 2007. **10**(11): p. 1361-8.
34. Iannitti, T., B.J. Kerr, and B.K. Taylor, *Mechanisms and Pharmacology of Neuropathic Pain in Multiple Sclerosis*. Current topics in behavioral neurosciences, 2014. **20**: p. 75-97.
35. Luo, C., et al., *Activity-dependent potentiation of calcium signals in spinal sensory networks in inflammatory pain states*. Pain, 2008. **140**(2): p. 358-367.
36. Sandkühler, J., et al., *Synaptic mechanisms of hyperalgesia*. Prog Brain Res, 2000. **129**: p. 81-100.
37. Taylor, B.K. and G. Corder, *Endogenous analgesia, dependence, and latent pain sensitization*. Curr Top Behav Neurosci, 2014. **20**: p. 283-325.
38. Sandkühler, J. and J. Lee, *How to erase memory traces of pain and fear*. Trends in Neurosciences, 2013. **36**(6): p. 343-352.
39. Gwak, Y.S. and C.E. Hulsebosch, *GABA and central neuropathic pain following spinal cord injury*. Neuropharmacology, 2011. **60**(5): p. 799-808.
40. Coull, J.A., et al., *Trans-synaptic shift in anion gradient in spinal lamina I neurons as a mechanism of neuropathic pain*. Nature, 2003. **424**(6951): p. 938-42.
41. Pertovaara, A., *Noradrenergic pain modulation*. Progress in neurobiology, 2006. **80**(2): p. 53-83.
42. Sonohata, M., et al., *Actions of noradrenaline on substantia gelatinosa neurones in the rat spinal cord revealed by in vivo patch recording*. The Journal of physiology, 2004. **555**(2): p. 515-526.
43. Jeong, C.Y., J.I. Choi, and M.H. Yoon, *Roles of serotonin receptor subtypes for the antinociception of 5-HT in the spinal cord of rats*. European Journal of Pharmacology, 2004. **502**(3): p. 205-211.
44. Bardin, L., J. Lavarenne, and A. Eschalier, *Serotonin receptor subtypes involved in the spinal antinociceptive effect of 5-HT in rats*. Pain, 2000. **86**(1-2): p. 11-18.
45. Abe, K., et al., *Responses to 5-HT in morphologically identified neurons in the rat substantia gelatinosa in vitro*. Neuroscience, 2009. **159**(1): p. 316-324.
46. Xie, D.J., et al., *Identification of 5-HT receptor subtypes enhancing inhibitory transmission in the rat spinal dorsal horn in vitro*. Molecular pain, 2012. **8**: p. 58.
47. Buritova, J., et al., *Effects of the high-efficacy 5-HT<sub>1A</sub> receptor agonist, F 13640 in the formalin pain model: A c-Fos study*. European Journal of Pharmacology, 2005. **514**(2): p. 121-130.
48. Millan, M.J., *Serotonin and pain: evidence that activation of 5-HT<sub>1A</sub> receptors does not elicit antinociception against noxious thermal, mechanical and chemical stimuli in mice*. Pain, 1994. **58**(1): p. 45-61.
49. Bardin, L., *The complex role of serotonin and 5-HT receptors in chronic pain*. Behav Pharmacol, 2011. **22**(5-6): p. 390-404.
50. Chiang, C.-Y., et al., *Astroglial Glutamate-Glutamine Shuttle Is Involved in Central Sensitization of Nociceptive Neurons in Rat Medullary Dorsal Horn*. The Journal of Neuroscience, 2007. **27**(34): p. 9068.

51. Scholz, J. and C.J. Woolf, *The neuropathic pain triad: neurons, immune cells and glia*. Nature Neuroscience, 2007. **10**(11): p. 1361-1368.
52. Ferrini, F., et al., *Morphine hyperalgesia gated through microglia-mediated disruption of neuronal Cl<sup>-</sup> homeostasis*. Nat Neurosci, 2013. **16**(2): p. 183-192.
53. Sorge, R.E., et al., *Different immune cells mediate mechanical pain hypersensitivity in male and female mice*. Nature Neuroscience, 2015. **18**(8): p. 1081-1083.
54. Mapplebeck, J.C., S. Beggs, and M.W. Salter, *Sex differences in pain: a tale of two immune cells*. Pain, 2016. **157 Suppl 1**: p. S2-6.
55. Brings, V.E. and M.J. Zylka, *Sex, drugs and pain control*. Nat Neurosci, 2015. **18**(8): p. 1059-60.
56. Ji, R.R., Z.Z. Xu, and Y.J. Gao, *Emerging targets in neuroinflammation-driven chronic pain*. Nat Rev Drug Discov, 2014. **13**(7): p. 533-48.
57. Tracey, I. and P.W. Mantyh, *The Cerebral Signature for Pain Perception and Its Modulation*. Neuron, 2007. **55**(3): p. 377-391.
58. Melzack, R., *From the gate to the neuromatrix*. Pain, 1999. **82**: p. S121-S126.
59. May, A., *Chronic pain may change the structure of the brain*. Pain, 2008. **137**(1): p. 7-15.
60. Legrain, V., et al., *The pain matrix reloaded: A salience detection system for the body*. Progress in neurobiology, 2011. **93**(1): p. 111-124.
61. Willis, W.D. and K.N. Westlund, *Neuroanatomy of the pain system and of the pathways that modulate pain*. J Clin Neurophysiol, 1997. **14**(1): p. 2-31.
62. Ab Aziz, C.B. and A.H. Ahmad, *The Role of the Thalamus in Modulating Pain*. The Malaysian Journal of Medical Sciences : MJMS, 2006. **13**(2): p. 11-18.
63. Feldmeyer, D., *Excitatory neuronal connectivity in the barrel cortex*. Frontiers in Neuroanatomy, 2012. **6**: p. 24.
64. Cruikshank, S.J., T.J. Lewis, and B.W. Connors, *Synaptic basis for intense thalamocortical activation of feedforward inhibitory cells in neocortex*. Nat Neurosci, 2007. **10**(4): p. 462-8.
65. Porter, J.T., C.K. Johnson, and A. Agmon, *Diverse Types of Interneurons Generate Thalamus-Evoked Feedforward Inhibition in the Mouse Barrel Cortex*. The Journal of Neuroscience, 2001. **21**(8): p. 2699.
66. Castro-Alamancos, M.A. and B.W. Connors, *THALAMOCORTICAL SYNAPSES*. Progress in neurobiology, 1997. **51**(6): p. 581-606.
67. Likavčanová, K., et al., *Metabolic changes in the thalamus after spinal cord injury followed by proton MR spectroscopy*. Magnetic Resonance in Medicine, 2008. **59**(3): p. 499-506.
68. Nakamura, A., et al., *Somatosensory Homunculus as Drawn by MEG*. NeuroImage, 1998. **7**(4): p. 377-386.
69. Liang, M., A. Mouraux, and G.D. Iannetti, *Parallel Processing of Nociceptive and Non-nociceptive Somatosensory Information in the Human Primary and Secondary Somatosensory Cortices: Evidence from Dynamic Causal Modeling of Functional Magnetic Resonance Imaging Data*. The Journal of Neuroscience, 2011. **31**(24): p. 8976.
70. Aronoff, R., et al., *Long-range connectivity of mouse primary somatosensory barrel cortex*. European Journal of Neuroscience, 2010. **31**(12): p. 2221-2233.
71. Mao, T., et al., *Long-Range Neuronal Circuits Underlying the Interaction between Sensory and Motor Cortex*. Neuron, 2011. **72**(1): p. 111-123.
72. Eto, K., et al., *Inter-regional contribution of enhanced activity of the primary somatosensory cortex to the anterior cingulate cortex accelerates chronic pain behavior*. J Neurosci, 2011. **31**(21): p. 7631-6.
73. Price, D.D., *Central neural mechanisms that interrelate sensory and affective dimensions of pain*. Mol Interv, 2002. **2**(6): p. 392-403, 339.
74. Lübke, J. and D. Feldmeyer, *Excitatory signal flow and connectivity in a cortical column: focus on barrel cortex*. Brain Structure and Function, 2007. **212**(1): p. 3-17.
75. Douglas, R.J. and K.A. Martin, *Neuronal circuits of the neocortex*. Annu Rev Neurosci, 2004. **27**: p. 419-51.

76. Lefort, S., et al., *The Excitatory Neuronal Network of the C2 Barrel Column in Mouse Primary Somatosensory Cortex*. Neuron. **61**(2): p. 301-316.
77. Isaacson, J.S. and M. Scanziani, *How Inhibition Shapes Cortical Activity*. Neuron, 2011. **72**(2): p. 231-243.
78. Markram, H., et al., *Interneurons of the neocortical inhibitory system*. Nat Rev Neurosci, 2004. **5**(10): p. 793-807.
79. Zhang, Z. and Q.-Q. Sun, *The Balance Between Excitation And Inhibition And Functional Sensory Processing In The Somatosensory Cortex*, in *International review of neurobiology*, N.K.K.I. Masayuki Kobayashi and L.W. John, Editors. 2011, Academic Press. p. 305-333.
80. Ascoli, G.A.Y., R., *Petilla terminology: nomenclature of features of GABAergic interneurons of the cerebral cortex*. Nat Rev Neurosci, 2008. **9**(7): p. 557-568.
81. Jones, E.G., *Cortical and subcortical contributions to activity-dependent plasticity in primate somatosensory cortex*. Annu Rev Neurosci, 2000. **23**: p. 1-37.
82. Feldman, D.E. and M. Brecht, *Map plasticity in somatosensory cortex*. Science, 2005. **310**(5749): p. 810-5.
83. Griffen, T.C. and A. Maffei, *GABAergic synapses: their plasticity and role in sensory cortex*. Frontiers in Cellular Neuroscience, 2014. **8**: p. 91.
84. Donato, F., S.B. Rompani, and P. Caroni, *Parvalbumin-expressing basket-cell network plasticity induced by experience regulates adult learning*. Nature, 2013. **504**(7479): p. 272-6.
85. Sugiyama, S., et al., *Experience-dependent transfer of Otx2 homeoprotein into the visual cortex activates postnatal plasticity*. Cell, 2008. **134**(3): p. 508-20.
86. Hensch, T.K. and M. Fagiolini, *Excitatory-inhibitory balance and critical period plasticity in developing visual cortex*. Prog Brain Res, 2005. **147**: p. 115-24.
87. Foeller, E. and D.E. Feldman, *Synaptic basis for developmental plasticity in somatosensory cortex*. Curr Opin Neurobiol, 2004. **14**(1): p. 89-95.
88. Hensch, T.K., *Critical period plasticity in local cortical circuits*. Nat Rev Neurosci, 2005. **6**(11): p. 877-888.
89. Fox, K., *A critical period for experience-dependent synaptic plasticity in rat barrel cortex*. J Neurosci, 1992. **12**(5): p. 1826-38.
90. Stern, E.A., M. Maravall, and K. Svoboda, *Rapid Development and Plasticity of Layer 2/3 Maps in Rat Barrel Cortex In Vivo*. Neuron. **31**(2): p. 305-315.
91. Diamond, M.E., M. Armstrong-James, and F.F. Ebner, *Experience-dependent plasticity in adult rat barrel cortex*. Proceedings of the National Academy of Sciences of the United States of America, 1993. **90**(5): p. 2082-6.
92. Trachtenberg, J.T., et al., *Long-term in vivo imaging of experience-dependent synaptic plasticity in adult cortex*. Nature, 2002. **420**(6917): p. 788-794.
93. Kim, S.K. and J. Nabekura, *Rapid synaptic remodeling in the adult somatosensory cortex following peripheral nerve injury and its association with neuropathic pain*. J Neurosci, 2011. **31**(14): p. 5477-82.
94. Komagata, S., et al., *Nociceptive cortical responses during capsaicin-induced tactile allodynia in mice with spinal dorsal column lesioning*. Neurosci Res, 2011. **69**(4): p. 348-51.
95. Fox, K., *Anatomical pathways and molecular mechanisms for plasticity in the barrel cortex*. Neuroscience, 2002. **111**(4): p. 799-814.
96. Carcea, I. and R.C. Froemke, *Cortical Plasticity, Excitatory-Inhibitory Balance, and Sensory Perception*. Prog Brain Res, 2013. **207**: p. 65-90.
97. Feldman, D.E., *Synaptic Mechanisms for Plasticity in Neocortex*. Annual review of neuroscience, 2009. **32**: p. 33-55.
98. Winship, I.R. and T.H. Murphy, *Remapping the somatosensory cortex after stroke: insight from imaging the synapse to network*. The Neuroscientist : a review journal bringing neurobiology, neurology and psychiatry, 2009. **15**(5): p. 507-24.

99. Li, C.X., J.C. Callaway, and R.S. Waters, *Removal of GABAergic inhibition alters subthreshold input in neurons in forepaw barrel subfield (FBS) in rat first somatosensory cortex (SI) after digit stimulation*. Experimental Brain Research, 2002. **145**(4): p. 411-428.
100. Petersen, C.C.H. and B. Sakmann, *Functionally Independent Columns of Rat Somatosensory Barrel Cortex Revealed with Voltage-Sensitive Dye Imaging*. The Journal of Neuroscience, 2001. **21**(21): p. 8435.
101. Moore, C.I. and S.B. Nelson, *Spatio-Temporal Subthreshold Receptive Fields in the Vibrissa Representation of Rat Primary Somatosensory Cortex*. Journal of neurophysiology, 1998. **80**(6): p. 2882.
102. Petersen, C.C.H., A. Grinvald, and B. Sakmann, *Spatiotemporal Dynamics of Sensory Responses in Layer 2/3 of Rat Barrel Cortex Measured &emdash; In Vivo &emdash; by Voltage-Sensitive Dye Imaging Combined with Whole-Cell Voltage Recordings and Neuron Reconstructions*. The Journal of Neuroscience, 2003. **23**(4): p. 1298.
103. Brown, C.E., et al., *In Vivo Voltage-Sensitive Dye Imaging in Adult Mice Reveals That Somatosensory Maps Lost to Stroke Are Replaced over Weeks by New Structural and Functional Circuits with Prolonged Modes of Activation within Both the Peri-Infarct Zone and Distant Sites*. The Journal of Neuroscience, 2009. **29**(6): p. 1719.
104. Bushnell, M.C., et al., *Pain perception: Is there a role for primary somatosensory cortex?* Proceedings of the National Academy of Sciences, 1999. **96**(14): p. 7705-7709.
105. Kim, W., S.K. Kim, and J. Nabekura, *Functional and structural plasticity in the primary somatosensory cortex associated with chronic pain*. Journal of neurochemistry, 2017. **141**(4): p. 499-506.
106. Kong, J., et al., *S1 is associated with chronic low back pain: a functional and structural MRI study*. Molecular pain, 2013. **9**: p. 43.
107. Kim, W. and S.K. Kim, *Neural circuit remodeling and structural plasticity in the cortex during chronic pain*. Korean J Physiol Pharmacol, 2016. **20**(1): p. 1-8.
108. DaSilva, A.F., et al., *Thickening in the somatosensory cortex of patients with migraine*. Neurology, 2007. **69**(21): p. 1990-5.
109. Kim, C.E., et al., *Large-scale plastic changes of the brain network in an animal model of neuropathic pain*. NeuroImage, 2014. **98**: p. 203-15.
110. Vierck, C.J., et al., *Role of primary somatosensory cortex in the coding of pain*. Pain, 2013. **154**(3): p. 334-44.
111. Kim, S.K., et al., *Phase-specific plasticity of synaptic structures in the somatosensory cortex of living mice during neuropathic pain*. Molecular pain, 2011. **7**: p. 87.
112. Kim, S.K., K. Eto, and J. Nabekura, *Synaptic structure and function in the mouse somatosensory cortex during chronic pain: in vivo two-photon imaging*. Neural Plast, 2012. **2012**: p. 640259.
113. Komagata, S., et al., *Initial phase of neuropathic pain within a few hours after nerve injury in mice*. J Neurosci, 2011. **31**(13): p. 4896-905.
114. Sharma, N.K., et al., *Primary somatosensory cortex in chronic low back pain - a H-MRS study*. J Pain Res, 2011. **4**: p. 143-50.
115. Christopherson, K.S., et al., *Thrombospondins Are Astrocyte-Secreted Proteins that Promote CNS Synaptogenesis*. Cell, 2005. **120**(3): p. 421-433.
116. Kim, S.K., et al., *Cortical astrocytes rewire somatosensory cortical circuits for peripheral neuropathic pain*. The Journal of clinical investigation, 2016. **126**(5): p. 1983-1997.
117. Vargová, L. and E. Syková, *Astrocytes and extracellular matrix in extrasynaptic volume transmission*. Philosophical Transactions of the Royal Society B: Biological Sciences, 2014. **369**(1654): p. 20130608.
118. Dityatev, A., M. Schachner, and P. Sonderegger, *The dual role of the extracellular matrix in synaptic plasticity and homeostasis*. Nat Rev Neurosci, 2010. **11**(11): p. 735-746.
119. Wang, D. and J. Fawcett, *The perineuronal net and the control of CNS plasticity*. Cell and tissue research, 2012. **349**(1): p. 147-160.

120. Zhuo, M., *Cortical excitation and chronic pain*. Trends in Neurosciences, 2008. **31**(4): p. 199-207.
121. Eto, K., et al., *Enhanced GABAergic Activity in the Mouse Primary Somatosensory Cortex Is Insufficient to Alleviate Chronic Pain Behavior with Reduced Expression of Neuronal Potassium-Chloride Cotransporter*. The Journal of Neuroscience, 2012. **32**(47): p. 16552.
122. Blom, S.M., et al., *Nerve injury-induced neuropathic pain causes disinhibition of the anterior cingulate cortex*. J Neurosci, 2014. **34**(17): p. 5754-64.
123. Kang, S.J., et al., *Bidirectional modulation of hyperalgesia via the specific control of excitatory and inhibitory neuronal activity in the ACC*. Mol Brain, 2015. **8**(1): p. 81.
124. Wrigley, P.J., et al., *Neuropathic pain and primary somatosensory cortex reorganization following spinal cord injury*. Pain, 2009. **141**(1-2): p. 52-9.
125. Yanagisawa, T., et al., *Induced sensorimotor brain plasticity controls pain in phantom limb patients*. Nat Commun, 2016. **7**: p. 13209.
126. Knecht, S., et al., *Cortical reorganization in human amputees and mislocalization of painful stimuli to the phantom limb*. Neuroscience letters, 1995. **201**(3): p. 262-264.
127. Gustin, S.M., et al., *Pain and plasticity: is chronic pain always associated with somatosensory cortex activity and reorganization?* J Neurosci, 2012. **32**(43): p. 14874-84.
128. Moseley, G.L. and H. Flor, *Targeting cortical representations in the treatment of chronic pain: a review*. Neurorehabil Neural Repair, 2012. **26**(6): p. 646-52.
129. Naro, A., et al., *Non-invasive Brain Stimulation, a Tool to Revert Maladaptive Plasticity in Neuropathic Pain*. Front Hum Neurosci, 2016. **10**: p. 376.
130. Fuchs, P.N., et al., *The anterior cingulate cortex and pain processing*. Frontiers in Integrative Neuroscience, 2014. **8**: p. 35.
131. Apkarian, A.V., et al., *Human brain mechanisms of pain perception and regulation in health and disease*. European journal of pain, 2005. **9**(4): p. 463-84.
132. Bliss, T.V., et al., *Synaptic plasticity in the anterior cingulate cortex in acute and chronic pain*. Nat Rev Neurosci, 2016. **17**(8): p. 485-96.
133. Xu, H., et al., *Presynaptic and postsynaptic amplifications of neuropathic pain in the anterior cingulate cortex*. J Neurosci, 2008. **28**(29): p. 7445-53.
134. Toyoda, H., M.G. Zhao, and M. Zhuo, *Enhanced quantal release of excitatory transmitter in anterior cingulate cortex of adult mice with chronic pain*. Molecular pain, 2009. **5**: p. 4.
135. Cao, X.Y., et al., *Characterization of intrinsic properties of cingulate pyramidal neurons in adult mice after nerve injury*. Molecular pain, 2009. **5**: p. 73.
136. Zhuo, M., *A synaptic model for pain: long-term potentiation in the anterior cingulate cortex*. Mol Cells, 2007. **23**(3): p. 259-71.
137. Johansen, J.P., H.L. Fields, and B.H. Manning, *The affective component of pain in rodents: Direct evidence for a contribution of the anterior cingulate cortex*. Proceedings of the National Academy of Sciences, 2001. **98**(14): p. 8077-8082.
138. Tolomeo, S., et al., *A causal role for the anterior mid-cingulate cortex in negative affect and cognitive control*. Brain, 2016. **139**(Pt 6): p. 1844-54.
139. Rainville, P., et al., *Pain Affect Encoded in Human Anterior Cingulate But Not Somatosensory Cortex*. Science, 1997. **277**(5328): p. 968.
140. Craig, A.D., et al., *Functional imaging of an illusion of pain*. Nature, 1996. **384**(6606): p. 258-60.
141. Gu, L., et al., *Pain inhibition by optogenetic activation of specific anterior cingulate cortical neurons*. PLoS ONE, 2015. **10**(2): p. e0117746.
142. Li, X.Y., et al., *Erasing injury-related cortical synaptic potentiation as a new treatment for chronic pain*. J Mol Med (Berl), 2011. **89**(9): p. 847-55.
143. Navratilova, E., et al., *Endogenous opioid activity in the anterior cingulate cortex is required for relief of pain*. J Neurosci, 2015. **35**(18): p. 7264-71.
144. Gorka, S.M., et al., *Opioid modulation of resting-state anterior cingulate cortex functional connectivity*. J Psychopharmacol, 2014. **28**(12): p. 1115-24.

145. Bingel, U., et al., *Mechanisms of placebo analgesia: rACC recruitment of a subcortical antinociceptive network*. Pain, 2006. **120**(1-2): p. 8-15.
146. Vogt, B.A., *Pain and emotion interactions in subregions of the cingulate gyrus*. Nat Rev Neurosci, 2005. **6**(7): p. 533-44.
147. Barthas, F., et al., *The anterior cingulate cortex is a critical hub for pain-induced depression*. Biol Psychiatry, 2015. **77**(3): p. 236-45.
148. Koga, K., et al., *Coexistence of two forms of LTP in ACC provides a synaptic mechanism for the interactions between anxiety and chronic pain*. Neuron, 2015. **85**(2): p. 377-89.
149. Zhuo, M., *Neural Mechanisms Underlying Anxiety-Chronic Pain Interactions*. Trends Neurosci, 2016. **39**(3): p. 136-45.
150. Calejesan, A.A., S.J. Kim, and M. Zhuo, *Descending facilitatory modulation of a behavioral nociceptive response by stimulation in the adult rat anterior cingulate cortex*. European journal of pain, 2000. **4**(1): p. 83-96.
151. Craig, A.D., *How do you feel? Interoception: the sense of the physiological condition of the body*. Nat Rev Neurosci, 2002. **3**(8): p. 655-666.
152. Craig, A.D., *Interoception: the sense of the physiological condition of the body*. Curr Opin Neurobiol, 2003. **13**(4): p. 500-505.
153. Brooks, J.C.W., et al., *Somatotopic organisation of the human insula to painful heat studied with high resolution functional imaging*. NeuroImage, 2005. **27**(1): p. 201-209.
154. Lu, C., et al., *Insular Cortex is Critical for the Perception, Modulation, and Chronification of Pain*. Neuroscience Bulletin, 2016. **32**(2): p. 191-201.
155. Wager, T.D., et al., *An fMRI-Based Neurologic Signature of Physical Pain*. New England Journal of Medicine, 2013. **368**(15): p. 1388-1397.
156. Segerdahl, A.R., et al., *The dorsal posterior insula subserves a fundamental role in human pain*. Nat Neurosci, 2015. **18**(4): p. 499-500.
157. Seifert, F. and C. Maihöfner, *Central mechanisms of experimental and chronic neuropathic pain: Findings from functional imaging studies*. Cellular and Molecular Life Sciences, 2008. **66**(3): p. 375.
158. Ostrowsky, K., et al., *Representation of pain and somatic sensation in the human insula: a study of responses to direct electrical cortical stimulation*. Cereb Cortex, 2002. **12**(4): p. 376-85.
159. Starr, C.J., et al., *Roles of the Insular Cortex in the Modulation of Pain: Insights from Brain Lesions*. J Neurosci, 2009. **29**(9): p. 2684-2694.
160. Watson, C.J., *Insular balance of glutamatergic and GABAergic signaling modulates pain processing*. Pain, 2016. **157**(10): p. 2194-2207.
161. Mutschler, I., et al., *Pain and emotion in the insular cortex: evidence for functional reorganization in major depression*. Neuroscience letters, 2012. **520**(2): p. 204-209.
162. Seminowicz, D.A. and M. Moayed, *The Dorsolateral Prefrontal Cortex in Acute and Chronic Pain*. The Journal of Pain.
163. Mouraux, A., et al., *A multisensory investigation of the functional significance of the "pain matrix"*. NeuroImage, 2011. **54**(3): p. 2237-2249.
164. Compston, A. and A. Coles, *Multiple sclerosis*. Lancet, 2002. **359**(9313): p. 1221-31.
165. Compston, A. and A. Coles, *Multiple sclerosis*. The Lancet. **372**(9648): p. 1502-1517.
166. Murray, T.J., *The history of multiple sclerosis: the changing frame of the disease over the centuries*. J Neurol Sci, 2009. **277** Suppl 1: p. S3-8.
167. Mallucci, G., et al., *The role of immune cells, glia and neurons in white and gray matter pathology in multiple sclerosis*. Progress in neurobiology, 2015. **0**: p. 1-22.
168. Hauser, S.L. and J.R. Oksenberg, *The Neurobiology of Multiple Sclerosis: Genes, Inflammation, and Neurodegeneration*. Neuron. **52**(1): p. 61-76.
169. Browne, P., et al., *Atlas of Multiple Sclerosis 2013: A growing global problem with widespread inequity*. Neurology, 2014. **83**(11): p. 1022-1024.

170. Dendrou, C.A., L. Fugger, and M.A. Friese, *Immunopathology of multiple sclerosis*. Nat Rev Immunol, 2015. **15**(9): p. 545-558.
171. Oksenberg, J.R., et al., *The genetics of multiple sclerosis: SNPs to pathways to pathogenesis*. Nat Rev Genet, 2008. **9**(7): p. 516-526.
172. Belbasis, L., et al., *Environmental risk factors and multiple sclerosis: an umbrella review of systematic reviews and meta-analyses*. The Lancet Neurology. **14**(3): p. 263-273.
173. O’Gorman, C., R. Lucas, and B. Taylor, *Environmental Risk Factors for Multiple Sclerosis: A Review with a Focus on Molecular Mechanisms*. International Journal of Molecular Sciences, 2012. **13**(9): p. 11718-11752.
174. Vollmer, T., *The natural history of relapses in multiple sclerosis*. Journal of the neurological sciences, 2007. **256**, **Supplement 1**: p. S5-S13.
175. Miller, D.H., D.T. Chard, and O. Ciccarelli, *Clinically isolated syndromes*. The Lancet Neurology. **11**(2): p. 157-169.
176. Ciccarelli, O. and A.T. Toosy, *Conversion from clinically isolated syndrome to multiple sclerosis: A large multicentre study*. Multiple Sclerosis Journal, 2015. **21**(8): p. 967-968.
177. Kuhle, J., et al., *Conversion from clinically isolated syndrome to multiple sclerosis: A large multicentre study*. Multiple sclerosis, 2015. **21**(8): p. 1013-24.
178. Fisniku, L.K., et al., *Disability and T2 MRI lesions: a 20-year follow-up of patients with relapse onset of multiple sclerosis*. Brain, 2008. **131**(Pt 3): p. 808-17.
179. Rovaris, M., et al., *Secondary progressive multiple sclerosis: current knowledge and future challenges*. The Lancet Neurology, 2006. **5**(4): p. 343-354.
180. Miller, D.H. and S.M. Leary, *Primary-progressive multiple sclerosis*. The Lancet Neurology, 2007. **6**(10): p. 903-912.
181. Lassmann, H., W. Bruck, and C. Lucchinetti, *Heterogeneity of multiple sclerosis pathogenesis: implications for diagnosis and therapy*. Trends in molecular medicine, 2001. **7**(3): p. 115-21.
182. Disanto, G., et al., *Heterogeneity in Multiple Sclerosis: Scratching the Surface of a Complex Disease*. Autoimmune Diseases, 2011. **2011**.
183. Franklin, R.J., *Why does remyelination fail in multiple sclerosis?* Nat Rev Neurosci, 2002. **3**(9): p. 705-14.
184. Dutta, R. and B.D. Trapp, *Mechanisms of neuronal dysfunction and degeneration in multiple sclerosis*. Progress in neurobiology, 2011. **93**(1): p. 1-12.
185. Stadelmann, C., C. Wegner, and W. Brück, *Inflammation, demyelination, and degeneration — Recent insights from MS pathology*. Biochimica et Biophysica Acta (BBA) - Molecular Basis of Disease, 2011. **1812**(2): p. 275-282.
186. Bar-Or, A., *The immunology of multiple sclerosis*. Semin Neurol, 2008. **28**(1): p. 29-45.
187. Sospedra, M. and R. Martin, *Immunology of multiple sclerosis*. Annu Rev Immunol, 2005. **23**: p. 683-747.
188. Becher, B., S. Spath, and J. Goverman, *Cytokine networks in neuroinflammation*. Nat Rev Immunol, 2017. **17**(1): p. 49-59.
189. Jangi, S., et al., *Alterations of the human gut microbiome in multiple sclerosis*. Nat Commun, 2016. **7**: p. 12015.
190. Geurts, J.J. and F. Barkhof, *Grey matter pathology in multiple sclerosis*. Lancet Neurol, 2008. **7**(9): p. 841-51.
191. Stadelmann, C., C. Wegner, and W. Bruck, *Inflammation, demyelination, and degeneration - recent insights from MS pathology*. Biochimica et biophysica acta, 2011. **1812**(2): p. 275-82.
192. Goverman, J., *Autoimmune T cell responses in the central nervous system*. Nature reviews. Immunology, 2009. **9**(6): p. 393.
193. Stys, P.K., et al., *Will the real multiple sclerosis please stand up?* Nat Rev Neurosci, 2012. **13**(7): p. 507-514.

194. Steinman, M.D.L., *Multiple Sclerosis: A Coordinated Immunological Attack against Myelin in the Central Nervous System*. Cell, 1996. **85**(3): p. 299-302.
195. Steinman, L., *Multiple sclerosis: a two-stage disease*. Nat Immunol, 2001. **2**(9): p. 762-764.
196. Stadelmann, C., *Multiple sclerosis as a neurodegenerative disease: pathology, mechanisms and therapeutic implications*. Curr Opin Neurol, 2011. **24**(3): p. 224-9.
197. Sospedra, M. and R. Martin, *Immunology of Multiple Sclerosis*. Semin Neurol, 2016. **36**(2): p. 115-27.
198. Turner, M.D., et al., *Cytokines and chemokines: At the crossroads of cell signalling and inflammatory disease*. Biochimica et Biophysica Acta (BBA) - Molecular Cell Research, 2014. **1843**(11): p. 2563-2582.
199. Maimone, D., G.C. Guazzi, and P. Annunziata, *IL-6 detection in multiple sclerosis brain*. J Neurol Sci, 1997. **146**(1): p. 59-65.
200. Carpintero, R. and D. Burger, *IFN $\beta$  and glatiramer acetate trigger different signaling pathways to regulate the IL-1 system in multiple sclerosis*. Communicative & integrative biology, 2011. **4**(1): p. 112-114.
201. Guo, H., J.B. Callaway, and J.P.Y. Ting, *Inflammasomes: mechanism of action, role in disease, and therapeutics*. Nat Med, 2015. **21**(7): p. 677-687.
202. Özenci, V., et al., *Multiple sclerosis is associated with an imbalance between tumour necrosis factor-alpha (TNF- $\alpha$ )- and IL-10-secreting blood cells that is corrected by interferon-beta (IFN- $\beta$ ) treatment*. Clinical and experimental immunology, 2000. **120**(1): p. 147-153.
203. Selmaj, K., et al., *Identification of lymphotoxin and tumor necrosis factor in multiple sclerosis lesions*. Journal of Clinical Investigation, 1991. **87**(3): p. 949-954.
204. *TNF neutralization in MS: results of a randomized, placebo-controlled multicenter study. The Lenercept Multiple Sclerosis Study Group and The University of British Columbia MS/MRI Analysis Group*. Neurology, 1999. **53**(3): p. 457-65.
205. Beattie, E.C., et al., *Control of Synaptic Strength by Glial TNF $\alpha$* . Science, 2002. **295**(5563): p. 2282-2285.
206. Mandolesi, G., et al., *IL-1beta dependent cerebellar synaptopathy in a mouse model of multiple sclerosis*. Cerebellum, 2015. **14**(1): p. 19-22.
207. Yang, G., et al., *Peripheral elevation of TNF-alpha leads to early synaptic abnormalities in the mouse somatosensory cortex in experimental autoimmune encephalomyelitis*. Proc Natl Acad Sci U S A, 2013. **110**(25): p. 10306-11.
208. Kawasaki, Y., et al., *Cytokine Mechanisms of Central Sensitization: Distinct and Overlapping Role of Interleukin-1 $\beta$ , Interleukin-6, and Tumor Necrosis Factor- $\alpha$  in Regulating Synaptic and Neuronal Activity in the Superficial Spinal Cord*. The Journal of Neuroscience, 2008. **28**(20): p. 5189-5194.
209. Khairova, R.A., et al., *A potential role for pro-inflammatory cytokines in regulating synaptic plasticity in major depressive disorder*. International Journal of Neuropsychopharmacology, 2009. **12**(4): p. 561-578.
210. Heesen, C., et al., *Fatigue in multiple sclerosis: an example of cytokine mediated sickness behaviour?* Journal of neurology, neurosurgery, and psychiatry, 2006. **77**(1): p. 34-39.
211. Di Filippo, M., et al., *Neuroinflammation and synaptic plasticity: theoretical basis for a novel, immune-centred, therapeutic approach to neurological disorders*. Trends Pharmacol Sci, 2008. **29**(8): p. 402-412.
212. McAfoose, J. and B.T. Baune, *Evidence for a cytokine model of cognitive function*. Neuroscience & Biobehavioral Reviews, 2009. **33**(3): p. 355-366.
213. Trapp, B.D. and K.A. Nave, *Multiple sclerosis: an immune or neurodegenerative disorder?* Annu Rev Neurosci, 2008. **31**: p. 247-69.
214. Trapp, B.D. and P.K. Stys, *Virtual hypoxia and chronic necrosis of demyelinated axons in multiple sclerosis*. The Lancet Neurology, 2009. **8**(3): p. 280-291.
215. Dutta, R., et al., *Mitochondrial dysfunction as a cause of axonal degeneration in multiple sclerosis patients*. Annals of neurology, 2006. **59**(3): p. 478-489.

216. Stys, P.K., S.G. Waxman, and B.R. Ransom, *Na(+)-Ca2+ exchanger mediates Ca2+ influx during anoxia in mammalian central nervous system white matter*. *Annals of neurology*, 1991. **30**(3): p. 375-80.
217. Stys, P.K., *General mechanisms of axonal damage and its prevention*. *Journal of the neurological sciences*, 2005. **233**(1-2): p. 3-13.
218. Mahad, D.H., B.D. Trapp, and H. Lassmann, *Pathological mechanisms in progressive multiple sclerosis*. *The Lancet Neurology*, 2015. **14**(2): p. 183-193.
219. Mathur, D., et al., *Perturbed Glucose Metabolism: Insights into Multiple Sclerosis Pathogenesis*. *Frontiers in neurology*, 2014. **5**: p. 250.
220. Mandolesi, G., et al., *Synaptopathy connects inflammation and neurodegeneration in multiple sclerosis*. *Nat Rev Neurol*, 2015. **11**(12): p. 711-24.
221. Nisticò, R., et al., *Synaptic plasticity in multiple sclerosis and in experimental autoimmune encephalomyelitis*. *Philosophical Transactions of the Royal Society B: Biological Sciences*, 2014. **369**(1633): p. 20130162.
222. Nistico, R., et al., *Inflammation subverts hippocampal synaptic plasticity in experimental multiple sclerosis*. *PLoS ONE*, 2013. **8**(1): p. e54666.
223. Falco, A., et al., *Reduction in parvalbumin-positive interneurons and inhibitory input in the cortex of mice with experimental autoimmune encephalomyelitis*. *Exp Brain Res*, 2014. **232**(7): p. 2439-49.
224. Ziehn, M.O., et al., *Hippocampal CA1 atrophy and synaptic loss during experimental autoimmune encephalomyelitis, EAE*. *Laboratory investigation; a journal of technical methods and pathology*, 2010. **90**(5): p. 774-786.
225. Rossi, S., et al., *Inflammation inhibits GABA transmission in multiple sclerosis*. *Multiple Sclerosis Journal*, 2012. **18**(11): p. 1633-1635.
226. Kettenmann, H., F. Kirchhoff, and A. Verkhratsky, *Microglia: New Roles for the Synaptic Stripper*. *Neuron*, 2013. **77**(1): p. 10-18.
227. Stephan, A.H., B.A. Barres, and B. Stevens, *The complement system: an unexpected role in synaptic pruning during development and disease*. *Annu Rev Neurosci*, 2012. **35**: p. 369-89.
228. Audoin, B., et al., *Compensatory cortical activation observed by fMRI during a cognitive task at the earliest stage of multiple sclerosis*. *Human Brain Mapping*, 2003. **20**(2): p. 51-58.
229. Rocca, M.A. and M. Filippi, *Functional MRI in Multiple Sclerosis*. *Journal of Neuroimaging*, 2007. **17**: p. 36S-41S.
230. Pantano, P., C. Mainero, and F. Caramia, *Functional Brain Reorganization in Multiple Sclerosis: Evidence from fMRI Studies*. *Journal of Neuroimaging*, 2006. **16**(2): p. 104-114.
231. Potter, L.E., et al., *Altered excitatory-inhibitory balance within somatosensory cortex is associated with enhanced plasticity and pain sensitivity in a mouse model of multiple sclerosis*. *Journal of neuroinflammation*, 2016. **13**(1): p. 142.
232. Cifelli, A. and P.M. Matthews, *Cerebral plasticity in multiple sclerosis: insights from fMRI*. *Multiple Sclerosis Journal*, 2002. **8**(3): p. 193-199.
233. Goldenberg, M.M., *Multiple Sclerosis Review*. *Pharmacy and Therapeutics*, 2012. **37**(3): p. 175-184.
234. Fox, E.J., *Management of worsening multiple sclerosis with mitoxantrone: a review*. *Clin Ther*, 2006. **28**(4): p. 461-74.
235. Atkins, H.L., et al., *Immunoablation and autologous haemopoietic stem-cell transplantation for aggressive multiple sclerosis: a multicentre single-group phase 2 trial*. *The Lancet*, 2016. **388**(10044): p. 576-585.
236. Branas, P., et al., *Treatments for fatigue in multiple sclerosis: a rapid and systematic review*. *Health Technol Assess*, 2000. **4**(27): p. 1-61.
237. Rizzo, M.A., et al., *Prevalence and treatment of spasticity reported by multiple sclerosis patients*. *Multiple Sclerosis Journal*, 2004. **10**(5): p. 589-595.
238. O'Carroll, C.B., et al., *Is donepezil effective for multiple sclerosis-related cognitive dysfunction? A critically appraised topic*. *The neurologist*, 2012. **18**(1): p. 51-4.

239. Canada, M.S.o. *Symptom Management (Treatments - Medications)*. [website] 2017 [cited 2017 6/12/2017]; Available from: <https://mssociety.ca/managing-ms/treatments/medications/symptom-management>.
240. Baxter, A.G., *The origin and application of experimental autoimmune encephalomyelitis*. Nat Rev Immunol, 2007. **7**(11): p. 904-912.
241. Constantinescu, C.S., et al., *Experimental autoimmune encephalomyelitis (EAE) as a model for multiple sclerosis (MS)*. British Journal of Pharmacology, 2011. **164**(4): p. 1079-1106.
242. Höftberger, R., et al., *Autoimmune encephalitis in humans: how closely does it reflect multiple sclerosis ?* Acta Neuropathologica Communications, 2015. **3**(1): p. 80.
243. Rivers, T.M., D.H. Sprunt, and G.P. Berry, *OBSERVATIONS ON ATTEMPTS TO PRODUCE ACUTE DISSEMINATED ENCEPHALOMYELITIS IN MONKEYS*. The Journal of experimental medicine, 1933. **58**(1): p. 39-53.
244. Rivers, T.M. and F.F. Schwentker, *ENCEPHALOMYELITIS ACCOMPANIED BY MYELIN DESTRUCTION EXPERIMENTALLY PRODUCED IN MONKEYS*. The Journal of experimental medicine, 1935. **61**(5): p. 689-702.
245. Gold, R., C. Linington, and H. Lassmann, *Understanding pathogenesis and therapy of multiple sclerosis via animal models: 70 years of merits and culprits in experimental autoimmune encephalomyelitis research*. Brain, 2006. **129**(8): p. 1953-1971.
246. Ransohoff, R.M., *Animal models of multiple sclerosis: the good, the bad and the bottom line*. Nat Neurosci, 2012. **15**(8): p. 1074-1077.
247. Robinson, A.P., et al., *The experimental autoimmune encephalomyelitis (EAE) model of MS: utility for understanding disease pathophysiology and treatment*. Handbook of clinical neurology, 2014. **122**: p. 173-189.
248. Furlan, R., C. Cuomo, and G. Martino, *Animal models of multiple sclerosis*. Methods in molecular biology, 2009. **549**: p. 157-73.
249. Croxford, A.L., F.C. Kurschus, and A. Waisman, *Mouse models for multiple sclerosis: Historical facts and future implications*. Biochimica et Biophysica Acta (BBA) - Molecular Basis of Disease, 2011. **1812**(2): p. 177-183.
250. Fletcher, J.M., et al., *T cells in multiple sclerosis and experimental autoimmune encephalomyelitis*. Clinical & Experimental Immunology, 2010. **162**(1): p. 1-11.
251. t Hart, B.A., B. Gran, and R. Weissert, *EAE: imperfect but useful models of multiple sclerosis*. Trends in molecular medicine, 2011. **17**(3): p. 119-25.
252. Yong, T., G.A. Meininger, and D.S. Linthicum, *Enhancement of histamine-induced vascular leakage by pertussis toxin in SJL/J mice but not BALB/c mice*. Journal of neuroimmunology, 1993. **45**(1-2): p. 47-52.
253. Linthicum, D.S., J.J. Munoz, and A. Blaskett, *Acute experimental autoimmune encephalomyelitis in mice. I. Adjuvant action of Bordetella pertussis is due to vasoactive amine sensitization and increased vascular permeability of the central nervous system*. Cell Immunol, 1982. **73**(2): p. 299-310.
254. Hofstetter, H.H., C.L. Shive, and T.G. Forsthuber, *Pertussis toxin modulates the immune response to neuroantigens injected in incomplete Freund's adjuvant: induction of Th1 cells and experimental autoimmune encephalomyelitis in the presence of high frequencies of Th2 cells*. Journal of immunology, 2002. **169**(1): p. 117-25.
255. Greter, M., et al., *Dendritic cells permit immune invasion of the CNS in an animal model of multiple sclerosis*. Nat Med, 2005. **11**(3): p. 328-334.
256. The Lenercept Multiple Sclerosis Study, G. and M.S.M.R.I.A.G. The University of British Columbia, *TNF neutralization in MS: Results of a randomized, placebo-controlled multicenter study*. Neurology, 1999. **53**(3): p. 457-457.
257. Burger, D., et al., *Glatiramer acetate increases IL-1 receptor antagonist but decreases T cell-induced IL-1beta in human monocytes and multiple sclerosis*. Proceedings of the National Academy of Sciences of the United States of America, 2009. **106**(11): p. 4355-9.

258. Glabinski, A.R. and R.M. Ransohoff, *The Chemokine System in Experimental Autoimmune Encephalomyelitis*, in *Experimental Models of Multiple Sclerosis*, E. Lavi and C.S. Constantinescu, Editors. 2005, Springer US: Boston, MA. p. 363-377.
259. Archelos, J.J., S.C. Previtali, and H.-P. Hartung, *The role of integrins in immune-mediated diseases of the nervous system*. Trends in Neurosciences. **22**(1): p. 30-38.
260. Sunnemark, D., et al., *CX3CL1 (fractalkine) and CX3CR1 expression in myelin oligodendrocyte glycoprotein-induced experimental autoimmune encephalomyelitis: kinetics and cellular origin*. Journal of neuroinflammation, 2005. **2**: p. 17.
261. Yong, V.W., et al., *Elevation of matrix metalloproteinases (MMPs) in multiple sclerosis and impact of immunomodulators*. Journal of the neurological sciences, 2007. **259**(1-2): p. 79-84.
262. MacKenzie-Graham, A., et al., *Cortical atrophy in experimental autoimmune encephalomyelitis: in vivo imaging*. NeuroImage, 2012. **60**(1): p. 95-104.
263. Musella, A., et al., *Linking synaptopathy and gray matter damage in multiple sclerosis*. Mult Scler, 2015.
264. Centonze, D., et al., *Inflammation Triggers Synaptic Alteration and Degeneration in Experimental Autoimmune Encephalomyelitis*. The Journal of Neuroscience, 2009. **29**(11): p. 3442.
265. Tambalo, S., et al., *Functional Magnetic Resonance Imaging of Rats with Experimental Autoimmune Encephalomyelitis Reveals Brain Cortex Remodeling*. J Neurosci, 2015. **35**(27): p. 10088-100.
266. Rossi, S., et al., *Impaired striatal GABA transmission in experimental autoimmune encephalomyelitis*. Brain, Behavior, and Immunity, 2011. **25**(5): p. 947-956.
267. Smith, T., et al., *Autoimmune encephalomyelitis ameliorated by AMPA antagonists*. Nat Med, 2000. **6**(1): p. 62-6.
268. Pitt, D., P. Werner, and C.S. Raine, *Glutamate excitotoxicity in a model of multiple sclerosis*. Nat Med, 2000. **6**(1): p. 67-70.
269. Rossi, S., et al., *Abnormal activity of the Na/Ca exchanger enhances glutamate transmission in experimental autoimmune encephalomyelitis*. Brain, Behavior, and Immunity, 2010. **24**(8): p. 1379-1385.
270. Mandolesi, G., et al., *Cognitive deficits in experimental autoimmune encephalomyelitis: neuroinflammation and synaptic degeneration*. Neurological Sciences, 2010. **31**(2): p. 255-259.
271. Acharjee, S., et al., *Altered cognitive-emotional behavior in early experimental autoimmune encephalitis – Cytokine and hormonal correlates*. Brain, Behavior, and Immunity, 2013. **33**: p. 164-172.
272. Pollak, Y., et al., *Experimental autoimmune encephalomyelitis-associated behavioral syndrome as a model of 'depression due to multiple sclerosis'*. Brain, Behavior, and Immunity, 2002. **16**(5): p. 533-543.
273. Olechowski, C.J., J.J. Truong, and B.J. Kerr, *Neuropathic pain behaviours in a chronic-relapsing model of experimental autoimmune encephalomyelitis (EAE)*. Pain, 2009. **141**(1-2): p. 156-64.
274. Olechowski, C.J., et al., *Changes in nociceptive sensitivity and object recognition in experimental autoimmune encephalomyelitis (EAE)*. Experimental neurology, 2013. **241**(0): p. 113-121.
275. Musgrave, T., C.J. Olechowski, and B.J. Kerr, *Learning new tricks from an old dog: using experimental autoimmune encephalomyelitis to study comorbid symptoms in multiple sclerosis*. Pain Management, 2011. **1**(6): p. 571-576.
276. O'Connor, A.B., et al., *Pain associated with multiple sclerosis: systematic review and proposed classification*. Pain, 2008. **137**(1): p. 96-111.
277. Foley, P.L., et al., *Prevalence and natural history of pain in adults with multiple sclerosis: Systematic review and meta-analysis*. PAIN®, 2013. **154**(5): p. 632-642.
278. Svendsen, K.B., et al., *Sensory function and quality of life in patients with multiple sclerosis and pain*. Pain, 2005. **114**(3): p. 473-81.
279. Martinelli Boneschi, F., et al., *Lifetime and actual prevalence of pain and headache in multiple sclerosis*. Multiple Sclerosis Journal, 2008. **14**(4): p. 514-521.

280. Bermejo, P.E., C. Oreja-Guevara, and E. Diez-Tejedor, [*Pain in multiple sclerosis: prevalence, mechanisms, types and treatment*]. *Revista de neurologia*, 2010. **50**(2): p. 101-8.
281. Stenager, E., L. Knudsen, and K. Jensen, *Acute and chronic pain syndromes in multiple sclerosis*. *Acta neurologica Scandinavica*, 1991. **84**(3): p. 197-200.
282. Broła, W., K. Mitosek-Szewczyk, and J. Opara, *Symptomatology and pathogenesis of different types of pain in multiple sclerosis*. *Neurol Neurochir Pol*, 2014. **48**(4): p. 272-9.
283. Österberg, A. and J. Boivie, *Central pain in multiple sclerosis – Sensory abnormalities*. *European journal of pain*, 2010. **14**(1): p. 104-110.
284. Osterberg, A., J. Boivie, and K.A. Thuomas, *Central pain in multiple sclerosis--prevalence and clinical characteristics*. *European journal of pain*, 2005. **9**(5): p. 531-42.
285. Seixas, D., et al., *Pain in multiple sclerosis: A systematic review of neuroimaging studies*. *NeuroImage: Clinical*, 2014. **5**: p. 322-331.
286. Nurmikko, T.J., S. Gupta, and K. MacIver, *Multiple sclerosis-related central pain disorders*. *Curr Pain Headache Rep*, 2010. **14**(3): p. 189-95.
287. Nick, S.T., et al., *Multiple sclerosis and pain*. *Neurological research*, 2012.
288. Truini, A., et al., *Mechanisms of pain in multiple sclerosis: a combined clinical and neurophysiological study*. *Pain*, 2012. **153**(10): p. 2048-54.
289. Scherder, E., et al., *Pain in Parkinson's disease and multiple sclerosis: Its relation to the medial and lateral pain systems*. *Neuroscience & Biobehavioral Reviews*, 2005. **29**(7): p. 1047-1056.
290. Khan, N. and M.T. Smith, *Multiple sclerosis-induced neuropathic pain: pharmacological management and pathophysiological insights from rodent EAE models*. *Inflammopharmacology*, 2014. **22**(1): p. 1-22.
291. Solaro, C. and M. Messmer Uccelli, *Pharmacological management of pain in patients with multiple sclerosis*. *Drugs*, 2010. **70**(10): p. 1245-54.
292. Solaro, C. and M.M. Uccelli, *Management of pain in multiple sclerosis: a pharmacological approach*. *Nat Rev Neurol*, 2011. **7**(9): p. 519-27.
293. Grau-López, L., et al., *Analysis of the pain in multiple sclerosis patients*. *Neurología (English Edition)*, 2011. **26**(4): p. 208-213.
294. Lu, J., et al., *Pain in experimental autoimmune encephalitis: a comparative study between different mouse models*. *Journal of neuroinflammation*, 2012. **9**(1): p. 233.
295. Thibault, K., B. Calvino, and S. Pezet, *Characterisation of sensory abnormalities observed in an animal model of multiple sclerosis: a behavioural and pharmacological study*. *Eur J Pain*, 2011. **15**(3): p. 231 e1-16.
296. Steinman, L. and S.S. Zamvil, *Virtues and pitfalls of EAE for the development of therapies for multiple sclerosis*. *Trends in Immunology*. **26**(11): p. 565-571.
297. Aicher, S.A., et al., *Hyperalgesia in an animal model of multiple sclerosis*. *Pain*, 2004. **110**(3): p. 560-70.
298. Thorburn, K.C., et al., *Facial hypersensitivity and trigeminal pathology in mice with experimental autoimmune encephalomyelitis*. *Pain*, 2016. **157**(3): p. 627-42.
299. Fu, W. and B.K. Taylor, *Activation of cannabinoid CB2 receptors reduces hyperalgesia in an experimental autoimmune encephalomyelitis mouse model of multiple sclerosis*. *Neuroscience letters*, 2015. **595**: p. 1-6.
300. Yuan, S., Y. Shi, and S.J. Tang, *Wnt signaling in the pathogenesis of multiple sclerosis-associated chronic pain*. *Journal of neuroimmune pharmacology : the official journal of the Society on NeuroImmune Pharmacology*, 2012. **7**(4): p. 904-13.
301. Campbell, A.M., I.S. Zagon, and P.J. McLaughlin, *Opioid growth factor arrests the progression of clinical disease and spinal cord pathology in established experimental autoimmune encephalomyelitis*. *Brain Res*, 2012. **1472**: p. 138-48.

302. Lisi, L., et al., *Rapamycin reduces clinical signs and neuropathic pain in a chronic model of experimental autoimmune encephalomyelitis*. Journal of neuroimmunology, 2012. **243**(1-2): p. 43-51.
303. Dutra, R.C., et al., *The role of kinin B1 and B2 receptors in the persistent pain induced by experimental autoimmune encephalomyelitis (EAE) in mice: evidence for the involvement of astrocytes*. Neurobiology of disease, 2013. **54**: p. 82-93.
304. Rodrigues, D.H., et al., *IL-1 $\beta$  Is Involved with the Generation of Pain in Experimental Autoimmune Encephalomyelitis*. Molecular neurobiology, 2016. **53**(9): p. 6540-6547.
305. Grace, P.M., et al., *Behavioral assessment of neuropathic pain, fatigue, and anxiety in experimental autoimmune encephalomyelitis (EAE) and attenuation by interleukin-10 gene therapy*. Brain, Behavior, and Immunity, 2017. **59**: p. 49-54.
306. Lu, J., et al., *Pain in experimental autoimmune encephalitis: a comparative study between different mouse models*. Journal of neuroinflammation, 2012. **9**: p. 233-233.
307. Khan, N., et al., *Antiallodynic effects of alpha lipoic acid in an optimized RR-EAE mouse model of MS-neuropathic pain are accompanied by attenuation of upregulated BDNF-TrkB-ERK signaling in the dorsal horn of the spinal cord*. Pharmacology Research & Perspectives, 2015. **3**(3): p. e00137.
308. Schmitz, K., et al., *Dichotomy of CCL21 and CXCR3 in nerve injury-evoked and autoimmunity-evoked hyperalgesia*. Brain Behav Immun, 2013. **32**: p. 186-200.
309. Pender, M.P. and T.A. Sears, *Involvement of the dorsal root ganglion in acute experimental allergic encephalomyelitis in the Lewis rat. A histological and electrophysiological study*. J Neurol Sci, 1986. **72**(2-3): p. 231-42.
310. Pender, M.P. and T.A. Sears, *Vulnerability of the dorsal root ganglion in experimental allergic encephalomyelitis*. Clin Exp Neurol, 1985. **21**: p. 211-23.
311. Pender, M.P. and T.A. Sears, *The pathophysiology of acute experimental allergic encephalomyelitis in the rabbit*. Brain, 1984. **107 ( Pt 3)**: p. 699-726.
312. Xu, Z.-Z., et al., *Inhibition of mechanical allodynia in neuropathic pain by TLR5-mediated A-fiber blockade*. Nature medicine, 2015. **21**(11): p. 1326-1331.
313. Duffy, S.S., et al., *Peripheral and Central Neuroinflammatory Changes and Pain Behaviors in an Animal Model of Multiple Sclerosis*. Frontiers in Immunology, 2016. **7**: p. 369.
314. Wang, I.C., et al., *Peripheral sensory neuron injury contributes to neuropathic pain in experimental autoimmune encephalomyelitis*. 2017. **7**: p. 42304.
315. Gritsch, S., et al., *Oligodendrocyte ablation triggers central pain independently of innate or adaptive immune responses in mice*. Nat Commun, 2014. **5**: p. 5472.
316. Moalem, G. and D.J. Tracey, *Immune and inflammatory mechanisms in neuropathic pain*. Brain Research Reviews, 2006. **51**(2): p. 240-264.
317. Duffy, S.S., J.G. Lees, and G. Moalem-Taylor, *The Contribution of Immune and Glial Cell Types in Experimental Autoimmune Encephalomyelitis and Multiple Sclerosis*. Multiple sclerosis international, 2014. **2014**: p. 285245.
318. Olechowski, C.J., et al., *A diminished response to formalin stimulation reveals a role for the glutamate transporters in the altered pain sensitivity of mice with experimental autoimmune encephalomyelitis (EAE)*. Pain, 2010. **149**(3): p. 565-72.
319. Musgrave, T., et al., *Tissue concentration changes of amino acids and biogenic amines in the central nervous system of mice with experimental autoimmune encephalomyelitis (EAE)*. Neurochemistry international, 2011. **59**(1): p. 28-38.
320. Marte, A., et al., *Alterations of glutamate release in the spinal cord of mice with experimental autoimmune encephalomyelitis*. Journal of neurochemistry, 2010. **115**(2): p. 343-52.
321. Doolen, S., et al., *Peripheral nerve injury increases glutamate-evoked calcium mobilization in adult spinal cord neurons*. Molecular pain, 2012. **8**: p. 56.

322. Sung, B., G. Lim, and J. Mao, *Altered expression and uptake activity of spinal glutamate transporters after nerve injury contribute to the pathogenesis of neuropathic pain in rats*. The Journal of neuroscience : the official journal of the Society for Neuroscience, 2003. **23**(7): p. 2899-910.
323. Aicher, S.A., et al., *Hyperalgesia in an animal model of multiple sclerosis*. Pain, 2004. **110**(3): p. 560-570.
324. Melanson, M., et al., *Experimental autoimmune encephalomyelitis-induced upregulation of tumor necrosis factor-alpha in the dorsal root ganglia*. Multiple sclerosis, 2009. **15**(10): p. 1135-45.
325. Begum, F., et al., *Elevation of tumor necrosis factor alpha in dorsal root ganglia and spinal cord is associated with neuroimmune modulation of pain in an animal model of multiple sclerosis*. Journal of neuroimmune pharmacology : the official journal of the Society on NeuroImmune Pharmacology, 2013. **8**(3): p. 677-90.
326. Zhu, W., et al., *Elevated expression of fractalkine (CX3CL1) and fractalkine receptor (CX3CR1) in the dorsal root ganglia and spinal cord in experimental autoimmune encephalomyelitis: implications in multiple sclerosis-induced neuropathic pain*. Biomed Res Int, 2013. **2013**: p. 480702.
327. Sloane, E., et al., *Anti-inflammatory cytokine gene therapy decreases sensory and motor dysfunction in experimental Multiple Sclerosis: MOG-EAE behavioral and anatomical symptom treatment with cytokine gene therapy*. Brain Behav Immun, 2009. **23**(1): p. 92-100.
328. Mahad, D.J. and R.M. Ransohoff, *The role of MCP-1 (CCL2) and CCR2 in multiple sclerosis and experimental autoimmune encephalomyelitis (EAE)*. Semin Immunol, 2003. **15**(1): p. 23-32.
329. Ji, R.-R., et al., *MMP regulation of neuropathic pain*. Trends Pharmacol Sci, 2009. **30**(7): p. 336-340.
330. Ji, R.-R., Z.-Z. Xu, and Y.-J. Gao, *Emerging targets in neuroinflammation-driven chronic pain*. Nat Rev Drug Discov, 2014. **13**(7): p. 533-548.
331. Sun, J.H., et al., *MCP-1 enhances excitability of nociceptive neurons in chronically compressed dorsal root ganglia*. Journal of neurophysiology, 2006. **96**(5): p. 2189-99.
332. Tsuda, M., et al., *Neuronal and microglial mechanisms for neuropathic pain in the spinal dorsal horn and anterior cingulate cortex*. Journal of neurochemistry, 2017. **141**(4): p. 486-498.
333. Schomberg, D. and J.K. Olson, *Immune responses of microglia in the spinal cord: contribution to pain states*. Experimental neurology, 2012. **234**(2): p. 262-70.
334. Ramesh, G., A.G. MacLean, and M.T. Philipp, *Cytokines and Chemokines at the Crossroads of Neuroinflammation, Neurodegeneration, and Neuropathic Pain*. Mediators of Inflammation, 2013. **2013**: p. 20.
335. Nessler, S., et al., *Effect of minocycline in experimental autoimmune encephalomyelitis*. Annals of neurology, 2002. **52**(5): p. 689-690.
336. Benson, C., et al., *Voluntary wheel running delays disease onset and reduces pain hypersensitivity in early experimental autoimmune encephalomyelitis (EAE)*. Experimental neurology, 2015. **271**: p. 279-290.
337. MacKenzie, E.M., et al., *Phenelzine: An Old Drug That May Hold Clues to The Development of New Neuroprotective Agents*. Klinik Psikofarmakoloji Bülteni-Bulletin of Clinical Psychopharmacology, 2010. **20**(2): p. 179-186.
338. Parent, M.B., M.K. Habib, and G.B. Baker, *Time-dependent changes in brain monoamine oxidase activity and in brain levels of monoamines and amino acids following acute administration of the antidepressant/antipanic drug phenelzine*. Biochem Pharmacol, 2000. **59**(10): p. 1253-63.
339. McManus, D.J., et al., *Effects of the antidepressant/antipanic drug phenelzine on GABA concentrations and GABA-transaminase activity in rat brain*. Biochemical pharmacology, 1992. **43**(11): p. 2486-2489.
340. Baker, G.B., et al., *Effects of the antidepressant phenelzine on brain levels of gamma-aminobutyric acid (GABA)*. J Affect Disord, 1991. **21**(3): p. 207-11.
341. Parent, M.B., et al., *Effects of the antidepressant/antipanic drug phenelzine and its putative metabolite phenylethylidenehydrazine on extracellular gamma-aminobutyric acid levels in the striatum*. Biochem Pharmacol, 2002. **63**(1): p. 57-64.

342. Baker, G.B., et al., *Insights into the mechanisms of action of the MAO inhibitors phenelzine and tranylcypromine: a review*. J Psychiatry Neurosci, 1992. **17**(5): p. 206-14.
343. Michael-Titus, A.T., et al., *Imipramine and phenelzine decrease glutamate overflow in the prefrontal cortex--a possible mechanism of neuroprotection in major depression?* Neuroscience, 2000. **100**(4): p. 681-4.
344. Yang, J. and J. Shen, *In vivo evidence for reduced cortical glutamate-glutamine cycling in rats treated with the antidepressant/antipanic drug phenelzine*. Neuroscience, 2005. **135**(3): p. 927-37.
345. Song, M.-S., et al., *The antidepressant phenelzine protects neurons and astrocytes against formaldehyde-induced toxicity*. Journal of neurochemistry, 2010. **114**(5): p. 1405-1413.
346. Mifflin, K.A., et al., *Manipulation of Neurotransmitter Levels Has Differential Effects on Formalin-Evoked Nociceptive Behavior in Male and Female Mice*. The Journal of Pain, 2016. **17**(4): p. 483-498.
347. Musgrave, T., et al., *The MAO inhibitor phenelzine improves functional outcomes in mice with experimental autoimmune encephalomyelitis (EAE)*. Brain, behavior, and immunity, 2011. **25**(8): p. 1677-88.
348. Benson, C.A., et al., *The MAO inhibitor phenelzine can improve functional outcomes in mice with established clinical signs in experimental autoimmune encephalomyelitis (EAE)*. Behav Brain Res, 2013. **252**: p. 302-11.

## Chapter 2

1. Fiedorowicz, J.G. and K.L. Swartz, *The Role of Monoamine Oxidase Inhibitors in Current Psychiatric Practice*. Journal of psychiatric practice, 2004. **10**(4): p. 239-248.
2. Rapaport, M.H., *Dietary restrictions and drug interactions with monoamine oxidase inhibitors: the state of the art*. J Clin Psychiatry, 2007. **68 Suppl 8**: p. 42-6.
3. Shulman, K.I., et al., *Current prescription patterns and safety profile of irreversible monoamine oxidase inhibitors: a population-based cohort study of older adults*. J Clin Psychiatry, 2009. **70**(12): p. 1681-6.
4. Parent, M.B., M.K. Habib, and G.B. Baker, *Time-dependent changes in brain monoamine oxidase activity and in brain levels of monoamines and amino acids following acute administration of the antidepressant/antipanic drug phenelzine*. Biochem Pharmacol, 2000. **59**(10): p. 1253-63.
5. McManus, D.J., et al., *Effects of the antidepressant/antipanic drug phenelzine on GABA concentrations and GABA-transaminase activity in rat brain*. Biochemical pharmacology, 1992. **43**(11): p. 2486-2489.
6. Paslawski, T., et al., *The antidepressant drug phenelzine produces antianxiety effects in the plus-maze and increases in rat brain GABA*. Psychopharmacology (Berl), 1996. **127**(1): p. 19-24.
7. Parent, M.B., et al., *Effects of the antidepressant/antipanic drug phenelzine and its putative metabolite phenylethylidenedihydrazone on extracellular gamma-aminobutyric acid levels in the striatum*. Biochem Pharmacol, 2002. **63**(1): p. 57-64.
8. Michael-Titus, A.T., et al., *Imipramine and phenelzine decrease glutamate overflow in the prefrontal cortex--a possible mechanism of neuroprotection in major depression?* Neuroscience, 2000. **100**(4): p. 681-4.
9. Song, M.-S., et al., *The antidepressant phenelzine protects neurons and astrocytes against formaldehyde-induced toxicity*. Journal of neurochemistry, 2010. **114**(5): p. 1405-1413.
10. MacKenzie, E.M., et al., *Phenelzine: An Old Drug That May Hold Clues to The Development of New Neuroprotective Agents*. Klinik Psikofarmakoloji Bülteni-Bulletin of Clinical Psychopharmacology, 2010. **20**(2): p. 179-186.
11. Song, M.-S., et al., *An update on amine oxidase inhibitors: Multifaceted drugs*. Progress in Neuro-Psychopharmacology and Biological Psychiatry, 2013. **44**: p. 118-124.

12. Potter, L.E., et al., *Altered excitatory-inhibitory balance within somatosensory cortex is associated with enhanced plasticity and pain sensitivity in a mouse model of multiple sclerosis*. Journal of neuroinflammation, 2016. **13**(1): p. 142.
13. Ransohoff, R.M., *Animal models of multiple sclerosis: the good, the bad and the bottom line*. Nat Neurosci, 2012. **15**(8): p. 1074-1077.
14. Mifflin, K.A., et al., *Manipulation of Neurotransmitter Levels Has Differential Effects on Formalin-Evoked Nociceptive Behavior in Male and Female Mice*. The Journal of Pain, 2016. **17**(4): p. 483-498.
15. Doolen, S., et al., *Peripheral nerve injury increases glutamate-evoked calcium mobilization in adult spinal cord neurons*. Molecular pain, 2012. **8**: p. 56.
16. Dubin, A.E. and A. Patapoutian, *Nociceptors: the sensors of the pain pathway*. The Journal of clinical investigation, 2010. **120**(11): p. 3760-3772.
17. Griebel, G., et al., *Behavioral effects of phenelzine in an experimental model for screening anxiolytic and anti-panic drugs: correlation with changes in monoamine-oxidase activity and monoamine levels*. Neuropharmacology, 1998. **37**(7): p. 927-935.
18. Musgrave, T., et al., *The MAO inhibitor phenelzine improves functional outcomes in mice with experimental autoimmune encephalomyelitis (EAE)*. Brain, Behavior, and Immunity, 2011. **25**(8): p. 1677-1688.
19. Gao, Y.J. and R.R. Ji, *c-Fos and pERK, which is a better marker for neuronal activation and central sensitization after noxious stimulation and tissue injury?* Open Pain J, 2009. **2**: p. 11-17.
20. Abbadie, C., et al., *Differential contribution of the two phases of the formalin test to the pattern of c-fos expression in the rat spinal cord: studies with remifentanyl and lidocaine*. Pain, 1997. **69**(1-2): p. 101-110.
21. Polgár, E., et al., *A Quantitative Study of Inhibitory Interneurons in Laminae I-III of the Mouse Spinal Dorsal Horn*. PLoS ONE, 2013. **8**(10): p. e78309.
22. Bardin, L., et al., *In the formalin model of tonic nociceptive pain, 8-OH-DPAT produces 5-HT<sub>1A</sub> receptor-mediated, behaviorally specific analgesia*. European Journal of Pharmacology, 2001. **421**(2): p. 109-114.
23. Abe, K., et al., *Responses to 5-HT in morphologically identified neurons in the rat substantia gelatinosa in vitro*. Neuroscience, 2009. **159**(1): p. 316-324.
24. Xie, D.J., et al., *Identification of 5-HT receptor subtypes enhancing inhibitory transmission in the rat spinal dorsal horn in vitro*. Molecular pain, 2012. **8**: p. 58.
25. Jeong, C.Y., J.I. Choi, and M.H. Yoon, *Roles of serotonin receptor subtypes for the antinociception of 5-HT in the spinal cord of rats*. European Journal of Pharmacology, 2004. **502**(3): p. 205-211.
26. Bardin, L., J. Lavarenne, and A. Eschalier, *Serotonin receptor subtypes involved in the spinal antinociceptive effect of 5-HT in rats*. Pain, 2000. **86**(1-2): p. 11-18.
27. Sonohata, M., et al., *Actions of noradrenaline on substantia gelatinosa neurones in the rat spinal cord revealed by in vivo patch recording*. The Journal of physiology, 2004. **555**(2): p. 515-526.
28. Fairbanks, C.A., L.S. Stone, and G.L. Wilcox, *Pharmacological Profiles of Alpha 2 Adrenergic Receptor Agonists Identified Using Genetically Altered Mice and Isobolographic Analysis*. Pharmacology & Therapeutics, 2009. **123**(2): p. 224-238.
29. Pertovaara, A., *Noradrenergic pain modulation*. Progress in neurobiology, 2006. **80**(2): p. 53-83.
30. Bourgoin, S., et al., *Monoaminergic control of the release of calcitonin gene-related peptide- and substance P-like materials from rat spinal cord slices*. Neuropharmacology, 1993. **32**(7): p. 633-640.
31. Hirono, M., et al., *Developmental enhancement of  $\alpha$ 2-adrenoceptor-mediated suppression of inhibitory synaptic transmission onto mouse cerebellar Purkinje cells*. Neuroscience, 2008. **156**(1): p. 143-154.
32. Dworkin, R.H., et al., *Pharmacologic management of neuropathic pain: evidence-based recommendations*. Pain, 2007. **132**(3): p. 237-51.
33. Millan, M.J., *Descending control of pain*. Progress in neurobiology, 2002. **66**(6): p. 355-474.
34. Patel, R. and A.H. Dickenson, *Mechanisms of the gabapentinoids and  $\alpha$ 2 $\delta$ -1 calcium channel subunit in neuropathic pain*. Pharmacology Research & Perspectives, 2016. **4**(2): p. n/a-n/a.

35. Dickenson, A.H., E.A. Matthews, and R. Suzuki, *Neurobiology of neuropathic pain: mode of action of anticonvulsants*. European journal of pain, 2002. **6**(SA): p. 51-60.
36. Finnerup, N.B., et al., *Pharmacotherapy for neuropathic pain in adults: a systematic review and meta-analysis*. The Lancet Neurology, 2015. **14**(2): p. 162-173.
37. Lee, I., et al., *Analgesic properties of meperidine, amitriptyline and phenelzine in mice*. Canadian Anaesthetists' Society Journal, 1983. **30**(5): p. 501-505.
38. Carter, R.B., *Differentiating analgesic and non-analgesic drug activities on rat hot plate: effect of behavioral endpoint*. Pain, 1991. **47**(2): p. 211-220.
- 39.Coderre, T.J., A.L. Vaccarino, and R. Melzack, *Central nervous system plasticity in the tonic pain response to subcutaneous formalin injection*. Brain Research, 1990. **535**(1): p. 155-158.
40. Coderre, T.J. and R. Melzack, *The contribution of excitatory amino acids to central sensitization and persistent nociception after formalin-induced tissue injury*. The Journal of Neuroscience, 1992. **12**(9): p. 3665.
41. Gogas, K.R., et al., *The antinociceptive action of supraspinal opioids results from an increase in descending inhibitory control: Correlation of nociceptive behavior and c-fos expression*. Neuroscience, 1991. **42**(3): p. 617-628.
42. Lu, Y. and E.R. Perl, *Selective action of noradrenaline and serotonin on neurones of the spinal superficial dorsal horn in the rat*. The Journal of physiology, 2007. **582**(Pt 1): p. 127-36.

### Chapter 3

1. Compston, A. and A. Coles, *Multiple sclerosis*. Lancet, 2002. 359(9313): p. 1221-31.
2. Svendsen, K.B., et al., *Sensory function and quality of life in patients with multiple sclerosis and pain*. Pain, 2005. 114(3): p. 473-81.
3. Svendsen, K.B., et al., *Pain in patients with multiple sclerosis: a population-based study*. Archives of neurology, 2003. 60(8): p. 1089-94.
4. O'Connor, A.B., et al., *Pain associated with multiple sclerosis: systematic review and proposed classification*. Pain, 2008. 137(1): p. 96-111.
5. Iannitti, T., B.J. Kerr, and B.K. Taylor, *Mechanisms and Pharmacology of Neuropathic Pain in Multiple Sclerosis*. Current topics in behavioral neurosciences, 2014. 20: p. 75-97.
6. Grau-López, L., et al., *Analysis of the pain in multiple sclerosis patients*. Neurología (English Edition), 2011. 26(4): p. 208-213.
7. Solaro, C. and M. Messmer Uccelli, *Pharmacological management of pain in patients with multiple sclerosis*. Drugs, 2010. 70(10): p. 1245-54.
8. Solaro, C. and M.M. Uccelli, *Management of pain in multiple sclerosis: a pharmacological approach*. Nat Rev Neurol, 2011. 7(9): p. 519-27.
9. Osterberg, A., J. Boivie, and K.A. Thuomas, *Central pain in multiple sclerosis--prevalence and clinical characteristics*. European journal of pain, 2005. 9(5): p. 531-42.
10. Österberg, A. and J. Boivie, *Central pain in multiple sclerosis – Sensory abnormalities*. European journal of pain, 2010. 14(1): p. 104-110.
11. Khan, F. and J. Pallant, *Chronic Pain in Multiple Sclerosis: Prevalence, Characteristics, and Impact on Quality of Life in an Australian Community Cohort*. The Journal of Pain, 2007. 8(8): p. 614-623.
12. Thibault, K., B. Calvino, and S. Pezet, *Characterisation of sensory abnormalities observed in an animal model of multiple sclerosis: a behavioural and pharmacological study*. Eur J Pain, 2011. 15(3): p. 231 e1-16.
13. Aicher, S.A., et al., *Hyperalgesia in an animal model of multiple sclerosis*. Pain, 2004. 110(3): p. 560-70.
14. Khan, N. and M.T. Smith, *Multiple sclerosis-induced neuropathic pain: pharmacological management and pathophysiological insights from rodent EAE models*. Inflammopharmacology, 2014. 22(1): p. 1-22.

15. Olechowski, C.J., J.J. Truong, and B.J. Kerr, *Neuropathic pain behaviours in a chronic-relapsing model of experimental autoimmune encephalomyelitis (EAE)*. *Pain*, 2009. 141(1-2): p. 156-64.
16. Croxford, A.L., F.C. Kurschus, and A. Waisman, *Mouse models for multiple sclerosis: Historical facts and future implications*. *Biochimica et Biophysica Acta (BBA) - Molecular Basis of Disease*, 2011. 1812(2): p. 177-183.
17. Ransohoff, R.M., *Animal models of multiple sclerosis: the good, the bad and the bottom line*. *Nat Neurosci*, 2012. 15(8): p. 1074-1077.
18. Olechowski, C.J., et al., *Changes in nociceptive sensitivity and object recognition in experimental autoimmune encephalomyelitis (EAE)*. *Experimental neurology*, 2013. 241(0): p. 113-121.
19. Aicher, S.A., et al., *Hyperalgesia in an animal model of multiple sclerosis*. *Pain*, 2004. 110(3): p. 560-570.
20. Latremoliere, A. and C.J. Woolf, *Central Sensitization: A Generator of Pain Hypersensitivity by Central Neural Plasticity*. *The journal of pain : official journal of the American Pain Society*, 2009. 10(9): p. 895-926.
21. Musgrave, T., et al., *Tissue concentration changes of amino acids and biogenic amines in the central nervous system of mice with experimental autoimmune encephalomyelitis (EAE)*. *Neurochemistry international*, 2011. 59(1): p. 28-38.
22. Parent, M.B., et al., *Effects of the antidepressant/antipanic drug phenelzine and its putative metabolite phenylethylidenehydrazine on extracellular gamma-aminobutyric acid levels in the striatum*. *Biochem Pharmacol*, 2002. 63(1): p. 57-64.
23. Parent, M.B., M.K. Habib, and G.B. Baker, *Time-dependent changes in brain monoamine oxidase activity and in brain levels of monoamines and amino acids following acute administration of the antidepressant/antipanic drug phenelzine*. *Biochem Pharmacol*, 2000. 59(10): p. 1253-63.
24. McManus, D.J., et al., *Effects of the antidepressant/antipanic drug phenelzine on GABA concentrations and GABA-transaminase activity in rat brain*. *Biochem Pharmacol*, 1992. 43(11): p. 2486-9.
25. Musgrave, T., et al., *The MAO inhibitor phenelzine improves functional outcomes in mice with experimental autoimmune encephalomyelitis (EAE)*. *Brain, Behavior, and Immunity*, 2011. 25(8): p. 1677-1688.
26. Olechowski, C.J., et al., *A diminished response to formalin stimulation reveals a role for the glutamate transporters in the altered pain sensitivity of mice with experimental autoimmune encephalomyelitis (EAE)*. *Pain*, 2010. 149(3): p. 565-72.
27. Abbadie, C., et al., *Differential contribution of the two phases of the formalin test to the pattern of c-fos expression in the rat spinal cord: studies with remifentanyl and lidocaine*. *Pain*, 1997. 69(1-2): p. 101-110.
- 28.Coderre, T.J., A.L. Vaccarino, and R. Melzack, *Central nervous system plasticity in the tonic pain response to subcutaneous formalin injection*. *Brain Research*, 1990. 535(1): p. 155-158.
29. Benson, C.A., et al., *The MAO inhibitor phenelzine can improve functional outcomes in mice with established clinical signs in experimental autoimmune encephalomyelitis (EAE)*. *Behavioural brain research*, 2013. 252: p. 302-11.
30. Barrot, M., *Tests and models of nociception and pain in rodents*. *Neuroscience*, 2012. 211: p. 39-50.
31. Lu, J., et al., *Pain in experimental autoimmune encephalitis: a comparative study between different mouse models*. *Journal of neuroinflammation*, 2012. 9(1): p. 233.
32. Duffy, S.S., et al., *Peripheral and Central Neuroinflammatory Changes and Pain Behaviors in an Animal Model of Multiple Sclerosis*. *Frontiers in Immunology*, 2016. 7: p. 369.
33. Sandkühler, J., *Models and Mechanisms of Hyperalgesia and Allodynia*. *Physiological Reviews*, 2009. 89(2): p. 707.
34. Kuner, R. and H. Flor, *Structural plasticity and reorganisation in chronic pain*. *Nat Rev Neurosci*, 2017. 18(1): p. 20-30.
35. Ji, R.-R., et al., *Central sensitization and LTP: do pain and memory share similar mechanisms?* *Trends in Neurosciences*, 2003. 26(12): p. 696-705.

36. Woolf, C.J. and M.W. Salter, *Neuronal plasticity: increasing the gain in pain*. *Science*, 2000. 288(5472): p. 1765-9.
37. Mandolesi, G., et al., *IL-1beta dependent cerebellar synaptopathy in a mouse model of multiple sclerosis*. *Cerebellum*, 2015. 14(1): p. 19-22.
38. Mandolesi, G., et al., *Synaptopathy connects inflammation and neurodegeneration in multiple sclerosis*. *Nat Rev Neurol*, 2015. 11(12): p. 711-24.
39. Nisticò, R., et al., *Synaptic plasticity in multiple sclerosis and in experimental autoimmune encephalomyelitis*. *Philosophical Transactions of the Royal Society B: Biological Sciences*, 2014. 369(1633): p. 20130162.
40. Centonze, D., et al., *Inflammation Triggers Synaptic Alteration and Degeneration in Experimental Autoimmune Encephalomyelitis*. *The Journal of Neuroscience*, 2009. 29(11): p. 3442.
41. Potter, L.E., et al., *Altered excitatory-inhibitory balance within somatosensory cortex is associated with enhanced plasticity and pain sensitivity in a mouse model of multiple sclerosis*. *Journal of neuroinflammation*, 2016. 13(1): p. 142.
42. Todd, A.J., *Neuronal circuitry for pain processing in the dorsal horn*. *Nature reviews. Neuroscience*, 2010. 11(12): p. 823-836.
43. Brumovsky, P.R., *VGLUTs in Peripheral Neurons and the Spinal Cord: Time for a Review*. *ISRN Neurology*, 2013. 2013: p. 28.
44. Todd, A.J., et al., *The expression of vesicular glutamate transporters VGLUT1 and VGLUT2 in neurochemically defined axonal populations in the rat spinal cord with emphasis on the dorsal horn*. *European Journal of Neuroscience*, 2003. 17(1): p. 13-27.
45. Benson, C.A., et al., *The MAO inhibitor phenelzine can improve functional outcomes in mice with established clinical signs in experimental autoimmune encephalomyelitis (EAE)*. *Behav Brain Res*, 2013. 252: p. 302-11.
46. Gao, Y.-J. and R.-R. Ji, *c-Fos and pERK, which is a better marker for neuronal activation and central sensitization after noxious stimulation and tissue injury?* *Open Pain J*, 2009. 2: p. 11-17.
47. Sheng, M. and M.E. Greenberg, *The regulation and function of c-fos and other immediate early genes in the nervous system*. *Neuron*, 1990. 4(4): p. 477-485.
48. Bullitt, E., *Expression of C-fos-like protein as a marker for neuronal activity following noxious stimulation in the rat*. *The Journal of comparative neurology*, 1990. 296(4): p. 517-530.
49. Sheng, M., G. McFadden, and M.E. Greenberg, *Membrane depolarization and calcium induce c-fos transcription via phosphorylation of transcription factor CREB*. *Neuron*, 1990. 4(4): p. 571-582.
50. Gao, Y.J. and R.R. Ji, *c-Fos and pERK, which is a better marker for neuronal activation and central sensitization after noxious stimulation and tissue injury?* *Open Pain J*, 2009. 2: p. 11-17.
51. Rodrigues, D.H., et al., *IL-1 $\beta$  Is Involved with the Generation of Pain in Experimental Autoimmune Encephalomyelitis*. *Molecular neurobiology*, 2016. 53(9): p. 6540-6547.
52. Yang, G., et al., *Peripheral elevation of TNF-alpha leads to early synaptic abnormalities in the mouse somatosensory cortex in experimental autoimmune encephalomyelitis*. *Proc Natl Acad Sci U S A*, 2013. 110(25): p. 10306-11.
53. Kim, H., et al., *Increased phosphorylation of cyclic AMP response element-binding protein in the spinal cord of Lewis rats with experimental autoimmune encephalomyelitis*. *Brain Research*, 2007. 1162: p. 113-120.
54. Moalem, G. and D.J. Tracey, *Immune and inflammatory mechanisms in neuropathic pain*. *Brain Research Reviews*, 2006. 51(2): p. 240-264.
55. Scholz, J. and C.J. Woolf, *The neuropathic pain triad: neurons, immune cells and glia*. *Nature Neuroscience*, 2007. 10(11): p. 1361-1368.
56. Ji, R.-R., Z.-Z. Xu, and Y.-J. Gao, *Emerging targets in neuroinflammation-driven chronic pain*. *Nat Rev Drug Discov*, 2014. 13(7): p. 533-548.
57. Yong, V.W., et al., *Elevation of matrix metalloproteinases (MMPs) in multiple sclerosis and impact of immunomodulators*. *Journal of the neurological sciences*, 2007. 259(1-2): p. 79-84.

58. Ji, R.-R., et al., *MMP regulation of neuropathic pain*. Trends Pharmacol Sci, 2009. 30(7): p. 336-340.
59. Szklarczyk, A. and K. Conant, *Matrix Metalloproteinases, Synaptic Injury, and Multiple Sclerosis*. Frontiers in Psychiatry, 2010. 1(130).
60. Lakhan, S.E. and M. Avramut, *Matrix Metalloproteinases in Neuropathic Pain and Migraine: Friends, Enemies, and Therapeutic Targets*. Pain Research and Treatment, 2012. 2012: p. 10.
61. Huntley, G.W., *Synaptic circuit remodelling by matrix metalloproteinases in health and disease*. Nat Rev Neurosci, 2012. 13(11): p. 743-757.
62. Peirs, C. and R.P. Seal, *Neural circuits for pain: Recent advances and current views*. Science, 2016. 354(6312): p. 578.
63. Peirs, C., et al., *Dorsal Horn Circuits for Persistent Mechanical Pain*. Neuron, 2015. 87(4): p. 797-812.
64. Gangadharan, V. and R. Kuner, *Unravelling Spinal Circuits of Pain and Mechanical Allodynia*. Neuron, 2015. 87(4): p. 673-675.
65. Braz, J., et al., *Transmitting pain and itch messages: A contemporary view of the spinal cord circuits that generate Gate Control*. Neuron, 2014. 82(3): p. 522-536.
66. Millan, M.J., *Descending control of pain*. Progress in neurobiology, 2002. 66(6): p. 355-474.
67. Polgár, E., et al., *A Quantitative Study of Inhibitory Interneurons in Laminae I-III of the Mouse Spinal Dorsal Horn*. PLoS ONE, 2013. 8(10): p. e78309.

#### Chapter 4

1. Demaree, H.A., E. Gaudino, and J. DeLuca, *The relationship between depressive symptoms and cognitive dysfunction in multiple sclerosis*. Cognitive neuropsychiatry, 2003. 8(3): p. 161-71.
2. Svendsen, K.B., et al., *Sensory function and quality of life in patients with multiple sclerosis and pain*. Pain, 2005. 114(3): p. 473-81.
3. Svendsen, K.B., et al., *Pain in patients with multiple sclerosis: a population-based study*. Archives of neurology, 2003. 60(8): p. 1089-94.
4. O'Connor, A.B., et al., *Pain associated with multiple sclerosis: systematic review and proposed classification*. Pain, 2008. 137(1): p. 96-111.
5. Osterberg, A., J. Boivie, and K.A. Thuomas, *Central pain in multiple sclerosis--prevalence and clinical characteristics*. European journal of pain, 2005. 9(5): p. 531-42.
6. Geurts, J.J.G., et al., *Measurement and clinical effect of grey matter pathology in multiple sclerosis*. The Lancet Neurology. 11(12): p. 1082-1092.
7. Eto, K., et al., *Inter-regional contribution of enhanced activity of the primary somatosensory cortex to the anterior cingulate cortex accelerates chronic pain behavior*. J Neurosci, 2011. 31(21): p. 7631-6.
8. Kim, S.K. and J. Nabekura, *Rapid synaptic remodeling in the adult somatosensory cortex following peripheral nerve injury and its association with neuropathic pain*. J Neurosci, 2011. 31(14): p. 5477-82.
9. Gustin, S.M., et al., *Pain and plasticity: is chronic pain always associated with somatosensory cortex activity and reorganization?* J Neurosci, 2012. 32(43): p. 14874-84.
10. Olechowski, C.J., et al., *A diminished response to formalin stimulation reveals a role for the glutamate transporters in the altered pain sensitivity of mice with experimental autoimmune encephalomyelitis (EAE)*. Pain, 2010. 149(3): p. 565-72.
11. Olechowski, C.J., et al., *Changes in nociceptive sensitivity and object recognition in experimental autoimmune encephalomyelitis (EAE)*. Experimental neurology, 2013. 241(0): p. 113-121.
12. Olechowski, C.J., J.J. Truong, and B.J. Kerr, *Neuropathic pain behaviours in a chronic-relapsing model of experimental autoimmune encephalomyelitis (EAE)*. Pain, 2009. 141(1-2): p. 156-64.
13. Rahn, E.J., et al., *Sex differences in a mouse model of multiple sclerosis: neuropathic pain behavior in females but not males and protection from neurological deficits during proestrus*. Biol Sex Differ, 2014. 5(1): p. 4.

14. Thibault, K., B. Calvino, and S. Pezet, *Characterisation of sensory abnormalities observed in an animal model of multiple sclerosis: a behavioural and pharmacological study*. European journal of pain, 2011. **15**(3): p. 231 e1-16.
15. Khan, N. and M.T. Smith, *Multiple sclerosis-induced neuropathic pain: pharmacological management and pathophysiological insights from rodent EAE models*. Inflammopharmacology, 2014. **22**(1): p. 1-22.
16. Gao, Y.J. and R.R. Ji, *c-Fos and pERK, which is a better marker for neuronal activation and central sensitization after noxious stimulation and tissue injury?* Open Pain J, 2009. **2**: p. 11-17.
17. Yang, G., et al., *Peripheral elevation of TNF-alpha leads to early synaptic abnormalities in the mouse somatosensory cortex in experimental autoimmune encephalomyelitis*. Proceedings of the National Academy of Sciences of the United States of America, 2013. **110**(25): p. 10306-11.
18. Tambalo, S., et al., *Functional Magnetic Resonance Imaging of Rats with Experimental Autoimmune Encephalomyelitis Reveals Brain Cortex Remodeling*. J Neurosci, 2015. **35**(27): p. 10088-100.
19. Falco, A., et al., *Reduction in parvalbumin-positive interneurons and inhibitory input in the cortex of mice with experimental autoimmune encephalomyelitis*. Experimental brain research. Experimentelle Hirnforschung. Experimentation cerebrale, 2014. **232**(7): p. 2439-49.
20. Shibuki K, H.R., Tohmi M, et al. Frostig RD, editor. , *Flavoprotein Fluorescence Imaging of Experience-Dependent Cortical Plasticity in Rodents*. In: *In Vivo Optical Imaging of Brain Function*. 2nd edition. Chapter 7.
21. Shibuki, K., et al., *Dynamic imaging of somatosensory cortical activity in the rat visualized by flavoprotein autofluorescence*. The Journal of physiology, 2003. **549**(Pt 3): p. 919-27.
22. Musgrave, T., et al., *Tissue concentration changes of amino acids and biogenic amines in the central nervous system of mice with experimental autoimmune encephalomyelitis (EAE)*. Neurochemistry international, 2011. **59**(1): p. 28-38.
23. Musgrave, T., et al., *The MAO inhibitor phenelzine improves functional outcomes in mice with experimental autoimmune encephalomyelitis (EAE)*. Brain, behavior, and immunity, 2011. **25**(8): p. 1677-88.
24. Hensch, T.K. and M. Fagiolini, *Excitatory-inhibitory balance and critical period plasticity in developing visual cortex*. Prog Brain Res, 2005. **147**: p. 115-24.
25. Woolf, C.J. and M.W. Salter, *Neuronal plasticity: increasing the gain in pain*. Science, 2000. **288**(5472): p. 1765-9.
26. Kalyvas, A.e.a. and S. David, *Cytosolic phospholipase A2 plays a key role in the pathogenesis of multiple sclerosis-like disease*. Neuron, 2004. **41**(3): p. 323-35.
27. Benson, C.A., et al., *The MAO inhibitor phenelzine can improve functional outcomes in mice with established clinical signs in experimental autoimmune encephalomyelitis (EAE)*. Behavioural brain research, 2013. **252**: p. 302-11.
28. Tohmi, M., et al., *Transcranial flavoprotein fluorescence imaging of mouse cortical activity and plasticity*. Journal of neurochemistry, 2009. **109 Suppl 1**: p. 3-9.
29. Drew, P.J., et al., *Chronic optical access through a polished and reinforced thinned skull*. Nature Methods, 2010. **7**(12): p. 981-984.
30. Bains, R., et al., *Volatile anaesthetics depolarize neural mitochondria by inhibition of the electron transport chain*. Acta Anaesthesiol Scand, 2006. **50**(5): p. 572-9.
31. T. Robert Husson and Naoum P. Issa. et al. Frostig RD, e., *Functional Imaging with Mitochondrial Flavoprotein Autofluorescence: Theory, Practice, and Applications*. In: *In Vivo Optical Imaging of Brain Function*. 2nd edition. Chapter 8.
32. Maggi, C.A. and A. Meli, *Suitability of urethane anesthesia for physiopharmacological investigations in various systems. Part 1: General considerations*. Experientia, 1986. **42**(2): p. 109-14.
33. Hara, K. and R.A. Harris, *The anesthetic mechanism of urethane: the effects on neurotransmitter-gated ion channels*. Anesthesia and analgesia, 2002. **94**(2): p. 313-8, table of contents.

34. Paxinos, G. and K.B.J. Franklin, *The mouse brain in stereotaxic coordinates*. Compact 2nd ed 2004, Amsterdam ; Boston: Elsevier Academic Press.
35. Winship, I.R. and T.H. Murphy, *In Vivo Calcium Imaging Reveals Functional Rewiring of Single Somatosensory Neurons after Stroke*. *Journal of Neuroscience*, 2008. **28**(26): p. 6592-6606.
36. Sigler, A.a.M., T. IO and VSD Signal Processor. 2012; Available from: [http://www.neuroscience.ubc.ca/faculty/murphy\\_software.html](http://www.neuroscience.ubc.ca/faculty/murphy_software.html).
37. Harrison, T.C., A. Sigler, and T.H. Murphy, *Simple and cost-effective hardware and software for functional brain mapping using intrinsic optical signal imaging*. *J Neurosci Methods*, 2009. **182**(2): p. 211-8.
38. Gibb, R. and B. Kolb, *A method for vibratome sectioning of Golgi-Cox stained whole rat brain*. *J Neurosci Methods*, 1998. **79**(1): p. 1-4.
39. Frostig, R.D., *Functional organization and plasticity in the adult rat barrel cortex: moving out-of-the-box*. *Curr Opin Neurobiol*, 2006. **16**(4): p. 445-50.
40. Lefort, S., et al., *The excitatory neuronal network of the C2 barrel column in mouse primary somatosensory cortex*. *Neuron*, 2009. **61**(2): p. 301-16.
41. Schindelin, J., et al., *Fiji: an open-source platform for biological-image analysis*. *Nat Methods*, 2012. **9**(7): p. 676-82.
42. Longair, M.H., D.A. Baker, and J.D. Armstrong, *Simple Neurite Tracer: open source software for reconstruction, visualization and analysis of neuronal processes*. *Bioinformatics*, 2011. **27**(17): p. 2453-4.
43. Lein, E.S., et al., *Genome-wide atlas of gene expression in the adult mouse brain*. *Nature*, 2007. **445**(7124): p. 168-76.
44. Kuo, T.e.a. *ITCN Cell Counter*. Available from: <http://rsb.info.nih.gov/ij/plugins/itcn.html>.
45. Komagata, S., et al., *Nociceptive cortical responses during capsaicin-induced tactile allodynia in mice with spinal dorsal column lesioning*. *Neuroscience Research*, 2011. **69**(4): p. 348-351.
46. Kim, S.K., K. Eto, and J. Nabekura, *Synaptic structure and function in the mouse somatosensory cortex during chronic pain: in vivo two-photon imaging*. *Neural Plast*, 2012. **2012**: p. 640259.
47. Watanabe, T., et al., *Spinal mechanisms underlying potentiation of hindpaw responses observed after transient hindpaw ischemia in mice*. *Sci Rep*, 2015. **5**: p. 11191.
48. Komagata, S., et al., *Initial phase of neuropathic pain within a few hours after nerve injury in mice*. *J Neurosci*, 2011. **31**(13): p. 4896-905.
49. Sachdev, R.N., M.R. Krause, and J.A. Mazer, *Surround suppression and sparse coding in visual and barrel cortices*. *Front Neural Circuits*, 2012. **6**: p. 43.
50. Margolis, D.J., H. Lutcke, and F. Helmchen, *Microcircuit dynamics of map plasticity in barrel cortex*. *Curr Opin Neurobiol*, 2014. **24**(1): p. 76-81.
51. Zhang, G., et al., *Upregulation of excitatory neurons and downregulation of inhibitory neurons in barrel cortex are associated with loss of whisker inputs*. *Mol Brain*, 2013. **6**: p. 2.
52. Reinert, K.C., et al., *Flavoprotein autofluorescence imaging of neuronal activation in the cerebellar cortex in vivo*. *Journal of neurophysiology*, 2004. **92**(1): p. 199-211.
53. Reinert, K.C., et al., *Flavoprotein autofluorescence imaging in the cerebellar cortex in vivo*. *J Neurosci Res*, 2007. **85**(15): p. 3221-32.
54. Reinert, K.C., et al., *Cellular and metabolic origins of flavoprotein autofluorescence in the cerebellar cortex in vivo*. *Cerebellum*, 2011. **10**(3): p. 585-99.
55. Holtmaat, A. and K. Svoboda, *Experience-dependent structural synaptic plasticity in the mammalian brain*. *Nat Rev Neurosci*, 2009. **10**(9): p. 647-58.
56. Karetko, M. and J. Skangiel-Kramska, *Diverse functions of perineuronal nets*. *Acta Neurobiol Exp (Wars)*, 2009. **69**(4): p. 564-77.
57. Hartig, W., et al., *Cortical neurons immunoreactive for the potassium channel Kv3.1b subunit are predominantly surrounded by perineuronal nets presumed as a buffering system for cations*. *Brain Res*, 1999. **842**(1): p. 15-29.

58. Levy, A.D., M.H. Omar, and A.J. Koleske, *Extracellular matrix control of dendritic spine and synapse structure and plasticity in adulthood*. Front Neuroanat, 2014. **8**: p. 116.
59. Soleman, S., et al., *Targeting the neural extracellular matrix in neurological disorders*. Neuroscience, 2013. **253**: p. 194-213.
60. Ye, Q. and Q.L. Miao, *Experience-dependent development of perineuronal nets and chondroitin sulfate proteoglycan receptors in mouse visual cortex*. Matrix Biol, 2013. **32**(6): p. 352-63.
61. Centonze, D., et al., *Inflammation triggers synaptic alteration and degeneration in experimental autoimmune encephalomyelitis*. J Neurosci, 2009. **29**(11): p. 3442-52.
62. Mandolesi, G., et al., *Cognitive deficits in experimental autoimmune encephalomyelitis: neuroinflammation and synaptic degeneration*. Neurological sciences : official journal of the Italian Neurological Society and of the Italian Society of Clinical Neurophysiology, 2010. **31**(Suppl 2): p. S255-9.
63. Gray, E., et al., *Elevated matrix metalloproteinase-9 and degradation of perineuronal nets in cerebrocortical multiple sclerosis plaques*. J Neuropathol Exp Neurol, 2008. **67**(9): p. 888-99.
64. Berard, J.L., et al., *Characterization of relapsing-remitting and chronic forms of experimental autoimmune encephalomyelitis in C57BL/6 mice*. Glia, 2010. **58**(4): p. 434-45.
65. Ahissar et al., S., *S1 laminar specialization*. Scholarpedia, 2010. **5**(8).
66. Murakami, H., et al., *Short-term plasticity visualized with flavoprotein autofluorescence in the somatosensory cortex of anaesthetized rats*. The European journal of neuroscience, 2004. **19**(5): p. 1352-60.
67. Feldman, D.E. and M. Brecht, *Map plasticity in somatosensory cortex*. Science, 2005. **310**(5749): p. 810-5.
68. Hensch, T.K., *Critical period regulation*. Annu Rev Neurosci, 2004. **27**: p. 549-79.
69. Donato, F., S.B. Rompani, and P. Caroni, *Parvalbumin-expressing basket-cell network plasticity induced by experience regulates adult learning*. Nature, 2013. **504**(7479): p. 272-6.
70. Toyozumi, T., et al., *A theory of the transition to critical period plasticity: inhibition selectively suppresses spontaneous activity*. Neuron, 2013. **80**(1): p. 51-63.
71. Mandolesi, G., et al., *IL-1beta dependent cerebellar synaptopathy in a mouse model of multiple sclerosis*. Cerebellum, 2015. **14**(1): p. 19-22.
72. Rossi, S., et al., *Impaired striatal GABA transmission in experimental autoimmune encephalomyelitis*. Brain, Behavior, and Immunity, 2011. **25**(5): p. 947-56.
73. Nistico, R., et al., *Synaptic plasticity in multiple sclerosis and in experimental autoimmune encephalomyelitis*. Philos Trans R Soc Lond B Biol Sci, 2014. **369**(1633): p. 20130162.
74. Pitt, D., P. Werner, and C.S. Raine, *Glutamate excitotoxicity in a model of multiple sclerosis*. Nat Med, 2000. **6**(1): p. 67-70.
75. Bar-Or, A., et al., *Analyses of all matrix metalloproteinase members in leukocytes emphasize monocytes as major inflammatory mediators in multiple sclerosis*. Brain, 2003. **126**(Pt 12): p. 2738-49.
76. Schafer, D.P., E.K. Lehrman, and B. Stevens, *The "quad-partite" synapse: microglia-synapse interactions in the developing and mature CNS*. Glia, 2013. **61**(1): p. 24-36.
77. Ramesh, G., A.G. MacLean, and M.T. Philipp, *Cytokines and chemokines at the crossroads of neuroinflammation, neurodegeneration, and neuropathic pain*. Mediators Inflamm, 2013. **2013**: p. 480739.
78. Eyo, U.B. and L.J. Wu, *Bidirectional microglia-neuron communication in the healthy brain*. Neural Plast, 2013. **2013**: p. 456857.
79. Nakamura, K., et al., *Transiently increased colocalization of vesicular glutamate transporters 1 and 2 at single axon terminals during postnatal development of mouse neocortex: a quantitative analysis with correlation coefficient*. The European journal of neuroscience, 2007. **26**(11): p. 3054-67.

80. Nakamura, K., et al., *Postnatal changes of vesicular glutamate transporter (VGluT)1 and VGluT2 immunoreactivities and their colocalization in the mouse forebrain*. The Journal of comparative neurology, 2005. **492**(3): p. 263-88.
81. Graziano, A., et al., *Vesicular glutamate transporters define two sets of glutamatergic afferents to the somatosensory thalamus and two thalamocortical projections in the mouse*. The Journal of comparative neurology, 2008. **507**(2): p. 1258-76.
82. Brumovsky, P.R., *VGLUTs in Peripheral Neurons and the Spinal Cord: Time for a Review*. ISRN Neurology, 2013. **2013**: p. 28.
83. Todd, A.J., et al., *The expression of vesicular glutamate transporters VGLUT1 and VGLUT2 in neurochemically defined axonal populations in the rat spinal cord with emphasis on the dorsal horn*. European Journal of Neuroscience, 2003. **17**(1): p. 13-27.
84. Shen, J. and J. Yang, *In Vivo Detection of Altered GABA Levels Following Acute Administration of Antidepressant/Antipanic Drug Phenelzine*. Proc. Intl. Soc. Mag. Reson. Med., 2005. **13**.
85. Parent, M.B., et al., *Effects of the antidepressant/antipanic drug phenelzine and its putative metabolite phenylethylidenehydrazine on extracellular gamma-aminobutyric acid levels in the striatum*. Biochemical pharmacology, 2002. **63**(1): p. 57-64.
86. Parent, M.B., M.K. Habib, and G.B. Baker, *Time-dependent changes in brain monoamine oxidase activity and in brain levels of monoamines and amino acids following acute administration of the antidepressant/antipanic drug phenelzine*. Biochemical pharmacology, 2000. **59**(10): p. 1253-63.
87. Benson, C.A., et al., *The MAO inhibitor phenelzine can improve functional outcomes in mice with established clinical signs in experimental autoimmune encephalomyelitis (EAE)*. Behav Brain Res, 2013. **252**: p. 302-11.
88. Aznar, S., et al., *The 5-HT1A serotonin receptor is located on calbindin- and parvalbumin-containing neurons in the rat brain*. Brain Res, 2003. **959**(1): p. 58-67.
89. Salgado, H., et al., *Pre- and postsynaptic effects of norepinephrine on  $\gamma$ -aminobutyric acid-mediated synaptic transmission in layer 2/3 of the rat auditory cortex*. Synapse, 2012. **66**(1): p. 20-28.
90. Kruglikov, I. and B. Rudy, *Perisomatic GABA release and thalamocortical integration onto neocortical excitatory cells are regulated by neuromodulators*. Neuron, 2008. **58**(6): p. 911-24.
91. Huang, Y., et al., *5-HT3a Receptors Modulate Hippocampal Gamma Oscillations by Regulating Synchrony of Parvalbumin-Positive Interneurons*. Cerebral Cortex, 2014.
92. Edeline, J.M., *Beyond traditional approaches to understanding the functional role of neuromodulators in sensory cortices*. Front Behav Neurosci, 2012. **6**: p. 45.
93. Yang, J. and J. Shen, *In vivo evidence for reduced cortical glutamate-glutamine cycling in rats treated with the antidepressant/antipanic drug phenelzine*. Neuroscience, 2005. **135**(3): p. 927-37.
94. Michael-Titus, A.T., et al., *Imipramine and phenelzine decrease glutamate overflow in the prefrontal cortex--a possible mechanism of neuroprotection in major depression?* Neuroscience, 2000. **100**(4): p. 681-4.
95. Kuhn, S.A., et al., *Microglia express GABA(B) receptors to modulate interleukin release*. Mol Cell Neurosci, 2004. **25**(2): p. 312-22.
96. Dello Russo, C., et al., *Inhibition of microglial inflammatory responses by norepinephrine: effects on nitric oxide and interleukin-1beta production*. J Neuroinflammation, 2004. **1**(1): p. 9.

## Chapter 5

1. Ban, T.A., *Capsules: History of Psychopharmacology*.
2. Heal, D.J., et al., *Amphetamine, past and present – a pharmacological and clinical perspective*. Journal of Psychopharmacology (Oxford, England), 2013. **27**(6): p. 479-496.
3. Stolerman, I.P., *Encyclopedia of Psychopharmacology*, I.P. Stolerman, Editor 2010, SpringerReference.

4. Nolan, C.M., S.V. Goldberg, and S.E. Buskin, *Hepatotoxicity associated with isoniazid preventive therapy: A 7-year survey from a public health tuberculosis clinic*. JAMA, 1999. **281**(11): p. 1014-1018.
5. Pleasure, H., *Psychiatric and neurological side-effects of isoniazid and iproniazid*. A.M.A. Archives of Neurology & Psychiatry, 1954. **72**(3): p. 313-320.
6. Shulman, K.I., N. Herrmann, and S.E. Walker, *Current Place of Monoamine Oxidase Inhibitors in the Treatment of Depression*. CNS drugs, 2013. **27**(10): p. 789-797.
7. Maxwell, M., *Drug Discovery*. 1990.
8. Ramachandrai, C.T., et al., *Antidepressants: From MAOIs to SSRIs and more*. Indian Journal of Psychiatry, 2011. **53**(2): p. 180-182.
9. Grady, M.M. and S.M. Stahl, *Practical guide for prescribing MAOIs: debunking myths and removing barriers*. CNS spectrums, 2012. **17**(1): p. 2-10.
10. McCabe-Sellers, B.J., C.G. Staggs, and M.L. Bogle, *Tyramine in foods and monoamine oxidase inhibitor drugs: A crossroad where medicine, nutrition, pharmacy, and food industry converge*. Journal of Food Composition and Analysis, 2006. **19**: p. S58-S65.
11. Folks, D.G., *Monoamine oxidase inhibitors: reappraisal of dietary considerations*. J Clin Psychopharmacol, 1983. **3**(4): p. 249-52.
12. Fiedorowicz, J.G. and K.L. Swartz, *The Role of Monoamine Oxidase Inhibitors in Current Psychiatric Practice*. Journal of psychiatric practice, 2004. **10**(4): p. 239-248.
13. Song, M.-S., et al., *An update on amine oxidase inhibitors: Multifaceted drugs*. Progress in Neuro-Psychopharmacology and Biological Psychiatry, 2013. **44**: p. 118-124.
14. Parent, M.B., et al., *Effects of the antidepressant/antipanic drug phenelzine and its putative metabolite phenylethylidenehydrazine on extracellular gamma-aminobutyric acid levels in the striatum*. Biochem Pharmacol, 2002. **63**(1): p. 57-64.
15. McManus, D.J., et al., *Effects of the antidepressant/antipanic drug phenelzine on GABA concentrations and GABA-transaminase activity in rat brain*. Biochem Pharmacol, 1992. **43**(11): p. 2486-9.
16. MacKenzie, E.M., et al., *Phenelzine: An Old Drug That May Hold Clues to The Development of New Neuroprotective Agents*. Klinik Psikofarmakoloji Bülteni-Bulletin of Clinical Psychopharmacology, 2010. **20**(2): p. 179-186.
17. Michael-Titus, A.T., et al., *Imipramine and phenelzine decrease glutamate overflow in the prefrontal cortex--a possible mechanism of neuroprotection in major depression?* Neuroscience, 2000. **100**(4): p. 681-4.
18. Yang, J. and J. Shen, *In vivo evidence for reduced cortical glutamate-glutamine cycling in rats treated with the antidepressant/antipanic drug phenelzine*. Neuroscience, 2005. **135**(3): p. 927-37.
19. Lee, I., et al., *Analgesic properties of meperidine, amitriptyline and phenelzine in mice*. Canadian Anaesthetists' Society Journal, 1983. **30**(5): p. 501-505.
20. EMELE, J.F., J. SHANAMAN, and M.R. WARREN, *THE ANALGESIC ACTIVITY OF PHENELZINE AND OTHER COMPOUNDS*. Journal of Pharmacology and Experimental Therapeutics, 1961. **134**(2): p. 206-209.
21. Schulze, D.R., F.I. Carroll, and L.R. McMahon, *Interactions between dopamine transporter and cannabinoid receptor ligands in rhesus monkeys*. Psychopharmacology (Berl), 2012. **222**(3): p. 425-38.
22. Excellium Pharmaceutical, I., *IMIPRAMINE HYDROCHLORIDE Prescribing Information*.
23. Medicine, N.-U.S.N.L.o. *Imipramine*. [cited 2017; Available from: <https://medlineplus.gov/druginfo/meds/a682389.html>].
24. Mifflin, K.A., et al., *Manipulation of Neurotransmitter Levels Has Differential Effects on Formalin-Evoked Nociceptive Behavior in Male and Female Mice*. The Journal of Pain, 2016. **17**(4): p. 483-498.
25. Hunskaar, S. and K. Hole, *The formalin test in mice: dissociation between inflammatory and non-inflammatory pain*. Pain, 1987. **30**(1): p. 103-14.

26. Abbadie, C., et al., *Differential contribution of the two phases of the formalin test to the pattern of c-fos expression in the rat spinal cord: studies with remifentanyl and lidocaine*. Pain, 1997. **69**(1-2): p. 101-110.
- 27.Coderre, T.J., A.L. Vaccarino, and R. Melzack, *Central nervous system plasticity in the tonic pain response to subcutaneous formalin injection*. Brain Research, 1990. **535**(1): p. 155-158.
28. Coderre, T.J. and R. Melzack, *The contribution of excitatory amino acids to central sensitization and persistent nociception after formalin-induced tissue injury*. The Journal of Neuroscience, 1992. **12**(9): p. 3665.
29. Benson, C.A., et al., *The MAO inhibitor phenelzine can improve functional outcomes in mice with established clinical signs in experimental autoimmune encephalomyelitis (EAE)*. Behav Brain Res, 2013. **252**: p. 302-11.
30. Musgrave, T., et al., *The MAO inhibitor phenelzine improves functional outcomes in mice with experimental autoimmune encephalomyelitis (EAE)*. Brain, behavior, and immunity, 2011. **25**(8): p. 1677-88.
31. Bullitt, E., *Expression of C-fos-like protein as a marker for neuronal activity following noxious stimulation in the rat*. The Journal of comparative neurology, 1990. **296**(4): p. 517-530.
32. Gao, Y.-J. and R.-R. Ji, *c-Fos and pERK, which is a better marker for neuronal activation and central sensitization after noxious stimulation and tissue injury?* Open Pain J, 2009. **2**: p. 11-17.
33. Sardella, T.C., et al., *Dynorphin is expressed primarily by GABAergic neurons that contain galanin in the rat dorsal horn*. Molecular pain, 2011. **7**(1): p. 76.
34. Polgár, E., et al., *A Quantitative Study of Inhibitory Interneurons in Laminae I-III of the Mouse Spinal Dorsal Horn*. PLoS ONE, 2013. **8**(10): p. e78309.
35. Doolen, S., et al., *Peripheral nerve injury increases glutamate-evoked calcium mobilization in adult spinal cord neurons*. Molecular pain, 2012. **8**: p. 56.
36. Malcolm, D.E., et al., *Phenelzine reduces plasma vitamin B6*. Journal of Psychiatry and Neuroscience, 1994. **19**(5): p. 332-334.
37. Olechowski, C.J., J.J. Truong, and B.J. Kerr, *Neuropathic pain behaviours in a chronic-relapsing model of experimental autoimmune encephalomyelitis (EAE)*. Pain, 2009. **141**(1-2): p. 156-64.
38. Olechowski, C.J., et al., *A diminished response to formalin stimulation reveals a role for the glutamate transporters in the altered pain sensitivity of mice with experimental autoimmune encephalomyelitis (EAE)*. Pain, 2010. **149**(3): p. 565-72.
39. Olechowski, C.J., et al., *Changes in nociceptive sensitivity and object recognition in experimental autoimmune encephalomyelitis (EAE)*. Experimental neurology, 2013. **241**(0): p. 113-121.
40. Peirs, C., et al., *Dorsal Horn Circuits for Persistent Mechanical Pain*. Neuron, 2015. **87**(4): p. 797-812.
41. Peirs, C. and R.P. Seal, *Neural circuits for pain: Recent advances and current views*. Science, 2016. **354**(6312): p. 578.
42. Lieu, A., G. Tenorio, and B.J. Kerr, *Protein kinase C gamma (PKCγ) as a novel marker to assess the functional status of the corticospinal tract in experimental autoimmune encephalomyelitis (EAE)*. Journal of neuroimmunology, 2013. **256**(1): p. 43-48.
43. Falco, A., et al., *Reduction in parvalbumin-positive interneurons and inhibitory input in the cortex of mice with experimental autoimmune encephalomyelitis*. Exp Brain Res, 2014. **232**(7): p. 2439-49.
44. Rossi, S., et al., *Impaired striatal GABA transmission in experimental autoimmune encephalomyelitis*. Brain, Behavior, and Immunity, 2011. **25**(5): p. 947-956.
45. Rossi, S., et al., *Tumor necrosis factor is elevated in progressive multiple sclerosis and causes excitotoxic neurodegeneration*. Multiple Sclerosis Journal, 2013. **20**(3): p. 304-312.
46. Mandolesi, G., et al., *IL-1beta dependent cerebellar synaptopathy in a mouse model of multiple sclerosis*. Cerebellum, 2015. **14**(1): p. 19-22.
47. Zhu, W., et al., *Elevated expression of fractalkine (CX3CL1) and fractalkine receptor (CX3CR1) in the dorsal root ganglia and spinal cord in experimental autoimmune encephalomyelitis: implications in multiple sclerosis-induced neuropathic pain*. Biomed Res Int, 2013. **2013**: p. 480702.

48. Begum, F., et al., *Elevation of tumor necrosis factor alpha in dorsal root ganglia and spinal cord is associated with neuroimmune modulation of pain in an animal model of multiple sclerosis*. Journal of neuroimmune pharmacology : the official journal of the Society on NeuroImmune Pharmacology, 2013. **8**(3): p. 677-90.
49. Melanson, M., et al., *Experimental autoimmune encephalomyelitis-induced upregulation of tumor necrosis factor-alpha in the dorsal root ganglia*. Multiple sclerosis, 2009. **15**(10): p. 1135-45.
50. Rodrigues, D.H., et al., *IL-1 $\beta$  Is Involved with the Generation of Pain in Experimental Autoimmune Encephalomyelitis*. Molecular neurobiology, 2016. **53**(9): p. 6540-6547.
51. Nessler, S., et al., *Effect of minocycline in experimental autoimmune encephalomyelitis*. Annals of neurology, 2002. **52**(5): p. 689-690.
52. Reinert, K.C., et al., *Cellular and metabolic origins of flavoprotein autofluorescence in the cerebellar cortex in vivo*. Cerebellum, 2011. **10**(3): p. 585-99.
53. Tambalo, S., et al., *Functional Magnetic Resonance Imaging of Rats with Experimental Autoimmune Encephalomyelitis Reveals Brain Cortex Remodeling*. J Neurosci, 2015. **35**(27): p. 10088-100.
54. Shih, Y.Y., et al., *Striatal and cortical BOLD, blood flow, blood volume, oxygen consumption, and glucose consumption changes in noxious forepaw electrical stimulation*. J Cereb Blood Flow Metab, 2011. **31**(3): p. 832-41.
55. Hiu, T., et al., *Enhanced phasic GABA inhibition during the repair phase of stroke: a novel therapeutic target*. Brain, 2016. **139**(2): p. 468-480.
56. Rudolph, U. and H. Möhler, *GABA(A) Receptor Subtypes: Therapeutic Potential in Down Syndrome, Affective Disorders, Schizophrenia, and Autism*. Annual review of pharmacology and toxicology, 2014. **54**: p. 483-507.
57. Lewis, D.A., et al., *Cortical parvalbumin interneurons and cognitive dysfunction in schizophrenia*. Trends in Neurosciences. **35**(1): p. 57-67.
58. Farrant, M. and Z. Nusser, *Variations on an inhibitory theme: phasic and tonic activation of GABA<sub>A</sub> receptors*. Nat Rev Neurosci, 2005. **6**(3): p. 215-229.
59. Fagiolini, M., et al., *Specific GABA<sub>A</sub> Circuits for Visual Cortical Plasticity*. Science, 2004. **303**(5664): p. 1681-1683.
60. Chow, A., et al., *K(+) channel expression distinguishes subpopulations of parvalbumin- and somatostatin-containing neocortical interneurons*. J Neurosci, 1999. **19**(21): p. 9332-45.
61. Rosato-Siri, M.D., et al., *A Novel Modulator of Kv3 Potassium Channels Regulates the Firing of Parvalbumin-Positive Cortical Interneurons*. The Journal of pharmacology and experimental therapeutics, 2015. **354**(3): p. 251-60.
62. Beurdeley, M., et al., *Otx2 binding to perineuronal nets persistently regulates plasticity in the mature visual cortex*. J Neurosci, 2012. **32**(27): p. 9429-37.
63. Bernard, C. and A. Prochiantz, *Otx2-PNN Interaction to Regulate Cortical Plasticity*. Neural Plast, 2016. **2016**: p. 7931693.
64. Sugiyama, S., et al., *Experience-dependent transfer of Otx2 homeoprotein into the visual cortex activates postnatal plasticity*. Cell, 2008. **134**(3): p. 508-20.
65. Yang, G., et al., *Peripheral elevation of TNF-alpha leads to early synaptic abnormalities in the mouse somatosensory cortex in experimental autoimmune encephalomyelitis*. Proc Natl Acad Sci U S A, 2013. **110**(25): p. 10306-11.
66. Kuo, M.-F., et al., *Focusing Effect of Acetylcholine on Neuroplasticity in the Human Motor Cortex*. The Journal of Neuroscience, 2007. **27**(52): p. 14442.
67. Bear, M.F. and W. Singer, *Modulation of visual cortical plasticity by acetylcholine and noradrenaline*. Nature, 1986. **320**(6058): p. 172-6.
68. Tisell, A., et al., *Increased Concentrations of Glutamate and Glutamine in Normal-Appearing White Matter of Patients with Multiple Sclerosis and Normal MR Imaging Brain Scans*. PLoS ONE, 2013. **8**(4): p. e61817.

69. Geurts, J.J.G., et al., *MR spectroscopic evidence for thalamic and hippocampal, but not cortical, damage in multiple sclerosis*. *Magnetic Resonance in Medicine*, 2006. **55**(3): p. 478-483.
70. Musgrave, T., et al., *The MAO inhibitor phenelzine improves functional outcomes in mice with experimental autoimmune encephalomyelitis (EAE)*. *Brain, Behavior, and Immunity*, 2011. **25**(8): p. 1677-1688.
71. Musgrave, T., et al., *Tissue concentration changes of amino acids and biogenic amines in the central nervous system of mice with experimental autoimmune encephalomyelitis (EAE)*. *Neurochemistry international*, 2011. **59**(1): p. 28-38.

# **Appendix**

## Published Papers

RESEARCH

Open Access



# Altered excitatory-inhibitory balance within somatosensory cortex is associated with enhanced plasticity and pain sensitivity in a mouse model of multiple sclerosis

Liam E. Potter<sup>1,5</sup>, John W. Paylor<sup>1,3</sup>, Jee Su Suh<sup>5</sup>, Gustavo Tenorio<sup>5</sup>, Jayalakshmi Caliaperumal<sup>1,4</sup>, Fred Colbourne<sup>1,4</sup>, Glen Baker<sup>1,3</sup>, Ian Winship<sup>1,3</sup> and Bradley J. Kerr<sup>1,2,5\*</sup>

## Abstract

**Background:** Chronic neuropathic pain is a common symptom of multiple sclerosis (MS). MOG<sub>35–55</sub>-induced experimental autoimmune encephalomyelitis (EAE) has been used as an animal model to investigate the mechanisms of pain in MS. Previous studies have implicated sensitization of spinal nociceptive networks in the pathogenesis of pain in EAE. However, the involvement of supraspinal sites of nociceptive integration, such as the primary somatosensory cortex (S1), has not been defined. We therefore examined functional, structural, and immunological alterations in S1 during the early stages of EAE, when pain behaviors first appear. We also assessed the effects of the antidepressant phenelzine (PLZ) on S1 alterations and nociceptive (mechanical) sensitivity in early EAE. PLZ has been shown to restore central nervous system (CNS) tissue concentrations of GABA and the monoamines (5-HT, NA) in EAE. We hypothesized that PLZ treatment would also normalize nociceptive sensitivity in EAE by restoring the balance of excitation and inhibition (E-I) in the CNS.

**Methods:** We used *in vivo* flavoprotein autofluorescence imaging (FAI) to assess neural ensemble responses in S1 to vibrotactile stimulation of the limbs in early EAE. We also used immunohistochemistry (IHC), and Golgi-Cox staining, to examine synaptic changes and neuroinflammation in S1. Mechanical sensitivity was assessed at the clinical onset of EAE with Von Frey hairs.

**Results:** Mice with early EAE exhibited significantly intensified and expanded FAI responses in S1 compared to controls. IHC revealed increased vesicular glutamate transporter (VGLUT1) expression and disrupted parvalbumin+ (PV+) interneuron connectivity in S1 of EAE mice. Furthermore, peri-neuronal nets (PNNs) were significantly reduced in S1. Morphological analysis of excitatory neurons in S1 revealed increased dendritic spine densities. Iba-1+ cortical microglia were significantly elevated early in the disease. Chronic PLZ treatment was found to normalize mechanical thresholds in EAE. PLZ also normalized S1 FAI responses, neuronal morphologies, and cortical microglia numbers and attenuated VGLUT1 reactivity—but did not significantly attenuate the loss of PNNs.

**Conclusions:** These findings implicate a pro-excitatory shift in the E-I balance of the somatosensory CNS, arising early in the pathogenesis EAE and leading to large-scale functional and structural plasticity in S1. They also suggest a novel antinociceptive effect of PLZ treatment.

\* Correspondence: [bradley.kerr@ualberta.ca](mailto:bradley.kerr@ualberta.ca)

<sup>1</sup>Neuroscience and Mental Health Institute, University of Alberta, Edmonton, AB T6G 2E1, Canada

<sup>2</sup>Department of Pharmacology, University of Alberta, Edmonton, AB T6E 2H7, Canada

Full list of author information is available at the end of the article

## Background

In addition to progressive paralysis and the formation of white matter plaques, multiple sclerosis (MS) is often associated with prominent secondary symptoms [1]. Sensory alterations, including pain and dysesthesia, are frequently reported in the clinical MS population [2, 3]. A substantial proportion of those affected (up to 40 %) suffer from pain of central neuropathic origin (CNP) [4, 5]. An increasing awareness of these issues has developed in parallel with an increased focus on the importance of gray matter alterations in the pathobiology of MS [6]. Furthermore, a connection between maladaptive plasticity within pain-associated gray matter regions of the brain—such as the primary somatosensory cortex (S1)—and CNP has been established in the literature [7–9].

Several recent studies and reviews have indicated that the disease model, experimental autoimmune encephalomyelitis (EAE), shares multiple pathobiological characteristics with MS beyond the hallmark symptoms of demyelination, paralysis, and frank neurodegeneration [10]. Wide-spread gray matter synaptopathy, driven by diffuse and persistent neuroinflammation throughout the central nervous system (CNS) is emerging as a critical contributing factor in the loss of function, sensory and cognitive abnormalities [11], and potentially in pain—which is also now known to feature prominently EAE. These reports provide an experimental foundation for investigations into the connections between these phenomena in diseases like MS/EAE. Specifically, earlier studies by Olechowski et al. [12–14] and others [15–17] established the suitability of the female C57/BL6 mouse model of EAE for the study of the underlying mechanisms of CNP in MS. These studies revealed that mice with EAE develop robust mechanical and thermal allodynia prior to the onset of paralytic symptoms. They also found evidence of hyperexcitability within the dorsal horn of the spinal cord (SC-DH), a form of central sensitization [12, 18]. While a few previous reports have highlighted the existence of altered neuronal structure and function in the neocortex of animals with EAE [19–21], no study to date has directly examined changes in neuronal activity and structure in higher sensory cortex in connection with altered pain behaviors in the early stages of the disease.

S1 is known to play a critical role in processing “sensory-discriminative” aspects of both painful and non-painful touch. Within S1, the body-centric locations of external stimuli are encoded as a spatially organized “somatotopic map” comprised by distinct regions of cortical activation. The intensity (or perceived intensity) of an external stimulus is encoded as the magnitude of cortical activation (the extent of neuronal spiking activity, within an ensemble) in S1. Painful stimuli, which are generally perceived as being more intense, are associated with a greater magnitude of activation in S1 [22]. Allodynia, such as in

EAE/MS with CNP, involves non-noxious stimuli being perceived as painful—and is thought to involve intense activation (hyperexcitability) in S1 and connected “pain-associated” brain regions [23–25]. Indeed, plasticity and enhanced activation in S1 has been shown to enhance activation in other “pain regions,” such as the anterior cingulate cortex, and to enhance chronic pain states [7, 23].

In the current study, we quantified synaptic densities and neuronal morphologies in S1 of female C57/BL6 mice with EAE using histological methods. This involved immunostaining for vesicular glutamate transporter (VGLUT1)+ presynaptic excitatory terminals and parvalbumin+ (PV+) inhibitory networks and reflectance-mode confocal microscopy of Golgi-Cox-stained cortical neurons. We also quantified sensory-evoked functional neuronal responses in S1 of EAE mice using *in vivo* flavoprotein autofluorescence imaging (FAI). FAI has recently been employed in several studies of cortical (S1) responses to noxious and non-noxious peripheral stimuli in rodents under acute urethane-induced anesthesia. This technique measures increases in endogenous green fluorescence, produced by oxidized flavoproteins within the mitochondrial respiratory chain, as a quantitative and non-hemodynamic index of neuronal energy metabolism and activity [26]. The FAI signal has been shown to exhibit a roughly linear correspondence with local-field potentials and intracellular calcium rises and with stimulus amplitude, frequency, and duration [27]. These features make FAI an ideal technique for investigating cortical nociceptive responses in EAE and for the assessment of novel antinociceptive treatments.

The antidepressant phenelzine (PLZ) is an atypical monoamine oxidase inhibitor (MAOI). We have previously demonstrated that EAE is associated with a reduction in CNS tissue concentrations of the monoamine neurotransmitters (NTs) serotonin (5-HT), noradrenaline (NA), and dopamine (DA), as well as gamma-aminobutyric acid (GABA) [28]. PLZ can restore CNS tissue concentrations of all of these NTs when given chronically to mice with EAE [29]. PLZ therefore combines the features of both an anticonvulsant and an antidepressant—the net effect of which, we predicted, would be a promotion of neuronal inhibition within the CNS. As two recent reviews have speculated that a chronic pro-excitatory/disinhibitory state may exist in the CNS in MS/EAE [10, 11], and as both pain and neocortical plasticity are thought to be regulated by a precise balance of CNS excitation and inhibition (E-I) [30, 31], we hypothesized that a disrupted E-I balance might underlie both conditions in EAE. We also hypothesized that restoring this balance, by bolstering CNS inhibition with PLZ, would be an effective approach to treatment for these symptoms of the disease.

## Methods

### Mice and behavioral testing

A total of 116, 8–12-week-old, female C57/BL6 mice (Charles River–Saint Constant, Quebec, Canada) were used in these experiments. Mice were housed 5 per cage, in standard cages, and fed ad libitum. All animal experiments and procedures were conducted in accordance with the Canadian Council on Animal Care's Guidelines and Policies and with protocols approved by the University of Alberta Health Sciences Animal Care and Use Committee.

### EAE induction

EAE was induced in mice by subcutaneous (S.C.) injection into the hindquarters of 50 µg of myelin oligodendrocyte glycoprotein (MOG<sub>35–55</sub>), obtained from the Peptide Synthesis Facility at the University of Calgary (Calgary, Alberta, Canada), and emulsified in Complete Freund's Adjuvant (CFA, 1.5 mg/mL) containing additional heat-killed *Mycobacterium tuberculosis* H37Ra (Difco Laboratories/BD Biosciences—Franklin Lakes, NJ, USA). Immunized mice also received two intraperitoneal (IP) injections of pertussis toxin (*Bordetella pertussis*) (PT, List Biological Labs—Campbell, CA, USA)—first, on the day of the induction and again 48 h later. Control mice received identical CFA with added *M. tuberculosis* H37Ra (S.C./hindquarters), but without MOG<sub>35–55</sub>. CFA mice also received PT injections on the same days.

### Disease scoring

Mice were scored daily for clinical disease severity by an observer blinded to the treatment groups, using a standard five-point scale (grades 0–4) defined as follows [32]: grade 0—*normal mouse, no loss of motor function*; grade 1—*flaccid tail, paralyzed in ≥50 % of the tail's length, or partial paralysis of the tail with visible weakness in one or more of the limbs*; grade 2—*completely paralyzed tail, some hindlimb weakness, preserved righting reflex*; grade 3—*severe hindlimb weakness, slowed righting reflex*; grade 4—*complete paralysis of one or both of the hindlimbs*. “Clinical onset” or “disease onset” was defined as the first day an animal scored a clinical grade of 1 or higher. Except in the “pre-symptomatic” experiments (and excluding CFA/naïve controls), only mice that developed clinical signs of EAE were included in the analyses.

### Drug treatments

For behavioral experiments, mice were divided into groups that, starting at 7 days post-induction (dpi), received daily IP injections of either vehicle (VEH, bacteriostatic water, 10 mL/kg body weight) or phenelzine (PLZ, 15 mg/kg body weight, Sigma-Aldrich—Oakville, ON, Canada). For EAE animals receiving PLZ, drug was

given on alternate days with injections of VEH given on the “off” day. This design was intended to control for multiple IP injections, as previous experiments showed that for longer experiments (a 21-dpi fixed endpoint was selected for this behavioral/“established” histology cohort), the effectiveness of GABA-transaminase (GABA-T) inhibition is better maintained by this injection schedule [33]. For the “onset” FAI/histology (Golgi-Cox) experiment, treatment was conducted in identical fashion; except animals in the (EAE- and CFA-) PLZ groups received the drug daily, rather than having the drug alternated with injections of VEH.

### Pain testing/Von Frey hair assay

The Von Frey hair (VF/VFH) assay was used to assess mechanical (tactile/punctate pressure) sensitivity and allodynia [34]. Animals were placed in transparent plexi-glass boxes over a screen that allowed access to the paws. Prior to the start of testing, all mice underwent a period of habituation to the boxes (5–10 min/day, for 3 days before baseline testing began). Mice were also given 5–10 min of habituation time in the testing boxes at the start of each test day. After this period, the plantar surface of each hindpaw was stimulated ×5 with a weighted Von Frey hair monofilament. An observer blinded to the experimental/treatment groups monitored and recorded behavioral responses to stimulation. “Noxious responding” (i.e., shaking, licking, or guarding of the paw) was noted. Hindpaw stimulation was repeated through a progressive series of filament weights (0.04–2.0 g), until a stimulus produced a “noxious response” ≥60 % of the time—the weight at which this occurred was taken to be the withdrawal threshold for that paw on that day. Left and right paw responses were averaged within each animal to provide a combined threshold for each test day, and these combined thresholds were used for subsequent analysis. Prior to disease induction, all animals underwent VFH testing on three separate days to establish baseline mechanical thresholds. After induction, mice were tested on days 3, 7, 9, and 12 post-induction and at clinical onset. CFA animals from 7–12 dpi were used in the “onset” analysis: *n* = 5 from each of days 7, 9, and 12 for the VEH group. PLZ-treated CFAs were taken at 12 dpi, following 7 daily drug injections.

### Rotorod

To confirm that there was no confounding influence of motor impairment in EAE mice at this stage of the disease, the Rotorod assay (Harvard Apparatus, Holliston, MA, USA) was also administered alongside the VFH assay. Any animals with a clinical grade of ≥2, or that could not successfully complete the Rotorod task, remaining on the Rotorod for the full duration of 180 s in at least one of the three attempts, and additionally failed to respond in the VFH (obtained a 2.0 g threshold, the maximum), were

excluded from the behavioral analysis ( $n = 3$ ). After excluding these animals, none of the groups differed in terms of their (mean) duration spent on the Rotorod (group means, avg. of 3 attempts/95 % C.I. of mean: CFA 173.6 s/ $\pm$ 6.1 s; EAE-VEH 126.7 s/ $\pm$ 68.6 s; EAE-PLZ 157.8 s/ $\pm$ 39.8 s—Kruskal-Wallis one-way analysis of variance (ANOVA) on ranks not significant,  $p = 0.242$ ).

#### **In vivo FAI of S1**

FAI through a thinned-skull window has several methodological advantages over other functional imaging techniques. It is minimally invasive to the animal and avoids certain experimental pitfalls common to more invasive methods, which frequently involve at minimum a craniotomy (electrophysiology, calcium imaging). By imaging through a thin window, we minimized the risk of exposing the brain to inadvertent physical trauma and/or periods of hypoxia/tissue exposure and avoided inducing excess inflammation/infection at the site of the cranial window. Furthermore, since the FAI signal is endogenous, no additional (and potentially disruptive or toxic) extrinsic compounds had to be applied to the brain [26, 35].

#### **Animal preparation (thin window)**

Mice at 7–9 dpi (“pre-symptomatic”) ( $n = 4$  EAE mice,  $n = 5$  CFA mice) or clinical onset ( $n = 8$  VEH-treated CFA mice at matched time points,  $n = 4$  PLZ-treated CFA mice at 14–17 dpi,  $n = 8$  VEH-treated EAE mice,  $n = 10$  PLZ-treated EAE mice) were imaged acutely through a thinned-skull window [36], before being euthanized for histological analysis. Animals did not receive any treatment injections on the day of the procedure. Prior to surgery, mice were lightly anesthetized with urethane (1.25 g/kg body weight IP, plus supplemental doses as required, dissolved at 20 % w/v in 0.9 % saline). Urethane was chosen as it provides stable and long-lasting anesthesia, and does not uncouple mitochondrial respiration in neurons (unlike volatile anesthetics [37]), making it suitable for FAI [38]. Relative to other anesthetics (such as pentobarbital or ketamine), urethane also does not strongly or preferentially modulate CNS GABA or glutamate function, and does not significantly interfere with evoked neuronal-ensemble responses, provided the dosage is appropriate and the achieved depth of anesthesia consistent [39, 40]. Anesthetized mice were placed in a modified stereotaxic apparatus, with body temperature continuously monitored and maintained at 37 °C by a rectal thermometer and heating pad. The hair of the scalp was grazed, and a local anesthetic (bupivacaine, 0.1 mg S.C.) was administered to the incision area. A rostrocaudal incision (approximately 1 cm in length) was made at the midline, and the overlying skin was pulled back to expose the dorsal surface of the skull. Any underlying connective tissue was cleared away to reveal the underlying bone. Under a dissecting

microscope, bregma was located and used as a reference to locate the region of interest (ROI) above the right primary somatosensory cortex (SIHL/FL, centered 2 mm lateral from midline, 0.5 mm caudal to bregma) [41]. A circle, 3 mm in diameter, was traced over the ROI to demarcate the boundaries of the window. Using a high-speed dental drill, the skull was progressively thinned to the point where the underlying vasculature was clearly visible (approximately 30 % of the original thickness). During this process, physiological saline was periodically dripped onto the skull to aid with visualizing the region and to prevent frictional heating. Particular attention was paid to ensuring that excessive mechanical pressure, which can cause blood to pool beneath the window, was not applied during the thinning process. This is necessary because blood absorbs light and scatters both the excitation and emission wavelengths for FA imaging. Once a smooth cranial surface was obtained at the appropriate depth, the animal was transferred to the imaging setup.

#### **FA imaging**

After preparation, animals in the stereotaxic frame and held at normothermia were positioned into the imaging setup. The imaging setup consists of a binocular epifluorescence microscope (TCS SP5 MP—Leica Microsystems, Wetzlar, Germany) equipped with  $\times 2.5$  objective lens. Under blue excitation light (450–490 nm, I3 filter-cube—Leica) generated by a 120-W metal-halide lamp (Leica EL6000), images of the brain’s endogenous green ( $>515$  nm) fluorescence were captured from a software-controlled frame-grabber (EPIX PIXCI™ EL1—EPIX Inc., Buffalo Grove, IL, USA) connected to a 12-bit CCD camera (DALSA Pantera™ DS-21-01 M60—Teledyne Dalsa, Waterloo, ON, Canada). This setup employs a dichroic mirror (510 nm) to accommodate separate light paths for excitation and emission wavelengths, preventing contamination and dilution of the relatively weak fluorescence signal by the much larger blue-green reflectance signal [27]. In order to improve detection of the weak fluorescence signal and enhance the signal-to-noise ratio, the camera was also set to  $4 \times 4$  spatial binning. The animal’s left fore- and hindlimb were positioned into computer-triggered vibromechanical stimulators incorporating piezoceramic actuators (Piezo Systems, Woburn, MA, USA) [42]. All external light sources were removed by dimming the light in the room and covering the imaging setup with an opaque black curtain. Extraneous vibrational sources were controlled by the use of an air table. Imaging trials involved the continuous capture of frames for 7.5 s at 4 hz (250 ms exposure, 31 frames) for “pre-symptomatic” imaging, or for 6 s at 5 hz (200 ms exposure, 31 frames) for “onset” imaging, with the stimulus (1 mm deflection, 100 hz, 1 s stimulus duration) being delivered after the first second. These relatively long exposure times were necessary to

reliably detect the weak fluorescence signal; however, the temporal resolution we obtained was adequate, as the time course of the in vivo sensory-evoked FA signal in mouse S1 is relatively slow (in the order of seconds). In order to obtain a consistent and accurately quantifiable FA response, each imaging session was comprised of 40 repeated trials per limb (alternating fore- and hind-), with a 20-s interstimulus interval to allow activity to return to baseline. All images were stored as uncompressed 256 × 256 pixel grayscale TIFF stacks.

#### **FA image processing and data analysis**

Data analysis was performed using NIH ImageJ 1.43/FIJI software equipped with the Intrinsic Signal and VSD Processor plugin (v1.0.8, written by Albrecht Sigler) obtained from the website of Dr. Timothy Murphy [43]. Briefly, in order to obtain a representative response and improve signal-to-noise ratio, all trials from a given limb and session were averaged to provide a mean time series. Prior to averaging, all trials were manually inspected for any obvious motion, light, or equipment artifacts that might obscure the signal (due to their much larger relative magnitudes). The plugin's automated data quality algorithm was also used to detect trials that deviated strongly from the mean response (i.e.,  $\geq 10$  % frame-by-frame deviation in the average gray value from the mean z-stack). Any trials contaminated by artifacts, or with a highly deviating response profile, were excluded from the analysis. A Gaussian filter ( $r = 1.0$  pixel) was applied to all images in the  $x, y$  directions to reduce high frequency noise. In order to control for global differences in basal cortical activity, tissue autofluorescence, and ambient light levels, all responses were normalized to a percent change in fluorescence vs. baseline ( $\% \Delta F/F$ ). A "baseline" image was calculated from the mean time series as the (pixel-by-pixel gray value) average of the frames immediately preceding the onset of stimulation. A "response" frame was defined for each session as the frames that, following the onset of stimulation, comprised the primary FA response (i.e., from the initial upward inflection point or signal onset—to the zero intercept, or signal offset), as determined from the intensity-vs.-time plot of the mean time series. The baseline image was subtracted from all images in the series to create a "difference series." All images in the response frame (of the difference series) were then divided by the baseline image (and multiplied by 100) to yield a time series of images in which the intensity of each pixel indicated the % change in intensity vs. baseline ( $\% \Delta F/F$ ) [44].

This ( $\% \Delta F/F$ ) time series was then quantified along the following parameters: time of signal onset, time to peak response, duration of the attack phase, duration of the decay phase, and total response duration (only decay-duration data is shown—although total response duration

differed between treatment groups, this was accounted for by changes in decay duration). In the spatial domain, the areal extent of the "cortical map" (i.e., response area) was quantified. This "cortical map" was defined as the area where the  $\% \Delta F/F$  was  $> 50$  % of its maximal value in a (mean) z-projected image of the response frame. An ROI was drawn around this "map" area, and the (ROI-wide) mean intensity ( $\% \Delta F/F$ ) was plotted vs. time, in order to determine the intensity at peak response. For the "surround-inhibitory" FA signal analysis, an ROI was drawn manually around the darkened regions adjacent to the "cortical map," and the peak (negative)  $\% \Delta F/F$  intensity value was thereby attained.

#### **Histology**

Histological analysis was performed on brain tissues extracted from CFA controls and EAE (untreated, VEH-treated, PLZ-treated) mice at the various experimental endpoints: "pre-symptomatic" (7–9 dpi/post-FAI), "clinical onset" (the day a mouse first presented as clinical grade 1 or higher, post-FAI; CFA endpoints matched) and at the "established disease" endpoint of 21 dpi. In order to improve certain group sizes and obtain greater statistical power, "additional onset" brains (referred to in the subsequent text) were obtained from a separate cohort of CFA/EAE mice that received no drug treatments, but did receive similar behavioral habituation and baseline assessments, were fixed at clinical onset (7–9 dpi for CFA animals) for tissues. Statistical comparisons confirmed that these mice did not differ significantly from the initial cohorts on the applicable measures.

#### **Tissue extraction and fixation**

For "pre-symptomatic" and "clinical-onset" cohorts, depth of anesthesia was assessed immediately after FAI. Any animals that required additional anesthesia were put into a chamber supplied with isoflurane/O<sub>2</sub> mixture at 5 % w/v, 3 L/min at 14.7 psi for approximately 1 min. For behavioral/histology cohorts ("additional onset" and "established disease" immunohistochemistry (IHC)), mice were anesthetized with sodium pentobarbital (1.7 g/kg IP). Fully anesthetized mice underwent exsanguination and fixation by transcardiac perfusion with 4 % w/v paraformaldehyde (PFA) in 0.1 M phosphate buffer (PB). For Golgi-Cox staining, extracted tissues (whole brains from the "clinical-onset" FAI experiment) were briefly immersed in ddH<sub>2</sub>O and then placed immediately into Golgi-Cox solution (see below). For IHC, extracted tissues were post-fixed in 4 % w/v PFA/0.1 M PB for at least 24 h and then immersed in 30 % w/v sucrose solution in 0.1 M PB overnight, before being snap frozen with isopentane on solid carbon dioxide. Frozen tissues were stored at  $-80$  °C prior to sectioning on a cryostat (50  $\mu$ m) as free-floating sections (see below, "established disease" cohort only) or immediately

mounted onto slides (“pre-symptomatic” and “onset” histology).

#### **Free-floating sectioning**

For “established disease” histology, free-floating sections were stored in phosphate-buffered saline solution (PBS) at 4 °C until they could be stained. After staining with a standard IHC protocol (see below), sections were mounted onto slides and coverslipped with Vectashield® Mounting Medium with DAPI (Vector Laboratories Inc., Burlingame, CA, USA).

#### **Golgi-Cox staining**

We performed Rapid Golgi-Cox staining, combined with reflectance-mode laser-scanning confocal microscopy, on tissue sections incorporating S1 from CFA, VEH-treated EAE, and PLZ-treated EAE mice at clinical onset. Immediately after FAI, extracted brains were immersed in Rapid Golgi-Cox solution (“Solutions A/B,” FD Rapid GolgiStain Kit™, FD Neurotechnologies—Columbia, MD, USA) for 14 days (changing the solution once after 24 h) at RT/low ambient light, before being transferred into cutting solution (“Solution C”). Brains were sectioned on a vibratome (Leica VT1200S) at 200 μm to ensure that whole (untransected) neuronal arbors could be accommodated [45] and then mounted on gelatin-coated slides. Slides were further developed and processed according to the manufacturer’s instructions, before being coverslipped with Permount™ Mounting Medium (Fisher Scientific Co., Waltham, MA, USA).

Spiny (excitatory/glutamatergic) neurons in cortical layers 2/3 and of S1—mainly pyramidal cells in layers 2/3, or stellate/star-pyramid (principal) cells in layer 4 [46, 47]—were located by reference to a stereotaxic atlas [41] and identified by their cytoarchitectonic/morphological characteristics. This step was performed under bright-field illumination on a Leica TCS SP-5 MP microscope by an unbiased observer. Three-dimensional z-stacks of these neurons were then acquired from the same microscope in confocal reflectance mode (488 nm argon laser, 30/70 R/T filter), equipped with a ×20 objective water-immersion lens (1.0 NA). Only neurons that were completely stained and unbroken were selected for acquisition to ensure that accurate quantifications could be obtained. Whenever staining permitted, at least two neurons from each layer were chosen from each animal for analysis. Z-stacks of the neurons’ entire dendritic arbors were acquired (2048 × 2048 pixels, pixel-size 240 × 240 nm, z-length: 0.54 μm, ×2 line/frame averaging) using Leica’s LAS-AF™ software suite. The observer then manually selected representative dendritic segments and manually counted the total number of spines (protruding in all three planes) along their lengths using FIJI/ImageJ [48]. Only protrusions with a distinctly formed neck and head were considered to be dendritic spines (“stubs” and filopodia were

not included in the counts). For each neuron, a minimum of 3 and a maximum of 9 dendritic segments were analyzed, with an effort made to sample equally from proximal and distal branches and from the apical and basilar tufts (when staining permitted). This resulted in a total of  $n = 42$  neurites from 8 layer 2/3 neurons and  $n = 47$  neurites from 10 layer 4 neurons (5 mice) for the CFA group. For the EAE-VEH group,  $n = 66$  neurites from 14 layer 2/3 neurons and  $n = 76$  neurites from 14 layer 4 neurons (8 mice) were obtained, and for the EAE-PLZ group,  $n = 79$  neurites from 18 layer 2/3 (9 mice) and  $n = 83$  neurites from 20 layer 4 neurons (10 mice). Dendritic segment lengths were determined using the Simple Neurite Tracer plugin for FIJI/ImageJ [49], and the spine density of each segment was calculated by dividing the total number of spines by the length of the corresponding segment.

#### **Immunohistochemistry: antibodies/reagents**

Tissues were stained using a standard IHC protocol with the following commercially available antibodies: rat anti-cluster of differentiation (CD)3 (1:200 concentration, AbD Serotec®—BioRad Laboratories Canada Ltd., Mississauga, ON, Canada), rat anti-CD45 (1:200, AbD Serotec®), rabbit anti-ionized calcium-binding adapter (Iba)-1 (1:500, Wako Chemicals USA Inc., Richmond, VA, USA), mouse anti-PV (1:2000, Cedar Lane, Burlington, ON, Canada), rabbit anti-VGLUT1 (1:1000, Cell Signaling Technology, Danvers, MA, USA), and *Wisteria floribunda* lectin (WFA, 1:1000, Vector Laboratories). Primary antibodies were visualized with the following fluorescent secondary antibodies: goat anti-rabbit Alexa Fluor®488 (1:200, Invitrogen™—Life Technologies Inc., Burlington, ON, Canada), donkey anti-rat 488 Alexa Fluor®488 (1:200), Alexa Fluor® 647 streptavidin (1:200), and goat anti-rabbit Alexa Fluor®594 (1:200). Selected PV-stained slides that were used in the “perisomatic” analysis were counterstained with NeuroTrace® 530/615 Red Fluorescent Nissl Stain (“fluoronissl”—ThermoFisher Scientific, Waltham, MA, USA) according to the manufacturer’s instructions. All slides were coverslipped using Vectashield® with DAPI.

#### **IHC: image acquisition**

Low-power images were captured on a Leica DMI 6000B microscope equipped with a ×5 objective lens (×50 total magnification). Higher magnification images required for the VGLUT1 analysis were acquired on a Zeiss Observer Z.1 inverted microscope equipped with a ×40 objective lens (×400 total magnification). For the “perisomatic” PV analysis, three-dimensional high-resolution (2048 × 2048 pixels, 0.301 μm × 0.301 μm pixel size, 0.615 μm optical slice thickness, ~30 slices) confocal fluorescence z-stack images were acquired (focused on L2/3 in S1HL, 1 image per section, 2 sections per slide, 2 slides per animal) with a Leica TCS SP-5 MP

microscope equipped with a  $\times 20$  objective water-immersion lens (1.0 NA). For VGLUT1 analysis, 4 images from (S1HL) layer 2/3, and 4 images from layer 4/5 were taken from at least 2 sections per slide and 1 or 2 slides per animal. All other measurements (Iba-1, WFA, and PV) were taken as the average of 3 sections per slide and 1 slide per animal (see Table 1 for histology sample sizes). Image acquisition parameters remained consistent within each analysis. All quantitative IHC image analyses were performed on either the original unmodified images or on images processed in a consistently applied manner as described elsewhere in the methods. Representative photomicrographs used in figures were additionally adjusted for brightness, contrast, color balance, and histogram scaling in order to improve the overall visibility of the images. These adjustments were performed only on whole images and were applied in a consistent manner such that the figures accurately reflect the entire contents and relative intensities of the original images.

#### **IHC: analysis**

CD3/CD45 staining was not quantified, as no infiltrating cells were present in any of the slides. For all other stains, images were quantified by an unbiased observer blind to treatment groups. Apart from the “perisomatic” PV analysis (see below), images were quantified with NIH ImageJ/FIJI. S1 hindlimb region (S1HL) and individual cortical layers therein were identified visually by inspecting cytoarchitectonic features and by making reference to stereotaxic atlases [41, 50]. An ROI over S1HL was manually drawn, and the total area of this ROI measured to ensure it remained consistent across all images and animals (the standard deviation for ROI area remained below 5 % at all times). Within this ROI, quantifications of parvalbumin-positive (PV+) and Iba-1+ cells were performed using the ITCN-automated cell-counting plugin for ImageJ (by Thomas Kuo et al. [51]). PV+ cell quantifications were performed for 7–9 dpi CFA control mice, “pre-symptomatic” EAE, and “additional onset” EAE groups, as well as for all “established” (21 dpi) groups (CFA, EAE-VEH, EAE-PLZ). Quantification of WFA staining was performed by manually counting peri-neuronal nets (PNNs) in the ROI. For VGLUT1 analysis, a custom Fiji macro was used to create an ROI of consistent dimensions/area in each image and subsequently return the integrated density within that ROI.

#### **IHC: analysis (“perisomatic” PV)**

Perisomatic PV staining was quantified using a custom Matlab application (created by Liam Potter, using elements of code and guidance from Dr. Majid Mohajerani, University of Lethbridge, Canada). This program was designed to operate on confocal images that had been “pre-processed” with a custom FIJI script, the purpose of which was to produce images of manageable file size, reduce image “noise,” and achieve better separation of the relevant foreground pixels from image background. Briefly, a 1-pixel-radius median filter was applied to each z-stack. Filtered stacks were group z-projected (by max intensity; 5 slices to 1 slice), followed by the manual selection of 2 or 3 consecutive “in-plane” (properly gained/artifact/distortion-free) z-projected images from each stack. These images were concatenated to form a new “compressed” z-stack. Compressed z-stacks were binarized using an automatic local thresholding function (Bernsen algorithm, 15-pixel radius). Following this pre-processing, a final “control” image was added at the end of the binarized stack by performing a watershed transform on a single “guide” image chosen from the stack. This “guide” image was selected to be one that contained many basket-cell outlines (i.e., “perisomatic” staining surrounding a putative pyramidal cell shadow). These shadows were later confirmed as pyramidal neurons by examining the fluoronissl counterstain. The watershed transform applied to the “guide” image served to close-off the spatial boundaries of these shadows so a region-growing algorithm could be applied.

Final processed/binarized stacks were loaded into the Matlab viewer, and an unbiased operator was then able to “click” inside these cell “shadows,” triggering the region-growing algorithm in the “control” image, followed by morphological dilation, to define the “perisomatic” ROI for that neuron. This ROI was then used as a Boolean mask to obtain the total number of “above-threshold” (white) pixels captured therein from each image in the stack (excluding the “control image”). After adding up the areas from each image in the stack (yielding a “pseudo-volume”), the resulting sum was normalized to the cross-sectional area of the “shadow neuron” (the initial undilated area of the ROI) and divided by the number of images in the (compressed) z-stack (excluding the “control image”). The final quantity obtained for each neuron was therefore a stack- (or “volume-”) averaged ratio of total

**Table 1** Immunohistochemistry group sizes (*n*'s)

Marker: group	CD3/CD45 (Early/Est.)	PV (cell counts) (Pre/Ons/Est.)	Perisomatic PV (Pre/Est.)	VGLUT1 (Pre/Est.)	WFA (Pre/Ons/Est.)	Iba-1 (Pre/Ons/Est.)
CFA	4/4	8/8/6	8/8	8/5	11/11/6	13/13/6
EAE (VEH)	4/4	4/4/7	4/4	4/5	4/8/7	4/8/7
EAE (PLZ)	4/4	–/–/4	–/4	–/4	–/–/4	–/–/4

stained area (adjacent the neuron) to the neuronal cross-sectional area. Approximately 25 “shadows” were analyzed per confocal stack (i.e., approx. 100 neurons per animal). The program operator was able to avoid inadvertently capturing any PV+ somas, confounding tissue artifacts, non-neuronal hypo/hyperintensities, and poorly binarized areas in the images by constant visual comparison with the unprocessed original confocal stacks during the analysis.

### Statistics

Statistical analyses were carried out using (the two-tailed) Student's *t* test or by one-way ANOVA with additional post hoc tests. The Holm-Sidak method was generally used for all pairwise post hoc comparisons (Student-Newmnn-Keuls (SNK) method was used for layer 4 2<sup>0</sup> branches Golgi-Cox analysis), whereas Dunnett's method was used when only post hoc comparisons against the control group were required. For non-parametric data, or cases where assumptions of normality/homogeneity of variances were not met, the Mann-Whitney rank-sum test or the Kruskal-Wallis one-way ANOVA (with post hoc comparisons against the control group by Dunn's method) was used. Significance ( $\alpha$ ) was set at  $p < 0.05$ .

### Results

#### Mice with EAE exhibit enhanced neuronal responses to tactile stimulation within S1 pre-symptomatically

To examine whether EAE involves changes in the functional (neuronal) activation of S1, we used FAI to measure responses in the forelimb (FL) and hindlimb (HL) cortex regions (S1FL/HL), evoked by a “non-noxious” vibrotactile (mechanical) stimulus. We first imaged naïve and CFA-only controls, along with EAE animals at a “pre-symptomatic” time point (7–9 dpi)—prior to any clinical signs of the disease, but when mechanical allodynia has been observed [14]. Vibrotactile-evoked FAI responses in S1HL were significantly more intense in the EAE group than in CFA-only controls or “naïve” animals (one-way ANOVA,  $p = 0.012$ ; all pairwise post hoc comparisons by Holm-Sidak method) (Fig. 1a, b). The area of cortical activation elicited by this stimulus was also significantly larger in the EAE group compared to naïve animals or mice treated with CFA only (one-way ANOVA,  $p = 0.009$ ; all pairwise post hoc comparisons by Holm-Sidak method) (Fig. 1c—an additional movie depicts representative HL responses (see Additional file 1: Video 1)).

When the HL-evoked FAI signal was analyzed in the temporal domain, we found that the overall signal duration—the time between stimulus onset and signal offset—was prolonged in the EAE group when compared to CFA-only or naïve animals. Specifically, the duration of the decay phase, or the time between signal-peak and signal-offset, was significantly prolonged and accounted for most of the overall increase in signal duration (one-way

ANOVA,  $p = 0.013$ ; all pairwise post hoc comparisons by Holm-Sidak method) (Fig. 1d). As CFA-only mice and naïve mice did not differ in terms of evoked functional activation of S1, and have also not been observed to differ in any of the other relevant parameters (such as mechanical sensitivity), CFA-only mice were used as the control group in subsequent analyses.

#### Early EAE is associated with changes in the density of inhibitory and excitatory synaptic markers within S1

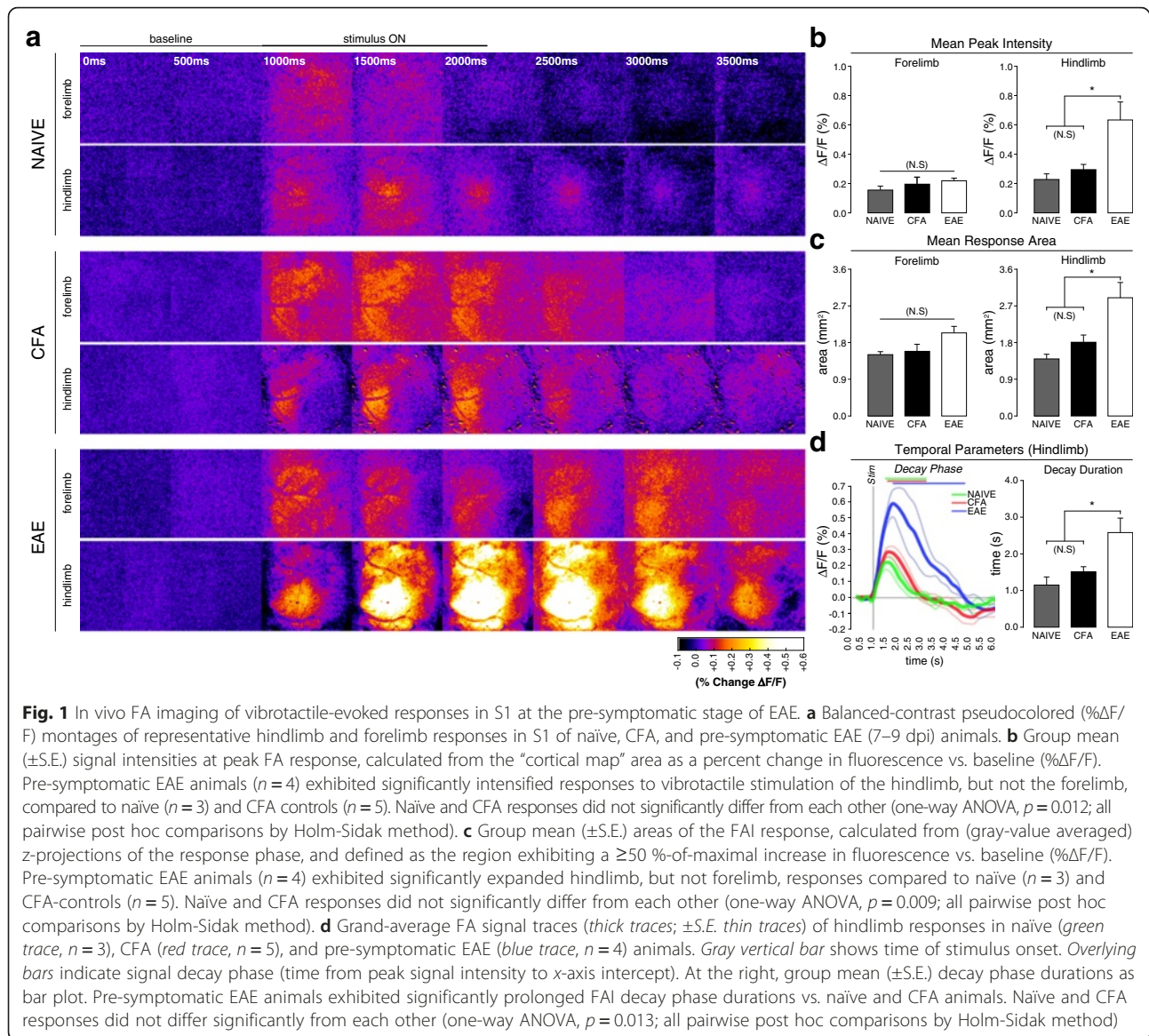
We next examined the possibility of a specific intracortical synaptic basis for the functional plasticity that we observed with FAI in S1 in EAE mice. To this end, we employed IHC on brain tissues collected post-FAI from CFA-only and pre-symptomatic EAE mice and examined the density of excitatory and inhibitory synaptic contacts in S1HL.

We found no significant difference in the number of parvalbumin-positive (PV+) inhibitory interneuron cell bodies in S1 from EAE or CFA control mice (see Additional file 2: Figure S1). However, we did observe a significant reduction in perisomatic PV-immunoreactivity around putative pyramidal neurons residing in cortical layers 2/3 of S1 at the earliest time point (two-tailed *t* test “pre” vs. CFA,  $p = 0.042$ ) (Fig. 2a–c). Hypo-intense regions or “shadows” in the dense PV staining, targeted in this analysis, were visually confirmed to correspond with neuronal (mostly pyramidal) cell-bodies using fluoronissl counterstaining (Fig. 2(a')).

The presynaptic marker of excitatory synapses, VGLUT1, is expressed at both thalamocortical and corticocortical glutamatergic terminals throughout S1. In contrast to PV, we found a significant increase in VGLUT1 density in layers 2/3 and 4/5 of S1 in pre-symptomatic EAE animals, compared to CFA controls (two-tailed *t* tests, L2/3:  $p = 0.041$ , L4/5:  $p = 0.047$ ) (Fig. 2d–i).

#### Chronic treatment with the antidepressant PLZ normalizes vibrotactile-evoked FAI responses in S1 of mice with EAE at clinical onset

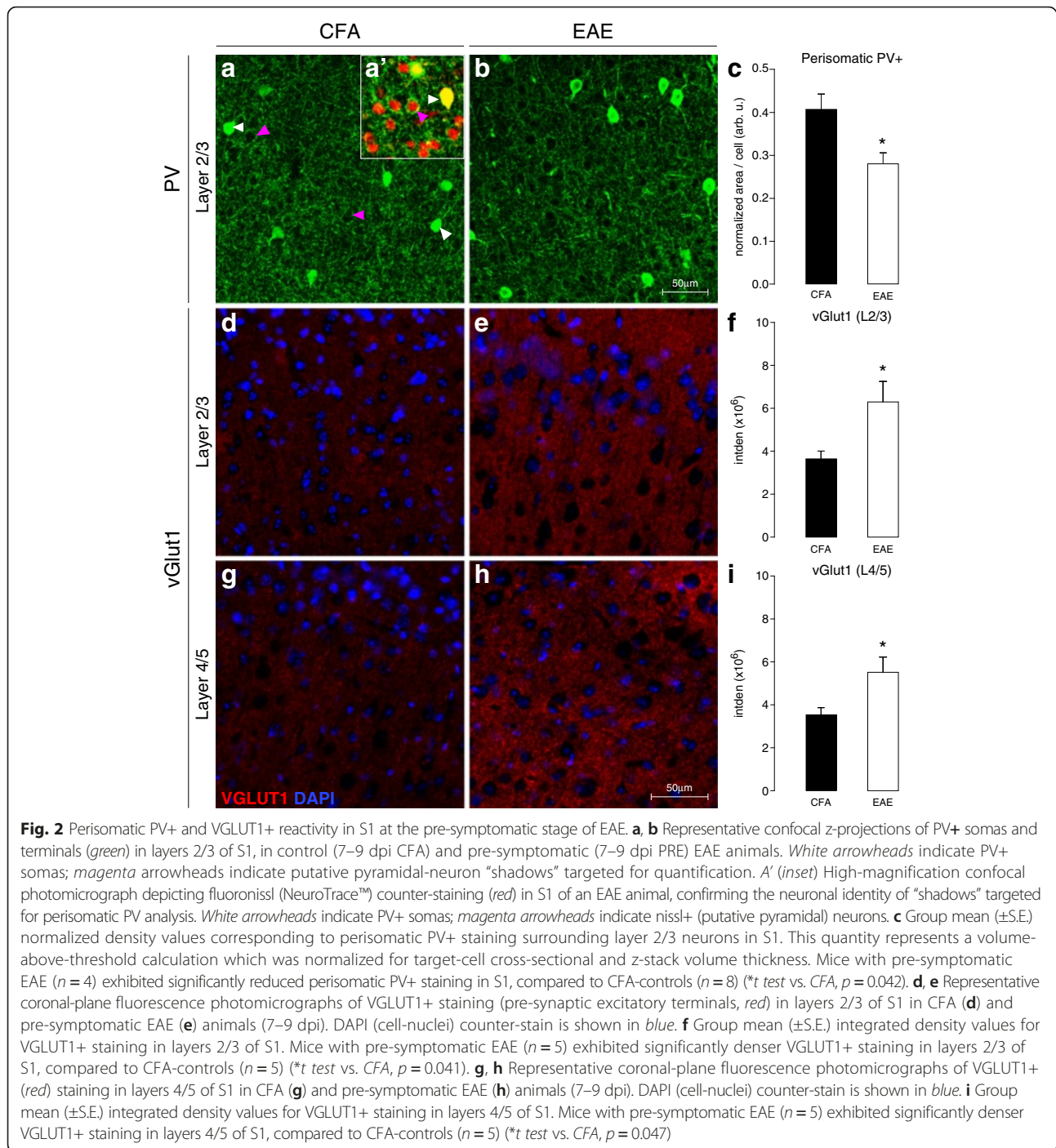
Our next experiment characterized the effects of PLZ treatment on vibrotactile-evoked FAI responses in S1 of CFA/EAE mice at the clinical onset of the disease, the time point when behaviorally measured allodynia is most prominent in EAE mice [14]. CFA-only controls and mice with EAE were treated with either vehicle (VEH) or PLZ, beginning at 7 dpi. S1 responses to vibrotactile stimulation of the limbs were imaged on the day when a mouse first presented with clinical signs of the disease (clinical onset/grade 1, flaccid paralyzed tail). As previously reported by Benson et al. [29, 33], PLZ treatment in EAE delays clinical onset by several days on average (see Additional file 3: Figure S2). Following onset, clinical severity progresses in PLZ-treated EAE mice along



an equivalent trajectory to that of VEH-treated EAE mice. As observed in pre-symptomatic animals, VEH-treated EAE mice exhibited significantly intensified HL-evoked S1 FAI responses at clinical onset, compared to control mice treated with CFA alone. Chronic PLZ treatment in EAE animals normalized the intensity of HL-evoked responses to levels similar to (VEH-treated) CFA controls. PLZ-treated CFA animals did not significantly differ from VEH-treated CFA or PLZ-treated EAE animals (one-way ANOVA,  $p < 0.001$ ; all post hoc comparisons by Holm-Sidak method) (Fig. 3a, b).

Similar to what we observed at the pre-symptomatic stage, the area of the HL-evoked S1 FAI response remained significantly expanded at clinical onset in EAE mice treated with vehicle. This functional “map” expansion in S1 of EAE animals was normalized by PLZ treatment. PLZ treatment

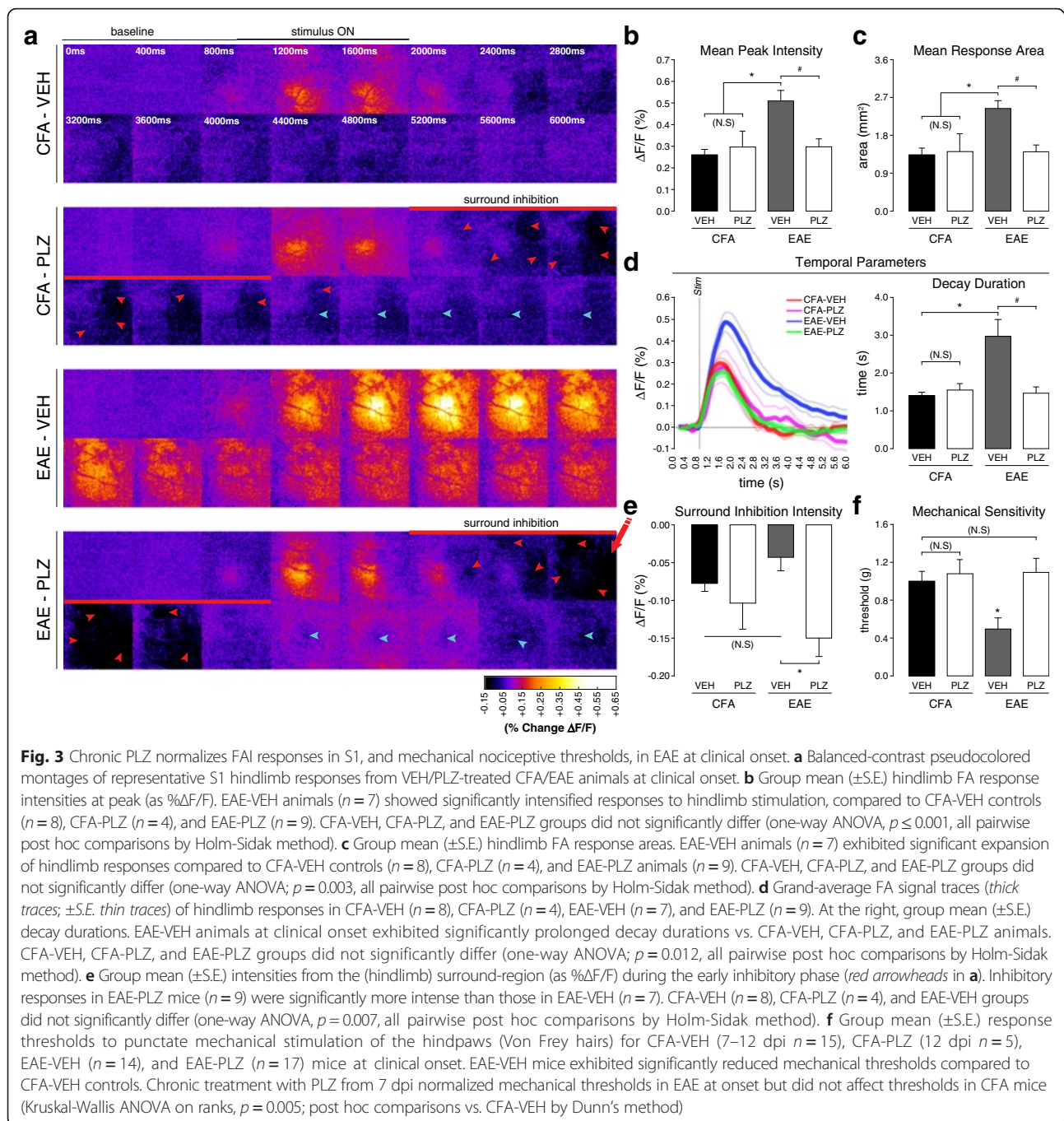
did not significantly affect HL-evoked response area in CFA animals (one-way ANOVA,  $p = 0.003$ ; all pairwise post hoc comparisons by Holm-Sidak method) (Fig. 3c). EAE animals at clinical onset also exhibited increased HL-evoked FAI signal duration, which was mainly the result of a significantly prolonged decay phase. Treatment with PLZ normalized HL-evoked response/decay durations in EAE animals at clinical onset but did not alter response durations in CFA animals (one-way ANOVA,  $p = 0.012$ , all pairwise post hoc comparisons by Holm-Sidak method) (Fig. 3d—an additional movie depicts representative HL responses (see Additional file 4: Video 2). VEH-treated EAE mice also displayed significantly more intense FAI responses in S1FL to forelimb stimulation at clinical onset. PLZ treatment in mice with EAE normalized the intensity of FL-evoked responses to CFA levels. Again, PLZ-treated



CFA animals did not significantly differ from VEH-treated CFA mice or PLZ-treated EAE animals for FL parameters (Kruskal-Wallis one-way ANOVA on ranks,  $p < 0.001$  post hoc comparisons vs. CFA by Dunn's method) (see Additional file 5: Figure S3).

To determine whether measurable changes in functional inhibition might contribute to the altered patterns of activation observed in S1 of EAE animals [52–54], we also quantified the magnitude of the early/adjacent

“surround-inhibitory/off-map” FAI signal. This signal component indicates reduced neuronal spiking and oxidative metabolism and has been shown to be GABA-A receptor-mediated [55–57]. There was no significant difference in the magnitude of this negative signal component between CFA control mice treated with either VEH or PLZ, nor did we find any differences between VEH-treated CFA controls and VEH-treated EAE mice (post hoc comparisons not significant,  $p > 0.05$ ). However, we



found that the magnitude of this negative signal was significantly greater in PLZ-treated EAE mice compared to EAE mice treated with VEH (one-way ANOVA,  $p = 0.007$ , all pairwise post hoc comparisons by Holm-Sidak method) (Fig. 3a, e).

#### PLZ treatment normalizes nociceptive sensitivity in mice with EAE

In order to confirm an association between S1 plasticity and nociception in the EAE model, we characterized the

effects of PLZ treatment on withdrawal thresholds in response to Von Frey hair (punctate mechanical) stimulation. For this analysis, a separate cohort of CFA-only and EAE mice were treated with either VEH or PLZ from 7 dpi and assessed with VF hairs on the day of clinical onset (CFA mice were assessed at matched time points as described in methods). As we have demonstrated previously [14], mice with EAE exhibit significantly decreased mechanical withdrawal thresholds at clinical onset. In contrast, withdrawal thresholds were

normalized in EAE mice treated with PLZ and were not significantly different from CFA controls. PLZ-treated CFA mice did not differ significantly from VEH-treated CFA or from PLZ-treated EAE animals (Kruskal-Wallis one-way ANOVA on ranks,  $p = 0.005$ ; all post hoc comparisons vs. CFA by Dunn's method) (Fig. 3f). As no differences were observed between the PLZ- and VEH-treated CFA groups in either evoked functional responses in S1 or behaviorally assessed nociceptive sensitivity, the PLZ-treated CFA group was not included in subsequent analyses.

#### **EAE is associated with morphological changes to excitatory neurons of cortical layers 2/3 and 4 of S1, which are prevented or reversed by PLZ treatment**

Altered functional responses in the neocortex are often a consequence of structural plasticity and modified connectivity amongst excitatory pyramidal/principal neurons [53]. Moreover, neuropathic pain states are associated with the rapid remodeling of dendritic spines, where the excitatory post-synaptic density is localized [58], in excitatory neurons of S1. We therefore investigated whether we could detect alterations in the density of dendritic spines along the processes of spiny excitatory (principal and pyramidal) neurons in cortical layer 4 and layers 2/3 of S1. Layer 2/3 and layer 4 spiny (excitatory) neurons were found to exhibit greater overall spine densities along the examined dendrites from the EAE-VEH group (Kruskal-Wallis one-way ANOVA on ranks, layers 2/3:  $p = 0.032$ , layer 4:  $p < 0.001$ , all post hoc comparisons vs. CFA by Dunn's method). This effect was normalized to CFA levels in the EAE-PLZ group (post hoc comparison between EAE-PLZ and CFA not significant,  $p > 0.05$ ) (Fig. 4a–c).

We next examined spine densities in the same set of neurons, grouping dendritic segments according to their relative position within their associated neuronal arbor. We classified dendritic segments as either apical or basilar branches and as primary, secondary, and tertiary branches. We then analyzed all possible permutations of these categories (primary apical, primary basilar, secondary apical, etc.). This “grouped” analysis allowed us to determine that the increased spine density we observed at the neurites of layer 2/3 neurons from the EAE-VEH group was almost completely localized to the tertiary (i.e., the most distal dendrites, in this classification) basilar branches. PLZ treatment prevented or reversed these changes, as spine densities at tertiary-basilar neurites were normalized to CFA levels (Kruskal-Wallis one-way ANOVA on ranks,  $p = 0.007$ , all post hoc comparisons vs. CFA by Dunn's method) (Fig. 4b). The distribution of layer 4 neuronal dendrites exhibiting elevated spine densities (i.e., from the EAE-VEH group) was less specifically localized within the arbor. These increases did not occur exclusively in either the apical or basilar tufts

or in the most proximal or distal dendrites. Rather, layer 4 neuronal dendrites from the EAE-VEH group exhibited a significant increase in spine density specifically when considering second-order branches. Again, we found that PLZ treatment normalized these densities to CFA levels (one-way ANOVA,  $p < 0.001$ , all pairwise post hoc comparisons by SNK method) (Fig. 4c).

#### **Chronic PLZ treatment partially normalizes pre-synaptic excitatory synaptic densities in S1 of mice with established EAE**

To investigate the long-term consequences of EAE on cortical plasticity and how PLZ can affect these processes, we assessed the effects of chronic PLZ treatment on cortical pre-synaptic alterations in tissue taken at the fixed endpoint of 21 dpi. This is a time past the “clinical-onset” phase, when the disease has been fully established in the majority of animals. At this later stage of the disease, perisomatic PV staining within S1 was not significantly different between CFA controls and VEH- or PLZ- treated EAE animals (one-way ANOVA not significant,  $p = 0.661$ ) (Fig. 5a, b). In contrast, VGLUT1 staining in S1 remained significantly denser in the VEH-treated EAE animals at 21 dpi compared to CFA controls. This elevated VGLUT1 density was partially diminished in the PLZ-treated EAE group, but not completely normalized to CFA levels (one-way ANOVA, layers 2/3:  $p = 0.014$ , layers 4/5:  $p = 0.007$ , all pairwise post hoc comparisons by Holm-Sidak method) (Fig. 5c, d).

#### **EAE is associated with a progressive loss of peri-neuronal nets and microgliosis in S1**

PV+ interneurons are often surrounded by organized components of the extracellular matrix (ECMCs) known as peri-neuronal nets (PNNs) [59]. Intact PNNs are essential to maintaining the fast-inhibitory activity of PV+ interneurons [60]. They are also known to be important regulators of plasticity [61] and may be disrupted in disease states [62]. We next assessed if PNNs were disrupted in the EAE somatosensory cortex by staining with WFA lectin [63]. The number of intact PNNs was significantly diminished in S1 of EAE animals beginning at clinical onset (one-way ANOVA,  $p = 0.008$ , post hoc comparisons vs. CFA by Dunnett's method) (see Additional file 2: Figure S1). This reduction in PNN numbers was persistent and was also observed in S1 of EAE animals at the later 21 dpi time point. Chronic PLZ treatment from 7 dpi did not restore or prevent the decline of PNN numbers in EAE animals assessed at the 21 dpi time point (one-way ANOVA,  $p = 0.021$ , post hoc comparisons vs. CFA by Dunnett's method) (Fig. 6a, b).

We next sought to identify the potential disease-related mechanism that leads to PNN loss and concurrent synaptic remodeling in EAE. As inflammation and immune-mediated mechanisms have been implicated in synaptic plasticity in EAE [20, 64, 65], and in the loss of

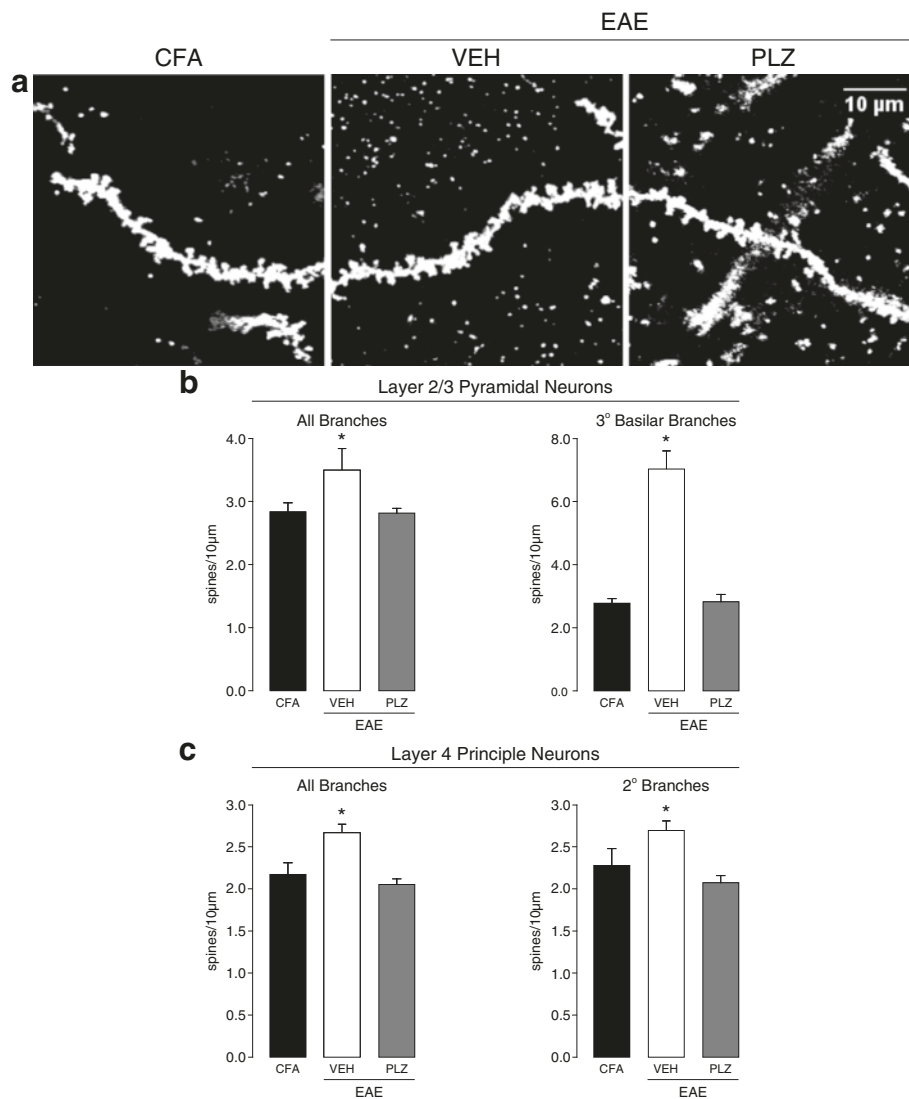


**Fig. 4** Morphological changes in spiny excitatory neurons of S1 in EAE, and PLZ-treated EAE, at clinical onset. **a** Representative maximum z-projected images showing appearance and density of spines on dendritic segments from spiny excitatory neurons in S1. Spines were visualized by reflectance-mode (488 nm) laser-scanning confocal microscopy on Golgi-Cox stained brains from VEH-treated CFA (CFA), VEH-treated EAE (VEH), and PLZ-treated EAE (PLZ) animals at clinical onset. **b** Mean ( $\pm$ S.E.) dendritic-spine densities assessed from the branches of spiny neurons in layers 2/3 of S1 from CFA-VEH ( $n = 42$  dendritic segments, 4 animals), EAE-VEH ( $n = 66$  dendritic segments, 8 animals), and EAE-PLZ mice ( $n = 78$  dendritic segments, 9 animals). Dendritic segments from EAE-VEH animals exhibited significantly increased spine-densities compared to segments from CFA-VEH mice. This increase was localized almost exclusively to the tertiary basilar branches (CFA-VEH  $n = 12$ , EAE-VEH  $n = 13$ , EAE-PLZ  $n = 14$  dendritic segments). Daily treatment with PLZ from 7 dpi prevented or reversed this increase—mean spine-densities along segments from EAE-PLZ animals did not significantly differ from CFA controls (Kruskal-Wallis one-way ANOVA on ranks; “all-branches”  $p = 0.032$ ; tertiary-basilar branches  $p = 0.007$ , all post hoc comparisons vs. CFA controls by Dunn’s method). **c** Mean ( $\pm$ S.E.) dendritic-spine densities assessed from the branches of spiny neurons in layer 4 of S1 from CFA-VEH ( $n = 36$  dendritic segments, 4 animals), EAE-VEH ( $n = 58$  dendritic segments, 8 animals), and EAE-PLZ mice ( $n = 83$  dendritic segments, 10 animals). Dendritic segments from EAE-VEH animals exhibited significantly increased spine-densities compared to segments from CFA-VEH mice. This increase was also specifically significant for second-order branches (CFA-VEH  $n = 23$ , EAE-VEH  $n = 43$ , EAE-PLZ  $n = 54$  dendritic segments). Daily treatment with PLZ prevented or reversed this increase—mean spine densities along segments from EAE-PLZ animals did not significantly differ from CFA-controls but were significantly reduced vs. the EAE-VEH group (“all-branches” analyzed by Kruskal-Wallis one-way ANOVA on ranks,  $p < 0.001$ ; post hoc comparisons vs. CFA controls by Dunn’s method. Secondary branches analyzed by one-way ANOVA,  $p < 0.001$ , all pairwise post hoc comparisons by SNK test)

PNNs in MS [66], we examined the state of neuroinflammation in S1. We first performed immunostaining for CD3 or CD45 expressing CNS-infiltrating leukocytes and

T cells. CD3<sup>+</sup> T cells and CD45<sup>+</sup> leukocytes were not present in S1 at either the pre-symptomatic or clinical-onset time points (see Additional file 6: Figure S4). We

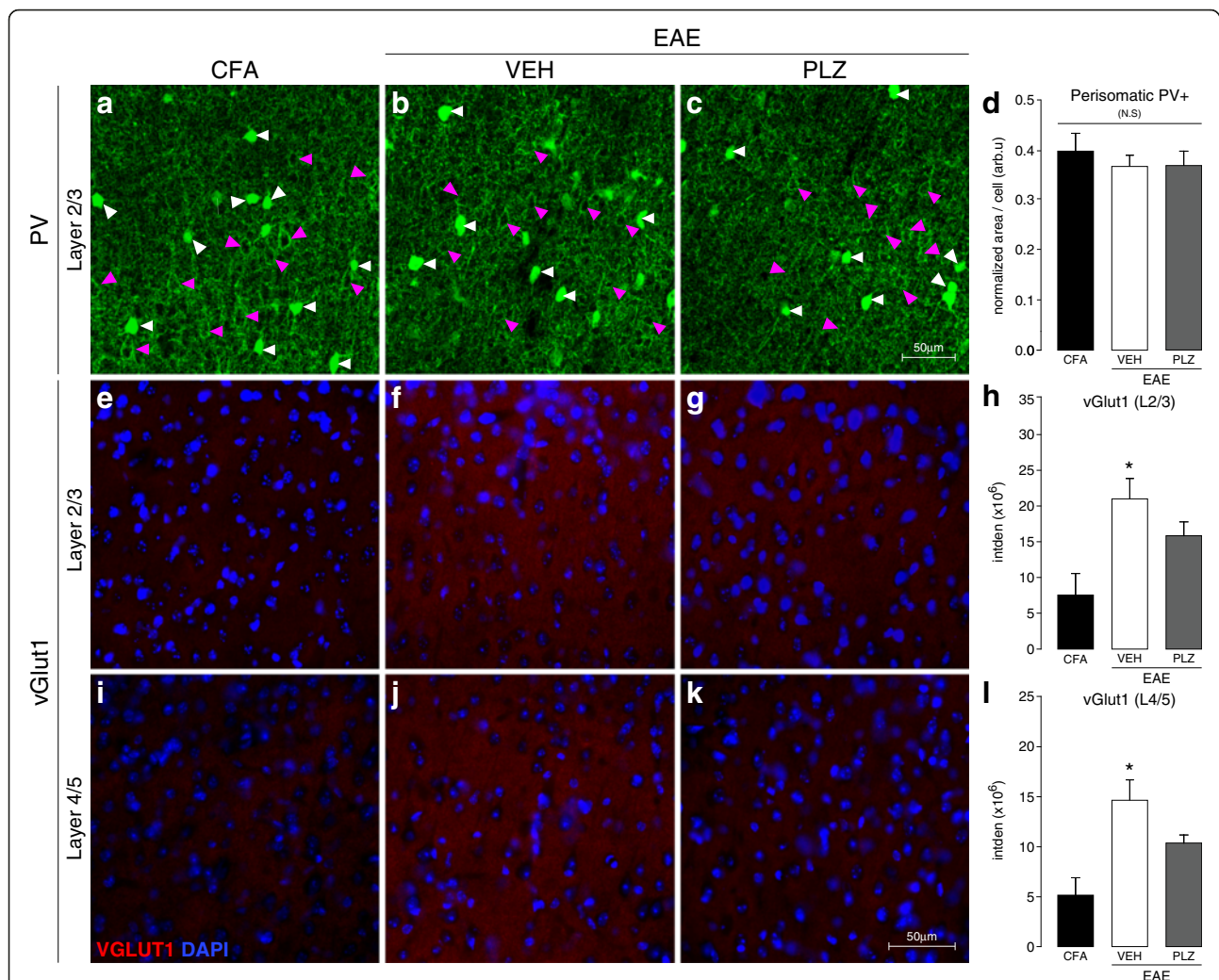


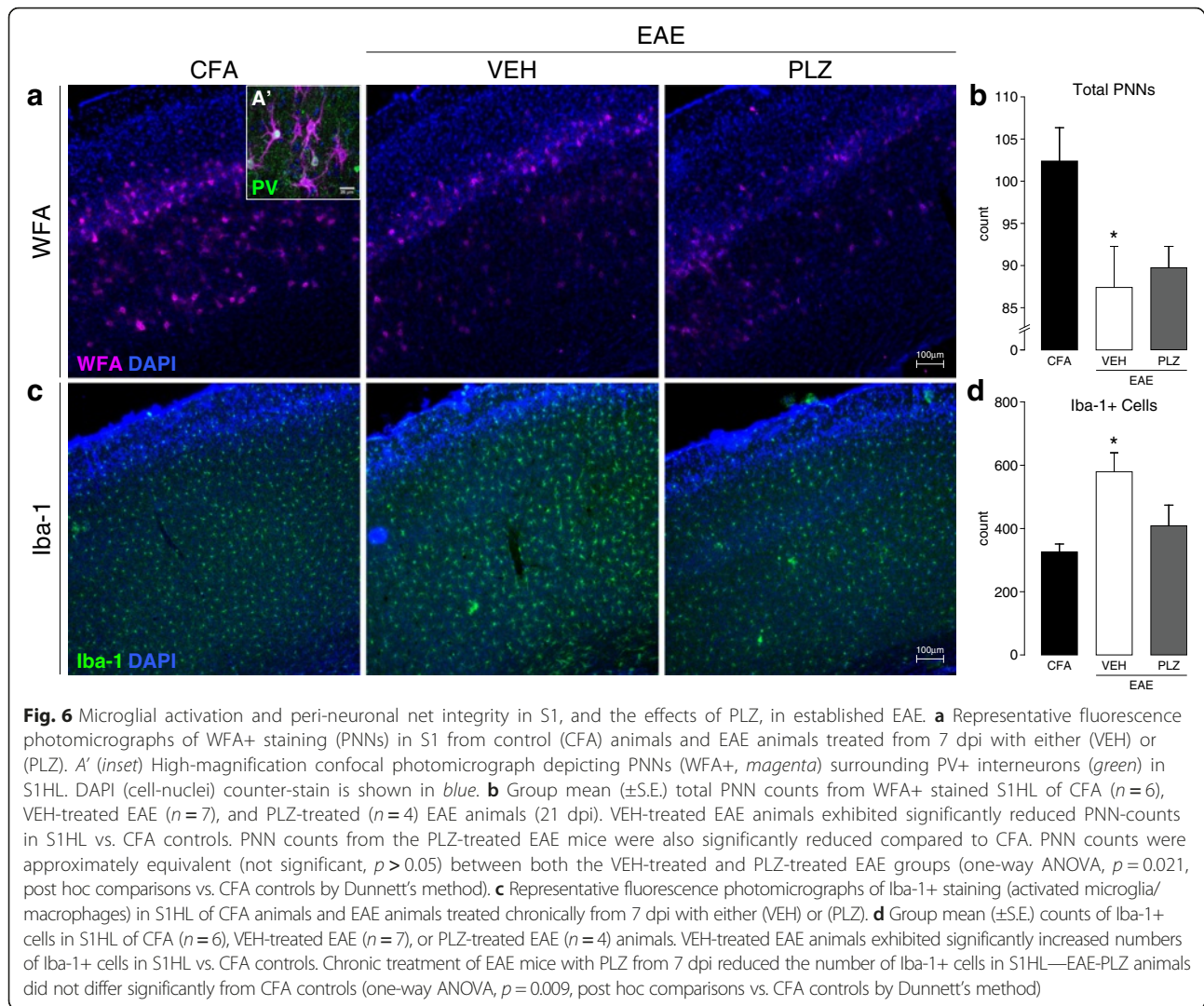
**Fig. 5** Perisomatic PV+ and VGLUT1+ reactivity and the effects of PLZ treatment in established EAE. **a–c** Representative confocal z-projections of PV+ somas and terminals (green) in layers 2/3 of S1, in control (CFA), VEH-treated EAE (21 dpi, VEH), and PLZ-treated EAE (21 dpi, PLZ) animals (treated from 7 dpi). White arrowheads indicate PV+ somas; magenta arrowheads indicate putative pyramidal-neuron “shadows” targeted for quantification. **d** Group mean ( $\pm$ S.E.) normalized density values corresponding to perisomatic PV+ staining surrounding layer 2/3 neurons in S1. Control (CFA) ( $n = 8$ ), VEH-treated EAE ( $n = 4$ ), and PLZ-treated EAE ( $n = 4$ ) animals did not differ from each another at this time point (one-way ANOVA not significant,  $p = 0.661$ ). **e–g** Representative fluorescence photomicrographs of VGLUT1+ staining (red) in layers 2/3 of S1; in control (CFA), VEH-treated EAE (21 dpi, VEH), and PLZ-treated EAE (21 dpi, PLZ) animals (treated from 7 dpi). DAPI (cell-nuclei) counter-stain is shown in blue. **h** Group mean ( $\pm$ S.E.) integrated densities of VGLUT1+ stained CFA ( $n = 5$ ), EAE-VEH ( $n = 5$ ), and EAE-PLZ ( $n = 4$ ) animals. VEH-treated EAE animals retained strongly increased VGLUT1+ density in layer 2/3 S1 vs. CFA controls. PLZ treatment from 7 dpi significantly reduced VGLUT1+ density in EAE animals but did not normalize to CFA-levels (one-way ANOVA,  $p = 0.014$ , all pairwise post hoc comparisons performed by Holm-Sidak method). **i–k** Representative fluorescence photomicrographs of VGLUT1+ staining (red) in layers 4/5 of S1; in control (CFA), VEH-treated EAE (21 dpi, VEH), and PLZ-treated EAE (21 dpi, PLZ) animals (treated from 7 dpi). DAPI (cell-nuclei) counter-stain is shown in blue. **l** Group mean ( $\pm$ S.E.) integrated densities of VGLUT1+ stained CFA ( $n = 5$ ), EAE-VEH ( $n = 5$ ), and EAE-PLZ ( $n = 4$ ) animals. VEH-treated EAE animals retained strongly increased VGLUT1+ density in layers 4/5 of S1 vs. CFA controls. PLZ treatment from 7 dpi significantly reduced VGLUT1+ density in EAE animals but did not normalize to CFA-levels (one-way ANOVA,  $p = 0.007$ , all pairwise post hoc comparisons performed by Holm-Sidak method)

did, however, observe significantly increased numbers of Iba-1+ microglia at both of these early disease time points (one-way ANOVA,  $p = 0.012$ , all post hoc comparisons vs. CFA by Dunnett’s method). This increase in cortical Iba-1+ microglia was also observed in tissues from late-stage EAE animals that were treated with VEH at 21 dpi. Notably, chronic PLZ treatment normalized Iba-1+ cell

counts in S1 of EAE animals at 21 dpi (one-way ANOVA,  $p = 0.009$ , all post hoc comparisons vs. CFA by Dunnett’s method) (Fig. 6c, d).

## Discussion

This study is the first investigation of functional neocortical plasticity along with persistent neuroanatomical



and synaptic changes occurring in S1 in the very early stages of the C57/BL6 MOG<sub>35–55</sub> EAE model. Specifically, we find in vivo evidence in early EAE of enhanced intensity and spread of the neuronal activation within S1 that is evoked by vibrotactile stimulation of the fore- or hindlimb. Interestingly, a delay exists between the “pre-symptomatic” and “clinical-onset” time points in the sensitization of responses to forelimb stimulation. This delay mirrors the caudal-to-rostral progression of spinal inflammation and paralysis in EAE [67] and suggests that ascending sensitization within the SC-DH [12] may precede (or initiate) sensitization of supraspinal sites, as has been observed in other models of neuropathic pain and allodynia [8, 23, 24].

In addition to the observed enhancement of functional responses, we find histological evidence of an increased density of excitatory pre-synaptic (VGLUT1+) terminals and post-synaptic contacts (dendritic spines) in cortical layers 2/3 and 4/5 of S1 in early EAE. These changes are

indicative of pro-excitatory remodeling of the major feed-forward circuit through S1 [47], in which layer 4 principal neurons receive thalamocortical inputs [68] and project vertically to pyramidal neurons of layer 2/3—primarily to the distal/basilar branches. Abundant transcolumellar connections in layer 2/3 mediate the horizontal spread of activation through S1, defining the areal extent of a “functional map” [53, 69]. Synaptic remodeling along this pathway therefore likely contributes to the intensification and expansion of S1 functional responses in early EAE [70]. These alterations occur prior to the onset of major paresis and temporally coincide with the appearance of prominent pain behaviors in the disease. Moreover, similar functional and synaptic alterations occurring in S1 have been shown to play a causal role in other neuropathic pain models [7, 8].

We also find evidence in EAE of an early, although transient, disruption of target-cell innervation by basket-forming PV+ inhibitory interneurons in S1. The central

role of PV-mediated fast-spiking inhibition in limiting the extent to which large-scale plastic changes may occur in the neocortex, during both adulthood and the perinatal critical period, is well documented in the literature [71, 72]. Even a transient loss of PV-mediated perisomatic inhibition in early EAE might therefore have profound and lasting consequences, leading to a dysregulated E-I balance and maladaptive cortical plasticity [73]. Moreover, we find that PV+ interneurons are affected in EAE by an early-appearing and persistent loss of their associated PNN structures. PNNs serve multiple supportive and protective functions for PV+ neurons, including sequestering cations (i.e.,  $\text{Ca}^{2+}$ ) to support fast-spiking activity, limiting synaptic modifications and alterations of connectivity, and protecting the neurons against chemical insults such as reactive oxygen species (ROS) [59]. The loss of PNNs may therefore be a key precipitating factor in the aberrant structural and synaptic plasticity we find in both the inhibitory and excitatory circuitry of S1 in early EAE. Loss of PNNs may additionally contribute to the unique susceptibility of PV+ interneurons to degeneration in the later stages of EAE/MS, which has been reported by several groups [21, 74, 75].

Collectively with our previous findings [12, 28], the multiple functional and synaptic changes in S1 evidenced in this study provide support for the hypothesis that EAE involves a profound, pro-excitatory, shift in the E-I balance of the entire somatosensory CNS, beginning very early in the disease course. This disrupted E-I balance promotes functional and structural plasticity within S1 [30, 71], leading to amplified cortical responses to peripheral stimuli and likely contributing to pain behaviors (i.e., allodynia) in the disease [7, 23, 31].

While we are the first group to find an increase in both pre- and post-synaptic glutamatergic markers and a concurrent reduction in perisomatic PV+ immunoreactivity in S1 in early EAE, several other groups have found similar or complementary changes in the EAE/MS brain [21, 74, 75]. A report by Yang et al. (2014) demonstrated enhanced turnover of dendritic spines and axonal boutons in layer 5 pyramidal neurons within S1 in early MOG<sub>35–55</sub> EAE [19]. As mentioned, loss of PV+ interneurons in EAE has also been demonstrated by several groups in multiple brain regions, including primary motor cortex [21, 64, 76]. A single report by Tambolo et al. (2015) also suggested, based on functional magnetic resonance imaging (*fMRI*)-blood-oxygen-level-dependent (BOLD) data, that the later stages (30–60 dpi) of the Lewis rat model of EAE involve functional expansion of the vibromechanically evoked S1 forelimb representation [20]. This study also found dendritic spine loss in layer 2/3 and 4 neurons of S1. While some of the findings and interpretations offered in Tambolo et al. (2015) appear to contrast with our observations, it is worth noting that there are significant methodological

differences between the studies. Furthermore, inferences about neural activation based strictly on the *fMRI*-BOLD signal may potentially be confounded by hemodynamic changes in the disease state. Nevertheless, much agreement exists between these various reports. Indeed, a substantial body of evidence is emerging that early synaptopathy in EAE and MS brains leads progressively to neuronal hyperexcitability, plasticity, excitotoxicity, and eventual dysfunction and degeneration [21, 65, 77]. In the majority of these studies, inflammation and circulating pro-inflammatory cytokines have been proposed as the proximal causative factors [10, 11].

In our examination of the role that inflammation plays in initiating or promoting cortical alterations in EAE, we first examined tissues for infiltrating CD3+ T cells and CD45+ leukocytes. As noted, brain-penetrating T cells were absent from S1 at these early stages in our model. However, intracortical Iba-1-reactive microglia were found to be significantly more abundant in EAE compared to CFA controls, both pre-symptomatically (7 dpi), and in the established disease (21 dpi). Previous groups have suggested multiple contributing roles for reactive microglia in EAE/MS-related synaptopathies [10, 11]. Microglia are capable of modifying neuronal connectivity through multiple mechanisms, including the secretion of diffusible factors such as matrix metalloproteases (i.e., matrix metalloproteinase (MMP)-2, MMP-9), which digest ECMCs such as PNNs, and are known to be elevated in the brain in EAE/MS [78]. Reactive microglia also secrete cytokines, such as soluble tumor necrosis factor (sTNF)- $\alpha$  and interleukin (IL)-1 $\beta$  [79, 80] which have been shown to promote synaptic plasticity and scaling, and neuronal hyperexcitability in EAE [19]. Microglia are furthermore responsive to many activity-dependent signals, such as extracellular glutamate and adenosine triphosphate (ATP) [81]. The pro-excitatory state found in early EAE cortex therefore likely acts to promote microglial reactivity in a feed-forward manner.

In addition to characterizing cortical functional and synaptic changes in early EAE, we also demonstrated a novel antinociceptive effect of PLZ treatment in the disease. Chronic treatment with PLZ from 7 dpi, when early cortical and behavioral alterations are already established, fully normalized mechanical withdrawal thresholds in EAE mice at clinical onset. Significantly, we also demonstrated that PLZ treatment normalizes S1 functional responses in EAE at onset. Furthermore, PLZ treatment attenuated S1 structural and synaptic abnormalities—normalizing dendritic spine densities at clinical onset and attenuating VGLUT1 reactivity in the established disease (21 dpi). Notably, this result highlights the possibility that, given the proper intervention, disease-related synaptopathies may be reversible. PLZ restores CNS levels of GABA in EAE through the inhibition of GABA-T by its active metabolite phenylethylidenehydrazine (PEH) and restores monoamine levels by the

irreversible inhibition of MAO-A and B [29]. PLZ has previously been shown to enhance functional intracortical GABA release [82–84]. The enhancement of the GABA-AR-mediated [55, 56] surround-inhibitory FAI signal we find in PLZ-treated EAE mice supports this proposed mechanism of action. Other groups have also suggested that PLZ may attenuate excessive cortical glutamate release by affecting glutamate-glutamine (neuron-astrocyte) shuttling and conversion [85, 86]. Defective astrocytic reuptake and metabolism has been suggested to promote excessive synaptic glutamate and CNS hyperexcitability in EAE/MS [10–12]. While PLZ treatment in EAE did not rescue disrupted PNNs, it significantly reduced Iba-1+ cells within S1. Just as excitatory signaling can promote microglial reactivity, inhibitory signaling through G protein-coupled receptors, such as GABA-BRs [87] and adrenergic receptors [88], can reduce microglial motility and reactivity. Enhancement of GABAergic/monoaminergic neurotransmission and the concomitant reduction of excitatory signaling may therefore be the means by which PLZ treatment reduces cortical microgliosis in EAE. This synergistic neuroglial action likely aids in the restoration of normal constraints on plasticity within the somatosensory CNS and contributes to the normalization of pain behaviors in EAE. PLZ treatment does not induce a generalized analgesic or sedative effect, as it produced no significant changes in basal mechanical sensitivity or motor function in control (CFA) animals. PLZ also did not affect evoked S1 functional responses in control (CFA) animals.

Although the current experiments did not involve direct manipulation of the sensory cortex in a way that might conclusively establish an immediate causal link between altered S1 structure/function and altered pain behaviors in EAE, the complete dissociation of responses to PLZ treatment in non-disease controls and EAE animals supports the hypothesis that maladaptive cortical plasticity and hyperexcitability within S1 directly contributes to pain in the disease.

## Conclusions

The evidence presented here supports a link between altered central E-I balance, maladaptive functional and structural plasticity in S1, and increased pain behaviors in early EAE. The PLZ experiments demonstrate, in principle, that a treatment which acts to restore lost CNS inhibitory function can normalize pain behaviors and S1 synaptic structure and function in EAE. By focusing our investigation on the early stages of EAE—when pain is first becoming established and when initiating pathogenic and synaptic changes occur—we hope to highlight the possibility that early therapeutic intervention, perhaps with a “combined-action” agent similar to PLZ, may be invaluable for preventing the development of CNP states in MS patients. For those patients with established CNP, and other “secondary”

symptoms of MS, the potentially reversible nature of CNS synaptopathy—as demonstrated here—also provides hope that certain aspects of the disease might also be effectively reverted through targeted interventions.

## Additional files

**Additional file 1:** Video 1. In vivo FA imaging of vibrotactile-evoked responses in S1 at the pre-symptomatic stage of EAE. Representative hindlimb-evoked FAI responses in S1 for naïve, CFA, and EAE animals at the pre-symptomatic time point. (MOV 10708 kb)

**Additional file 2: Figure S1.** S1 IHC in pre-symptomatic and clinical-onset EAE: PV+ cell counts, PNN counts, and Iba-1+ microglia counts. A) Representative fluorescence photomicrographs of PV+ staining (low-mag) in S1 from control (CFA) and EAE animals at the pre-symptomatic stage (7–9 dpi PRE) or clinical onset (ONS). B) Group mean ( $\pm$ S.E.) total PV+ cell counts from S1HL of CFA ( $n=8$ ), PRE ( $n=4$ ), and ONS ( $n=4$ ) EAE animals. No significant differences were observed between groups (one-way ANOVA N.S.). C) Representative fluorescence photomicrographs of WFA+ staining (PNNs) in S1 from control (CFA) and EAE animals at the pre-symptomatic stage (7–9 dpi PRE) or clinical onset (ONS). D) Group mean ( $\pm$ S.E.) total PNN counts from S1HL of CFA ( $n=11$ ), PRE ( $n=4$ ), and ONS ( $n=8$ ) EAE animals. EAE animals exhibited significantly reduced PNN-counts vs. CFA-controls at clinical onset (one-way ANOVA,  $p=0.007$ , post hoc comparisons vs. CFA-controls by Dunnett’s method). E) Representative fluorescence photomicrographs of Iba-1+ staining (PNNs) in S1 from control (CFA) and EAE animals at the pre-symptomatic stage (7–9 dpi PRE) or clinical onset (ONS). F) Group mean ( $\pm$ S.E.) total Iba-1+ counts from S1HL of CFA ( $n=13$ ), PRE ( $n=4$ ), and ONS ( $n=8$ ) EAE animals. EAE animals exhibited significantly increased numbers of Iba-1+ cells (microglial activation) in S1HL vs. CFA-controls at all time points (one-way ANOVA,  $p=0.012$ , post hoc comparisons vs. CFA-controls by Dunnett’s method). (PDF 6418 kb)

**Additional file 3: Figure S2.** PLZ-treatment delays the onset of clinical symptoms of EAE. Mean number of days (post-induction) to clinical onset (grade >0) in animals treated with vehicle (VEH,  $n=26$ ) or phenelzine (PLZ,  $n=27$ ) since 7 dpi. PLZ delayed the clinical onset of EAE by several days ( $t$  test,  $p=0.041$ ). (PDF 76 kb)

**Additional file 4:** Video 2. In vivo FAI of vibrotactile-evoked responses in S1 of EAE and PLZ-treated EAE animals at clinical onset. Representative hindlimb-evoked FA responses in S1 for vehicle-treated CFA (CFA-VEH), phenelzine-treated CFA (CFA-PLZ), vehicle-treated EAE (EAE-VEH), and phenelzine-treated EAE (EAE-PLZ) animals at clinical onset. (MOV 19447 kb)

**Additional file 5: Figure S3.** In vivo FAI of forelimb vibrotactile-evoked responses in S1 of EAE and PLZ-treated EAE animals at clinical onset. A) Balanced-contrast pseudocolored montages of representative S1 hindlimb responses from VEH/PLZ-treated CFA/EAE animals at clinical onset. B) Group mean ( $\pm$ S.E.) forelimb intensities at peak FA response, calculated from the “cortical map” area as a percent change in fluorescence vs. baseline (% $\Delta$ F/F). VEH-treated EAE animals at clinical onset ( $n=7$ ) exhibited significantly intensified responses to vibrotactile stimulation of the forelimb, compared to CFA controls ( $n=8$ ). PLZ-treated EAE ( $n=9$ ) and PLZ-treated CFA ( $n=4$ ) animals did not significantly differ from CFA (Kruskall-Wallis one-way ANOVA on ranks,  $p<0.001$ ; all post hoc comparisons vs. CFA-VEH controls by Dunn’s method). C) Group mean ( $\pm$ S.E.) forelimb FA response areas. EAE-VEH animals at onset ( $n=7$ ) exhibited significant expansion of hindlimb responses compared to CFA-VEH controls ( $n=8$ ), CFA-PLZ ( $n=4$ ), and EAE-PLZ animals ( $n=9$ ). CFA-VEH, CFA-PLZ, and EAE-PLZ groups did not significantly differ (Kruskall-Wallis one-way ANOVA on ranks not significant,  $p=0.912$ ). (PDF 545 kb)

**Additional file 6: Figure S4.** S1 IHC in pre-symptomatic and clinical-onset EAE: absence of cortical-infiltrating CD3+ and/or CD45+ T cells. A) Representative fluorescence photomicrographs of CD3+ staining in S1 from control (CFA) and EAE animals at the pre-symptomatic stage (7–9 dpi PRE) or clinical onset (ONS). No infiltrating T cells were apparent. B) Representative fluorescence photomicrographs of CD45+ staining in S1 from control (CFA) and EAE animals at the pre-symptomatic stage (7–9 dpi PRE) or clinical onset (ONS). No infiltrating T cells were apparent. (PDF 1663 kb)

### Abbreviations

5-HT, 5-hydroxytryptamine (serotonin); ANOVA, analysis of variance; ATP, adenosine triphosphate; BOLD, blood-oxygen-level dependent (signal); CD, cluster of differentiation; CFA, complete Freund's adjuvant; CNP, chronic neuropathic pain; CNS, central nervous system; DH, dorsal horn; dpi, days post-inoculation; EAE, experimental autoimmune encephalomyelitis; ECMC, extracellular matrix component; E-I, excitatory-inhibitory; FA/FAI, flavoprotein autofluorescence (imaging); FL, forelimb; GABA, gamma-aminobutyric acid; DA, dopamine; GABA-T, GABA-transaminase; HL, hindlimb; Iba, ionized calcium-binding adapter; IHC, immunohistochemistry; fMRI, functional magnetic resonance imaging; IL, interleukin; IP, intraperitoneal; MAO, monoamine oxidase; MAOI, monoamine oxidase inhibitor; MMP, matrix metalloproteinase; MOG, myelin oligodendrocyte glycoprotein; MS, multiple sclerosis; NA, noradrenaline; NT, neurotransmitter; PB, phosphate buffer; PBS, phosphate-buffered saline; PEH, phenylethylidenehydrazine; PFA, paraformaldehyde; PLZ, phenelzine; PNN, peri-neuronal net; PT, pertussis toxin; PV, parvalbumin; ROI, region of interest; S.C., subcutaneous; S1, primary somatosensory cortex; SC, spinal cord; SNK, Student-Newman-Keuls; sTNF, soluble tumor necrosis factor; VEH, vehicle; VF/VFH, Von Frey hair; VGLUT, vesicular glutamate transporter; WFA, *Wisteria floribunda* agglutinin

### Acknowledgements

The authors would also like to acknowledge the technical assistance provided by Bin Dong and Kasia Zubkow from the University of Alberta, as well as Dr. Majid Mohajerani of the University of Lethbridge.

### Funding

Funding for this project was provided by the operating grants from the Canadian Institutes of Health Research (CIHR) MOP-119338 and MOP-86712, the University of Alberta, Pfizer Canada, and the MS Society of Canada (MSSC). LP was supported by a studentship from the MSSC and BJK by a Donald Paty Career Development Award from the MSSC. FC is a Canada Research Chair in Intracerebral Hemorrhage. IW is supported by a scholarship from Alberta Innovates - Health Solutions.

### Availability of data and materials

Raw data upon which the conclusions in the manuscript are based will not be made publicly available at this time due to time constraints and to the large volume and diverse formatting of these materials.

### Authors' contributions

The study was primarily conceived and designed and written by LP/BK, with major intellectual, technical, and conceptual input and material (i.e., equipment/training) contributions from IW, as well as GB. GT and BK carried out the EAE inductions, and GT assisted with the behavioral assays and with processing tissues for histology, and with figures, alongside LP. LP was the primary contributor to the animal scoring, behavioral assays, and drug treatments. LP also conducted all of the FAI imaging studies, in the lab of IW, and also designed the custom Matlab program. FC and JC provided the technical expertise, training, and materials for the Golgi-Cox study. JS assisted with the immunostaining and performed the analysis. JWP carried out the IHC and assisted in the data analysis. All authors read and approved the final manuscript.

### Competing interests

The authors declare that they have no competing interests.

### Consent for publication

Not applicable.

### Ethics approval and consent to participate

All animal experiments and procedures were conducted in accordance with the Canadian Council on Animal Care's Guidelines and Policies and with protocols approved by the University of Alberta Health Sciences Animal Care and Use Committee (AUP#00000274).

### Author details

<sup>1</sup>Neuroscience and Mental Health Institute, University of Alberta, Edmonton, AB T6G 2E1, Canada. <sup>2</sup>Department of Pharmacology, University of Alberta, Edmonton, AB T6E 2H7, Canada. <sup>3</sup>Department of Psychiatry (NRU), University of Alberta, Edmonton, AB T6G 2B7, Canada. <sup>4</sup>Department of Psychology,

University of Alberta, Edmonton, AB T6G 2E9, Canada. <sup>5</sup>Department of Anesthesiology and Pain Medicine, University of Alberta, Clinical Sciences Building, 8-120, Edmonton, AB T6G 2G3, Canada.

Received: 30 March 2016 Accepted: 1 June 2016

Published online: 10 June 2016

### References

- Demaree HA, Gaudino E, DeLuca J. The relationship between depressive symptoms and cognitive dysfunction in multiple sclerosis. *Cogn Neuropsychiatry*. 2003;8(3):161–71.
- Svensden KB et al. Sensory function and quality of life in patients with multiple sclerosis and pain. *Pain*. 2005;114(3):473–81.
- Svensden KB et al. Pain in patients with multiple sclerosis: a population-based study. *Arch Neurol*. 2003;60(8):1089–94.
- O'Connor AB et al. Pain associated with multiple sclerosis: systematic review and proposed classification. *Pain*. 2008;137(1):96–111.
- Osterberg A, Boivie J, Thuomas KA. Central pain in multiple sclerosis—prevalence and clinical characteristics. *Eur J Pain*. 2005;9(5):531–42.
- Geurts JGG, Calabrese M, Fisher E, Rudick RA. Measurement and clinical effect of grey matter pathology in multiple sclerosis. *Lancet Neurol*. 2012;11(12): p. 1082–1092. doi:10.1016/S1474-4422(12)70230-2.
- Eto K et al. Inter-regional contribution of enhanced activity of the primary somatosensory cortex to the anterior cingulate cortex accelerates chronic pain behavior. *J Neurosci*. 2011;31(21):7631–6.
- Kim SK, Nabekura J. Rapid synaptic remodeling in the adult somatosensory cortex following peripheral nerve injury and its association with neuropathic pain. *J Neurosci*. 2011;31(14):5477–82.
- Gustin SM et al. Pain and plasticity: is chronic pain always associated with somatosensory cortex activity and reorganization? *J Neurosci*. 2012;32(43):14874–84.
- Mandolesi G et al. Synaptopathy connects inflammation and neurodegeneration in multiple sclerosis. *Nat Rev Neurol*. 2015;11(12):711–24.
- Musella A et al. Linking synaptopathy and gray matter damage in multiple sclerosis. *Mult Scler J*. 2016;22(2):146–9.
- Olechowski CJ et al. A diminished response to formalin stimulation reveals a role for the glutamate transporters in the altered pain sensitivity of mice with experimental autoimmune encephalomyelitis (EAE). *Pain*. 2010;149(3):565–72.
- Olechowski CJ et al. Changes in nociceptive sensitivity and object recognition in experimental autoimmune encephalomyelitis (EAE). *Exp Neurol*. 2013;241:113–21.
- Olechowski CJ, Truong JJ, Kerr BJ. Neuropathic pain behaviours in a chronic-relapsing model of experimental autoimmune encephalomyelitis (EAE). *Pain*. 2009;141(1–2):156–64.
- Rahn EJ et al. Sex differences in a mouse model of multiple sclerosis: neuropathic pain behavior in females but not males and protection from neurological deficits during proestrus. *Biol Sex Differ*. 2014;5(1):4.
- Thibault K, Calvino B, Pezet S. Characterisation of sensory abnormalities observed in an animal model of multiple sclerosis: a behavioural and pharmacological study. *Eur J Pain*. 2011;15(3):231. e1–16.
- Khan N, Smith MT. Multiple sclerosis-induced neuropathic pain: pharmacological management and pathophysiological insights from rodent EAE models. *Inflammopharmacology*. 2014;22(1):1–22.
- Gao YJ, Ji RR. c-Fos and pERK, which is a better marker for neuronal activation and central sensitization after noxious stimulation and tissue injury? *Open Pain J*. 2009;2:11–7.
- Yang G et al. Peripheral elevation of TNF-alpha leads to early synaptic abnormalities in the mouse somatosensory cortex in experimental autoimmune encephalomyelitis. *Proc Natl Acad Sci U S A*. 2013;110(25):10306–11.
- Tambalo S et al. Functional magnetic resonance imaging of rats with experimental autoimmune encephalomyelitis reveals brain cortex remodeling. *J Neurosci*. 2015;35(27):10088–100.
- Falco A et al. Reduction in parvalbumin-positive interneurons and inhibitory input in the cortex of mice with experimental autoimmune encephalomyelitis. *Experimental brain research. Experimentelle Hirnforschung. Experimentation Cerebrale*. 2014;232(7):2439–49.
- Komagata S et al. Nociceptive cortical responses during capsaicin-induced tactile allodynia in mice with spinal dorsal column lesioning. *Neurosci Res*. 2011;69(4):348–51.

23. Kim SK, Eto K, Nabekura J. Synaptic structure and function in the mouse somatosensory cortex during chronic pain: in vivo two-photon imaging. *Neural Plast.* 2012;2012:640259.
24. Watanabe T et al. Spinal mechanisms underlying potentiation of hindpaw responses observed after transient hindpaw ischemia in mice. *Sci Rep.* 2015;5:11191.
25. Komagata S et al. Initial phase of neuropathic pain within a few hours after nerve injury in mice. *J Neurosci.* 2011;31(13):4896–905.
26. Shibuki K, H.R., Tohmi M, et al. Frostig RD, editor., Flavoprotein fluorescence imaging of experience-dependent cortical plasticity in rodents. In: *in vivo optical imaging of brain function*. 2nd edition. Chapter 7.
27. Shibuki K et al. Dynamic imaging of somatosensory cortical activity in the rat visualized by flavoprotein autofluorescence. *J Physiol.* 2003;549(Pt 3):919–27.
28. Musgrave T et al. Tissue concentration changes of amino acids and biogenic amines in the central nervous system of mice with experimental autoimmune encephalomyelitis (EAE). *Neurochem Int.* 2011;59(1):28–38.
29. Musgrave T et al. The MAO inhibitor phenelzine improves functional outcomes in mice with experimental autoimmune encephalomyelitis (EAE). *Brain Behav Immun.* 2011;25(8):1677–88.
30. Hensch TK, Fagioli M. Excitatory-inhibitory balance and critical period plasticity in developing visual cortex. *Prog Brain Res.* 2005;147:115–24.
31. Woolf CJ, Salter MW. Neuronal plasticity: increasing the gain in pain. *Science.* 2000;288(5472):1765–9.
32. Kalyvas A, David S. Cytosolic phospholipase A2 plays a key role in the pathogenesis of multiple sclerosis-like disease. *Neuron.* 2004;41(3):323–35.
33. Benson CA et al. The MAO inhibitor phenelzine can improve functional outcomes in mice with established clinical signs in experimental autoimmune encephalomyelitis (EAE). *Behav Brain Res.* 2013;252:302–11.
34. Barrot M. Tests and models of nociception and pain in rodents. *Neuroscience.* 2012;211:39–50.
35. Tohmi M et al. Transcranial flavoprotein fluorescence imaging of mouse cortical activity and plasticity. *J Neurochem.* 2009;109 Suppl 1:3–9.
36. Drew PJ et al. Chronic optical access through a polished and reinforced thinned skull. *Nat Methods.* 2010;7(12):981–4.
37. Bains R et al. Volatile anaesthetics depolarize neural mitochondria by inhibition of the electron transport chain. *Acta Anaesthesiol Scand.* 2006;50(5):572–9.
38. T. Robert Husson and Naoum P. Issa, et al. Frostig RD, e., Functional imaging with mitochondrial flavoprotein autofluorescence: theory, practice, and applications. In: *in vivo optical imaging of brain function*. 2nd edition. Chapter 8.
39. Maggi CA, Meli A. Suitability of urethane anesthesia for physiopharmacological investigations in various systems. Part 1: general considerations. *Experientia.* 1986;42(2):109–14.
40. Hara K, Harris RA. The anesthetic mechanism of urethane: the effects on neurotransmitter-gated ion channels. *Anesth Analg.* 2002;94(2):313–8. table of contents.
41. Paxinos G and Franklin KBJ. *The mouse brain in stereotaxic coordinates*. Compact 2nd ed 2004, Amsterdam; Boston: Elsevier Academic Press.
42. Winship IR, Murphy TH. In vivo calcium imaging reveals functional rewiring of single somatosensory neurons after stroke. *J Neurosci.* 2008;28(26):6592–606.
43. Sigler, A.a.M., T. IO and VSD signal processor. 2012; Available from: [http://www.neuroscience.ubc.ca/faculty/murphy\\_software.html](http://www.neuroscience.ubc.ca/faculty/murphy_software.html).
44. Harrison TC, Sigler A, Murphy TH. Simple and cost-effective hardware and software for functional brain mapping using intrinsic optical signal imaging. *J Neurosci Methods.* 2009;182(2):211–8.
45. Gibb R, Kolb B. A method for vibratome sectioning of Golgi-Cox stained whole rat brain. *J Neurosci Methods.* 1998;79(1):1–4.
46. Frostig RD. Functional organization and plasticity in the adult rat barrel cortex: moving out-of-the-box. *Curr Opin Neurobiol.* 2006;16(4):445–50.
47. Lefort S et al. The excitatory neuronal network of the C2 barrel column in mouse primary somatosensory cortex. *Neuron.* 2009;61(2):301–16.
48. Schindelin J et al. Fiji: an open-source platform for biological-image analysis. *Nat Methods.* 2012;9(7):676–82.
49. Longair MH, Baker DA, Armstrong JD. Simple neurite tracer: open source software for reconstruction, visualization and analysis of neuronal processes. *Bioinformatics.* 2011;27(17):2453–4.
50. Lein ES et al. Genome-wide atlas of gene expression in the adult mouse brain. *Nature.* 2007;445(7124):168–76.
51. Kuo, T.e.a. ITCN cell counter. Available from: <http://rsb.info.nih.gov/ij/plugins/itcn.html>.
52. Sachdev RN, Krause MR, Mazer JA. Surround suppression and sparse coding in visual and barrel cortices. *Front Neural Circuits.* 2012;6:43.
53. Margolis DJ, Lutcke H, Helmchen F. Microcircuit dynamics of map plasticity in barrel cortex. *Curr Opin Neurobiol.* 2014;24(1):76–81.
54. Zhang G et al. Upregulation of excitatory neurons and downregulation of inhibitory neurons in barrel cortex are associated with loss of whisker inputs. *Mol Brain.* 2013;6:2.
55. Reinert KC et al. Flavoprotein autofluorescence imaging of neuronal activation in the cerebellar cortex in vivo. *J Neurophysiol.* 2004;92(1):199–211.
56. Reinert KC et al. Flavoprotein autofluorescence imaging in the cerebellar cortex in vivo. *J Neurosci Res.* 2007;85(15):3221–32.
57. Reinert KC et al. Cellular and metabolic origins of flavoprotein autofluorescence in the cerebellar cortex in vivo. *Cerebellum.* 2011;10(3):585–99.
58. Holtmaat A, Svoboda K. Experience-dependent structural synaptic plasticity in the mammalian brain. *Nat Rev Neurosci.* 2009;10(9):647–58.
59. Karetko M, Skangiel-Kramska J. Diverse functions of perineuronal nets. *Acta Neurobiol Exp (Wars).* 2009;69(4):564–77.
60. Hartig W et al. Cortical neurons immunoreactive for the potassium channel Kv3.1b subunit are predominantly surrounded by perineuronal nets presumed as a buffering system for cations. *Brain Res.* 1999;842(1):15–29.
61. Levy AD, Omar MH, Koleske AJ. Extracellular matrix control of dendritic spine and synapse structure and plasticity in adulthood. *Front Neuroanat.* 2014;8:116.
62. Soleman S et al. Targeting the neural extracellular matrix in neurological disorders. *Neuroscience.* 2013;253:194–213.
63. Ye Q, Miao QL. Experience-dependent development of perineuronal nets and chondroitin sulfate proteoglycan receptors in mouse visual cortex. *Matrix Biol.* 2013;32(6):352–63.
64. Centonze D et al. Inflammation triggers synaptic alteration and degeneration in experimental autoimmune encephalomyelitis. *J Neurosci.* 2009;29(11):3442–52.
65. Mandolesi G et al. Cognitive deficits in experimental autoimmune encephalomyelitis: neuroinflammation and synaptic degeneration. *Neuro Sci.* 2010;31 Suppl 2:S255–9.
66. Gray E et al. Elevated matrix metalloproteinase-9 and degradation of perineuronal nets in cerebrocortical multiple sclerosis plaques. *J Neuropathol Exp Neurol.* 2008;67(9):888–99.
67. Berard JL et al. Characterization of relapsing-remitting and chronic forms of experimental autoimmune encephalomyelitis in C57BL/6 mice. *Glia.* 2010;58(4):434–45.
68. Ahissar E, Staiger J. S1 laminar specialization. *Scholarpedia.* 2010;5(8):7457. [http://www.scholarpedia.org/article/S1\\_laminar\\_specialization](http://www.scholarpedia.org/article/S1_laminar_specialization).
69. Murakami H et al. Short-term plasticity visualized with flavoprotein autofluorescence in the somatosensory cortex of anesthetized rats. *Eur J Neurosci.* 2004;19(5):1352–60.
70. Feldman DE, Brecht M. Map plasticity in somatosensory cortex. *Science.* 2005;310(5749):810–5.
71. Hensch TK. Critical period regulation. *Annu Rev Neurosci.* 2004;27:549–79.
72. Donato F, Rompani SB, Caroni P. Parvalbumin-expressing basket-cell network plasticity induced by experience regulates adult learning. *Nature.* 2013;504(7479):272–6.
73. Toyozumi T et al. A theory of the transition to critical period plasticity: inhibition selectively suppresses spontaneous activity. *Neuron.* 2013;80(1):51–63.
74. Mandolesi G et al. IL-1beta dependent cerebellar synaptopathy in a mouse model of multiple sclerosis. *Cerebellum.* 2015;14(1):19–22.
75. Rossi S et al. Impaired striatal GABA transmission in experimental autoimmune encephalomyelitis. *Brain Behav Immun.* 2011;25(5):947–56.
76. Nistico R et al. Synaptic plasticity in multiple sclerosis and in experimental autoimmune encephalomyelitis. *Philos Trans R Soc Lond B Biol Sci.* 2014; 369(1633):20130162.
77. Pitt D, Werner P, Raine CS. Glutamate excitotoxicity in a model of multiple sclerosis. *Nat Med.* 2000;6(1):67–70.
78. Bar-Or A et al. Analyses of all matrix metalloproteinase members in leukocytes emphasize monocytes as major inflammatory mediators in multiple sclerosis. *Brain.* 2003;126(Pt 12):2738–49.
79. Schafer DP, Lehrman EK, Stevens B. The “quad-partite” synapse: microglia-synapse interactions in the developing and mature CNS. *Glia.* 2013; 61(1):24–36.
80. Ramesh G, MacLean AG, Philipp MT. Cytokines and chemokines at the crossroads of neuroinflammation, neurodegeneration, and neuropathic pain. *Mediators Inflamm.* 2013;2013:480739.

81. Eyo UB, Wu LJ. Bidirectional microglia-neuron communication in the healthy brain. *Neural Plast.* 2013;2013:456857.
82. Shen J and Yang J. In vivo detection of altered GABA levels following acute administration of antidepressant/antipanic drug phenelzine - *Proc. Intl. Soc. Mag. Reson. Med.* 2005;13:546.
83. Parent MB et al. Effects of the antidepressant/antipanic drug phenelzine and its putative metabolite phenylethylidenehydrazine on extracellular gamma-aminobutyric acid levels in the striatum. *Biochem Pharmacol.* 2002;63(1):57–64.
84. Parent MB, Habib MK, Baker GB. Time-dependent changes in brain monoamine oxidase activity and in brain levels of monoamines and amino acids following acute administration of the antidepressant/antipanic drug phenelzine. *Biochem Pharmacol.* 2000;59(10):1253–63.
85. Yang J, Shen J. In vivo evidence for reduced cortical glutamate-glutamine cycling in rats treated with the antidepressant/antipanic drug phenelzine. *Neuroscience.* 2005;135(3):927–37.
86. Michael-Titus AT et al. Imipramine and phenelzine decrease glutamate overflow in the prefrontal cortex—a possible mechanism of neuroprotection in major depression? *Neuroscience.* 2000;100(4):681–4.
87. Kuhn SA et al. Microglia express GABA(B) receptors to modulate interleukin release. *Mol Cell Neurosci.* 2004;25(2):312–22.
88. Dello Russo C et al. Inhibition of microglial inflammatory responses by norepinephrine: effects on nitric oxide and interleukin-1beta production. *J Neuroinflammation.* 2004;1(1):9.